Microalgae for Combined Nutrient Recovery and Biofuel Production from Sewage

Nicola Jeanne Wood

Submitted in accordance with the requirements for the degree of

Doctor of Philosophy

The University of Leeds

School of Civil Engineering

School of Molecular and Cellular Biology

School of Chemical and Process Engineering

May 2020

The candidate confirms that the work submitted is his/her own and that appropriate credit has been given where reference has been made to the work of others

Acknowledgments

First and foremost, I would like to thank my supervisors, Dr Miller Alonso Camargo-Valero and Professor Alison Baker for both their expertise and constant support and encouragement throughout the project. I am incredibly grateful for the opportunity to conduct my PhD in their groups and have thoroughly enjoyed working with them. I would also like to thank my co-supervisor Dr Andrew Ross for his expertise and guidance.

I am grateful to the EPSRC centre for doctoral training in Bioenergy (grant number EP/L014912/1) for their financial support and to Professor Jenny Jones, James McKay and Emily Bryan-Kinns for their support throughout my time at The University of Leeds.

I would also like to thank the technical teams in Engineering and Biological Sciences in particular, Dr Dave Elliott, Sue Marcus and Adrian Cunliffe for their training and support, the group of Professor Alison Smith at the University of Cambridge who provided invaluable training at the start of this project, Dr Rupert Quinnell for teaching me the necessary statistics, Dr Yasuko Kamisugi and Dr Andrew Cuming for kindly allowing me to use their fluorescence microscope and Dr Jeanine Williams and Iram Razaq for their training and help with the GC-MS equipment. Thanks also to Dr Lili Chu and the whole of the Baker group for their support and friendship during my time in the laboratory.

Finally, I would like to especially thank my family and friends, including everyone in the Bioenergy CDT, who have always been there to provide moral support, a confidence boost or a much needed tea break.

Abstract

It is critical that we move towards a more sustainable society. Three of our largest challenges are the need for sustainable energy generation, currently dominated by fossil fuel combustion, sustainable food supply, reliant on energy intensive fertiliser production, and a sustainable supply of fresh water, the treatment of which is often unreliable or economically prohibitive.

The use of microalgae for low-cost and effective nutrient removal in wastewater treatment works (WWTW) was established in the mid-20th century, but microalgae have gained renewed attention for their ability to accumulate lipids for biodiesel production. Furthermore, the ability of microalgae to accumulate high nutrient concentrations offers an opportunity to shift the focus of nutrient control in WWTW from removal to reuse (i.e. in agricultural fertilisers). This project addresses the hypothesis that microalgae may be cultivated within WWTW to simultaneously recover essential nutrients, produce biomass suitable for biodiesel production and contribute to the wastewater treatment process.

A new method to measure algal biomass density using digital image analysis was developed. The method facilitates the use of small volume cultures for screening studies without compromising robust growth data. The effect of environmental conditions, present within WWTW, on the growth, nutrient uptake and lipid accumulation in the model microalga *Chlamydomonas reinhardtii* are presented. Results demonstrate that pH control to near-neutral is preferable for nutrient removal, nutrient recovery and biofuel potential, owing to the increase in biomass density. In ammonium-rich wastewaters, pH control is critical to prevent ammonia toxicity. The choice of nitrogen source (ammonium vs. nitrate) had no significant effect on microalgal growth or biomass composition, microalgal nutrient removal therefore facilitates removal of wastewater nitrification processes. Finally, the small molecule, diphenyl methylphosphonate is shown to cause oil retention in *C.reinhardtii* and offers a means to improve lipid quality for biodiesel production.

Table of Contents

List of Figures

List of Tables

Abbreviations

ACCase	Acetyl-CoA Carboxylase
ACP	Acyl Carrier Protein
AD	Anaerobic Digestion
ADP	Adenosine Diphosphate
AGPase	ADP-glucose Pyrophosphorylase
AOB	Ammonia Oxidising Bacteria
ATP	Adenosine Triphosphate
BBM	Bold's Basal Media
BFA	Brefeldin A
BOD	Biological Oxygen Demand
CFPP	Cold Filter Plugging Point
CFU	Colony Forming Units
Chl	Chlorophyll
CIS	Citrate Synthase
CN	Cetane Number
DAG	Diacylglycerol
DGAT	Diacylglycerol Acyltransferase
DGTS	Diacylglyceryltrimethylhomoserine
dH_2O	Deionised Water
DMP	Diphenyl Methylphosphonate
DMSO	Dimethyl Sulfoxide
DSP	Diarrhetic Shellfish Poisoning
DU	Degree of Unsaturation
EBPR	Enhanced Biological Phosphorus Removal
ER	Endoplasmic Reticulum
EROI	Energy Return on Investment
EU	European Union
FAME	Fatty Acid Methyl Ester
FFA	Free Fatty Acid
G3P	Glycerol-3-Phosphate
GAO	Glycogen Accumulating Organism
GC-MS	Gas Chromatography Mass Spectrometry
GMO	Genetically Modified Organism
GPAT	Glycerol-3-acyltransferase

GPI	Green Pixel Intensity
HHV	Higher Heating Value
HRAP	High Rate Algal Pond
HRT	Hydraulic Retention Time
IV	Iodine Value
LB	Luria Broth
LCSF	Long Chain Saturation Factor
LPA	Lysophosphatide
MCT	Malonyl-CoA:ACP Transacylase
MUFA	Mono-unsaturated Fatty Acid
N	Nitrogen
NOEC	No Observable Effect Concentration
OD	Optical Density
OSI	Oxidation Stability Index
P	Phosphorus
PA	Phosphatidic Acid
PAP	Phosphatidic Acid Phosphatase
PAO	Polyphosphate Accumulating Organism
PBR	Photobioreactor
PDAT	Phospholipid Diacylglycerol Acyltransferase
PolyP	Polyphosphate
PPK	Polyphosphate Kinase
PSR1	Phosphate Starvation Response 1
PST	Paralytic Shellfish Toxin
PUFA	Poly-unsaturated Fatty Acid
RGB	Red Green Blue
SD	Standard Deviation
SFA	Saturated Fatty Acid
STW	Sewage Treatment Works
SV	Saponification Value
SWW	Synthetic Wastewater
TAG	Triacylglycerol
TAP	Tris-Acetate-Phosphate
TCA	Tricarboxylic Acid
TEM	Transmission Electron Microscopy

TGA	Thermogravimetric Analysis
TSS	Total Suspended Solids
UK	United Kingdom
UNFCC	United Nations Framework Convention on Climate Change
US(A)	United States (of America)
VSS	Volatile Suspended Solids
VTC	Vacuolar Transport Chaperone
WSP	Waste Stabilisation Pond
WWT	Wastewater Treatment
WWTW	Wastewater Treatment Works

Chapter One – Literature Review and Project Rationale

1.1 Introduction

Global population is set to rise from 7.3 billion (2015) to 8.5 billion by 2030 and 9.7 billion by 2050 (UN, 2015). With this comes an increased demand for fundamental resources. Together, known as the Water-Energy-Food Nexus, the interconnected supply and demand of water, food and energy is the most fundamental challenge to a sustainable society, essential for human well-being and sustainable development (FAO, 2014).

Clean water is a necessity for food security and economic development, particularly in industrial and agricultural sectors. With agriculture accounting for 70 % of global freshwater withdrawals, water is set to become one of the key constraints to food production if better means of water and land management are not adopted (FAO, 2011a). Food production, including transport and distribution as well as collection and treatment of the required water, additionally consumes approximately 30 % of global energy supply (FAO, 2011b).

As a result of our increasing population it is predicted that 60 % more food will need to be produced by 2050 with total water use for irrigation subsequently expected to rise by 10 % within the same time frame (FAO, 2011a). Similarly, global energy needs are predicted to increase by up to 50 % by 2040 (IEO, 2016). In 2009, John Beddington, then the UK chief scientific advisor, stated that the increasing demands for food, water and energy, along with our need to mitigate and adapt to climate change, are in danger of creating a 'perfect storm' of events with global implications (Beddington, 2009).

In response to climate change, 2008 saw the world's first legally binding climate change target established in the UK, the 2008 Climate Change Act, which commits the UK to reducing net carbon emissions by 80 % of 1990 baseline levels by 2050 (Climate Change Act 2008). Additionally, the recent Paris Agreement, which came into force in November 2016, ratified by all but three United Nations Framework Convention on Climate Change (UNFCCC) eligible member countries, sees the largest unified agreement on climate change since the Kyoto Protocol with targets to reduce global warming to "well below 2°C" and commitments to reduce carbon emissions to net zero by the latter half of the 21st century (Paris Agreement 2015; CCC, 2016).

Current and future scenarios therefore demand prompt actions encouraging a sustainable and integrated balance to achieve energy, food and water security.

1.1.1. Energy production and climate change

Current energy supply is dependent on the burning of fossil fuels and this is set to continue with fossil fuels estimated to account for 78 % of global energy consumption as late as 2040 (IEO, 2016). The burning of fossil fuels releases vast quantities of carbon dioxide into the atmosphere leading to global warming and climate change. As of 2010, fossil fuel related CO_2 emissions from the energy sector accounted for 69 % of all greenhouse gas emissions (IPCC, 2014), but as the effects of climate change intensify, a change to so-called 'green' energy sources is imperative.

Atmospheric CO_2 concentrations are at a record high, consistently exceeding 400 ppm (CO2 Earth, 2020) in comparison with pre-industrial times when CO_2 concentrations never reportedly exceeded 300 ppm (Etheridge *et al*., 1998). Furthermore, atmospheric CO_2 is set to continue increasing, with current growth rate at approximately 2.4 ppm/year (CO2 Earth, 2020). The increasing atmospheric CO_2 is expected to have dramatic effects on our climate in the coming decades with the recent increase in weather extremes such as heat waves, tropical cyclones and severe flooding believed to be directly connected to increasing atmospheric CO_2 (IPCC, 2007a).

Global temperature has risen 0.85°C since 1880 (IPCC, 2013) leading to dramatic reductions in polar ice. Subsequent sea-level rise is predicted between 0.52 and 0.98 m by 2100 (IPCC, 2013) jeopardising low lying communities and increasing flood risks. Additionally, ocean acidification caused by excessive CO_2 absorption is leading to coral reef destruction (Hoegh-Guldburg *et al*., 2007; Andersson and Gledhill, 2013). Coral reefs are some of the world's most biodiverse ecosystems and are relied on heavily by industries such as fishing and tourism. Their destruction will have serious consequences on low-income and isolated communities within reef regions (Hoegh-Guldburg *et al*., 2007 and sources therein).

An increase in global temperature is, both directly and indirectly, expected to have significant implications for human health. Global temperature rise is expected to cause reductions in crop yield (Lobell and Asner, 2003; Battisti and Naylor, 2009), increasing disease transmission, particularly for vector-borne diseases such as malaria and dengue-fever where warming will most likely increase the habitable area for disease-carriers such as mosquitos (Pascual *et al*., 2006; *Lancet* 2009), and worsening air quality particularly in cities (*Lancet* 2009; IPCC, 2007b).

With food and water supply dependent on energy security, and energy demand predicted to rise by nearly 50 % by 2040 (IEO, 2016) as a result of population rise and increasing development, our need for sustainable energy production is critical.

1.1.2 Water and wastewater

Rising temperatures and increasing eutrophication are leading to increasingly poor water quality and intensifying the occurrence and duration of droughts. Economically less developed countries located in West Asia and North Africa are currently the worst affected by water shortages, while developed regions such as the US mid-west and Australia are also significantly affected but with the economic freedom to circumvent the worst effects (Seckler *et al*., 1998). Assessments predict that North Africa as well as much of Asia will be the worst affected by increasing water scarcity approaching 2050 (Brauman *et al*., 2016; Kummu *et al*., 2016; Liu *et al*., 2017).

Additionally, increasing industrialisation and urbanisation are leading to increasing quantities of municipal wastewater. An average city of half a million inhabitants produces approximately 85,000 tonnes of municipal wastewater per day, all of which needs to be thoroughly cleaned and treated before it can be recycled in order to prevent harmful pollutants entering water supplies or the environment (Pescod, 1992).

In addition to the presence of harmful pathogens and chemicals condemning untreated wastewaters unsuitable as a drinking source, high concentrations of nutrients, particularly nitrogen and phosphorus, as a result of sewage and agricultural run-off, act as harmful environmental contaminants (Pittman *et al*., 2011). Eutrophication, the rapid and unwanted growth of phytoplankton as a result of excessive nutrient concentrations, has become a more serious and widespread problem since the middle of the 20th century (Cai *et al*., 2013). Increasing demand for food requiring nutrient-rich fertilisers (Lam and Ho, 1989 – cited in Blackburn *et al*, 2004), industrial growth worldwide (phosphates being one of the primary constituents of detergents) and increasing temperatures, as a result of global warming, are all expected to contribute to the increasing occurrence and severity of algal blooms and dead zones (Joyce, 2000).

Photosynthetic algal blooms impose diurnal variations in water pH due to consumption and release of CO_2 (Mara, 2003). During dark-hours, algal blooms compete with other aquatic life for oxygen, whilst consumption of CO_2 during photosynthesis causes water pH to rise creating high concentrations of harmful non-ionised ammonia (NH_3) (Abdel-Rouf *et al*., 2012). Under severe circumstances, algal blooms may completely restrict light penetration below the surface, halting photosynthesis, resulting in oxygen starvation and eventual death of marine life (Cai *et al*., 2013).

Blooms of cyanobacteria (formerly blue-green algae) also produce toxins which directly contribute to marine death. Toxins include paralytic shellfish toxins (PSTs), microcystins, okadaic

acid and polyether toxins such as those found in diarrhetic shellfish poisoning (DSP)-causing dinoflagellates (Blackburn, 2004 and sources therein). Some of the effects of algal toxins can be extended to human life through transfer up the food chain. Algal blooms exacerbate water shortages through contamination of drinking water supplies. Effects such as the death of fish have also been linked to a decrease in tourism and subsequent economic decline in regions where industries such as fishing are vital (Cai *et al.*, 2013).

Furthermore, if untreated, wastewaters serve as a sink, removing valuable nutrients from circulation and leaving us reliant on finite sources elsewhere.

1.1.3 Food and the need for sustainable fertilisers

With plants unable to obtain phosphorus from the atmosphere and often struggling to extract phosphorus from soils due to varying soil fixing ability or it being locked up in organic forms unavailable for uptake (Kochian, 2012), phosphorus is limiting for plant growth on over half of the worlds arable soils (Lynch, 2011). As such, agriculture in many areas, including in the UK, is dependent upon the application of phosphate fertilisers, produced from imported rock phosphate, for food security (Elser and Bennett, 2011).

In usable forms for fertiliser, phosphorus supply is finite. Furthermore, demand is set to increase with population rise, particularly with the increased popularity of meat and dairy-based diets requiring a higher phosphorus input than other food sources (Cordell *et al*., 2009). World consumption of P_2O_5 is expected to rise from 47 million tons in 2019 to 50 million tons per year by 2023 (U.S. Geological Survey, 2020) with 82 % of all phosphate used for fertiliser production (Prud'Homme, 2010). Despite the heavy use of phosphate fertilisers, only 20 % of that used makes it to the dinner plate, with 60 % of all losses due to erosion, leaching and run-off from farms (Elser and Bennett, 2011) and eventual removal during wastewater treatment or biological uptake in eutrophic water systems.

The panic ensued by pre-2010 studies, which estimated the exhaustion of rock phosphate supplies by 2130 (Abelson, 1999; Schröder *et al.,* 2011), has subsided with new evidence of significant rock phosphate reserves (Elser and Bennett, 2011). The U.S. Geological Survey estimates that rock phosphate reserves stand at over 300 billion tons, stating that we are not facing imminent shortages (U.S. Geological Survey, 2020).

Regardless of the quantity of global reserves, the distribution of rock phosphate is such that four countries/territories (the USA, China, Morocco and Western Sahara) hold over 80 % of raw rock phosphate supply, with Morocco and Western Sahara alone in control of over 70 % of all global reserves (Van Kauwenbergh, 2010; U.S. Geological Survey, 2020). As such, almost all

of the EUs supply of phosphorus comes from imported rock phosphate, leaving it vulnerable to volatile prices and supply security. This was starkly highlighted in 2007-2008 when the price of rock phosphate temporarily rose by 700 % of its 2006 prices over fears of dwindling supplies (Elser and Bennett, 2011).

Despite our reliance on phosphate for food security, of all phosphorus consumed in food globally (almost 100 % of which is later excreted), it is estimated that only 10 % is reused either before or after treatment with the remainder ending in water systems, non-agricultural land or landfill (Cordell *et al*., 2009; Schroder *et al*., 2011). Our wastewaters contain huge quantities of valuable phosphorus which, if harnessed, could form part of a sustainable phosphorus supply independent of the need for imports.

In addition, while not a finite resource, atmospheric nitrogen harnessed for fertiliser through the Haber-Bosch process to produce ammonia is done so at the expense of 1-2 % of global energy and approximately 2 L of fossil fuels per kilogram of nitrogen (Smith, 2002). Nitrification/denitrification processes in wastewater treatment see the majority of this nitrogen converted back into N_2 gas for safe release back into the atmosphere (see Section 1.3.3.1).

1.2 Microalgae

With approximately 4,500 times global energy demand reaching the earth's surface every year in the form of solar energy (Larkum, 2010), energy from biomass (bioenergy) is now widely adopted. Biomass currently constitutes approximately 10 % of global energy use, however the majority of this is still used for basic heat production for cooking in developing countries (IRENA, 2014).

Unlike other renewables, biomass offers an easily transportable, storable and highly versatile means to harness solar energy with the potential to be converted into several energy forms, including electricity, biogas and transport fuels, depending on demand (Saxena *et al*., 2009). Indeed, the vast majority of current energy supply is reliant on the release of solar energy stored long-term in the chemical bonds of fossil fuels. Furthermore, the fast growth rate and intrinsically carbon neutral nature of biomass combustion means that bioenergy offers a sustainable means to produce energy whilst minimising harmful atmospheric emissions.

Despite the promising potential of bioenergy, biomass production is severely limited by the availability of land and fresh water. Furthermore, if climate change mitigation policies are adopted, irrigation of bioenergy crops is predicted to have by far the greatest impact on water demand approaching 2100 (Mouratiadou *et al*., 2016). Similarly, as demand for food increases, so does demand for arable crop land; there are already reports of increasing food prices in the

USA, Brazil and parts of East Asia due to the production of bioenergy crops on land previously used for food production (Larkum, 2010 and sources therein). Given the constraints on land at risk of degradation, vulnerable drylands and the risk of tropical forest encroachment, it is estimated that it will be impossible for traditional bioenergy crops to provide more than 20-30 % of primary global energy demand by 2050 and even this will cause considerable pressure on land supply (Haberl *et al*., 2013).

The 'food vs. fuel' debate and the need for copious amounts of fresh water, alongside other constraints such as the need for agricultural fertiliser, currently limit the potential of biomass as a long-term global energy solution. However, the emergence of microalgae as a research topic for bioenergy production offers a means to circumvent the majority of problems associated with traditional bioenergy sources.

Microalgae are a large and diverse group of unicellular organisms capable of both phototrophic and heterotrophic growth through carbon fixation (Chisti, 2007; Greenwell *et al*., 2010). The term 'microalgae' refers to eukaryotic species such as green algae, however older reports may also include cyanobacteria, formerly blue-green algae, as prokaryotic microalga. Compared with traditional land-based biomass crops, microalgae offer several advantages:

- Microalgae can be grown year-round and do not compete with food for land, being capable of efficient growth on non-arable land, in marine ponds or in brackish waters (Cai *et al*., 2013; Gonçalves *et al*., 2016).
- Similarly, they do not require a supply of fresh water and are able to grow in a range of water systems including wastewater. This is coupled with their ability to extract nutrients from wastewater systems, essential for microalgal growth but which would otherwise act as harmful contaminants in water systems such as lakes, ponds and reservoirs.
- Due to their unicellular structure and the absence of stems, roots, bark and other structures unable to photosynthesise, the efficiency at which microalgae are able to convert solar energy into biomass comes much closer to the theoretical maximum (approx. 9-11 %) than it does for land plants (van Bielen *et al*., 2010). Additionally, microalgae do not produce lignocellulosic biomass which is hard to process and subsequently often goes to waste in energy production systems (Beer *et al*., 2009).
- Their unicellular structure also facilitates rapid growth and reproduction with doubling times of approximately 6-8 hours under favourable growth conditions.

Furthermore, microalgae are reportedly capable of much greater oil yields than terrestrial bioenergy crops (Chisti, 2007; Scott *et al*., 2010; Demirbas and Demirbas, 2011)

meaning a much smaller land area would be required to satisfy energy demand. Estimates of oil yield from microalgae range from 8,200 to 60,000 $Lha^{-1}year^{-1}$, depending on the study and microalgal strain, compared with 544 and 2,700 $Lha^{-1}year^{-1}$ for soya and canola respectively (Chisti, 2007; Scott *et al*., 2010). These figures should however be used with caution as research has so far primarily been conducted under heavily controlled conditions at lab or pilot scale and recent evidence suggests that yields will be lower for scaled-up processes (Amaro *et al*., 2011).

1.2.1 Economic constraint on microalgal biodiesel

While, in theory, microalgae offer great potential as a biofuel source, in order to be competitive as an alternative to petrodiesel, microalgal biodiesel must also be economically comparable. Current diesel prices at pump range from US $0.02-1.88/L across the world with the average price standing at US $1.02/L (Global Petrol Prices, 2019a). In biodiesels favour, fossil derived fuel prices are increasing with average world gasoline prices almost doubling since 2002 from US $0.58/L (The World Bank, 2020) to current estimates of US $1.11/L (Global Petrol Prices, 2019b).

Optimistic estimates for the cost of microalgal biodiesel range from US $1.40-3.53/L (Chisti, 2007; Campbell *et al*., 2011; Delrue *et al*., 2012; Slade and Bauen, 2013) meaning microalgal oil production costs need to fall at least 2.5-fold, however other reports predict reductions of up to seven times current costs may be necessary (Chisti, 2007).

Regardless of the ranging total costs reported, cultivation costs, including nutrients, carbon dioxide and water, are consistently reported as one of, if not the most significant, contributor to microalgal biodiesel costs from cultivation in open raceway ponds (Campbell *et al*., 2011; Delrue *et al*., 2012; Nagarajan *et al*., 2013; Slade and Bauen, 2013) with nitrogen and phosphorus alone costing up to 10 % of total costs (Delrue *et al*., 2012; Slade and Bauen, 2013). These costs could be saved if nutrients can be obtained free of charge (i.e. from wastewater) with up to 50 % of costs avoidable if carbon dioxide can additionally be obtained for free (i.e. from flue gas emissions) (Slade and Bauen, 2013). Additionally, the supply of nutrients reportedly contributes up to 50 % of all energy requirements associated with algal cultivation (Delrue *et al*., 2012), as such a source of easily obtainable nutrients could significantly improve the energy return on investment (EROI) of microalgal biodiesel. These reports stand only for cultivation in raceway ponds; the cost of microalgal biodiesel from cultivation in photobioreactors (PBRs) is dominated by capital costs and economic feasibility is unlikely even if free water and nutrients can be obtained.

It is clear that lipid yield along with the supply of nutrients and water are two of the largest bottlenecks affecting the economic feasibility of microalgal biodiesel.

1.2.2 The closed-loop cycle of microalgal wastewater treatment, nutrient recovery and biofuel production

In recent years there has been considerable interest in combining microalgae cultivation with wastewater treatment, making use of the free water and nutrients provided by wastewater, for combined nutrient recovery and biofuel production. The high nitrogen and phosphorus content of microalgae (approximately 10 % and 1 % respectively) make them advantageous organisms for the bioremediation of these nutrients from waste systems (van Harmelen and Oonk, 2006) thus allowing for recycling of essential nutrients back into fertilisers. The use of microalgae for nutrient removal from wastewaters additionally provides a low-cost, high efficiency contribution to the wastewater treatment process.

By combining with wastewater treatment, the cultivation of biomass can be done at a considerably reduced cost due to the free source of water and nutrients provided by wastewater. Additionally, the contributions of microalgae to the wastewater treatment process and the ability to recycle high-value nutrients further reduce the total cost of microalgal biodiesel. Throughout the process, wastewaters and CO_2 produced may be recycled to feed the growing algal culture and residual biomass after nutrient and oil extraction can potentially be anaerobically digested to produce biogas as an additional source of energy. Together these form the closed loop cycle of water, energy and nutrients for combined wastewater treatment, nutrient recovery and biofuel production (Figure 1.1).

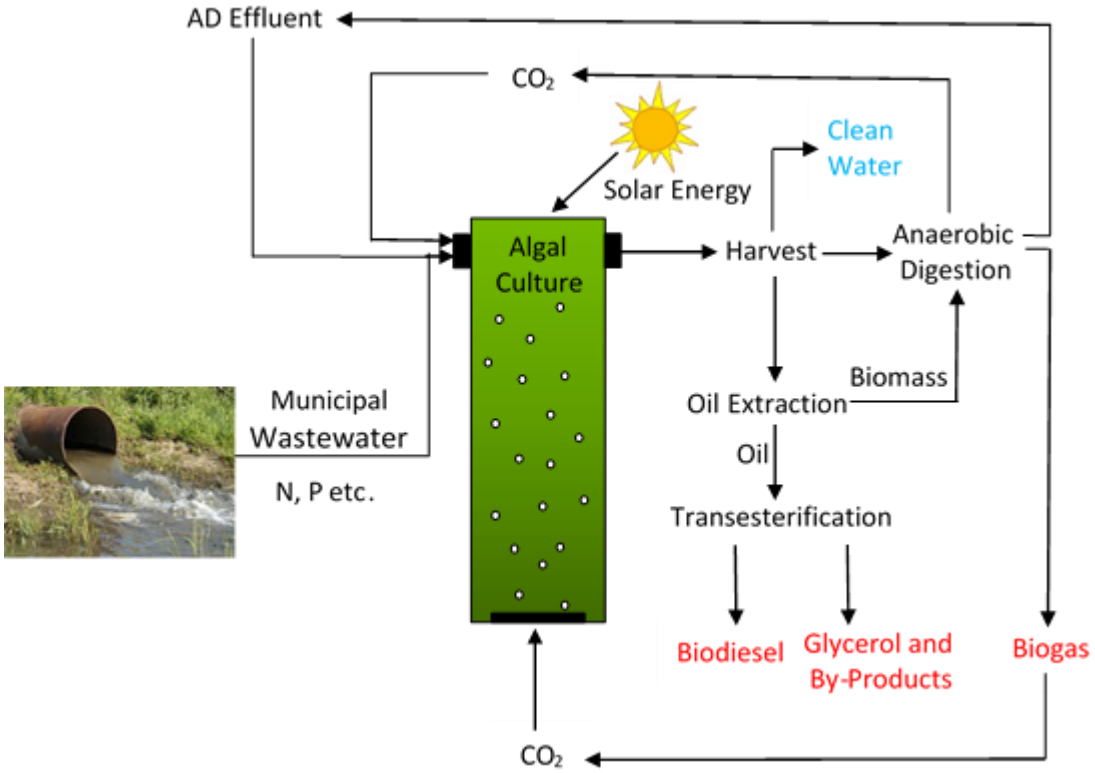

Figure 1.1 The proposed closed loop cycle of energy, water and nutrients for combined wastewater treatment, nutrient recovery and biofuel production. Inspired by Sivakumar et al, (2012). Algae grown within WWTW can be used to clean the wastewater of contaminating nutrients (N and P etc.). The produced biomass can then be used to produce biodiesel and biogas with all waste products recycled back to the cultivation stage. N and P may be extracted for recycling from biomass either before or after lipid extraction, from AD effluent, or by use of microalgae directly as a fertiliser.

This project focusses on improving our understanding of the impact of environmental conditions on biomass cultivation, nutrient uptake and net lipid production and therefore the opportunities for simultaneous bioenergy generation and nutrient recovery from wastewater. As such, the remainder of this review will discuss recent advances in the areas of:

- Microalgal growth and nutrient uptake in wastewaters for combined wastewater treatment and nutrient remediation,
- Strategies for over-accumulation of phosphate in microalgae in the form of polyphosphate for the production of high-value fertilisers and
- Microalgal biofuel production and lipid optimisation strategies

1.2.3 Chlamydomonas as a model organism

Bioremediation of essential nutrients from wastewaters using *Chlorella* and *Duniliella* has been investigated for the last 50 years and *Chlorella* is still the most popular choice for bioremediation research largely due to its common presence within wastewater treatment facilities, robustness to a wide range of growth conditions and its potential to be used for

biofuels, animal feeds and fertilisers (Abdel-Raouf *et al.,* 2012; Sun *et al.,* 2013; Asmare *et al.,* 2014; Gonçalves *et al.,* 2014; Zhang *et al.,* 2014a; Caporgno *et al.,* 2015; Mujtaba *et al.,* 2015; Lu *et al.,* 2015; Cho *et al.,* 2016; Wang *et al.,* 2016). In recent years, as microalgae have gained increasing attention as a potential biofuel feedstock, research into microalgal wastewater treatment has expanded to investigate a wide range of microalgal species including *Desmodesmus* (Samori *et al.,* 2013), *Scenedesmus* (Asmare *et al.,* 2014; Xu *et al.,* 2015; Zhang *et al.,* 2015; Yu *et al.,* 2015; Wang *et al.,* 2016; Lutzu *et al.,* 2016), *Pseudokirchneriella* (Gonçalves *et al.,* 2014; Morales-Amaral *et al.,* 2015), *Muriellopsis* (Morales-Amaral *et al.,* 2015), *Chlorococcum* (Karemore and Sen, 2015) and *Chlamydomonas* (Zhang *et al.,* 2014a; Yu *et al.,* 2015; Hernandez *et al.,* 2016).

The chlorophyte *Chlamydomonas* has emerged as a model organism for the study of algal metabolism and the production of valuable bioproducts (Salomé and Merchant, 2019). Over 500 species of *Chlamydomonas* have been identified and cells have been isolated across the globe from a range of habitats including freshwaters, oceans and sewage ponds and from a range of climates including some arctic regions (Harris, 1988). A recent study on the use of microalgae for phosphorus remediation from WWTW in New Zealand identified *Chlamydomonas* as one of only a few luxury phosphorus accumulating microalgae present commonly within WWTW across three climate zones (Crimp *et al*., 2018). Specifically, the now fully sequenced *Chlamydomonas reinhardtii* genome is a first for microalgae, and facilitates in depth understanding of photosynthesis, cell division and the effect of environmental conditions at a genetic level (Merchant *et al*., 2007). As such *Chlamydomonas reinhardtii* has become one of the most widely researched algal organisms with many isolated mutants, allowing for the study of many specific functions within the cell, and a large knowledgebase regarding its structure and biochemical functions (Harris *et al*., 1988; The Chlamydomonas Resource Center,a).

The ability of *Chlamydomonas* to grow in a wide range of environments including wastewaters and ammonia rich media, under both phototrophic and heterotrophic conditions (when supplied with an organic carbon source) make it especially promising as a potential organism for nutrient removal within WWTW (Mara, 2003). While other species of microalgae such as *Chlorella*, *Scenedesmus* and *Botryococcus* have demonstrated greater potential as biofuel feedstocks (Rodolfi *et al*., 2013; Islam *et al*., 2013), the emergence of *Chlamydomonas reinhardtii* as a model organism with a wide range of available mutants and a wealth of published literature is of particular use for this project which aims to understand the specific effects of various culture conditions on algal metabolism. As such, this project focusses on *Chlamydomonas reinhardtii* for nutrient recovery and biodiesel production from wastewaters.

1.3 Sewage Treatment Processes and Microalgal Bioremediation

Domestic wastewater is comprised of approximately 99.9 % water with contaminants including organic and inorganic matter, nutrients, particularly nitrogen and phosphorus, dissolved and suspended solids and microorganisms such as faecal coliforms (von Sperling, 2007).

Conventional wastewater treatment within a wastewater treatment works (WWTW) or sewage treatment works (STW) comprises physical, biological and chemical processes to remove solids, organics and nutrients. Limits on contaminants within wastewater effluent are imposed depending on effluent use (e.g. irrigation or human consumption) and contain restrictions on the quantity of organics, pathogens and nutrients in the final treated effluent. An example of a sewage treatment process is presented in Figure 1.2.

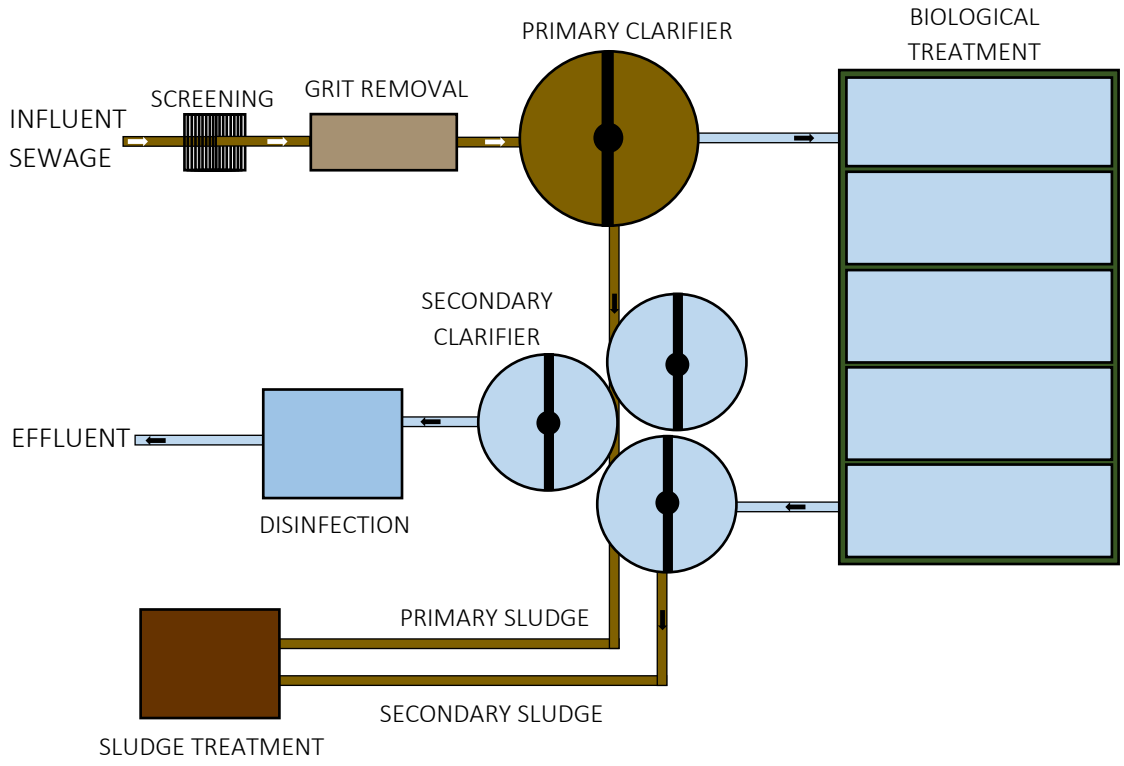

Figure 1.2 An example of a sewage treatment process. Influent wastewater first passes through screenings, a grit removal chamber and a primary clarifier (or settling tank) to remove the bulk of the solid phase. Organics and suspended solids are removed via biological treatment consisting of a trickling filter, activated sludge facility or waste satabilisation ponds. Finally, residual solids are removed in the secondary clarifier and effluent faces final disinfection before release. Sludge from clarifiers is removed via specialist sludge treatment.

1.3.1 Solids removal

Large solid matter is initially removed from influent wastewater by passing the water through a bar screen with spacing ranging from 20-60 mm. Following initial screening, water is

passed into a grit chamber, a long thin chamber which serves to reduce the flow rate, allowing smaller settleable solids such as grit and sand to settle while organic matter remains in solution (Abdel-Raouf *et al*., 2012).

Water and dissolved/colloidal organic matter are then passed into the primary clarifier, a large container typically 3-5 metres deep, where the long retention time of a few hours allows for up to half of the remaining solids to settle where they are removed by pumps for sludge treatment and disposal. Large skimmers remove floating materials such as oil and scum which are similarly disposed of *via* sludge treatment (Pescod, 1992).

1.3.2 Removal of organics and suspended solids

Organics, measured as biological oxygen demand (BOD), and suspended solids are removed in secondary treatment using aerobic microorganisms (principally bacteria) able to assimilate organic matter (See Figure 1.2 – Biological Treatment). The three most common treatment methods are the trickling filter, activated sludge processes and the use of oxidation, or waste stabilisation, ponds.

Trickling filters are a collection of stones, plastic blocks or wooden slats held within a basin or tank. These objects provide a surface on which a biological layer of microbes, a biofilm, forms creating a filter to breakdown organic matter. Wastewater is allowed to flow slowly (or trickle) through the filter where organics are metabolised by the biofilm. Air is typically provided either naturally from the atmosphere or pumped through the filters to provide oxygen for microbial growth (Pescod, 1992; Muralikrishna and Manickam, 2017; Gerber and Pepper, 2019).

The activated sludge process takes place within a large basin or aeration tank where fresh sludge from a secondary clarifier is added to a suspension of wastewater and microbes and aerated using air pumped from the base of the tank. This aeration also serves to efficiently mix the contents of the tank. The aerated suspension provides the perfect environment for aerobic microbes, which grow to form a suspension of biological solids (activated sludge). A retention time of between 3 and 8 hours (or longer for high organic content wastewaters) allows the microorganisms to absorb and metabolise dissolved organics from the wastewater. The treated wastewater then flows into a secondary clarifier which, acting like the primary clarifier, removes solid matter, including the microbial sludge. Approximately 30 % of the removed sludge is recirculated into the aeration tank to serve the activated sludge process. The remainder is removed and treated along with solid wastes from the preceding processes (Pescod, 1992; Grady *et al*., 2011; Muralikrishna and Manickam, 2017).

Alternatively, a series of oxidation tanks, or waste stabilisation ponds, which use a combination of bacteria and algae can be used (Pescod, 1992; Mara, 2003; Grady *et al*., 2011). Waste stabilisation ponds (WSPs) are the favoured technology in developing countries owing to the low capital and operational costs and because the typically warmer temperatures are more favourable for their operation (Mara, 2003). There are typically three types of pond, anaerobic, facultative and maturation (aerobic) ponds, although raw wastewaters may flow directly into facultative ponds (named primary facultative ponds). The pond type is determined by the pond depth and surface area which control the level of dissolved oxygen and sunlight penetration. Anaerobic ponds are the deepest ensuring anaerobic conditions in the sludge layer at the bottom of the tank, while maturation ponds are much shallower and have a greater surface area to promote photosynthesis. Facultative ponds rely on both anaerobic bacteria and an algal layer on the surface. Wastewaters flow first into anaerobic ponds where organics sediment and are digested in the sludge layer at the bottom of the tank by anaerobic bacteria. Anaerobic ponds also remove contaminants such as heavy metals which are toxic to algae and so must be removed before treatment in facultative ponds (Mara, 2003).

Following treatment in anaerobic ponds, wastewaters are received into secondary facultative ponds (or primary facultative ponds in the case of low BOD in the raw wastewater where anaerobic ponds are not required). In facultative ponds, the growth of algae produces the oxygen required for bacterial BOD removal. This symbiotic relationship between anaerobic bacteria and algae minimises the aeration needed to the pond, however additional aeration is often supplied to reduce the required size of the pond or the hydraulic retention time (Ambulkar & Nathanson, 2010). Digested sludge from anaerobic and facultative ponds is removed at much lower frequencies than in activated sludge treatments, requiring removal only every 1-3 years for anaerobic ponds and approximately every 10 years for facultative ponds (Mara, 2003). Effluent from facultative ponds is then removed into a single or series of maturation ponds designed for pathogen and nutrient removal.

Pathogen removal, typically monitored by the concentration of faecal coliforms, happens in most cases fortuitously with the primary objective of reducing BOD (Curtis, 2003). Up to 50 % of faecal coliforms are removed during primary sedimentation with the remainder (or as much as possible) removed during secondary treatment. In activated sludge plants and in anaerobic and facultative ponds, 90-99 % of remaining faecal coliforms and other pathogens including helminth eggs and protozoan cysts are removed primarily by adsorption onto solids such as algae and other bacteria which sediment when they die and are removed as sludge (Curtis, 2003; Mara, 2003).

Unlike other technologies, in waste stabilisation ponds, the maturation ponds are designed to optimise pathogen removal. The shallow depth (approx. 1m) allows for greater light penetration through the pond (Mara, 2003). The high sunlight coupled with the high oxygen concentrations afforded by algal growth leads to photooxidation contributing to the death of a large proportion of the remaining pathogens (Curtis *et al.*, 1992). Furthermore, the diurnal variations in pH due to algal growth mean that during daylight hours pH at the surface of the pond can rise to >10 causing faecal bacteria to rapidly die off (Mara, 2003).

1.3.3 Nutrient removal

Due to the problems associated with high nutrient concentrations in natural systems such as lakes and reservoirs, wastewater treatment must be meet strict nutrient effluent restrictions (around 10-15 mg/L N and 1-2 mg/L P, Environment Agency, 2019). Current nutrient removal technologies focus on removal, rather than recovery, of nutrients in order to meet strict effluent requirements designed primarily for environmental protection.

1.3.3.1 Nitrogen removal

Domestic wastewater contains nitrogen predominantly in organic, i.e. urea, and ammonium forms and early bacterial decomposition and hydrolysis convert much of the organic nitrogen forms into ammonium (Eckenfelder and Argaman, 1991). The most popular method for nitrogen control within wastewater treatment plants is through the action of nitrifying and denitrifying bacteria (Jeyanayagam, 2005; McCarty, 2018; Halling-Sørensen and Jørgensen, 1993). Nitrification is the oxidation of ammonium to nitrite and then nitrate by ammonia oxidising bacteria (AOB) under aerobic conditions (Eq. 1.1 & 1.2). This is followed by denitrification which involves the reduction of nitrate to nitrogen gas by heterotrophic bacteria under anoxic conditions (Eq. 1.3). Nitrogen gas can then be released into the environment without harm.

$$2NH_4^+ + 3O_2 \rightarrow 2NO_2^- + 2H_2O + 4H^+ \quad (1.1)$$

$$2NO_2^- + O_2 \rightarrow 2NO_3^- \quad (1.2)$$

$$NO_3^- + Organics \rightarrow N_2(gas) + CO_2 + H_2O + OH^- \quad (1.3)$$

As with other processes, aeration is usually required for the growth of nitrifying bacteria and as such nitrogen removal adds significantly to the cost of wastewater treatment processes. Less oxygen, and therefore less energy, intensive processes have since been developed such as direct denitrification of nitrite rather than nitrate, removing the additional oxidation step (McCarty, 2018). Cost and energy savings can be achieved through use of anaerobic ammonium oxidation (anammox) bacteria, which convert a mix of ammonium and nitrite directly into

nitrogen gas. Discovered in the 1980s (Mulder, 1989), the process is almost ubiquitous in freshwaters and the infrastructure has now been developed to make use of anammox for efficient nitrogen removal in WWTW without the need for aeration (Kuenen, 2008). However, widely used nitrogen removal processes do not consider recovery of nitrogen species with almost all nitrogen removed from wastewaters as nitrogen gas to the atmosphere. The same nitrogen gas which is then removed from the atmosphere by the Haber-Bosch process for fertiliser production at great expense in terms of both energy and greenhouse gas emissions.

In contrast, waste stabilisation ponds are designed for nitrogen removal through microbial (predominantly algal) uptake (Mara, 2003). At high pH, ammonia may also be lost to the atmosphere in the gaseous form through volatilisation, however recent research has demonstrated that losses to volatilisation provide minimal contributions to total nitrogen removal (Camargo Valero and Mara, 2007a). In depth research by Camargo-Valero and Mara investigating the fate of nitrogen species within waste stabilisation ponds also identifies the importance of simultaneous nitrification and denitrification for nitrogen removal in maturation ponds particularly during colder months (water temperature 3.1 - 6.4°C) when conditions are less favourable for algal growth (Camargo Valero *et al*., 2010a). Furthermore, algal sediment (sludge) containing approximately 10 % nitrogen by weight (Stumm and Morgan, 1996), is later anaerobically digested by bacteria recycling much of the stored nitrogen back into the water column (Camargo Valero *et al*., 2010b). As such, efficient solid removal processes (i.e. algal harvesting) are required to permanently remove nitrogen from waste stabilisation ponds.

1.3.3.2 Phosphorus removal

As with nitrogen control in wastewater treatment plants, the most common methods for phosphorus removal focus on removal, with little or no attention to the needs or opportunities for phosphorus recovery. The most popular methods for phosphorus removal involve chemical dosing with alum (aluminium sulphate), iron (ferric chloride) or lime metal salts to promote phosphorus precipitation (Mara, 2003; Bunce *et al*., 2018). Precipitants are then removed either by sedimentation into the sludge layer or by filtration. These processes are successful at removing total phosphorus to <0.1 mg/L P but come with heavy costs associated with the addition of metal salts (Smith *et al*., 2008) and often require pH control of the effluent prior to discharge due to the effect of added metal salts on water pH (Bunce *et al*. 2018). Despite the phosphorus rich precipitates, chemically bonded P is difficult to separate making sustainable phosphorus recovery from such processes almost impossible (Likosova *et al*., 2013; Oleszkiewicz *et al*., 2015).

Methods for more controlled precipitation (e.g. as struvite, $NH_4MgPO_4.6H_2O$) and reactive filters systems involving P-sorption have been developed but with varied success (Bunce

et al., 2018). While struvite precipitation is well-developed, and struvite can be used as an agricultural fertiliser with good properties, the addition of magnesium and need for pH adjustment significantly increase operation costs (Bhuiyan *et al*., 2008). In contrast, while the research into active filter technology demonstrates effective removal of P (Renman and Renman, 2010), it is yet to be proved at scale or over a sustained period of time (Shilton *et al*., 2006; Bunce *et al*., 2018).

Alternative biological removal processes offer advantages in terms of cost and sustainability. The widely used enhanced biological phosphorus removal (EBPR) process is traditionally applied within activated sludge systems and works by polyphosphate accumulating organisms (PAOs) removing phosphate from the bulk liquid phase of activated sludge and storing it as polyphosphate granules within the cell (Oehmen *et al*., 2007; Bunce *et al*., 2018). The process comprises of an anaerobic phase followed by an aerobic phase. The anaerobic phase acts as a conditioning phase for PAOs and contains a large supply of readily available organic matter. Although they are unable to reproduce in anaerobic conditions, PAOs consume volatile fatty acids, formed from biodegradable organic matter, to form stored carbon compounds. Energy for the process is obtained by mobilising stored polyphosphate and as such, prior to entering the aerobic zone, PAOs are low in phosphate but contain large carbon reserves. In the aerobic phase, being able to multiply and oxidising stored carbon allows for storage of greater phosphate than was previously released, leading to a net removal of phosphate from the liquid phase (MPCA, 2006).

EBPR processes can achieve effluent P levels as low as 0.1 mg/L (Blackall *et al*., 2002) and the increasing use of anaerobic digestion in sludge management means that phosphorus eventually ends up in the nutrient rich digestate liquor with potential for P recovery through struvite precipitation (Pastor *et al*., 2008, Yuan *et al*., 2012). However, the reliability of EBPR processes can be a problem with disturbances such as increased rainfall, nutrient limitation or increased nutrient loading leading to process upsets (Oehmen *et al*, 2007). Additionally, microbial competition between PAOs and glycogen accumulating organisms (GAOs) has been shown to decrease P removal performance (Oehmen *et al*., 2007) and the need for anaerobic and aerobic zones means that aeration costs can be high. The provision for chemical P removal methods at most WWTW demonstrates that there are wide-spread problems with the performance of EBPR processes (Blackall *et al*., 2002).

1.3.4 Microalgal bioremediation of N, P and C

As a means to both meet tightening effluent discharge limits and recycle nitrogen and phosphorus, research into microalgal bioremediation of essential nutrients from wastewater

has increased significantly in recent years. The high nitrogen and phosphorus concentrations within microalgal cells (approximately 10 % and 1 % respectively) make them advantageous organisms for recycling N and P from waste streams (van Harmelen and Oonk, 2006). Nutrients can then be either extracted from algae or the algae can be used directly as an agricultural fertiliser. Unlike bacteria, microalgae do not require oxygen supplementation, and therefore allow for the potential removal of energy intensive aeration processes. The ability to assimilate large quantities of carbon dioxide and the potential for coupling microalgal cultivation with flue gas emissions or biogas upgrading, through removal of biogas CO_2 to increase methane percentage, make microalgae especially favourable for combined wastewater treatment and carbon dioxide sequestration (Park *et al*., 2011; Sivakumar *et al*., 2012; Xu *et al*., 2015).

The use of microalgae for nutrient bioremediation was initially proposed in the middle of the 20th century as a means to control unwanted growth through selective eutrophication in a controlled environment (Oswald and Golueke, 1966). Since then High Rate Algal Ponds (HRAPs) have been developed and are now operated for wastewater treatment in several countries including, but not limited to, the USA where they were developed, France, the United Kingdom and New Zealand (Young *et al*., 2017). High rate algal ponds are shallow ponds typically 0.2-1.0 m in depth, (Park *et al*., 2011) designed to optimise algal growth for the removal of nutrients. They typically follow a covered anaerobic pond designed for initial solids removal (Craggs *et al*., 2014).

There is a wealth of research reporting the efficiency of microalgae to remove essential nutrients (namely nitrogen and phosphorus) in both real and synthetic wastewaters from a wide variety of sources including municipal/industrial wastewater (Karemore *et al*., 2015; Yu *et al*., 2015), dairy wastewater (Asmare *et al*., 2014; Lu *et al*., 2015), cheese whey effluent (Tsolcha *et al*., 2015), swine wastewater (Zhang *et al*., 2014a), brewery wastewater (Lutzu *et al*., 2016) as well as from laboratory designed synthetic wastewaters (Mujtaba *et al*., 2015; Cho *et al*., 2016; Goncalves *et al*., 2014; Yulistyorini, 2016). Nutrient removal efficiencies are typically up to 100 % and 88 % for nitrogen and phosphorus removal respectively (Bhatt *et al*., 2014).

Emerging research in this area is investigating the use of microalgae for nutrient bioremediation from the liquid digestate formed during anaerobic digestion (AD) of primary and secondary sludge. AD has become a popular means of sludge management but the digestate produced is typically rich in nutrients and is often returned to the head of the wastewater treatment process where the high irregular nutrient loads increase treatment costs and can cause process upsets (Halfhide *et al*., 2015; Stiles *et al*., 2018). The high nutrient concentrations in digestate are proposed to increase biomass growth (Halfhide *et al*., 2015) and promising results have been reported (Morales-Amaral *et al*., 2015; Xu *et al*., 2015; Al Momani and Örmeci, 2016; Bohutskyi *et al*., 2016; Ramsundar *et al*., 2017). However, excessive ammonium

concentrations have been shown to hinder growth in some cases (Morales-Amaral *et al*., 2015b; Stiles *et al*., 2018) and dilution using effluent from other stages of the treatment process may be necessary (Arias *et al*., 2018).

In existing HRAPs, total nitrogen and phosphorus removal is currently comparable, if not better, than conventional WSPs (Craggs *et al*., 2014) with sunlight intensity and duration widely accepted to be the most important factors for efficient algal growth and subsequently for bioremediation (Samori *et al*., 2013; Craggs *et al*., 2014; Gonçalves *et al*., 2014; Zhang *et al*., 2015); bioremediation ability is, in general, proportional to biomass productivity. However, biological systems for nutrient removal are still heavily variable and season dependent and more research is needed to critically understand the effect of both physicochemical and nutritional conditions on algal bioremediation efficiency. The discovery that, like PAOs used in the EBPR process, microalgae can accumulate and store phosphorus, beyond the requirements for growth, as polyphosphate (Komine *et al*., 2000; Ruiz *et al*., 2001a; Powell *et al*., 2009), opens new avenues of research for improving phosphorus removal in HRAPs (see Section 1.4).

Furthermore, while HRAPSs were initially developed in the 1950s (Craggs *et al*., 2014), interest in using microalgae for wastewater treatment has been renewed recently due to the potential for biofuel production from the resultant microalgal biomass (Gupta and Bux, 2019). Microalgae are already a popular research topic for their potential to produce lipids as a biodiesel starting product. Combining wastewater treatment with microalgal cultivation has been identified as a promising means by which to make microalgal biodiesel economically feasible (see Section 1.2.1). In order to realise this, there is a need for research aimed at optimising lipid production in microalgae under conditions both replicable within a wastewater treatment works and which do not compromise the ability of the microalgae to perform their primary function of nutrient removal.

Research investigating the biofuel potential of microalgae when grown in wastewater has been conducted on a wide range of species and wastewaters. Similarly to nitrogen removal (see Section 1.5.2), studies have demonstrated that continued cultivation after the exhaustion of available nitrogen leads to increased lipid accumulation (Caporgno *et al*., 2015; Tsolcha *et al*., 2015; Lutzu *et al*., 2016). Further, recent research aimed at optimising the growth conditions for phosphorus and lipid accumulation are described in the following sections (see sections 1.4 and 1.5) however, the conditions needed for efficient biofuel production, in particular culture conditions such as pH or nutrient sources, are rarely reported in the context of wastewater with studies choosing instead to focus heavily on species or strain selection (Chinnasamy *et al*., 2010; Zhou *et al*., 2011; Abou-Shanab *et al*., 2013; Pachés *et al*., 2020) or simply measuring the

potential of a single microalgal strain in a single source of wastewater (Zheng *et al*., 2011; Chen *et al*., 2020) with little investigation into how or why the conditions are or are not successful.

There is a need for a much greater understanding of the effect of varying culture conditions on the biomass productivity, nutrient removal and biofuel potential of microalgae simultaneously. This knowledge would allow for informed decisions to be made about the feasibility of bioremediation by microalgae depending on the wastewater characteristics at various sources as well as the most profitable bioproducts (e.g. fertilisers, biodiesel etc.) which could be obtained.

1.4 Polyphosphate Accumulation in Microalgae

Under normal circumstances microalgal biomass contains approximately 1 % phosphorus by weight (Oswald, 1988; Stumm and Morgan, 1996; van Harmelen and Oonk, 2006). However, under certain circumstances, microalgae can be stimulated to accumulate phosphorus in excess of that needed for growth (up to 3 %), storing the additional phosphorus in inorganic polyphosphate granules (Komine *et al*., 2000; Ruiz *et al*., 2001a; Powell *et al*., 2009). Harnessing this ability could allow, not only for effective phosphorus removal from waste streams, but also a phosphorus rich biomass for phosphorus recycling into agricultural fertiliser.

Polyphosphate (polyP) (Figure 1.3) is a long-chain linear polymer comprised of tens or hundreds of phosphate residues (Pi) linked together by high-energy phospho-anhydride bonds similar to those in ATP (Gomez-Garcia and Kornberg, 2004; Rao *et al*., 2009). Phosphorus is essential in many processes necessary to sustain life, including nucleic acid and membrane synthesis and activity, and the regulation and modification of proteins, however the pathways of synthesis and degradation of polyphosphate are different between organisms. Additionally, phosphate serves signalling through amino acid phosphorylation and the regulation of gene expression and translation (Moseley *et al*., 2006; Freimoser *et al*., 2006 and sources therein; Hurlimann, 2007).

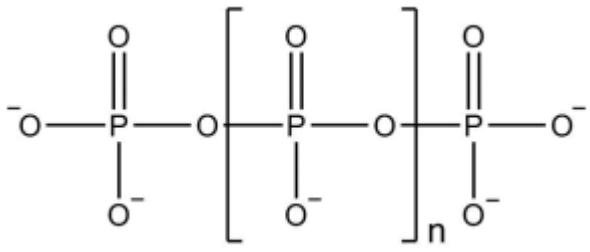

Figure 1.3 Inorganic polyphosphate. 'n' may take a range of values from tens to hundreds.

1.4.1 Polyphosphate metabolism

Microalgae are known to accumulate polyphosphate under two distinct conditions. The first, termed 'over-compensation' or 'phosphate overplus', requires a pre-starvation stage whereby cells are deprived of phosphate. Transferral to phosphate replete medium causes excessive phosphate accumulation and polyphosphate storage (Aitchison and Butt, 1973; Vagabov *et al*., 2008; Powell *et al*., 2009). The second condition, 'luxury uptake', occurs when cells are exposed to high concentrations of phosphorus (Powell *et al*., 2009). Luxury uptake is a more promising route for polyphosphate accumulation in wastewaters due to high phosphate concentrations present in waste streams and the costs and time associated with introducing a pre-starvation step, however the conditions which influence luxury uptake and its role in microalgae are less well understood.

Despite a basic understanding of the effect of phosphate availability on polyphosphate accumulation in microalgae, the mechanisms of its uptake and storage remain elusive. Almost all knowledge of polyP accumulation in microalgae comes from extrapolation from other, very different, microorganisms such as yeast and bacteria. A whole genome screen of non-essential knock out mutants in bakers' yeast (*Saccharomyces cerevisiae*) identified 255 mutants with altered polyP accumulation (Freimoser *et al*., 2006). The vast array of influential genes demonstrates the complexity of polyP metabolism and the sensitivity, highly intertwined with primary cellular metabolism, involved with maintaining normal polyP levels.

In bacteria, polyP is formed from ATP by polyphosphate kinase (PPK1) by transferral of the terminal ATP phosphoryl group to the growing polyP chain (Harold, 1966; Gerasimaitė *et al*., 2014). By reversing the process, ATP can be synthesised from ADP and polyP. PPK1 is not found in eukaryotes except *Dictyostelium discoidum* (slime mould) (Zhang *et al*., 2005) nor has any homologue of PPK1 been found in yeast (Ogawa *et al*., 2000). Breakdown of polyP in bacteria is catalysed primarily by the exopolyphosphatase PPX1 (Gerasimaite *et al*., 2014; Bolesch and Keasling, 2000).

In eukaryotes, polyP is stored in membrane-bound organelles, acidocalcisomes, which are also responsible for accumulating high concentrations of divalent cations including Ca^{2+}, Zn^{2+}, Mg^{2+} and Mn^{2+} (Gerasimaite *et al*., 2014). Initially, polyP synthesis is dependent upon the uptake of Pi into the cell from the surrounding media. Five phosphate transporters have been identified in the yeast *S.cerevisiae*, Pho84, Pho87, Pho89m Pho90 and Pho91, of which Pho84 is the most important; *S. cerevisiae* mutants deficient in all but Pho84 can accumulate polyP similarly to the wild-type (Hurlimann, 2007). The two high-affinity transporters, Pho84 and Pho85, are regulated by the *PHO* pathway (Hurlimann, 2007 and sources therein). The remaining three low-affinity

transporters have been shown to perform phosphate transport in the absence of high-affinity transporters but are primarily responsible for external phosphate sensing and regulation of the phosphate synthesis pathway (Hurlimann, 2007). Proteins housed within the Vacuolar Transport Chaperone (VTC) complex are then responsible for the synthesis of polyP (Ogawa *et al*., 2000; Hothorn *et al*., 2009).

Three enzymes responsible for polyP degradation have been identified in the yeast *S.cerevisiae*: a cytosolic exopolyphosphatase, Ppx1 (Wurst and Kornberg, 1994) and endopolyphosphatase, Ddp1 (Lonetti *et al*., 2011) and an acidocalsisome localised endopolyphosphatase, Ppn1 (Kumble and Kornberg, 1996; Sethuraman *et al*., 2001). Pho91 is proposed as a specific phosphate transporter responsible for exporting phosphate out of the acidocalsisome into the cytosol and deletion of Pho91 results in an increase in polyphosphate (Hurlimann, 2007).

Like yeast, microalgae have been shown to accumulate polyphosphate in granules resembling acidocalcisomes, with as many as 40 polyphosphate containing granules present at any one time (Komine *et al*., 2000; Ruiz *et al*., 2001a). Microalgae have also been shown to be dependent on VTC1 with mutants deficient in the gene exhibiting significantly reduced polyphosphate accumulation under normal conditions and a limited lifespan when deprived of phosphate (Aksoy *et al*., 2014). *Chlamydomonas* also contains a set of Pi transporters homologous to the high-affinity Pho84 and Pho89 transporters found in yeast known as the PTA and PTB transporters (Moseley *et al*., 2006). The demonstrated similarities suggest a similar polyphosphate accumulation pathway could operate in microalgae as that present in yeast.

There is a crucial difference however in the response to phosphate deficiency between microalgae and yeast. In contrast to yeast, the main regulator of phosphate deficiency in *Chlamydomonas reinhardtii* is the transcription factor PSR1 (Phosphorus Starvation Response 1) which when absent leads to defects in the phosphorus deprivation response within the cell (Wykoff *et al*., 1999). In the absence of PSR1, cells do not develop a high-affinity uptake system for Pi or excrete extracellular phosphatases and have a much lower survival rate under phosphorus deprivation, whereas overexpression of PSR1 leads to increased P accumulation under conditions of high and low phosphorus availability (Bajhaiya *et al*., 2016). PSR1 does not resemble any of the proteins found in yeast and is instead functionally homologous to the PHR1 regulon system in higher plants (Wykoff *et al*., 1999; Ogawa *et al*., 2000).

1.4.2 The role of polyphosphate and the conditions leading to its accumulation

The reason for phosphate over-accumulation is not fully understood, however understanding the roles of polyphosphate within microalgal cells will help to determine

potential environmental conditions for optimising polyphosphate accumulation. Similarly, understanding the environmental conditions that cause increased polyphosphate accumulation can shed light on its purpose within the cell.

Polyphosphate undoubtedly acts as an internal store of phosphate, with microalgae observed to rapidly mobilise stored polyphosphate during phosphate starvation (Harold, 1962; Miyachi *et al*., 1964; Vagabov *et al*., 2008; Powell *et al*., 2009). This likely explains polyphosphate 'over-compensation'.

Storage of phosphate as polyphosphate has also been proposed as a means of keeping Pi and H^+ levels stable within the cell (Harold *et al*., 1966) and reduce the osmotic stress caused by large pools of phosphate ions (Docampo and Moreno, 2001; Docampo *et al*., 2005). In epimastigotes of the protozoa *Trypanosoma cruzi*, hyper-osmotic and hypo-osmotic stress resulted in the respective increase and decrease in short and long chain polyphosphates with hypo-osmotic stress causing almost complete hydrolysis of long chain polyphosphates (Ruiz *et al*., 2001b). The link between the acidocalcisome and the contractile vacuole (responsible for water extrusion during hypo-osmotic stress) demonstrated in *C.reinhardtii* (Ruiz *et al*., 2001) is supportive of an osmotic homeostasis function of polyphosphate in microalgae.

In the yeast *Saccharomyces cerevisiae*, a shortening of polyphosphates has similarly been observed as a result of a sudden increase in media pH and subsequent intracellular alkalisation (Castro *et al*., 1995). Prolonged incubation resulted in neutralisation of internal pH and the recovery of central polyphosphate residues, indicating a restoration of long chain polyphosphates. Recovery of internal pH as a result of polyphosphate hydrolysis was later confirmed in *S.cerevisiae* (Castrol *et al*., 1999) demonstrating that polyphosphate plays a role in buffering intracellular pH in yeast.

Evidence suggests that alkaline growth media causes increased phosphate uptake in microalgae; polyphosphate was shown to accumulate in greater quantities in microalgae collected from a waste stabilisation pond when pH was allowed to rise naturally in contrast to buffered medium (Sells *et al*., 2018). By comparison with that shown in *S.cerevisiae*, the increase in polyphosphate in response to gradually increasing media pH may be so as to equip cells for the subsequent increase in internal pH. However, studies of this nature typically estimate algal phosphate concentration as that removed from the medium and rarely account for media phosphate lost through precipitation which significantly increases with increasing pH (Diamadopoulos and Benedek, 1984).

The homeostatic functions of polyphosphate may, at least in part, explain the 'luxury uptake' of phosphate.

Chlorella sp. (Zhu *et al*., 2015) and *Chlorella vulgaris* (Chu *et al*., 2015) have been demonstrated to accumulate additional polyphosphate when deprived of nitrogen, indicating that nitrogen stress may enhance polyphosphate accumulation in microalgae. A similar observation has been reported in *S.cerevisiae* where increased intracellular phosphate was observed when cells were starved of nitrogen (Breus *et al*., 2012) compared to the control (Kulakovskaya *et al*., 2005). The distinct functions of N and P within the cell limit the possibility that additional phosphate is accumulated to replace the lost nitrogen however. The similarity of the phospho-anhydride bonds in polyphosphate with those in ATP has led to the hypothesis that polyphosphate, like triacylglycerols, is accumulated as an energy store during nitrogen deprivation to be rapidly remobilised once favourable growth conditions are restored (Solovchenko *et al*., 2016).

A recent study demonstrated up to 4 % P by weight could be achieved in *C.reinhardtii* when grown in a mixed nitrogen source (1:1 NH_4:NO_3) (Yulistyorini, 2016). Cells were shown to preferentially accumulate ammonium before shifting to growth predominantly on nitrate, at which point phosphate levels within the cell were observed to increase rapidly. This is proposed to be due to the additional energy requirement for nitrate assimilation over ammonium resulting in a nitrogen stress response like that of nitrogen deprivation. An alternative hypothesis is that the presence of ammonium ions inhibits polyphosphate accumulation. In *S.cerevisiae*, addition of ammonium led to a reduction of long-chain polyphosphates (Greenfield *et al*., 1987) and this effect was most pronounced at pH 8.0 compared with pH 5-6 indicating that intracellular ammonia may play a role in polyphosphate hydrolysis.

Polyphosphate has additionally been shown to play a role in heavy metal tolerance in cells, with heavy metals typically reducing the accumulation of polyphosphate. Addition of cadmium to *Chlamydomonas acidophila* can result in almost complete loss of polyphosphate and an increase in vacuolar phosphate indicating that cadmium can induce polyphosphate hydrolysis (Nishikawa *et al*., 2003). Similar results have been shown for bacteria in the presence of cadmium, copper or zinc with a simultaneous increase in Pi export from the cell (Rachlin *et al*., 1984; Alvarez and Jerez, 2004). Additionally, at high concentrations cadmium and zinc can be incorporated into acidocalcisomes, replacing Mg^{2+} and Ca^{2+} ions in polyphosphate in some cases, indicating that the acidocalcisomes act as a storage pool for other elements (Rachlin *et al*., 1984; Ruiz *et al*., 2001). More recently, polyphosphate has been found in the cell walls of *C.reinhardtii* during cytokinesis and in new daughter cells proposed as a means by which to bind heavy metals and prevent them entering the cell before the cell wall has fully reformed (Werner *et al*., 2007).

Polyphosphate has also been shown in some cases to be influenced by light intensity, temperature and media phosphate concentration (Powell *et al*., 2008; Powell *et al*., 2009) although there is currently less understood about how and why these factors are influential.

In the context of wastewater treatment, the effect of pH and nitrogen availability/source could be particularly influential, with both varying substantially during conventional sewage treatment processes. In depth research into the effect of these conditions is necessary in order to identify the potential and possible inhibitory factors for microalgal phosphate recovery from wastewater.

1.5 Lipid Production and Optimisation in Microalgae

Lipids are a structurally diverse group of compounds containing a long tail (or fused ring in the case of steroids) and a head group and are typically defined as either polar or neutral (non-polar) depending on their nature. Polar lipids, such as phospholipids and galactolipids, act as major components of biological membranes creating cellular compartmentalisation (Buchannan *et al*., 2006; Campbell and Farrell, 2008; Li-Beisson *et al*., 2015). Neutral lipids, in particular triacylglycerols (TAGs), have gained attention owing to their high carbon content and suitability as a biodiesel starting product. TAGs comprise three fatty acid tail groups, most commonly 16 or 18 carbons in length, esterified to a single glycerol head group. They represent the most efficient form of energy and carbon storage within eukaryotic cells with an energy density twice that of starch or protein (Buchannan *et al*., 2006; Fan *et al*., 2011; Gonçalves *et al*., 2016).

Under suboptimal/stress conditions, microalgae have been shown to accumulate high quantities of TAGs within discrete oil bodies, lipid droplets, as an energy store to facilitate rapid cell recovery once adequate growth conditions are regained (Klok *et al*., 2014). The most well studied trigger of TAG accumulation is nitrogen starvation. Removal of available nitrogen causes rapid accumulation of TAGs which are subsequently degraded when nitrogen is resupplied (Siaut *et al*., 2011; Valledor *et al*., 2014; Schmollinger *et al*., 2014; Gonçalves *et al*., 2016). Once extracted, TAGs can be converted to biodiesel through a transesterification process in which TAGs and methanol are reacted in the presence of a catalyst to produce glycerol and biodiesel (methyl esters). The optimisation of TAG accumulation in microalgae is currently a popular and rapidly expanding field of research due to the potential for efficient biodiesel production (Gonçalves *et al*., 2016).

1.5.1 TAG metabolism

In green algae, *de novo* TAG synthesis begins in the chloroplast with acetyl-CoA conversion to malonyl-CoA catalysed by acetyl-CoA carboxylase (ACCase), the rate limiting

enzyme in TAG biosynthesis (Reverdatto *et al*., 1999; Gonçalves *et al*., 2016) (Figure 1.4). The malonyl group is then transferred to form malonyl-ACP (acyl carrier protein) catalysed by malonyl-CoA:ACP transacylase (MCT) (Klock *et al*., 2014). Fatty acid synthase then catalyses the continued reaction of acetyl-CoA with malonyl-ACP to elongate the acyl chains forming free fatty acids (FFAs) typically 16 or 18 carbons in length (Campbell and Farrell, 2008; Gonçalves *et al*., 2016).

Within the chloroplast, fatty acids can be used to acylate glycerol-3-phosphate (G3P) catalysed by resident acyl-transferases. The resultant phosphatidic acid (PA) is subsequently dephosphorylated by PA phosphatase (PAP) producing diacylglycerol (DAG). Within the chloroplast DAGs are primarily used as precursors to the structural membrane lipids of the photosynthetic apparatus (Fan *et al*., 2011 and sources therein; Klock *et al*., 2014; Gonçalves *et al*., 2016 and sources therein).

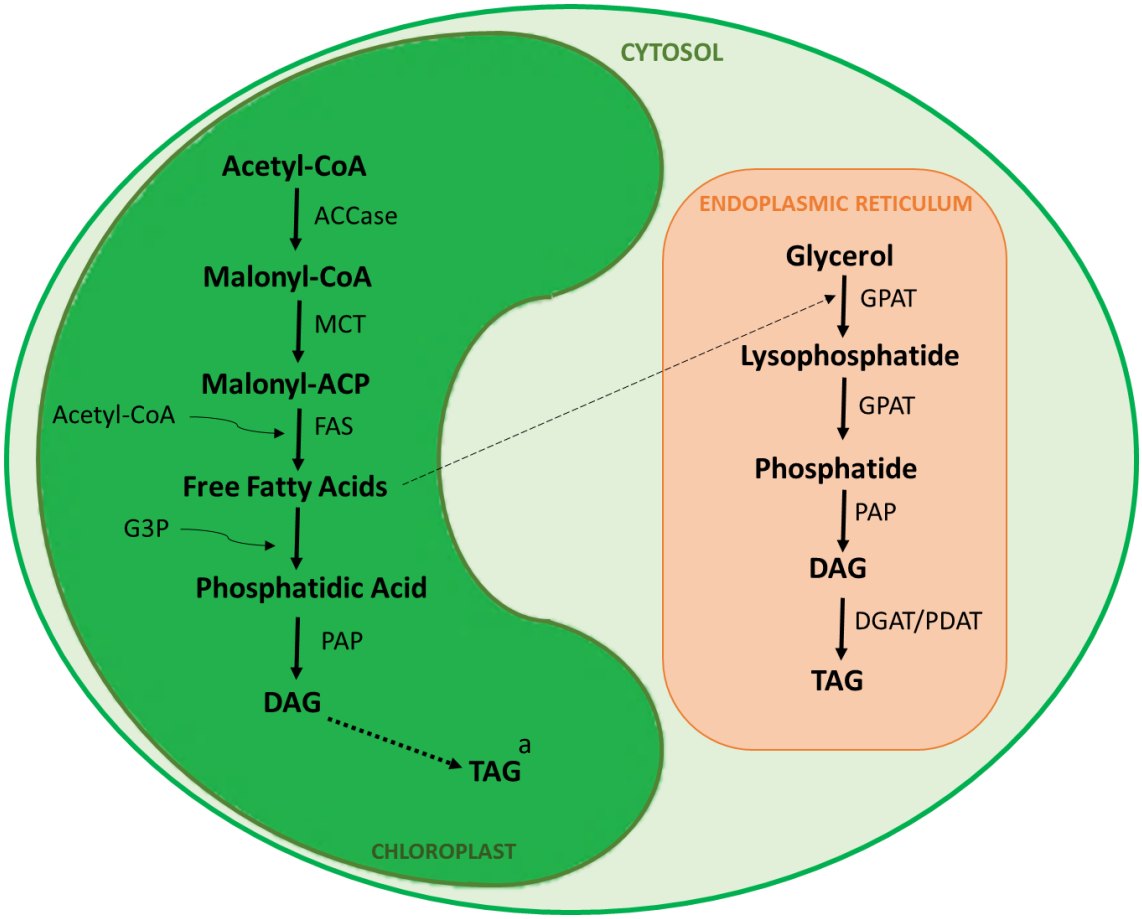

Figure 1.4 Synthesis of TAGs in microalgae. Free fatty acids (FFAs) are produced in the chloroplast by the continued reaction of acetyl-coA and malonyl-ACP. FFAs are converted to diacylglycerol (DAG) in the chloroplast or are exported to the endoplasmic reticulum where three fatty acid chains are bound to a glycerol head group to form TAG. ACCase = Acetyl-CoA carboxylase; MCT = Malonyl-CoA-ACP transacylase; FAS = Fatty acid synthase; G3P = Glycerol-3-phosphate; PAP = Phosphatidic acid phosphatase; GPAT = Glycerol-3-acetyltransferase; DGAT = Diacylglycerol acyltransferase; PDAT = Phospholipid diacylglycerol acyltransferase. [a]TAG production pathway from DAG within the chloroplast elucidated by Fan et al 2011.

Alternatively, FFAs can be exported to the endoplasmic reticulum (ER) where they are added to a glycerol head group to sequentially form lysophosphatide (LPA) and phosphatidate (PA) by glycerol-3-acyltransferase (GPAT) catalysed acylation at the sn-1 and sn-2 positions respectively. PA is subsequently dephosphorylated to produce DAG by removal of the sn-3 phosphate. TAG is formed by the final acylation of a free fatty acid or existing membrane fatty acid to the glycerol sn-3 position catalysed by diacylglycerol acyltransferase (DGAT) or phospholipid diacylglycerol acyltransferase (PDAT) respectively (Johnson and Alric, 2013; Goncalves *et al*., 2016).

Recently, a second TAG biosynthesis pathway was elucidated in which TAGs are synthesised directly from DAGs within the chloroplast, however the mechanism and enzymes are still unknown (Fan *et al*., 2011). The results indicate a preference for this novel chloroplast pathway under stress conditions, particularly nitrogen starvation, consistent with observed oil bodies in the chloroplast. This mechanism is further supported by the identification of additional plastid targeted acetyltransferases in microalgae (Vieler *et al*., 2012; Zienkiewicz *et al*., 2016).

Two families of diacylglycerol acyltransferase (DGAT) have been identified in *Chlamydomonas reinhardtii*, DGAT1 and DGAT2 (the latter consisting of five family members numbered 1-5). Under nitrogen sufficiency, transcriptional analysis revealed that mRNA levels of DGAT2-1 and DGAT2-5 are expressed highest of all DGATs. Similarly, under nitrogen deficiency DGAT2-1, DGAT2-5 and DGAT1 expression levels were the highest observed compared to transcripts of the remaining DGAT2 genes which were significantly decreased on nitrogen removal. The results suggest that DGAT2-1 and DGAT2-5 play dominant roles in TAG biosynthesis and, additionally DGAT1, in TAG accumulation (Deng *et al*., 2012). Overexpression of DGAT2-1 and DGAT2-5 successfully led to a 27.25 % and 48.25 % increase in lipid content respectively but interestingly, silencing DGAT2-2 increased lipid content by 24-34 % and silencing DGAT2-2 or DGAT2-3 had no observable effect on lipid content.

In an attempt to increase lipid content in *C.reinhardtii*, Zhu and co-workers expressed a PDAT from *S.cerevisae* in *Chlamydomonas reinhardtii* (Zhu *et al*., 2018). The *Chlamydomonas* mutant harbouring the ScPDAT demonstrated slower initial growth than wild-type *C.reinhardtii* however total fatty acid and TAG content were successfully increased by 22 % and 32 %, respectively.

A comprehensive review of lipid catabolism in microalgae, with a focus on *Chlamydomonas*, can be found in (Kong *et al*., 2018). In brief, fatty acids are first released from the glycerol head group by lipolysis catalysed by lipases within lipid droplets. Degradation of fatty acids to acetyl-CoA then occurs *via* the β-oxidation pathway. In plants, β-oxidation occurs

exclusively in the peroxisome (Poirier *et al*., 2006) and the recent localisation of an acyl-CoA oxidase within the peroxisomes ('microbodies') of *Chlamydomonas reinhardtii* provides conclusive evidence of a peroxisomal β-oxidation pathway in chlorophytes (Kong *et al*., 2017).

So far, of the enzymes responsible for lipid catabolism, only one DAG lipase, CrLIP1 (Li *et al*., 2012), one TAG lipase, CrLIP4 (Warakanont *et al*., 2019), and one acyl-oxidase, CrACX2, (catalysing the first step of the β-oxidation pathway) (Kong *et al*., 2017) have been identified in microalgae. The limited successes in upregulation of the TAG biosynthesis pathway for increased TAG accumulation, means that research surrounding the catabolism pathway is accelerating in the hope that its downregulation may improve oil yields in microalgae.

Use of an artificial micro-RNA to reduce CrLIP1 expression led to a delay in the remobilisation of TAGs on reintroduction of nitrogen (Li *et al*., 2012). 24 hours after N resupply, total TAG content per cell was significantly raised in CrLIP1 knockout mutants compared to empty vector controls, however TAG remobilisation was delayed rather than prevented with negligible TAG content measured after 110 hours in both the mutant and control samples. Similar results are observed in *C.reinhardtii* with reduced LIP4 transcription (Warakanont *et al*., 2019) and in the *cracx2* mutant (Kong *et al*., 2017), however growth was significantly restricted in *cracx2* mutants suggesting a need for efficient TAG remobilisation for sustained growth. No growth data is provided for either the *lip1* or *lip4* mutants.

A hypothesis for the limited success of genetic engineering attempts to increase lipid accumulation in microalgae centres on the competition for substrates (e.g. acyl-CoA) and carbon between pathways for TAG synthesis, cellular growth and other carbon rich storage products (Tan and Lee, 2016).

Citrate synthase (CIS) is a rate-limiting enzyme in the first step of the tricarboxylic acid (TCA) cycle (Deng *et al*., 2013) which releases stored chemical energy. Both the TCA and fatty-acid synthesis pathways are thought to compete for pyruvate, the end product of glycolysis. Artificial silencing of the CIS gene in *Chlamydomonas reinhardtii* (*CrCIS*) led to a 169.5 % increase in TAG content after six days cultivation in TAP media compared to the control and had no observable effect on the growth of the culture (Deng *et al*., 2013).

Arguably, the most successful attempt at genetic engineering to improve oil yields has been through downregulation of the starch accumulation pathway. In green microalgae, starch and lipid synthesis share many of the same precursors and as such their pathways are inseparably linked (Li *et al*., 2010a). Under most growth conditions, starch is shown to be the preferred storage product with TAG accumulation occurring significantly only when the carbon available is in excess of the demand for starch synthesis (Fan *et al*., 2012). The first committed

step in starch synthesis, converting ATP and glucose-1-phosphate to ADP-glucose and PPi, is catalysed by ADP-glucose pyrophosphorylase (AGPase). Silencing of the STA6 gene, encoding AGPase, (*C.reinhardtii* strain BAFJ5) leads to 2-10 times the TAG accumulation compared with the wild-type when subjected to nitrogen deprivation (Li *et al*., 2010a; Li *et al*., 2010b).

For a complete review of genetic engineering approaches in *Chlamydomonas reinhardtii* to increase oil content, readers are referred to the review paper by Kong *et al*., (2019).

1.5.2 TAG accumulation in response to nutritional stressors

Microalgae have been shown to accumulate large quantities of TAGs in response to nutritional stressors, the most well studied being nitrogen deprivation. Many studies have demonstrated a clear relationship between nitrogen deprivation and high TAG productivity in green microalgae with TAG accumulation increasing as the starvation period continues (Siaut *et al*., 2011; Valledor *et al*., 2014; Schmollinger *et al*., 2014). However, nitrogen starvation has been shown to cause complete cessation of cell division and a halt in biomass productivity within 24 hours of nitrogen removal, likely as a result of low nitrogen availability for protein and nucleotide biosynthesis (Siaut *et al*., 2011; Park *et al*., 2015).

Analysis of lipid composition during nitrogen starvation reveals a significant increase in saturated and mono-unsaturated lipids and a reduction in polyunsaturated lipids within the first 24 hours, indicating that large changes in lipid profile occur most rapidly at the onset of nitrogen starvation (Siaut *et al*., 2011). Transmission electron microscopy (TEM) imaging demonstrates a reduction of plastidial membranes and thylakoid membranes in nitrogen starved microalgae (Moellering and Benning, 2010; Siaut *et al*., 2011), including those of the chloroplast membrane. Nitrogen deprivation additionally leads to a reduction in the production of photosynthetic proteins together resulting in the breakdown of photosynthesis and an observable colour change from green to yellow (Gonçalves *et al*., 2016; Valledor *et al*., 2014).

Lipidomic analysis during nitrogen starvation has revealed upregulation of a lipase gene, proposed to be responsible for the breakdown of membrane lipids (Gargouri *et al*., 2015). Additionally, enzymes involved in the biosynthesis of diacylglyceryltrimethylhomoserine (DGTS), the main class of membrane lipids in *Chlamydomonas*, are shown to be downregulated within 24 hours of nitrogen starvation (Gargouri *et al*., 2015). Some part of the sudden TAG accumulation observed upon nitrogen starvation is widely believed to be due to the breakdown and recycling of membrane lipids into TAGs.

Upon reintroduction of nitrogen, photosynthesis and culture growth resumes rapidly (Gonçalves *et al*., 2016) with TAG content decreasing back to pre-starvation levels within 24

hours (Siaut *et al*., 2011; Valledor *et al*., 2014). As such, the rapid cellular rearrangement and accumulation of TAGs is proposed as a response designed to maximise carbon and energy storage in order to rapidly facilitate the regeneration of normal cell function upon the return of suitable growth conditions (Siaut *et al*., 2011; Schmollinger *et al*., 2014; Gonçalves *et al*., 2016).

Similarly to nitrogen starvation, phosphorus starvation has been proposed as a trigger of TAG accumulation, however the results are variable between species and as such there are disagreements about whether phosphorus starvation can be used reliably as a trigger of TAG accumulation. Studies have demonstrated an increase in TAG accumulation in species such as *Chlorella zofingiensis* (Feng *et al*., 2012) and *Nannochloropsis* sp. (Rodolfi *et al*., 2009) in response to phosphorus starvation while other studies in *Chlorella* (*pyrenidosa* and sp.) show no change in TAG content (Fan *et al*., 2014; Paveenkumar *et al*., 2012). Genomic analysis of *C.reinhardtii*, targeting the DGAT1, DGTT1 and PDAT1 acyltransferase genes, known to be upregulated during nitrogen starvation, revealed no change during phosphorus starvation (Boyle *et al*., 2012) suggesting that phosphorus starvation has little effect on TAG accumulation in *Chlamydomonas*.

In contrast, DGAT1 and PDAT1 in *C.reinhardtii* showed significant upregulation during iron deficiency (Boyle *et al*., 2012). Several studies have shown that iron deprivation, similarly to nitrogen deprivation, can trigger TAG accumulation significantly higher than that in control cultures (Liu and Wang, 2008; Fan *et al*., 2014; Urzika *et al*., 2013). There is some evidence to suggest that the reduction in biomass productivity is less severe than when starved of nitrogen (Fan *et al*., 2014) however, the TAG accumulation is similarly less significant and so it is difficult, at this stage, to determine whether iron stress leads to a net increase in TAG accumulation compared with nitrogen deficiency.

Nutrient availability is heavily dependent on the culture pH and the pH of wastewater can vary significantly due to diurnal variations imposed by microalgal growth; pH >10 is not uncommon in WWTW (Mara, 2003). Alkaline pH has been identified as a potential TAG accumulating stressor in some microalgae such as *Dunaliella* (Byrd and Burkholder, 2017), *Scenedesmus* (Gardner *et al*., 2013), *Phaeodactylum* (Mus *et al*., 2013) and *Chlorella* (Skrupski *et al*., 2013), however reports are often inconsistent and the majority of studies investigating pH struggle to limit the number of additional variables.

A study investigating the effect of pH on the growth rate and lipid production of *Chlorella pyrenoidosa* monitored the alga when grown in media with an initial pH ranging from 5.7-9.6 (Tan *et al*., 2016). Increasing the pH resulted in a decrease in growth rate but an increase in lipid content of approximately 45 % in cultures grown at pH 8.3 compared to the optimal pH

range for growth of 5.5-7.3, however there was an increase in the proportion of unsaturated fatty acids (particularly poly-unsaturated fatty acids, PUFA) which make the lipids less suitable for use as a biodiesel starting product (Ramos *et al*., 2009). The reduction in growth rate is proposed to be due to the increase in free ammonia (*pKa* NH_3-N = 9.3) which is toxic to algae beyond species specific concentrations; it is unclear how much the increased lipid content is due to the increased pH or the stress afforded by high concentrations of free ammonia.

In contrast Zhang and co-workers found no change in the growth of *Chlorella* sp. when grown in media of different starting pH (pH 5-11) and lipid accumulation was highest at pH 7, however no pH control was used and as such all cultures tended towards pH 6-8 within the timeframe of the experiment (Zhang *et al*., 2014b).

A common method of pH control is through the addition of bubbled CO_2 or sodium bicarbonate (Guihéneuf and Stengel, 2013; Posadas *et al*., 2015; Qiu *et al*., 2017) and there is a severe lack of research investigating the effect of pH performed in the absence of additional carbon sources. In particular, there are a significant number of studies linking bicarbonate addition to an increase in lipid accumulation (Guihéneuf and Stengel, 2013; Gardner *et al*., 2013), thus questioning whether increases in lipid content are as a result of increasing pH or simply the increased availability of carbon.

Furthermore, despite being one of the most widely studied species and a model organism, there is minimal research on the effect of pH in *Chlamydomonas*. A search for "Chlamydomonas" AND "pH" AND "Lipid" yielded only 65 hits in the Web of Science database (as of 13.03.2020) and only one of these reports were found to be relevant but used an additional carbon source, acetic acid, to mediate pH (Ochoa-Alfaro *et al*., 2019). The study found that of the three pH values tested (7.0, 7.8 and 8.5), pH 7.8 resulted in biomass with the highest lipid accumulation followed by pH 8.5, however cultures at pH 8.5 grew minimally. The increase in lipid content with increasing pH, despite the reduced acetic acid concentration, suggests that the relationship between pH and lipid accumulation is not as simple as an increase in carbon availability from carbon mediated pH control measures.

One study, using a mixed microalgal culture collected from a local lake, aimed to isolate the effects of pH, salinity and carbon supplementation on lipid accumulation by use of an orthogonal design (Chiranjeevi and Mohan, 2016). Specific quantitative data describing the effect of pH is hard to extract, however comparing all pH values and lipid contents reveals that, of the parameters tested, pH had the largest effect on total lipid content but no significant effect on neutral lipid (TAG) accumulation. Of the values tested (pH 4-10), pH 6 resulted in the highest total lipid content while pH 8 showed marginally higher neutral lipid content.

A report found to test of the effect of pH in the absence of other variables, using only a range of buffers for pH control and nitrate as the sole nitrogen source, demonstrated increased TAG accumulation in *Scenedesmus* sp. and *Coelastrella* sp. in response to increased pH (pH >9.4 compared to pH 7.5) (Gardner *et al*., 2012). Furthermore, unbuffered cultures which reached the highest final pH of 11.1 yielded the highest TAG accumulation suggesting a direct correlation between pH and TAG accumulation. The result of this study does suggest that pH may have a role in increasing useful lipid content for the production of biofuels, however much more research is needed to understand the effect of varying pH on lipid productivity given the highly variable pH of microalgal cultures within WWTW.

In addition, a range of physicochemical factors have been shown to influence TAG accumulation in microalgae including light intensity, photoperiod and temperature. These factors are beyond the scope of this project but have been comprehensively reviewed in the following reports (Ferreira and Sant'Anna, 2017; Morales *et al*., 2018).

1.5.3 TAG accumulation in response to chemical triggers

To circumvent the reduced biomass yields, and therefore reduced overall lipid yields, as a result of nutrient starvation, the use of chemical triggers is under investigation as a potential means to induce increased TAG accumulation whilst maintaining enough nutrients for efficient biomass production.

The drug Brefeldin A (BFA) is a known inhibitor of vesicular transport out of the endoplasmic reticulum. Investigations into the effect of BFA on *C.reinhardtii* have demonstrated that BFA can act as both a trigger for TAG accumulation and a suppressor of TAG mobilisation after nitrogen resupply following a dose dependent response (Kim *et al*., 2013; Kato *et al*., 2013). Addition of 2.5 µM BFA on nitrogen resupply to cells cultured in TAP-N for 24 hours led to 76 % Nile-red fluorescence retention after 16 hours compared to only 10 % retention in the control indicating that BFA can supress TAG remobilisation (Kato *et al*., 2013). Similarly, addition of 75 µg/mL (0.27 mM) BFA to mid-log phase cells under normal growth conditions resulted in an increase in Nile-red fluorescence intensity nearly four-fold within 15 hours of BFA addition compared to the control, with only limited retardation of biomass productivity (Kim *et al*., 2013) demonstrating the ability of BFA to induce TAG accumulation.

The effect of BFA on biomass productivity is however contradicted by a similar study which demonstrated that addition of 2.5 µM BFA led to a 50 % increase in Nile-red fluorescence but growth rate reduced similarly to that shown under nitrogen deprivation (Kato *et al*., 2013).

Of the chemical triggers investigated, BFA is still the most studied for inducing TAG accumulation in *C.reinhardtii*. In 2015, a high-throughput screen tested 1717 chemical compounds from the National Cancer Institute for their potential to induce growth or lipid accumulation in *Chlamydomonas reinhardtii*. Of the compounds tested, the drug Brefeldin A (BFA) was shown to be the most successful inducer of lipid accumulation with nearly 10 times the TAG accumulation when grown in the presence of 10 µM BFA compared to the control (Wase *et al*., 2015). Of the remaining tested compounds only six others were shown to cause increased TAG accumulation without severe retardation of growth but each presented TAG accumulation of less than one third that of BFA.

An exciting study revealed the potential of the fungicide fenpropimorph for improving lipid quality for biofuels in *Chlamydomonas reinhardtii* (Kim *et al*., 2015). Fenpropimorph inhibits reduction and isomerisation in the sterol biosynthetic pathway effectively inhibiting sterol biosynthesis; altering sterol levels has been shown to affect both the sterol and fatty acid metabolism in animal and fungal cells. Treatment of late log-phase *C.reinhardtii* with 10 µM fenpropimorph led to a four-fold increase in the quantity of TAGs compared to the control. Furthermore, the quantity of TAGs measured was two-fold higher than that in cultures without acetate starved of nitrogen for 9 days indicating that fenpropimorph is a more potent trigger of TAG accumulation than nitrogen starvation. Treatment with fenpropimorph did lead to rapid cell death and analysis revealed that the majority of TAGs accumulated on treatment were derived from chloroplast membrane lipids (Kim *et al*., 2015). However, the fast action of fenpropimorph at inducing conversion of polar membrane lipids into TAGs suggests it may be used for a late improvement of lipid quality for biofuel production.

Brown and co-workers identified that the small molecule, diphenyl methylphosphonate (DMP) can block breakdown of existing oil bodies in seedlings of the terrestrial plant *Arabidopsis thaliana* (Brown *et al*., 2013). When grown on agar containing 25 µM DMP, seedlings retained 64 % of dry seed TAGs after 5 days compared with only 7 % in the control. DMP addition resulted in clustering of peroxisomes around spherical oil bodies in hypocotyl cells. Neither germination nor any other organelles were affected, however growth was significantly reduced in DMP treated seedlings with seedlings noticeably stunted and pale compared to the control. Comparison with known *Arabidopsis* oil catabolism mutants indicated that DMP inhibits an early step in the fatty acid β-oxidation spiral. DMP failed to induce TAG accumulation in seedlings with little initial TAGs indicating that DMP has a role in supressing TAG catabolism but cannot induce TAG synthesis.

From our limited knowledge of TAG degradation in microalgae, the mechanisms are expected to be conserved between microalgae and higher plants (Li-Biesson *et al*., 2015). It is

therefore likely that DMP will play a similar role in suppression of TAG catabolism in microalgae although this hypothesis is yet to be tested. The study of Brown and co-workers is the first reported example of DMP as an inhibitor of TAG catabolism.

1.6 Project Rationale

1.6.1 Research Gap

The use of microalgae for wastewater treatment (i.e. nutrient removal) has gained renewed attention stimulated by the potential for microalgae to be used additionally as a source of biofuels and as a means to recycle nutrients. Indeed, combining microalgal cultivation with wastewater treatment, to provide a free source of water and essential nutrients, has been suggested as a necessary step to make microalgal biodiesel economically feasible. The question stands therefore: can we use HRAPs to produce microalgae of sufficient quality for biodiesel production without limiting their ability for nutrient removal?

In order for the potential of microalgae for simultaneous wastewater treatment, nutrient recovery and biofuel production to be realised, there is a need for a much more critical understanding of the effect of wastewater culture conditions on lipid production in microalgae. With microalgal growth favoured by high nutrient concentrations and lipid production (for conversion into biodiesel) favoured by stress conditions (e.g. nitrogen starvation) there is undoubtedly a compromise to be had between biomass density, bioremediation efficiency and biofuel potential.

To date, the majority of research investigating microalgal bioremediation or lipid accumulation focus either on strategies that are unfeasible within a wastewater treatment works (e.g. nitrogen starvation or the use of genetically modified strains) or simply assess the nutrient removal ability or lipid production in microalgae in a particular wastewater without considering the specific cultivation conditions (e.g. wastewater composition) which may have led to the result.

In particular, the effect of some factors, such as pH, which vary significantly within a WWTW, on bioremediation efficiency and lipid accumulation are woefully understudied; no studies were found documenting the direct effect of pH on TAG accumulation in *Chlamydomonas* despite it being widely regarded as a model organism for a variety of research topics including algal metabolism and the production of valuable bioproducts (see Section 1.2.3).

This project therefore takes a different approach. Rather than targeting strategies to optimise the bioremediation efficiency and lipid accumulation in microalgae, the bulk of this project focusses on identifying crucial variables within a WWTW, with a focus on nutritional

rather than physicochemical factors (i.e. nutrient concentration, pH and nitrogen source), and aims to identify the effect of each of these conditions on simultaneous nutrient recovery and lipid accumulation. With factors such as nitrogen source and pH varying significantly depending on the treatment stage within a WWTW, an understanding of the significance of these conditions will allow for informed decisions to be made about both the feasibility of HRAPs for combined nutrient recovery and biodiesel production and the most strategic stage of WWT to utilise for microalgal cultivation.

1.6.2 Project Aim and Objectives

The **overall aim** of this project is to understand how the conditions present within a wastewater treatment works can affect the growth, nutrient uptake and lipid accumulation of microalgae for combined nutrient recycling and biodiesel production from sewage. The project focusses on the model organism *Chlamydomonas reinhardtii*. The objectives designed to accomplish this aim are as follows:

Objective one is to develop a method to facilitate the robust monitoring of algal growth in small cultures. Current methods for monitoring algal growth require large sample volumes and in many cases are sample destructive. As such, the number of experiments that can be run in parallel is often severely space limited owing to the need for relatively large algal cultures. By developing a method that is robust for small cultures (< 5 mL), several experiments can be run in parallel thus allowing for rapid investigation of a much wider range of conditions. This objective is addressed in Chapter 3.

Starting with a synthetic wastewater, **objective two** is to identify potential conditions present within wastewater that could be significant for achieving combined nutrient removal and biofuel production from microalgae grown within a sewage treatment plant. This objective is addressed in Chapter 4.

Objective three takes these conditions and tests them in isolation in order to identify their effect on microalgal growth, nutrient uptake (nitrogen and phosphorus) and biofuel potential *via* accumulation of lipids for the production of biodiesel. The main focus is on the effect of pH (with and without bicarbonate addition) and the effect of inorganic nitrogen source. This objective is addressed in Chapters 4 and 5.

Finally, **objective four** looks at the effect of the chemical diphenyl methylphosphonate (DMP), previously shown to inhibit lipid catabolism in *Arabidopsis thaliana*, on lipid catabolism in *Chlamydomonas reinhardtii*. While genetic upregulation of lipid biosynthesis has had limited success in improving oil yields, an emerging area of research is focussed instead on

downregulation of lipid catabolism. We look at its effect both on lipid catabolism and biomass potential and therefore the potential of chemical lipid catabolism inhibitors or lipid catabolism mutants to improve biodiesel yields from microalgae. This objective is addressed in Chapter 6.

Chapter Two – Materials and Methods

This chapter describes the materials and methods used to cultivate *Chlamydomonas reinhardtii* under different culture conditions and monitor the growth, nutrient uptake and lipid content of the resulting biomass. The chapter is split into five main sections: (i) the choice of *Chlamydomonas reinhardtii* strains and growth media; (ii) the cultivation conditions and sample collection protocol for time-course studies; (iii) methods used to monitor biomass growth during cultivation; (iv) methods for the analysis of growth media and; (v) methods for the analysis of the collected biomass.

2.1 *Chlamydomonas reinhardtii* Strains

Chlamydomonas reinhardtii strains were purchased from the Chlamydomonas Resource Center, University of Minnesota, USA (https://www.chlamycollection.org/). Three strains of *C.reinhardtii* were chosen for initial investigation and are detailed in Table 2.1.

Table 2.1 Strains of C.reinhardtii used for investigation throughout this project.

Strain	Phenotype	Description
CC-1690 (*wt, mt+*)	'Wild-type'	Also known as 21 gr. This is a basic wild-type strain from the lab of Ruth Sagar. The NIT1 and NIT2 loci harbour wild-type alleles and strain CC-1690 can therefore grow on either ammonium or nitrate.
CC-125 (*wt, mt+)*	'Wild-type'	Basic "137" wild-type strain. CC-125 carries the *nit1* and *nit2* mutations and therefore cannot grow solely on nitrate as the available nitrogen source.
CC-400 (*cw15, mt+*)	Wall deficient	This strain contains the cell-wall deficient mutation and is the most widely used of the cell-wall deficient mutants.

Further information on the origin of standard laboratory strains of *C.reinhardtii* can be found in the following publication (Pröschold *et al*., 2005).

2.2 Growth Media

Throughout this project, algal cultivation was in one of the following growth media or modifications thereof. All media were made in deionised water (dH_2O) and sterilised by autoclaving at 121°C for a minimum of 20 minutes prior to use.

2.2.1 Tris-Acetate Phosphate (TAP) Media

Tris-Acetate Phosphate (TAP) media was made according to the recipe of the Chlamydomonas Resource Center (The Chlamydomonas Resource Center,b) and is considered

the standard growth media for the cultivation of *Chlamydomonas*. The recipe is given in Tables 2.2 and 2.3.

Table 2.2 Stock solution recipe for Tris-Acetate-Phosphate (TAP) medium

Pre-stock 1	EDTA-Na_2 (125 mM)	- 13.959 g EDTA-Na_2 in approx. 250 ml dH_2O - Make to pH 8.0 using KOH (approx. 1.7 g; trace element grade) - Fill to 300 ml total with dH_2O
Pre-stock 2	$(NH_4)_6Mo_7O_{24}$ (285 µM)	- 0.088 g $(NH_4)_6Mo_7O_{24}.4H_2O$ in dH_2O
Trace Element 1 (TE1)	EDTA-Na_2 (25 mM)	- 50 ml Pre1 made up to 250 ml with dH_2O
Trace Element 2 (TE2)	$(NH_4)_6Mo_7O_{24}$ (28.5 µM)	- 25 ml Pre2 made up to 250 ml with dH_2O
Trace Element 3 (TE3)	Zn.EDTA (2.5 mM)	- 0.18 g $ZnSO_4.7H_2O$ - 5.5 ml Pre1 - Make up to 250 ml with dH_2O
Trace Element 4 (TE4)	Mn.EDTA (6 mM)	- 0.297 g $MnCl_2.4H_2O$ - 12 ml Pre1 - Make up to 250 ml with dH_2O
Trace Element 5 (TE5)	Fe.EDTA (20 mM)	- 2.05 g EDTA-Na_2 - 0.58 g Na_2CO_3 - Dissolve in approx. 150 ml dH_2O - 1.35 g $FeCl_3.6H_2O$ - Make up to 250 ml with dH_2O
Trace Element 6 (TE6)	Cu.EDTA (2 mM)	- 0.085 g $CuCl_2.2H_2O$ - 4 ml Pre1 - Make up to 250 ml with dH_2O
Phos	Phosphate Buffer II	- 10.8 g K_2HPO_4 - 5.6 g KH_2PO_4 - Make up to 100 ml with dH_2O
A	Solution A	- 20 g NH_4Cl - 5 g $MgSO_4.7H_2O$ - 2.5 g $CaCl_2.2H_2O$ - Make up to 500 ml with dH_2O
Tris	Tris base – Trizma (1 M)	- 60.57 g Trizma - Make up to 500 ml with dH_2O

Table 2.3 Final TAP medium composition

TAP Media (pH 7.0)	- Add the following solutions to approx. 750 ml dH_2O - 20 ml Tris - 1.0 ml Phos - 10.0 ml A - 1.0 ml TE1 - 1.0 ml TE2 - 1.0 ml TE3 - 1.0 ml TE4 - 1.0 ml TE5 - 1.0 ml TE6 - 1.0 ml Glacial Acetic Acid - Adjust to pH 7.0 using HCl/KOH - Make up to 1 L with dH_2O

2.2.1.1 Modifications to TAP medium

To test the effect of varying culture conditions, modifications were made to TAP medium as detailed in Table 2.4.

Table 2.4 Modifications to standard TAP medium used in Chapters 4 and 5 to test the effect of differing culture conditions.

Media	Modification
TAP –N	TAP omitting NH_4Cl
TA-	Pi omitted and replaced with 1.5 mM KCl
TAP (NO_3)	NH_4Cl omitted and replaced with 7.5 mM $NaNO_3$
CAP (NH_4) High pH	Tris base replaced with 10 mM CAPS buffer and the pH set to 9.55 with 1 M KOH
CAP (NH_4) High pH + Bicarbonate	Tris base replaced with 10 mM CAPS buffer and 3.32 mM $NaHCO_3$ added. The pH set to 9.55 with 1 M KOH
CAP (NO_3) High pH	NH_4Cl replaced with 7.5 mM $NaNO_3$. Tris base replaced with 10 mM CAPS buffer and the pH set to 9.55 with 1 M KOH
CAP (NO_3) High pH + Bicarbonate	NH_4Cl replaced with 7.5 mM $NaNO_3$. Tris base replaced with 10 mM CAPS buffer and 3.32 mM $NaHCO_3$ added. The pH set to 9.55 with 1 M KOH
TAP with varying ammonium:nitrate ratio	NH_4Cl replaced with a total molar concentration of 3.25 mM NH_4Cl + $NaNO_3$ in the following ratios 100:0, 75:25, 50:50, 25:75 and 0:100

2.2.2 Bold's Basal Media (BBM) and Synthetic Wastewater (SWW)

Synthetic wastewater (SWW) was made according to the recipe reported by Yulistyorini (2016) (PhD thesis, University of Leeds, 2016). The recipe is based on Bold's Basal Media (BBM) for freshwater algae (recipe according to the Culture Collection of Algae and Protozoa, CCAP,

available at https://www.ccap.ac.uk/media/documents/BB.pdf) with modified nutrient concentrations. Carbon, nitrate and phosphate concentrations have been adapted to represent those present in wastewater samples taken from Esholt Wastewater Treatment Works, Bradford, UK. Recipes for both BBM and SWW are given in Table 2.5.

Table 2.5 Media recipe for Bold's Basal Medium (BBM) and a synthetic wastewater (SWW).

Stock	Composition	BBM (mL stock per L media)	SWW (mL stock per L media)
1	-25 g/L $NaNO_3$	10	6.1
2	-7.5 g/L $MgSO_4.7H_2O$	10	10
3	-2.5 g/L NaCl	10	10
4	-7.5 g/L K_2HPO_4	10	11.2
5	-17.5 g/L KH_2PO_4	10	-
6	-2.5 g/L $CaCl_2.2H_2O$	10	10
7	Trace Elements Solution -8.82 g/L $ZnSO_47H_2O$ -1.44 g/L $MnCl_2.4H2O$ -0.71 g/L MoO_3 -1.57 g/L $CuSO_4.5H2O$ -0.49 g/L $Co(NO_3)_2.6H_2O$	1	1
8	-11.42 g/L H_3BO_3	1	1
9	-50 g/L EDTA -31 g/L KOH	1	1
10	-4.98 g/L $FeSO_4.7H_2O$ -1mL/L H_2SO_4	1	1
Ammonium Acetate	-25 g/L $C_2H_3O_2NH_4$	-	5.5
Sodium Acetate	-25 g/L $C_2H_3NaO_2.3H_2O$	-	13.6
Sodium Bicarbonate	-45 g/L $NaHCO_3$	-	62

Once autoclaved the final media have an approximate pH of 6.8 and 9.1 for BBM and SWW respectively.

Table 2.6 gives the initial nutrient concentrations of carbon, nitrogen and phosphorus and the initial pH of each of the media preparations used.

Table 2.6 Nutrient concentrations (N, P and C) and initial pH of media preparations used within this project.

	Nitrogen as NH_4/NO_3 (mg/L)	Phosphorus as PO_4 (mg/L)	Carbon organic (mg/L)	Carbon inorganic (mg/L)	Initial pH
BBM	0/41	53	0	0	6.7
SWW	25/25	15	100	400	9.1
TAP	105/0	32	420	0.3	7.0
TAP –N	0/0	32	420	0.3	7.0
TA-	105/0	0	420	0.3	7.0
TAP (NO_3)	0/105	32	420	0.3	7.0
CAP (NH_4) High pH	105/0	32	420	0.3	9.5
CAP (NH_4) High pH + Bicarbonate	105/0	32	420	400	9.5
CAP (NO_3) High pH	0/105	32	420	0.3	9.5
CAP (NO_3) High pH + Bicarbonate	0/105	32	420	400	9.5
TAP with varying ammonium:nitrate ratio					
100:0	50/0	32	420	0.3	7.0
75:25	37.5/12.5	32	420	0.3	7.0
50:50	25/25	32	420	0.3	7.0
25:75	12.5/37.5	32	420	0.3	7.0
0:100	0/50	32	420	0.3	7.0

2.2.3 Preparation of DMP containing media

A stock solution of Diphenyl methylphosphonate (DMP) (TCI Europe nv Zwijndrecht, Belgium) was made up in DMSO (dimethyl sulfoxide) to 100 mM. The required volume of DMP stock solution was added to TAP medium (after autoclaving) and DMSO added, where necessary, to a final concentration of 0.1 % (v/v). Control cultures contained 0.1 % (v/v) DMSO in TAP medium only.

2.3 Long-term Storage of *Chlamydomonas*

Chlamydomonas reinhardtii strains were stored on sterile agar-slopes for up to three months. Agar slopes were made by adding 15 g/L agar to TAP medium before autoclaving. The agar-medium (approx. 15 mL) was poured into 30 mL flasks and allowed to set at an angle by resting the flask on its side with the open end slightly elevated. Approximately 10 µL of liquid

culture was spread onto each slope using a 10 µL inoculating loop and the slope was stored at 20°C (approx. 50 µE light, 16 hr photoperiod) for two weeks to allow the culture to grow before being moved to a laboratory bench for long-term storage. Strains were transferred to fresh slopes approximately every three months by resuspending cells in fresh TAP medium using an inoculating loop, allowing the culture to grow for 2-3 days, and respreading on fresh slopes.

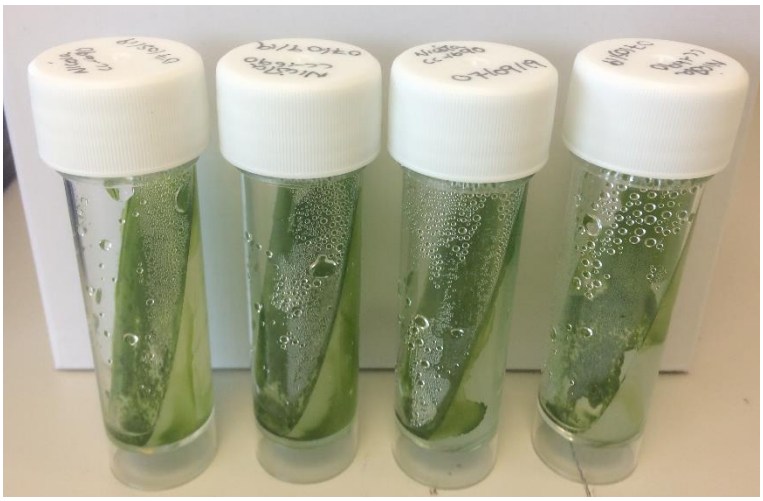

Figure 2.1 Agar slopes used for long-term storage of C.reinhardtii strains.

2.4 Microalgae Cultivation

All work with algal cells was conducted in a Class II laminar flow hood in order to maintain sterile conditions. All culture flasks were either sterile upon arrival (Bijou flasks) or autoclaved prior to use (121°C, 20 minutes).

2.4.1 Starter cultures

Starter cultures were made by scraping cells from an agar-slope onto an inoculating loop and resuspending them in 5 mL TAP media (unless otherwise stated) contained within sealed 7 mL Bijou flasks. The starter cultures were left to grow under controlled conditions (20°C, approx. 50 µE light, 16 hr photoperiod) without shaking for 2-7 days or until there was sufficient biomass for inoculation into culture vessels ($OD_{750} \simeq$ 1.0-2.5).

2.4.2 Cultivation for time-course analysis

The majority of experiments in this project are run as time-course studies monitoring the growth of an algal culture and media properties at time points for the duration of growth (growth curves) under different environmental conditions.

Unless otherwise stated, cultures were inoculated from liquid starter culture to an optical density (OD_{750}) of 0.005 in 125 mL media contained within 250 mL conical flasks and grown to stationary phase. The inoculation volume of starter culture was calculated from the

optical density of the starter culture immediately prior to inoculation. Conical flasks were fitted with a foam bung and the top covered with foil prior to autoclaving to allow gas transfer whilst maintaining sterile conditions. Cultures were grown within the Photon Systems Instruments (PSI) AlgaeTron AG 230 fitted with a shaking platform (PSI SHK-2013) (25°C, 150 rpm, 100 µE light, 24 hr photoperiod).

Samples were taken daily for analysis according to the protocol described in Figure 2.2 and Table 2.7.

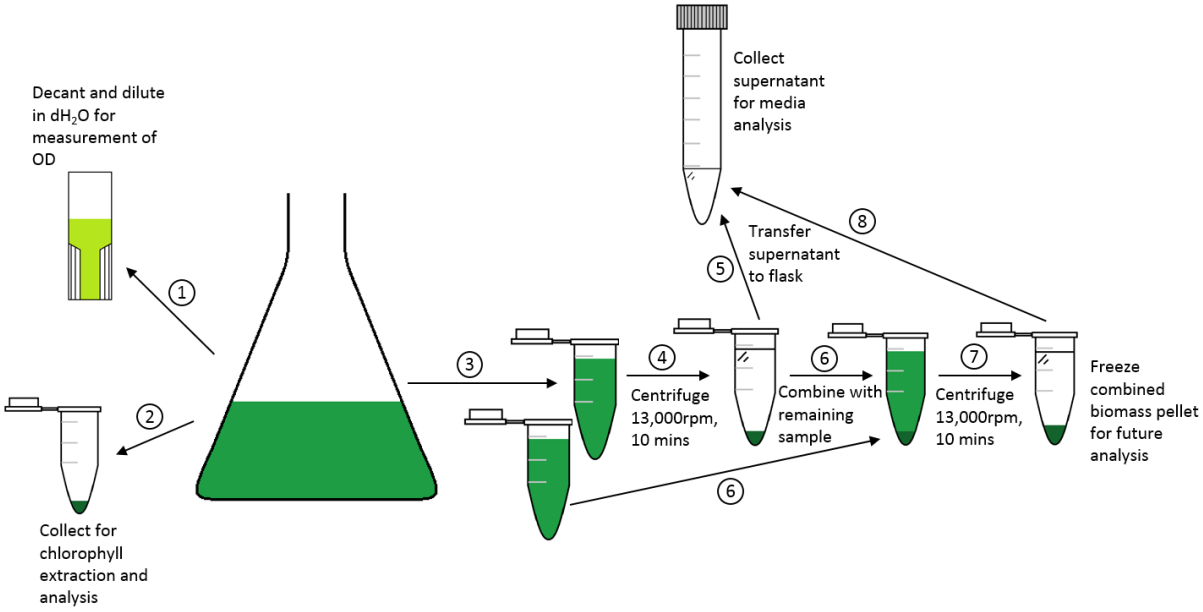

Figure 2.2 Sample collection protocol for collection of samples for optical denisty, chlorophyll, biomass and media analysis from time-course studies.

Table 2.7 General day-by-day protocol for collection and analysis of samples during time-course analysis (growth curves) of microalgal cultures.

Day	Protocol
0	**1. Take one sample per culture for optical density analysis into 1.5 mL cuvettes (up to 1mL sample) and make up to 1mL with dH_2O[a,b]** **2. Take approx. 10 mL fresh media into a 15 mL falcon tube** 3. Measure optical density of samples in cuvettes at 750 nm (see Section 2.5.1) 4. Measure pH of media in falcon tube **5. Filter pH sample through a 0.22 µm syringe filter into a new sterile 15 mL falcon tube and store at -20°C for media nutrient analysis**
1	**1. Take one sample per culture for optical density analysis into 1.5 mL cuvettes (up to 1mL sample) and make up to 1mL with dH_2O** **2. Take 3 mL of each culture into individual 15 mL falcon tubes** 3. Measure optical density of samples in cuvettes at 750 nm 4. Measure pH of samples in falcon tubes 5. **Filter pH samples through a 0.22 µm syringe filter into new sterile 15 mL falcon tubes and store at -20°C for media nutrient analysis**

2 - end	1. Label one 1.5 mL Eppendorf tube per culture (culture and date) and pre-weigh using a four decimal place balance **2. Take one sample per culture for optical density analysis into 1.5 mL cuvettes (up to 1mL sample) and make up to 1mL with dH_2O** **3. Take 2 x 1.5 mL aliquots of each culture into 1.5 mL Eppendorf tubes (for pH analysis and biomass collection). One of each aliquot should be placed in the pre-weighed tube**[c] **4. Take one sample per culture for chlorophyll analysis (100-500 µL) into a 1.5 mL Eppendorf tube**[b,c] 5. Measure optical density of samples in cuvettes at 750 nm 6. Measure chlorophyll content of chlorophyll samples (see Section 2.5.2). After initial pelleting step, decant supernatant into a falcon tube to be used for pH analysis 7. Pellet biomass in the pre-weighed Eppendorf tube (10 minutes, 13,000 rpm, approx. 16,000 g) 8. Decant supernatant into a falcon tube to combine with chlorophyll supernatant 9. Combine remaining culture aliquot with pellet and repeat steps 7 and 8 10. Wash final pellet twice with deionised water, resuspending the sample and pelleting each time as above. Store the final combined pellet at -70°C for future analysis 11. Measure pH of the combined supernatant sample **12. Filter pH sample through a 0.22 µm syringe filter into new sterile 15 mL falcon tubes and store at -20°C for media nutrient analysis**

[a] *Steps in bold indicate steps conducted under sterile conditions (class II laminar flow hood)*
[b] *For optical density and chlorophyll analysis, sample sizes were chosen to maintain a final absorbance of 0.4 and 1.0 respectively*
[c] *Collection of biomass samples and chlorophyll quantification were not conducted prior to Day 2 owing to the low density of cultures on Day 0 and Day 1*

On the final day of cultivation an aliquot of sample was taken from the final culture for observation of neutral lipid bodies by Nile-red fluorescence staining (see Section 2.5.4). All remaining biomass was harvested in 50 mL falcon tubes by centrifuging (4,500 rpm, 3,893 x g, 10 minutes) and washing twice in deionised water before storing at -70°C until required for analysis.

2.4.3 Media exchange

In some cases, the culture medium was changed part way through the experiment to observe the effects of particular culture conditions.

The culture media was exchanged by first harvesting the biomass by centrifugation in 50 mL falcon tubes (6,000 rpm, 2,540 x g, 10 minutes) and discarding the supernatant. Where total culture volume per flask did not fit in a single falcon tube, the remaining culture was added after the first centrifugation step such that all biomass in a single culture flask was harvested in

a single falcon tube. The pellet was then washed once in new media before being thoroughly resuspended in new media by shaking vigorously.

In order to control the starting OD of the exchanged culture, the OD of the culture within the falcon tube was measured and the required amount inoculated into the necessary volume of fresh media in order to obtain the required culture volume at the desired OD.

2.4.4 Monitoring bacterial contamination

Cultures were confirmed to be free from bacterial contamination at the end of growth by testing for bacterial growth when a small aliquot of the culture was spread onto LB-Agar plates. LB-medium is suitable culture medium for the growth of yeast and bacteria but cannot support the growth of microalgae and therefore can be used to check for contamination without microalgal interference.

Except preparing the agar-medium, all steps were performed under sterile conditions (Class II laminar flow). Plates were made by adding 15g/L agar to Luria Broth (LB) made according to the following recipe in deionised water:

-10g/L Tryptone
- 5g/L Yeast Extract
- 10g/L NaCl

The solution was autoclaved to dissolve the agar and to sterilise the medium before being poured into Petri-dishes (approx. 20-25 mL per dish) and allowed to set with the lids ajar to facilitate the removal of steam and prevent condensation on the inside of the plates. Unused plates were store upside down at 4°C until required.

Each culture was plated in triplicate on separate plates by dipping a 10 µL inoculation loop into the culture and spreading in a small area of the plate. The plates were stored upside down one each at room temperature, 29°C (to test for yeast contamination) and 37°C (to test for bacterial contamination). At each temperature a negative control was included by spreading a clean loop onto the plates. Cultures were confirmed to be sterile if all plates remained clean after 48 hours incubation.

2.5 Culture Analysis

During cultivation, cultures were analysed daily for optical density and chlorophyll concentration. All absorbance values for spectrophotometric analysis were measured using a Jenway 6715 UV/Vis spectrophotometer.

2.5.1 Optical density

Optical density was measured at 750 nm in 1.5 mL polystyrene semi-micro cuvettes by diluting a known volume of culture in deionised water to an absorbance ≤ 0.4. Cuvettes were topped with Parafilm and shaken vigorously for 5-10 seconds or until any settled/adhered sample was homogeneously suspended before measurement.

2.5.2 Chlorophyll quantification

Chlorophyll quantification was conducted spectrophotometrically *via* solvent extraction in 80 % (v/v) acetone/20 % (v/v) methanol. A known volume of sample was pelleted in a microcentrifuge (13,000 rpm, ~16,000 x g, 10 minutes) and the supernatant removed; sample volume was selected to maintain an absorbance <1.00 after chlorophyll extraction. The pellet was resuspended in 1 mL 80 % (v/v) acetone in methanol by vortexing before being further centrifuged (13,000 rpm, approximately 16,000 x g, 5 minutes) to remove cell debris. The absorbance of the supernatant was measured at 646.6 nm, 663.6 nm and 750 nm in a glass cuvette against an 80 % acetone/20 % (v/v) methanol blank. Once chlorophyll extraction had taken place, all samples were kept in the dark until analysis to prevent chlorophyll degradation.

Chlorophyll content was calculated according to the extinction coefficients described in Porra *et al.* (1989) as follows:

$$Chl\ a\ (\mu g/ml) = \frac{12.25\ E_{663.6} - 2.55\ E_{646.6}}{sample\ volume(ml)} \quad (2.1)$$

$$Chl\ b\ (\mu g/ml) = \frac{20.31\ E_{646.6} - 4.91\ E_{663.6}}{sample\ volume\ (ml)} \quad (2.2)$$

$$Chl\ a + b\ (\mu g/ml) = \frac{17.76\ E_{646.6} + 7.34\ E_{663.6}}{sample\ volume\ (ml)} \quad (2.3)$$

where $E_{663.6}$ and $E_{646.6}$ represent absorbances at 663.6 nm and 646.6 nm minus absorbance at 750 nm respectively.

2.5.3 Colony forming units

Colony forming units (cfu) were used to determine the concentration of live cells within a culture. Aliquots of culture were diluted by serial dilutions in TAP to a total 5,000 x dilution. 100 µL was then pipetted onto TAP-Agar plates and spread evenly using a 10 µL inoculation loop to minimise losses. A negative control was also plated using the same TAP medium used to create the dilutions. Plates were then left for 4-7 days (20°C, approx. 50 µE light, 16 hr photoperiod), or until colonies were visible, before the number of colonies on each plate was counted manually.

Image J software was used to calculate the mean colony area seven days after plating using the ColonyArea plugin. Colony clusters were separated using the Watershed function or manually where necessary. Colony area was then calculated as the average colony area of all detected colonies.

2.5.4 Fluorescence microscopy

Neutral lipid bodies were observed by staining with the fluorescent dye Nile-red which emits a yellow fluorescence signal (approximately 580 nm) in the presence of neutral lipids.

Nile-red stock solution was made up in methanol (0.1 mg/mL) and stored in the dark at -20°C. Samples were diluted to an approximate OD (OD_{750}) = 0.5 – 1.0 with deionised water and Nile-red stain added to a working concentration of 0.1 µg/mL. The samples were incubated in the dark for a minimum of 20 minutes before imaging. 10 µL sample was then placed on a microscope slide and covered with a cover slip. Samples were imaged using the Zeiss Axio Imager.M2 fluorescence microscope equipped with an EC Plan-Neofluar 40x/0.75 M27 air objective lens. Nile-red neutral lipid florescence was viewed using filter excitation and emission wavelengths of 540-552 nm and 575-640 nm respectively.

2.6 Biomass Analysis

With the exception of volatile suspended solids (VSS) all biomass analysis was conducted on freeze-dried biomass.

Biomass was freeze-dried for a minimum of 24 hours using a Christ Alpha 1-2 LDplus freeze dryer following a period stored at -70°C. *Chlamydomonas* cells do not survive freezing without cryoprotectant (The Chlamydomonas Resource Center,c; Harris *et al*., 1988) due to expanding ice crystals within the cells which cause the cells to burst. Storage at -70°C was therefore used both as a stable means by which to store biomass prior to analysis and as a means to crack cells for biomass analysis.

Given the -70°C freezer and the freeze-drier are housed in separate university departments, the biomass was transferred on ice and stored at -20°C for one hour immediately before being placed in the freeze-drier to ensure that the biomass was completely frozen before drying.

2.6.1 Volatile suspended solids

Volatile suspended solids were measured according to standard methods used for the examination of water and wastewater samples (Method 2540 D, E; APHA, 2012).

15 mL fresh culture was filtered onto individual, dried (550°C, 2 hours) and pre-weighed 90 mm diameter glass fibre filters (Fisherbrand™ Microglass Fiber Filters, Grade 261, product code 11714083) using a Buchner funnel connected to a vacuum pump. Samples were then placed in a 105°C drying oven for a minimum of 4 hours and the dried filters weighed to obtain the total suspended solid (TSS) mass. Samples were then placed in a 550°C muffle furnace to drive off the volatile matter for 2 hours and the final filters weighed to obtain the mass of inorganic solids. VSS was then calculated as the difference between total and inorganic solid mass according to the following equation. In each case the mass of the original filter was removed from the filter + sample mass.

$$VSS\ (g/L) = (Total\ Suspended\ Solids - Inorganic\ Solids) \times \frac{1000}{Sample\ Volume} \quad (2.4)$$

2.6.2 Biomass dry weight

Biomass dry weight was calculated from the mass of freeze-dried biomass contained within a pre-weighed 1.5 mL Eppendorf tube according to the following equation.

$$Biomass\ dry\ weight\ (g/L) = \frac{(Eppendorf\ mass\ after\ drying) - (Mass\ of\ empty\ Eppendorf)}{Volume\ of\ sample\ harvested} \quad (2.5)$$

2.6.3 Lipid analysis

2.6.3.1 Total lipids

Lipid analysis was conducted using Gas Chromatography Mass Spectrometry (GC-MS). Total lipids were extracted from approximately 5 mg dry biomass with in-situ transesterification by addition of 200 µL 2:1 chloroform methanol and 300 µL 0.6 M HCl in methanol and heated at 70°C for one hour in sealed glass vials (protocol modified from Bligh and Dyer, 1959). Once cooled 1 mL Hexane was added and the vials shaken before being allowed to settle for approximately 30 minutes. 500 µL of the upper organic layer was then removed to a fresh vial and 10 µL C17:0 internal standard (Sigma-Aldrich, Cat no. 51633-1G) added from one of two stocks made up in hexane (68.5 mg/mL and 16.3 mg/mL).

FAME analysis was conducted on a Schimadzu 2010 GC-MS using a polar Rtx®-Wax column (Restek, 30.0 m length, 0.25 µm film thickness, 0.25 mm internal diameter) with helium as the carrier gas. The injector temperature, ion source temperature and interface temperature were maintained at 250°C, 260°C and 250°C respectively. The sample was injected in splitless mode at an initial oven temperature of 50°C. After 1 minute the oven temperature was raised to 200°C at 25°C/min and then to 230°C at 3°C/min and held at 230°C for a further 18 minutes. FAMEs were identified by the fragmentation pattern and retention time by comparison with FAME external standard and previous literature (Siaut *et al*., 2011).

Different compounds have different detector response factors when analysed by GC-MS therefore the relationship between peak area and absolute concentration can vary depending on the compound of interest. In order to account for this, calibration curves were made by analysing the chromatogram of a known FAME mix external standard. In addition, a known concentration of a C17:0 internal standard was added to each sample to calibrate for any changes between individual analyses – e.g. sample injection volume. C8:0 – C24:0 fatty acid standard was purchased (Sigma-Aldrich, F.A.M.E. Mix C8-C24, Cat no. CRM18918) and a stock made up to approximately 20 mg/mL in hexane. C17:0 internal standard was added as described above and the external standard analysed according to the method described above at a range of concentrations. The following calibration curves were made for each of the compounds of interest by dividing the peak area of the compound of interest by that of the internal standard (Figure 2.3). A new standard curve was made for each concentration of C17:0 internal standard used.

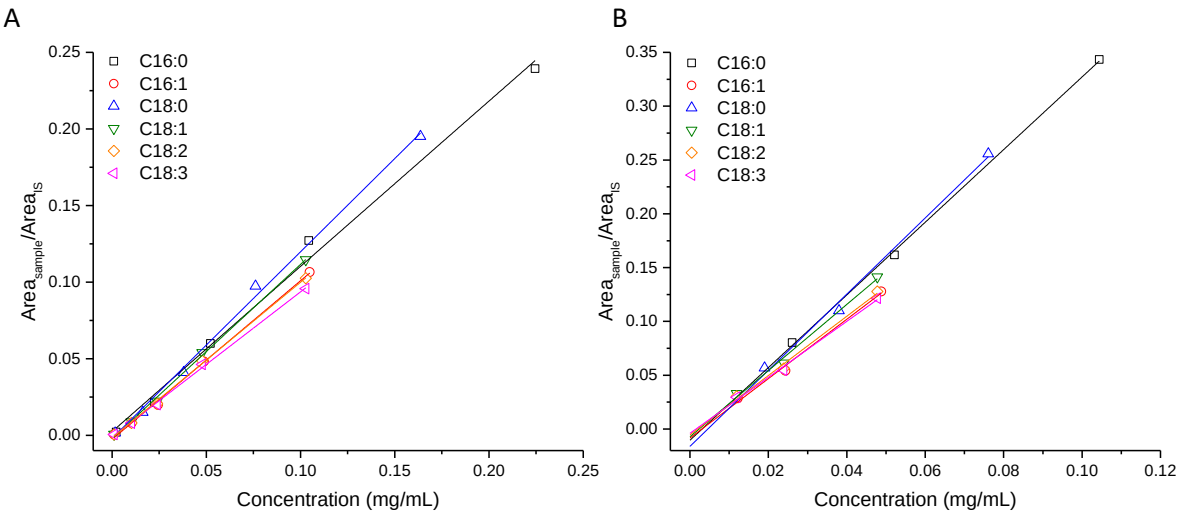

Figure 2.3 Calibration curves for each fatty acid of interest with two concentrations of C17:0 internal standard (A) 68.5 mg/mL, (B) 16.3 mg/mL. Standard curves are plotted as fatty acid peak area/peak area of the internal standard vs. concentration of fatty acid per mL solvent used to extract fatty acids.

The calibration equations for each of the fatty acids are presented in Table 2.8. Where there was a fatty acid in the sample that is not present in the external standard, the closest available compound was used to calculate the concentration from the peak areas – i.e. C18:4 was calculated from the C18:3 standard equation.

Table 2.8 Calibration equations from GC-MS external FAME standard at each of two concentrations of internal standard (A) 68.5 mg/mL, (B) 16.3 mg/mL. y is the peak area of the fatty acid of interest/peak area of the internal standard (C17:0). x is the concentration of fatty acid in mg/mL solvent used to extract fatty acids.

A	**Equation**	**R^2**
C16:0	y = 1.0792x + 0.0024	0.9972
C16:1	y = 1.0360x - 0.0027	0.9992
C18:0	y = 1.2177x - 0.0020	0.9986
C18:1	y = 1.1382x - 0.0022	0.9992
C18:2	y = 1.0166x - 0.0017	0.9993
C18:3	y = 0.9476x - 0.0011	0.9993

B	**Equation**	**R^2**
C16:0	y = 3.3751x - 0.0103	0.9997
C16:1	y = 2.7589x - 0.0083	0.9967
C18:0	y = 3.5369x - 0.0160	0.9974
C18:1	y = 3.0724x - 0.0070	0.9970
C18:2	y = 2.7539x - 0.0053	0.9972
C18:3	y = 2.6000x - 0.0039	0.9977

In each case the concentration of fatty acid present in the sample was calculated from the fatty acid peak area and the peak area of the internal standard using the above calibration equations. Fatty acid concentration is calculated per mg dry biomass according to the following equation:

$$FAME\ (mg/mg\ dry\ biomass) = \frac{FAME\ (mg/mL)\ x\ 1.14333\ (mL)}{mass\ biomass\ (mg)} \quad (2.6)$$

where *FAME (mg/mL)* is the concentration obtained from calibration curves, *1.14333 (mL)* is the total volume of organic solvent used in the extraction process (hexane + chloroform + internal standard solution) and *mass biomass (mg)* is the starting mass of biomass on which the extraction was performed.

2.6.3.2 Neutral lipids

Neutral lipids were measured gravimetrically to 0.01 mg (method modified from Usher, 2014). Neutral lipids were extracted in the non-polar solvent hexane. 1 mL hexane was added to approximately 5 mg dry biomass in a glass vial and the vial shaken and allowed to stand for 1 hour for neutral lipids to be extracted. 500 µL dH_2O was then added to facilitate phase separation of the organic and aqueous phases and the solution allowed to stand until the layers could be clearly defined (approximately 30 minutes). The upper organic layer was then removed by pipetting into a second pre-weighed vial. A further 1 mL of hexane was added, the vial shaken, and the layers allowed to separate before the organic layer was combined with the previous extract.

Due to the difficulty in fully removing the organic layer, the extraction process was conducted a total of 6 times. Assuming a minimum 50 % recovery of the organic layer at each extraction this ensures a recovery efficiency of at least 98.4 % of extracted lipids. Once all

extractions had been completed, the hexane was allowed to evaporate, and the vials re-weighed to determine the weight of neutral lipids extracted.

To confirm the result and for compositional analysis of the extracted lipids, the extracted lipids were then transesterified and analysed by GC-MS according to the method for total lipids starting with the addition of 200 µL 2:1 chloroform methanol and 300 µL 0.6 M HCl.

2.6.3.3 Biodiesel quality parameters

Biodiesel quality parameters were calculated according to the following equations (Krisnangkura, 1986; Francisco *et al*., 2009; Ramos *et al*., 2009; Islam *et al*., 2013; Rai and Gupta, 2017):

$$Degree\ of\ Unsaturation\ (DU) = (MUFA, wt\%) + (2xPUFA, wt\%) \quad (2.7)$$

$$Long\ Chain\ Saturation\ Factor\ (LCSF) = 0.1\ \times\ C16(wt\%) + 0.5 \times C18(wt\%) + 1 \times C20(wt\%) + 1.5 \times C22(wt\%) + 2 \times C24(wt\%) \quad (2.8)$$

$$Saponification\ Value\ (SV, mgKOHg^{-1}) = \sum \frac{560 \times N_i(mol\%)}{M_i} \quad (2.9)$$

$$Iodine\ Value\ (IV, gI_2 100g^{-1}) = \sum \frac{254 \times D_i \times N_i(mol\%)}{M_i} \quad (2.10)$$

$$Cetane\ Number\ (CN) = 46.3 + \frac{5458}{SV} - (0.225\ \times\ IV) \quad (2.11)$$

$$Cold\ Filter\ Plugging\ Point\ (CFPP, °C) = (3.1417 \times LCSF) - 16.477 \quad (2.12)$$

$$Oxidation\ Stability\ Index\ (OSI, h) = \frac{117.9295}{C18{:}2 + C18{:}3\ (wt\%)} + 2.5905 \quad (2.13)$$

$$Density\ (\rho, gcm^{-3}) = \sum \frac{N_i(wt\%)}{100} \times \left(0.8463 + \frac{4.9}{M_i} + 0.0118 \times D_i\right) \quad (2.14)$$

$$Kinematic\ Viscosity\ (\upsilon, mm^2 s^{-1}) = = \sum \frac{N_i(wt\%)}{100} \times EXP(-12.503 + 2.496 \times \ln M_i\ - 0.178 \times D_i) \quad (2.15)$$

$$Higher\ Heating\ Value\ (HHV, MJkg^{-1}) = \sum \frac{N_i(wt\%)}{100} \times \left(46.19 - \frac{1794}{M_i} - 0.21 \times D_i\right) \quad (2.16)$$

where N_i is the % of each fatty acid, M_i is the fatty acid molecular weight and D_i is the number of double bonds.

2.6.5 Thermogravimetric and elemental analysis

Thermogravimetric analysis (TGA) was conducted on a Mettler Toledo TGA/DSC1. Approximately 5-10 mg sample was accurately weighed into a 70 µL ceramic crucible, the lid attached, and the sample loaded onto the instrument.

The method was run according to the following profile to obtain the moisture, volatile matter, fixed carbon and ash content.

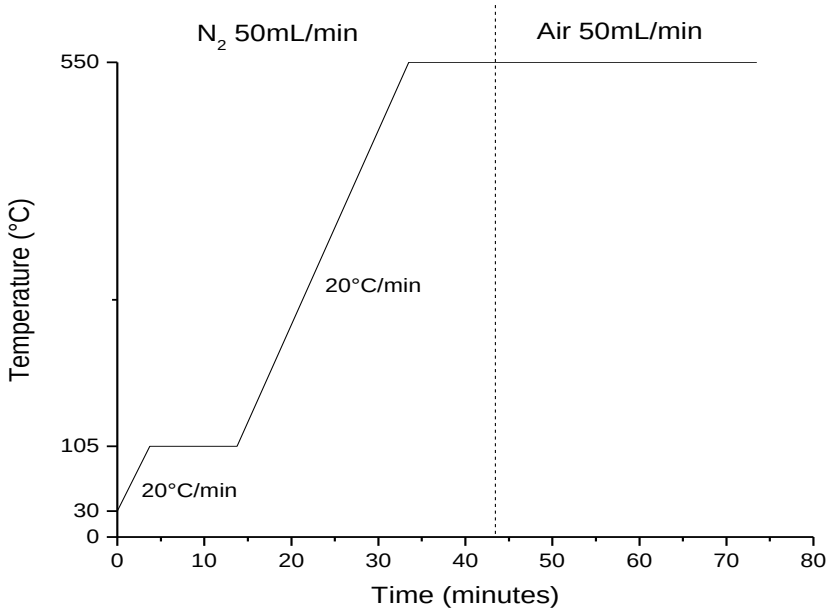

Figure 2.4 TGA heating profile to obtain the moisture, volatile matter, fixed carbon and ash content of dried C.reinhardtii samples.

Freeze-dried microalgae is hygroscopic and therefore fluctuations were observed between the original weighed mass and the mass as measured by the instrument. This is due to adsorption and evaporation of moisture. It is assumed that this moisture is not intrinsic to the biomass and as such percentages of moisture, volatiles, fixed carbon and ash were calculated based on the mass of the sample measured by the instrument immediately prior to analysis.

Elemental analysis was conducted to obtain the C, H, N, S and O (by difference) content of dry biomass samples using a Thermo Scientific FLASH 2000 elemental analyser. The instrument was calibrated using BBOT (2,5-Bis (5-tert- butyl-benzoxazol-2-yl) thiophene) and oatmeal standards (72.53 % C, 5.98 % H, 6.58 % N, 7.54 % S and 41.59 % C, 5.85 % H, 1.90 % N, 0.00 % S respectively). Approximately 2.5-3.5 mg sample was weighed into duplicate tin capsules and the capsules sealed and squeezed to remove air. Samples were combusted in the analyser in the presence of oxygen and elemental analysis calculated by the analyser by measuring concentrations of H_2O, CO_2, NO_x and SO_2 in the product gas.

TGA and elemental analysis were used to calculate the biomass nitrogen percentage, presented in chapters 4 and 5, and the elemental composition (presented in the appendix) on a dry basis according to the following equations:

$$\%C,N,S,Ash(dry) = \%C,N,S,Ash(ar) / \frac{\left(100-\%\left(moisture(ar)\right)\right)}{100} \quad (2.17)$$

$$\%H(dry) = \left(\%H(ar) - \left(\frac{2}{18}\right) \times \%moisture(ar)\right) / \frac{\left(100-\%\left(moisture(ar)\right)\right)}{100} \quad (2.18)$$

$$\%O(dry) = 100 - \%(C + H + N + S + Ash)(dry) \quad (2.19)$$

where *%C,H,N,S,O and Ash (dry)* are the % mass on a dry basis and *%C,H,N,S,O, Ash and Moisture (ar)* are the mass % as received from the instrument.

2.7 Media Analysis

Media was collected from the supernatant of harvested biomass (see Figure 2.2) and the pH measured. The sample was then filtered through a syringe filter (0.2 µm pore size) under sterile conditions into fresh, sterile tubes before storing at -20°C until further analysis.

The availability of nutrients is highly dependent on the pH of the culture. In order to be sure that measured nutrients reflect those available for biomass growth it is essential to filter the media samples prior to freezing to remove precipitation and prevent the solubilisation of any precipitated nutrients during the assays when dilution of the sample causes significant changes in the pH. Filtering the sample prior to freezing also removes any bacterial contamination obtained during the collection and pH measurement of media samples.

2.7.1 pH

pH was measured using a Mettler Toledo FiveEasy™ pH meter.

2.7.2 Phosphate quantification

The following method was modified from the Methods of Phosphorus Analysis for Soils, Sediments, Residuals and Waters (Pierzynski *et al.*, 2000).

Detergents and tap water contain large concentrations of phosphate. All glassware was therefore acid-washed to remove any phosphate prior use. Glassware was filled with 0.1 M HCl in deionised water and left overnight. The acid was then removed and the glassware thoroughly rinsed in deionised water and allowed to dry overnight.

The following reagents were prepared for the assay:

1. 2.5 M H_2SO_4
2. 40 g/L Ammonium molybdate tetrahydrate
3. 0.1 M Ascorbic Acid (stable for one month in an opaque bottle)
4. 2.75 g/L Potassium antimonyl tartarate
5. 5 g/L Phenolphthalein (50 % v/v ethanol in dH_2O)

With the exception of sulphuric acid, all reagents were stored at 4°C. For the preparation of phenolphthalein indicator solution, phenolphthalein was first dissolved in ethanol in a volumetric flask and made up to the required volume with deionised water to a final ratio of 1:1 (v/v) ethanol: dH_2O.

The reagents were combined on the day of use as follows and in the following order:

- 500 mL/L (1)
- 50 mL/L (4)
- 150 mL/L (2)
- 300 mL/L (3)

The combined reagent is stable for approximately 4 hours after preparation.

The reaction was performed in individual 1.5 mL semi-micro polystyrene cuvettes. 10 µL sample was added to 990 µL dH_2O and mixed by pipetting up and down several times. 10 µL phenolphthalein solution was added to test the pH of the solution and 2.5 M H_2SO_4 added in 10 µL increments to remove any colour (phenolphthalein pK_{In} = 9.4 where pK_{In} is the indicator dissociation constant). 160 µL combined reagent was added and the cuvette shaken gently to mix. The absorbance was measured at 880 nm exactly 20 minutes after the addition of the combined reagent against a blank containing 10 µL additional dH_2O in place of the sample.

A standard curve was constructed for each batch of combined reagent. A 20 µM P solution was made through serial dilutions starting from a 1 M solution of KH_2PO_4 made up in a volumetric flask. The standard curve was made by measuring the phosphate absorbance according to the following table:

Table 2.9 P concentrations and set up for construction of phosphate assay standard curve

P concentration µM	mL dH_2O	mL 20 µM P solution
20	0	1.0
16	0.2	0.8
12	0.4	0.6
10	0.5	0.5
8	0.6	0.4
6	0.7	0.3
4	0.8	0.2
2	0.9	0.1
1	0.95	0.05
0	1.0	0

2.7.3 Nitrogen quantification

The nitrate and ammonium concentrations in the media were determined by use of Hach® cuvette tests and the Hach Lange DR1900 spectrophotometer (Hach®, Manchester, UK) which has built-in the necessary blanks and calibration curves for each of the tests used. For measurement of ammonium, all samples were diluted a minimum of 20 x in deionised water to reduce the concentration of species that may interfere with the reaction.

The following tests were used depending on the estimated nitrogen concentration in the measured sample.

Table 2.10 Hach® cuvette tests used for the measurement of nitrate and ammonium in C.reinhardtii growth media

Nitrogen species	Test	Concentration (mg/L N)
Nitrate	LCK339	0.23-13.5
	LCK340	5-35
Ammonium	LCK304	0.015-2.0
	LCK305	1.0-12.0

Owing to unknown interferences in TAP medium which were observed to affect the accurate measurement of ammonium concentration, calibration curves were created for each kit and each dilution used using TAP medium containing known NH_4Cl concentrations. Samples of known concentration were made by serial dilutions of TAP medium (105 mg/L N) with TAP-N. All samples were filtered (0.2 µm) prior to final dilution (20-100 times) with deionised water to remove any precipitants. The following calibration curves were obtained (Figure 2.5).

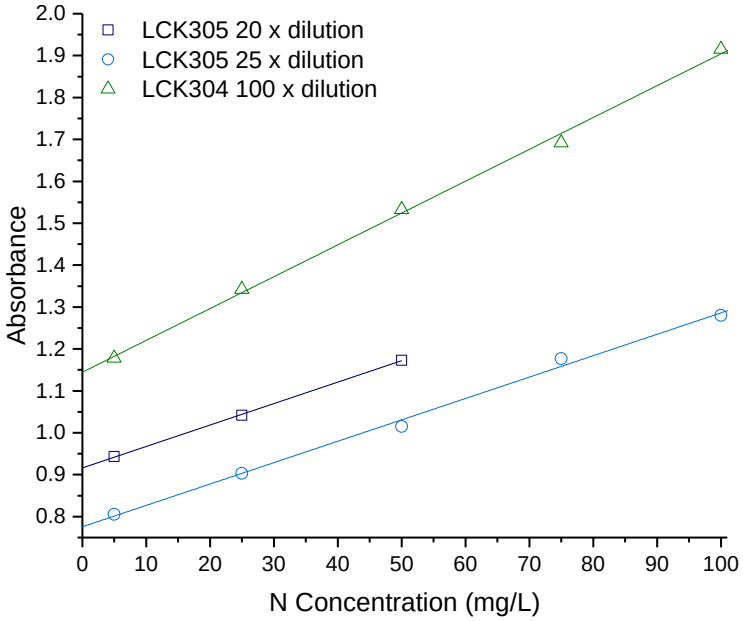

	Equation	R^2
LCK305 20 x dilution	y = 0.0051x + 0.9162	0.9999
LCK305 25 x dilution	y = 0.0051x + 0.7757	0.9979
LCK304 100 x dilution	y = 0.0076x + 1.1446	0.9989

Figure 2.5 Calibration curves for LCK304 and LCK305 Ammonium Hach® cuvette kits. Calibration curves were created from TAP medium with varying known concentrations of NH_4Cl.

Chapter Three – A Simple and Non-Destructive Method for Chlorophyll Quantification of Microalgal Cultures Using Digital Image Analysis

3.1 Background

Photosynthetic microalgae have gained attention for their ability to efficiently convert solar energy into biomass as a potential source of biofuels and high-value chemicals (Chisti *et al*., 2007; Wijffels and Barbosa, 2010; Liu and Benning, 2013; Goncalves *et al*., 2016). Chlorophylls *a* and *b* are the primary photosynthetic pigments in microalgae and are responsible for the characteristic green colour of chlorophyte cultures. The quantity of these pigments is therefore related to biomass production and can provide an indication of the growth of the culture (Wood *et al*., 2005). In industrial applications the production of neutral lipids (i.e. triacylglycerols, TAGs), which are favoured for use as a biodiesel starting product, has been linked to breakdown and recycling of membrane lipids including the chloroplast membrane. (Moellering and Benning, 2010; Siaut et al., 2011). Decrease in chlorophyll content can therefore be used as an indicator of possible neutral lipid production in microalgal cultures. Additionally, unlike growth measurements such as optical density or dry biomass weight, chlorophyll content can be used as a measurement of culture density without interference from non-photosynthetic organisms such as bacterial contaminants.

Conventional methods for chlorophyll quantification involve destructive solvent extraction and subsequent spectroscopic chlorophyll analysis (Porra *et al*., 1989). These methods are time consuming, require removal of sample from the culture vessel and subsequent destruction of the sample and require careful disposal of the resultant solvent waste. The removal and destruction of sample can be problematic, in particular for time course studies, where culture volume can limit the number of measurable parameters.

Fluorescence is widely used as a non-destructive method of chlorophyll detection and quantification in both plants (Buschmann *et al*., 2000) and algae (Vincent, 1983) including in environmental samples (Wang *et al*., 2018), and commercial products are available. However, there is a need for a simple, inexpensive, non-destructive method that does not require multiple sampling of small volume cultures which need to be maintained axenically.

Recently, digital imaging techniques have emerged as a means by which to rapidly and non-destructively measure chlorophyll content. In particular, the almost universal presence of smartphones has enabled the use of smartphone cameras in laboratory digital analysis (Rignon *et al*., 2016). A handful of studies over the last ten years have made use of the RGB colour model

for chlorophyll determination in plant leaves such as maize (Friedman *et al*., 2016), potato plants (Gupta *et al*., 2013) and in marine microalgal cultures (e.g. *N. oculta*; Su *et al*., 2008) *via* digital imaging. The RGB colour scale represents the intensity of red, green and blue components of a pixel within a digital computer image. Intensity ranges on a scale from 0 to 255 for each colour, where white has RGB values (255,255,255) and black has values (0,0,0). However, many methods published to date require the use of advanced modelling software or complex mathematical processing (Dey *et al*., 2016; Friedman *et al*., 2016; Su *et al*., 2008).

In this study, the microalga *Chlamydomonas reinhardtii* has been used to develop a simple and rapid method to quantify chlorophyll concentration of algal cultures non-destructively *in situ* using the RGB scale to quantify pixel colour intensity from digital photographs. The effect of bacterial contamination, sample volume, pH and neutral lipid production on the accuracy and reproducibility of the method is also evaluated. The method presented here is much simplified compared with other digital analysis methods for chlorophyll determination. Furthermore, the method is non-destructive and can be conducted without removal of sample from the culture vessel. This method requires minimal data manipulation and the use of only easily accessible software packages present as standard on most Microsoft (MS) Windows operated PCs.

The standard curve presented here is for cultures of *C.reinhardtii* grown in 7mL Bijou flasks. Digital images have been acquired under constant light conditions at a specific location using a smartphone digital camera. By creating a standard curve for the specific organism, culture vessel and photographic set-up available, the method presented here could be used to determine chlorophyll concentration for a range of algal species or consortia grown in a range of culture vessels. In addition, the method is robust to changes in sample volume and small changes in culture pH and bacterial contamination.

3.2 Method Development

3.2.1 Cultivation and sample preparation

Cultures of *C.reinhardtii* strain CC-1690 were grown statically in 5 mL TAP media contained within 7 mL plastic Bijou flasks fitted with screw-top lids at 20°C with a 16-hour photoperiod (approximately 50 µmol photons m^{-2} s^{-1}) (see Chapter 2, Section 2.4.1). All cultures were grown to stationary phase before being aliquoted, with a range of sample volumes, into fresh 7 mL flasks. Unless otherwise stated, all samples were made up to a total volume of 5 mL with TAP media, to create a range of absorbance values (A_{600} = 0.005-2.5), before analysis. Control cultures (sterile CC-1690, 5mL sample volume, pH 7.0-8.5) were initially analysed to assess the viability of the method.

3.2.2 Photographic chlorophyll analysis

Analysis was first conducted *via* the photographic digital analysis method demonstrated here, followed by comparison with a standard analytical method for chlorophyll quantification of microalgal cultures, detailed in Chapter 2, Section 2.5.2.

Photographic analysis was conducted by photographing each sample in triplicate (the three photographs were taken immediately one after another without disturbing the sample or camera position) using a smartphone (iPhone 5s, Apple Inc.) digital camera (8 megapixel, 1.5 µm pixels) mounted on a tripod. The camera was positioned at an angle of 30° from vertical at a height of 6.5 cm above the base of the sample flask and a horizontal distance of 8.5 cm from the flask edge; camera position was chosen to centre the sample within the photograph and minimise shadowing (Figure 3.1). All measurements were taken from the centre of the camera lens. Samples were shaken vigorously to resuspend any sedimented cells and positioned against a constant white background created by mounting white paper against a card box. The light concentration, measured at the sample position, was approximately 10 ± 1 µmol photons m^{-2} s^{1}.

Figure 3.1 Set up showing the sample and tripod positioning for photographic chlorophyll analysis.

'Green Pixel Intensity' (GPI) was determined from each photograph using Microsoft Paint software (MS Windows 7, version 6.1). Red, green and blue pixel intensities were obtained using the RGB colour model; pixels were selected using the 'color picker' tool and the RGB components extracted from the 'edit colors' feature.

Three individual pixels were selected each from the culture and from the white paper both to the immediate left and right of the flask as a background. Given the shadow present from the flask lid in each image, pixel selections for the culture were made one each from the different shadowed and un-shadowed regions (Figure 3.2).

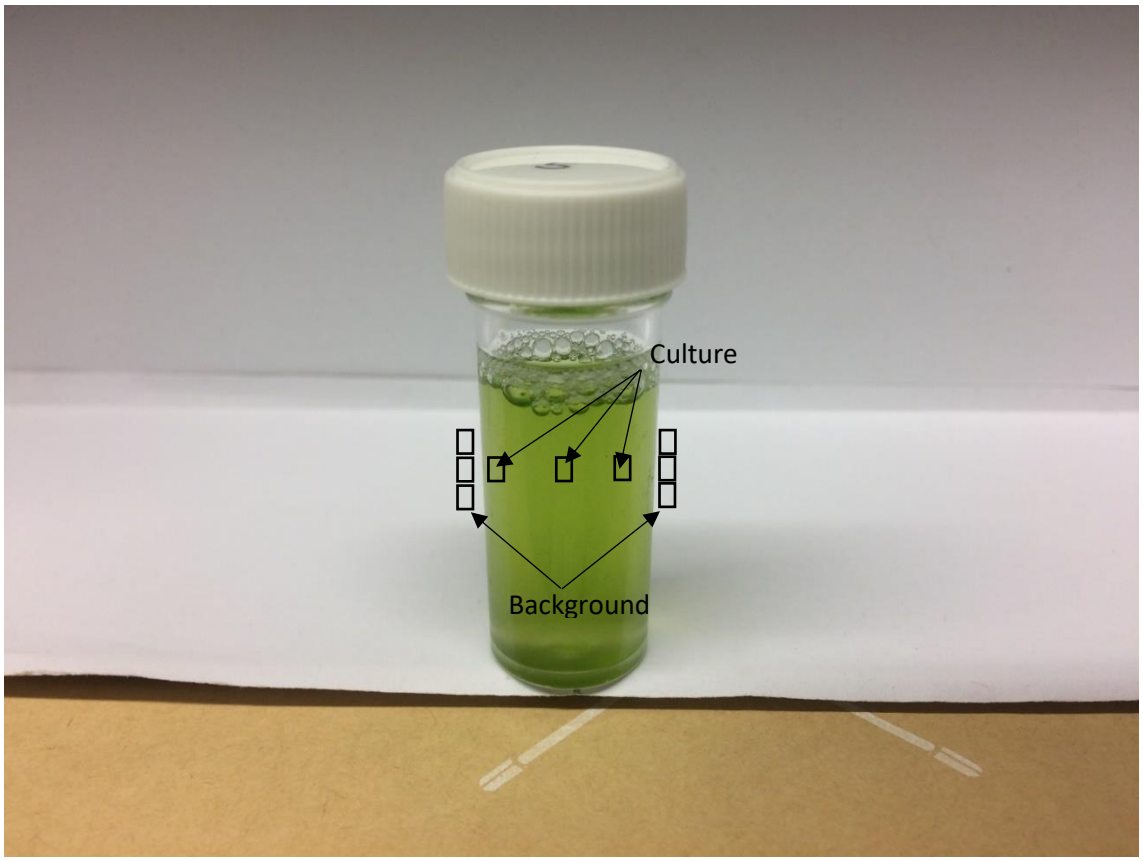

Figure 3.2 Pixel selection regions within sample photographs for photographic RGB data analysis.

Green pixel intensity (*GPI*) was calculated for each pixel from RGB data according to Equation 1.

$$Green\ Pixel\ Intensity\ (GPI) = \frac{G}{R+G+B} \tag{3.1}$$

where R, G, and B are the red, green and blue pixel intensities respectively.

For each photograph, *GPI* was calculated for each selected culture and background pixel and the mean *GPI* for each of the culture and background calculated. The mean background *GPI* was subtracted from the mean culture *GPI* such that:

$$GPI_{sample} = GPI_{culture} - GPI_{background} \quad (3.2)$$

where $GPI_{culture}$ is the mean *GPI* of three pixels selected from the culture and $GPI_{background}$ is the mean of six pixels taken from the white paper background to the immediate left and right of the culture.

On each day of sampling, a baseline green pixel intensity was obtained as described above from a sample vessel containing medium in the absence of culture and analysed as above such that:

$$GPI_{baseline} = GPI_{media} - GPI_{background} \quad (3.3)$$

where GPI_{media} is the mean *GPI* of three pixels selected from the media and $GPI_{background}$ is the mean of six pixels taken from the white paper background to the immediate left and right of the media.

Once each photograph had been analysed as above, the mean GPI_{sample} and mean $GPI_{baseline}$ were calculated from the corresponding GPI_{sample} and $GPI_{baseline}$ calculated values for each of the three photographs taken.

Final green pixel intensity (GPI_{final}) for each sample was obtained by subtracting the mean green pixel intensity of the baseline from that of the sample according to Equation 3.4.

$$Final\ Green\ Pixel\ Intensity\ (GPI_{final}) = mean\ GPI_{sample} - mean\ GPI_{baseline} \quad (3.4)$$

such that GPI_{final} represents the mean of the three photographs taken.

3.2.3 Investigating the effect of environmental interference

In order to test the reproducibility of the analysis when environmental interference is present, a range of commonly encountered parameters were chosen, and the analysis compared against the control.

To test the effect of sample volume 'Low volume' samples (sterile CC-1690, 3.5 mL volume, pH 7.0-8.5) were cultured as above but made up to a final volume of 3.5 mL with TAP media. 3.5 mL TAP media was used as a baseline.

In order to test the effect of pH on the analysis, 'High pH' samples (sterile CC-1690, 3.5 mL volume, pH 9.5) were created by exchanging cultures (see Chapter 2, Section 2.4.3) into CAPS-Acetate-Phosphate media (TAP media containing 10mM CAPS buffer in place of the Tris buffer, adjusted to pH 9.5 by addition of 1M KOH) and resuspending to a range of biomass concentrations. 5mL CAPS-Acetate-Phosphate media was used as a baseline.

To test the effect of bacterial contamination, contaminated samples (CC-1690 + *E.coli*, 5mL, pH 7.0-8.5) were created by the addition of two different quantities of stationary phase *Escherichia coli* (*E.coli*) culture (A_{600}=3.64). The *E.coli* culture was decanted into 1.5 mL aliquots contained within 1.5 mL Eppendorf tubes and pelleted (13,000 rpm, ~16,000 g, 10 minutes) in a microcentrifuge, the supernatant removed and the cultures resuspended in TAP medium. Sixteen *C.reinhardtii* samples were prepared; each sample was prepared to one of eight optical densities (A_{600} = 0.005-1.0) in duplicate. Each duplicate was spiked with 1.5ml or 0.325ml *E.coli* resuspended in TAP (approximate A_{600} = 1.0 and 0.25 respectively) to create a range of algal biomass concentrations containing two different *E.coli* contaminant concentrations.

Large quantities of neutral lipids are known to accumulate in microalgae under nitrogen starvation (Siaut *et al*., 2011; Valledor *et al*., 2014). 'TAP-N' samples (sterile CC-1690, 5mL, pH 7.0-8.5, TAP-N media) were created to test the effect of neutral lipid accumulation on photographic chlorophyll determination. Cultures were exchanged into TAP-N medium and resuspended to a range of biomass concentrations. Analysis was conducted over eight days as chlorophyll concentration fell and lipids were accumulated.

3.2.4 Statistical analysis

G*power (version 3.1) (Faul *et al*., 2009), was used to conduct a sensitivity power analysis (two tailed; linear bivariate regression: two groups, difference between slopes; $\alpha = 0.05$; power = $1 - \beta = 0.80$) to determine the detectable effect size ($|\Delta slope|$) between each environmental variable and the control dataset for the given sample sizes.

The relationship between Final Green Pixel Intensity (GPI_{final}) from photographic digital image analysis and chlorophyll concentration determined by extraction in 80 % (v/v) acetone in methanol for the control dataset was analysed by linear regression. Microsoft Excel software was used to calculate the coefficient of determination (R^2) for the correlation assuming a linear relationship between total chlorophyll concentration and green pixel intensity. Data points were subsequently removed (starting with the highest chlorophyll concentration) and the R^2 value recalculated as each additional point was removed. The linear portion of the correlation was chosen as the range of points (>2 points) responsible for the R^2 closest to 1.00. Regressions for all potential environmental interferences were considered linear within the same region as that of the control dataset.

OriginPro (Origin® 9.1) software was used to compute the 95 % confidence band for the linear portion of each curve. The 95 % confidence band represents the region in which there is 95 % certainty of the true linear fit residing.

IBM® SPSS Statistics® (version 22) was used to compare the slopes and intercepts of different standard curves using a univariate general linear model. A full model was fitted, with different slopes and intercepts for each fitted line. A significant difference between slopes was tested by examining the interaction term; if this was not significant, the interaction term was removed from the model and a significant difference between intercepts was tested. Normality of residuals was checked by visual inspection of Q-Q plots.

3.3 Results

3.3.1 Validity of the RGB model for predicting chlorophyll content

To test the validity of the RGB method (Eq. 3.1) to estimate the chlorophyll content of a microalgal culture, a series of sterile 5ml *C.reinhardtii* samples were made to a range of optical densities in standard Tris-Acetate Phosphate (TAP) Media, pH 7.0-8.5. Samples were first photographed for digital analysis before being aliquoted for standard spectroscopic chlorophyll quantification *via* extraction in 80 % (v/v) acetone in methanol (see Chapter 2, Section 2.5.2).

Example pictures for a range of biomass concentrations show a clear distinction between sample colours dependent on the chlorophyll concentration (Figure 3.3).

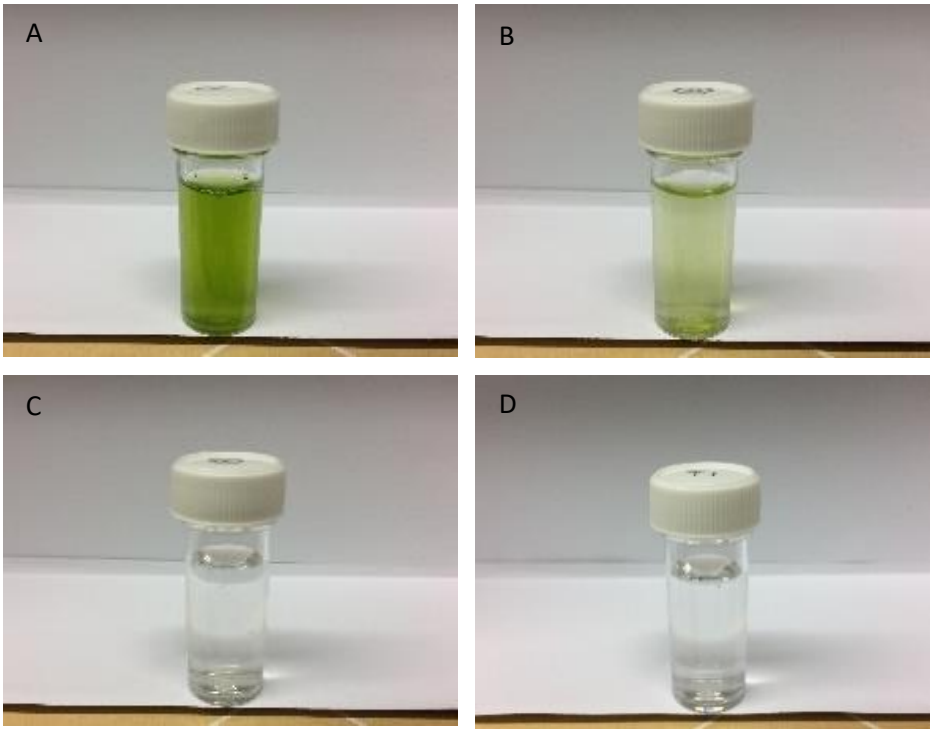

Figure 3.3 Photographs of C.reinhardtii samples for RGB digital analysis of chlorophyll concentrations: chlorophyll a + b = (A) 18.2 µg/ml; (B) 3.7 µg/ml; (C) 0.1 µg/ml; (D) 0 µg/ml (TAP blank).

Plotting final GPI, as measured by photographic digital analysis, against chlorophyll concentration, as measured by standard spectroscopic analysis, gives the correlation between the methods (Figure 3.4). The linear region of the correlation was determined by linear regression analysis (see Section 3.2.4). Adding points individually with increasing chlorophyll concentration resulted in a constant gradient up to a chlorophyll *a* + *b* concentration (*X*) of 16 µg/ml (final green pixel intensity = 0.125). Including points above *X* = 16 µg/ml resulted in the steady reduction of the gradient of the fitted line, indicating that the plot tends towards a plateau at high chlorophyll concentrations. In addition, above *X* = 16 µg/ml there is a noticeable increase in the scatter of the plot. The reduction in gradient as well as increased scatter beyond *X* = 16 µg/ml suggests a reduced sensitivity of the RGB method above this point; points above *X* = 16 µg/ml have therefore been excluded from the fitting model and all subsequent plots. For cultures of higher chlorophyll concentration, samples would need to be removed and diluted before analysis.

There is an excellent correlation between the RGB and standard methods for chlorophyll quantification for chlorophyll *a*, *b* and total chlorophyll as shown by the R^2 values of 0.988, 0.985 and 0.988 respectively. 95 % confidence bands demonstrate a high level of precision in the slopes and intercepts of the fitted lines. Data for the control dataset was acquired on three separate days and combined, there was no difference between days in the slopes ($F_{2,16} = 0.952$, $p = 0.407$) or intercepts ($F_{2,16} = 1.345$, $p = 0.285$), thus demonstrating the reproducibility of the method over different sampling periods.

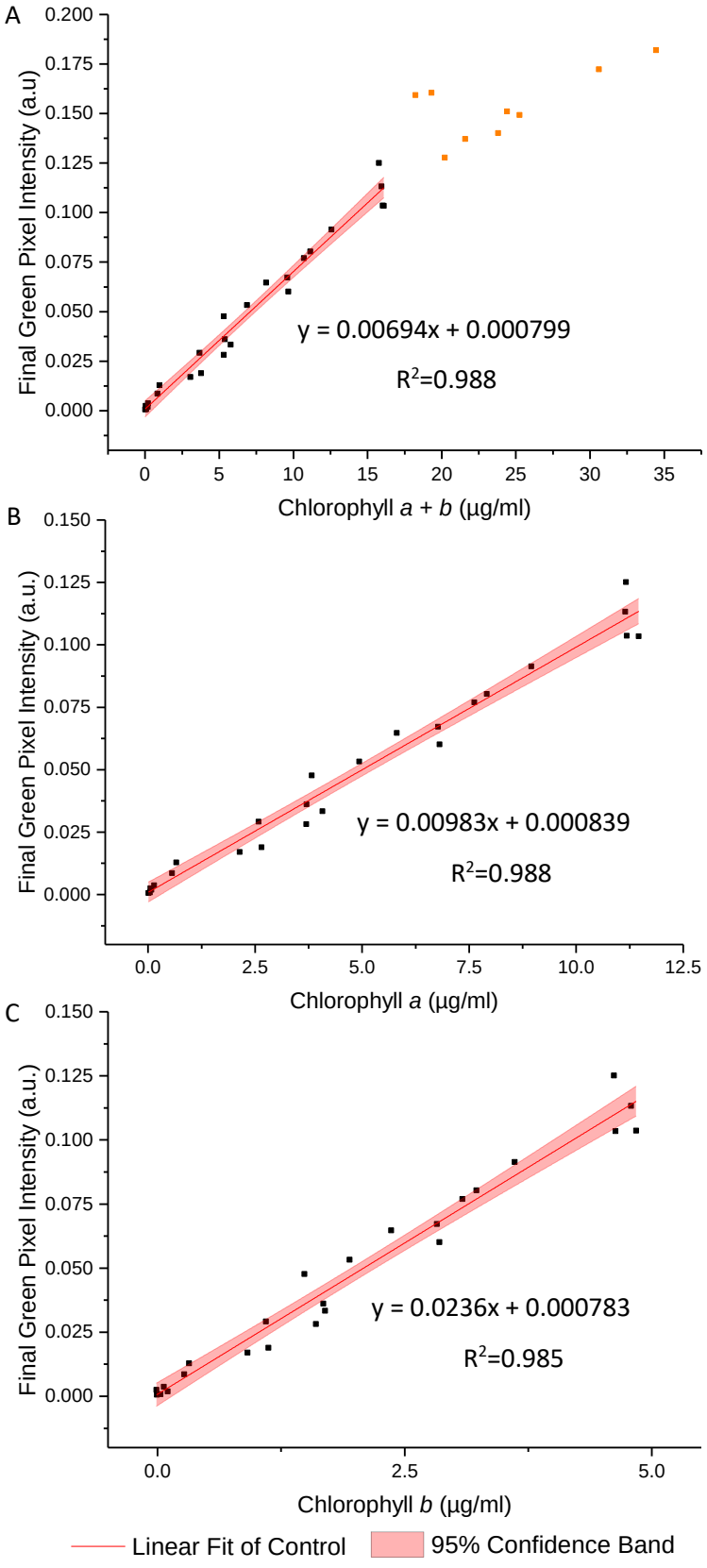

Figure 3.4 The correlation between (A) chlorophyll a + b, (B) chlorophyll a and (C) chlorophyll b concentrations, measured by standard extraction method in 80 % acetone, and final GPI calculated from the RGB colour model for sterile C.reinhardtii CC-1690 cultivated in TAP media and diluted to a range of biomass concentrations for analysis. Data points are the mean GPI of three photographs (y) and the mean chlorophyll concentration of three sample aliquots (x). Orange points indicate those excluded from the fitting model due to lack of continued linearity.

The regression parameters for the control dataset are given in Table 3.1. The high *p*-values for the intercept show that the intercept is not significantly different from zero in each case which is expected given the green pixel intensity of the TAP blank has been subtracted from each data point.

Table 3.1 Regression parameters for the control dataset.

	Equation	R^2	$F_{1,23}$	p^a
Chl *a* + *b*	y=0.00694(±0.00029)x + 0.000799(±0.00198)	0.988	0.162	0.691
Chl *a*	y=0.00983(±0.00032)x + 0.000839(±0.00193)	0.988	0.190	0.667
Chl *b*	y=0.02361(±0.00086)x + 0.000783(±0.00217)	0.985	0.129	0.722

[a]p-values indicating whether the intercept is significantly different from zero in each case

3.3.2 Effect of environmental interference on the chlorophyll/RGB correlation

To investigate whether a single standard curve, for the given experimental conditions (e.g. algal species, culture vessel etc.), could be used to estimate chlorophyll concentration from green pixel intensity in spite of potential environmental interference, four commonly encountered environmental variables were introduced and their effect on the correlation individually investigated. In each case, linear regression analysis was used to determine whether the slopes and intercepts of each correlation could be considered statistically similar to that of the control dataset (Figure 3.4). Owing to the loss of linearity in the correlation at concentrations above chlorophyll *a* + *b* = 16 µg/ml (green pixel intensity = 0.125) correlations have only been compared up to green pixel intensity = 0.125; data points above this have been removed from the fitted lines.

Table 3.2 gives the minimum detectable effect size (|Δslope|) for the given sample sizes. The effect size, in this case, is the smallest difference in slope between the RGB/chlorophyll correlations for control and variable datasets that can be distinguished with the given sample sizes.

Table 3.2 Detectable effect size (|Δslope|).

Sample Set vs. Control	Detectable Effect Size (|Δslope|)[a]
Low Volume	0.00115
High pH	0.00106
+1.5 ml *E.coli*	0.00107
+0.325 ml *E.coli*	0.00122

*[a]between each measured variable and the control dataset as calculated from G*power software; α=0.05; power = 1 – β = 0.80*

Figure 3.5 shows the effect on the relationship between green pixel intensity and chlorophyll *a*, *b* and total chlorophyll when the photographed sample volume is reduced from 5.0 ml to 3.5 ml. Samples were photographed at a volume of 3.5 ml for comparison with the control samples (5 ml) before being analysed for chlorophyll concentration by extraction in 80 % (v/v) acetone in methanol. In each case the linear fit for the low volume samples (red) is shown next to that of the control dataset (grey) with the 95 % confidence bands of each fit. In each case the R^2 values of 0.988, 0.989 and 0.985 for total chlorophyll (*a* + *b*), chlorophyll *a* and chlorophyll *b*, respectively demonstrate an excellent correlation between the green pixel intensity and chlorophyll concentration for the lower sample volume.

Comparing the low volume and control datasets we found no significant difference between the slopes of the two lines ($p > 0.05$, Table 3.3); this is corroborated by the overlapping 95 % confidence bands in each case.

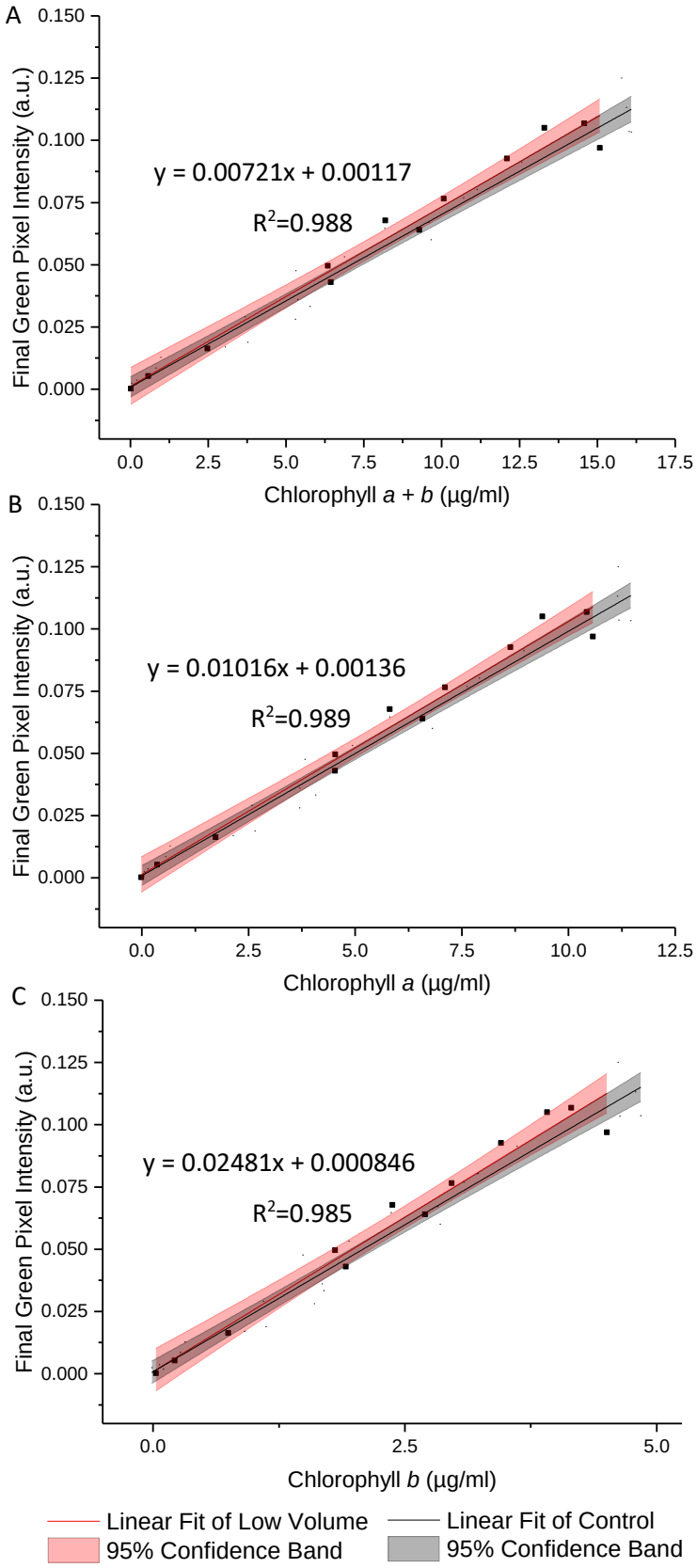

Figure 3.5 Relationship between final GPI, calculated from the RGB colour method, and (A) chlorophyll a + b, (B) chlorophyll a and (C) chlorophyll b concentrations, measured by standard extraction method in 80 % acetone, for C.reinhardtii photographed at two different culture volumes. Red = 'low volume', 3.5 ml samples; Grey = control, 5 ml samples. Data points are the mean GPI of three photographs (y) and the mean chlorophyll concentration of three sample aliquots (x).

Similarly, we found no significant difference between the intercepts of the low volume and control datasets ($p > 0.05$, Table 3.3).

Table 3.3 Regression parameters for 'Low Volume' samples.

			Slope[a]		Intercept[b]	
	Equation	R^2	$F_{1,33}$	p	$F_{1,34}$	p
Chl *a* + *b*	y=0.00721(±0.00035)x + 0.00117(±0.00337)	0.988	0.405	0.529	1.292	0.264
Chl *a*	y=0.01016(±0.00047)x + 0.00136(±0.00320)	0.989	0.335	0.567	1.251	0.271
Chl *b*	y=0.02481(±0.00139)x + 0.00085(±0.00388)	0.985	0.545	0.466	1.328	0.257

[a]p-values indicating whether the slope of the fitted line is significantly different from that of the control dataset in each case.
[b]p-values indicating whether the intercept of the fitted line is significantly different from zero and from the control dataset in each case.

During growth, even buffered cultures can vary in their pH owing to the consumption and release of carbon dioxide during photosynthesis and respiration. A selection of samples were transferred into high pH media (pH 9.5) immediately before being photographed in order to test the effect of pH on the RGB method. Figure 3.6 shows the relationship between green pixel intensity and conventional chlorophyll quantification for high pH samples compared to the control dataset (pH 7.0-8.5). The control dataset is present at a range of pH values owing to the increase in pH as the culture grows. The strong linear relationship is maintained despite the increase in pH as is evident from the high R^2 values ($R^2 > 0.995$ in each case).

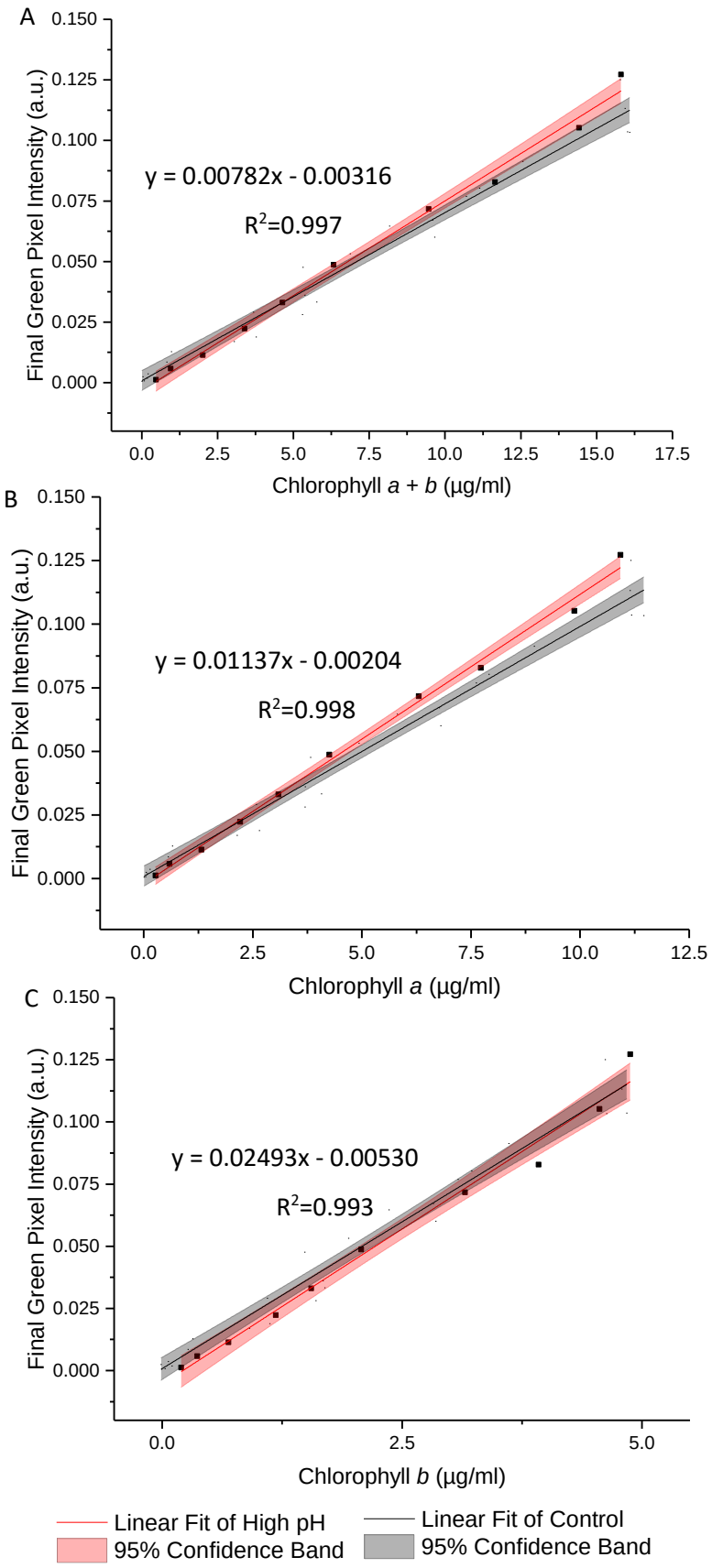

Figure 3.6 Relationship between final GPI, calculated from the RGB colour method, and (A) chlorophyll a + b, (B) chlorophyll a and (C) chlorophyll b concentrations, measured by standard extraction method in 80 % acetone, for C.reinhardtii photographed at two different culture pHs. Red = 'high pH', pH 9.5; Grey = control, pH 7.0-8.5. Data points are the mean GPI of three photographs (y) and the mean chlorophyll concentration of three sample aliquots (x).

We found a significant difference between the slopes of the high pH and control data for total chlorophyll and chlorophyll *a* (p = 0.035 and 0.009 respectively, Table 3.4). In contrast, for chlorophyll *b* there is no significant difference in the slope or intercept compared with that of the control data (p = 0.383) indicating that chlorophyll *b* concentration determined from the RGB colour method is less sensitive to changes in the culture pH. This can be seen clearly from the plots of the correlations against the control correlation (Figure 3.6). With the exception of chlorophyll *b*, the high pH correlation is steeper than the corresponding correlation for the control dataset.

Table 3.4 Regression parameters for 'High pH' samples.

			Slope[a]		Intercept[b]	
	Equation	R^2	$F_{1,31}$	p	$F_{1,32}$	p
Chl *a* + *b*	y=0.00782(±0.00021)x - 0.00316(±0.00186)	0.997	4.868	0.035	-	-
Chl *a*	y=0.01137(±0.00026)x - 0.00204(±0.00154)	0.998	7.890	0.009	-	-
Chl *b*	y=0.02493(±0.00104)x - 0.00530(±0.00292)	0.993	0.783	0.383	1.825	0.186

[a]p-values indicating whether the slope of the fitted line is significantly different from that of the control dataset in each case.
[b]p-values indicating whether the intercept of the fitted line is significantly different from zero and from the control dataset in each case.

E.coli was added at two different concentrations (A_{600} = 1.00 and 0.25) to a range of *C.reinhardtii* samples to investigate the effect of bacterial contamination on the RGB method. Figure 3.7 shows the relationship between the two methods for each concentration of *E.coli* (red) compared to the control dataset (grey). The clear linear relationship between the two methods is maintained despite the bacterial contamination (R^2 > 0.995 in both cases). There was no significant difference between the slopes of the contaminated samples and control data for chlorophyll *a*, *b* or total chlorophyll concentration (Table 3.5).

However, when fitting two lines with the same slope, there was a significant difference between the intercepts of the contaminated and control datasets for both the high and low *E.coli* cases, except for low *E.coli* chlorophyll *b* (Table 3.5). This difference in the intercepts of the contaminated and control correlations can be clearly seen in Figure 3.7, indicating that the high *E.coli* contamination is causing a zero error in the intercept.

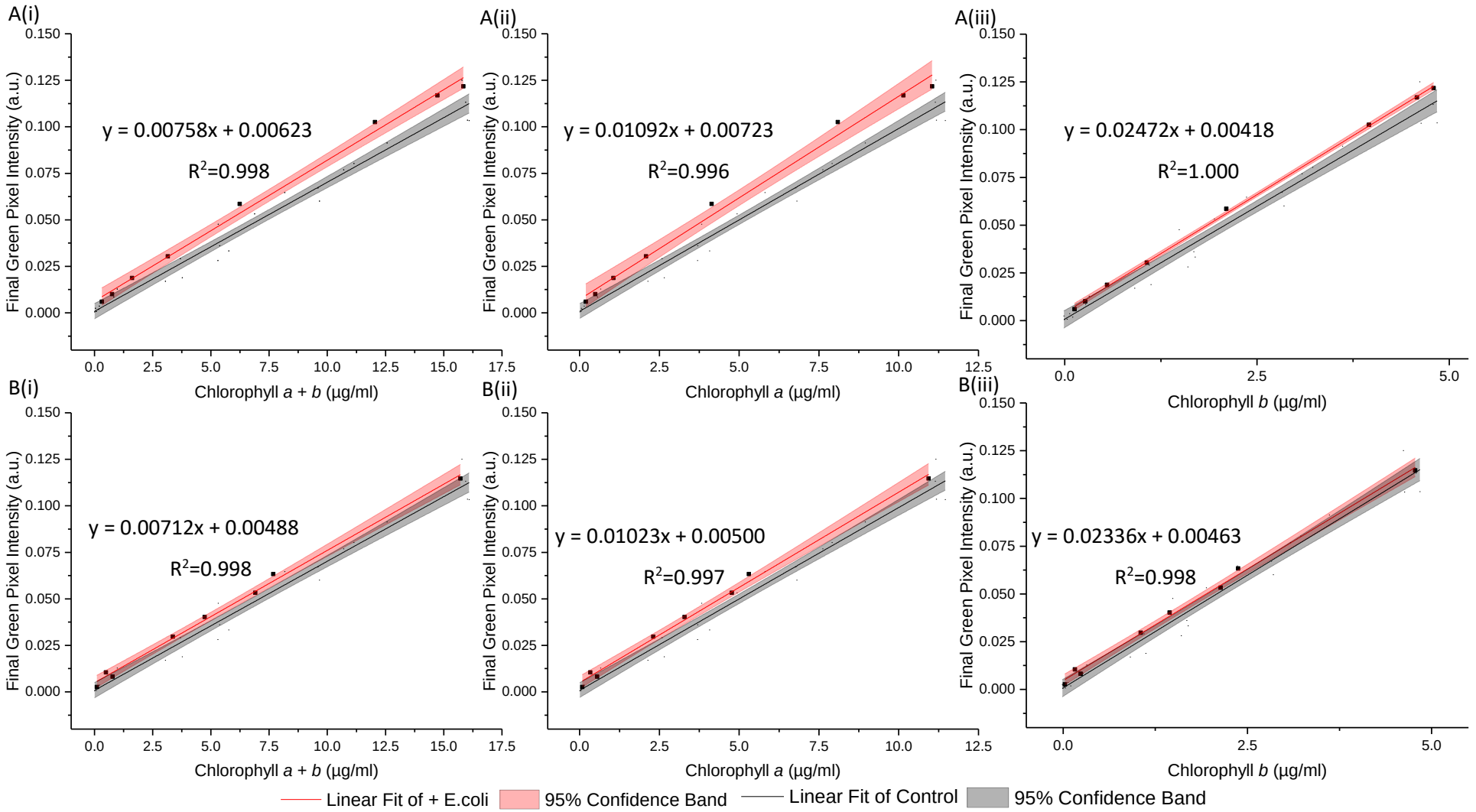

Figure 3.7 Relationship between final GPI, calculated from RGB colour method, and (i) chlorophyll a + b, (ii) chlorophyll a and (iii) chlorophyll b concentrations, by standard extraction method in 80 % acetone, for C.reinhardtii contaminated with E.coli. (A) Red = + 1.5 ml E.coli (A_{600} = 1.00); (B) Red = + 0.325 ml E.coli (A_{600} = 0.25); Grey = control, sterile samples. Data points are the mean GPI of three photographs (y) and the mean chlorophyll concentration of three sample aliquots (x).

Table 3.5 Regression parameters for contaminated samples.

				Slope[a]		Intercept[b]	
		Equation	R^2	$F_{1,29}$	*p*	$F_{1,30}$	*p*
+ 1.5 mL *E.coli*	**Chl *a* + *b***	y=0.00758(±0.00022)x + 0.00623(±0.00198)	0.998	2.526	0.123	16.156	<0.001
	Chl *a*	y=0.01092(±0.00041)x + 0.00723(±0.00257)	0.996	3.542	0.070	21.394	<0.001
	Chl *b*	y=0.02472(±0.00025)x + 0.00418(±0.00071)	1.000	0.623	0.436	5.301	0.028
+ 0.325 mL *E.coli*	**Chl *a* + *b***	y=0.00712(±0.00019)x + 0.00488(±0.00132)	0.998	0.142	0.709	4.704	0.038
	Chl *a*	y=0.01023(±0.00029)x + 0.00500(±0.00139)	0.997	0.395	0.535	6.233	0.018
	Chl *b*	y=0.02336(±0.00056)x + 0.00463(±0.00118)	0.998	0.022	0.882	1.894	0.179

[a]p-values indicating whether the slope of the fitted line is significantly different from that of the control dataset in each case.
[b]p-values indicating whether the intercept of the fitted line is significantly different from zero and from the control dataset in each case.

When starved of nitrogen, microalgae typically accumulate neutral lipids and cellular chlorophyll content is seen to deplete; this is proposed to be due to recycling of the chloroplast membrane lipids in favour of neutral lipid accumulation as an energy store (Valledor *et al*., 2014; Moellering and Benning, 2010). Reduction in chlorophyll concentration therefore has the potential to be used in many cases as an early indicator of neutral lipid accumulation. To test the effect of this process on the RGB method, a series of samples at three optical densities (A_{600} = 1.6 – 0.6) were transferred into TAP-N media and analysed periodically one sample per starting optical density over eight days as the chlorophyll content gradually decreased. Figure 3.8 shows the effect of nitrogen starvation on the correlation between green pixel intensity and chlorophyll concentration; individual symbols represent different starting optical densities.

As can be seen from the correlations between chlorophyll and final GPI, for nitrogen starved cultures final GPI is dependent on both the chlorophyll concentration and the initial biomass density (A_{600}); at similar chlorophyll concentrations a lower initial A_{600} resulted in a lower final GPI. Similarly, the intercept of the correlation with the y-axis (0 µg/mL chlorophyll) is increased with increasing initial A_{600}. For nitrogen starved *C.reinhardtii* there is a clear difference in the correlations between methods compared with that of the control dataset.

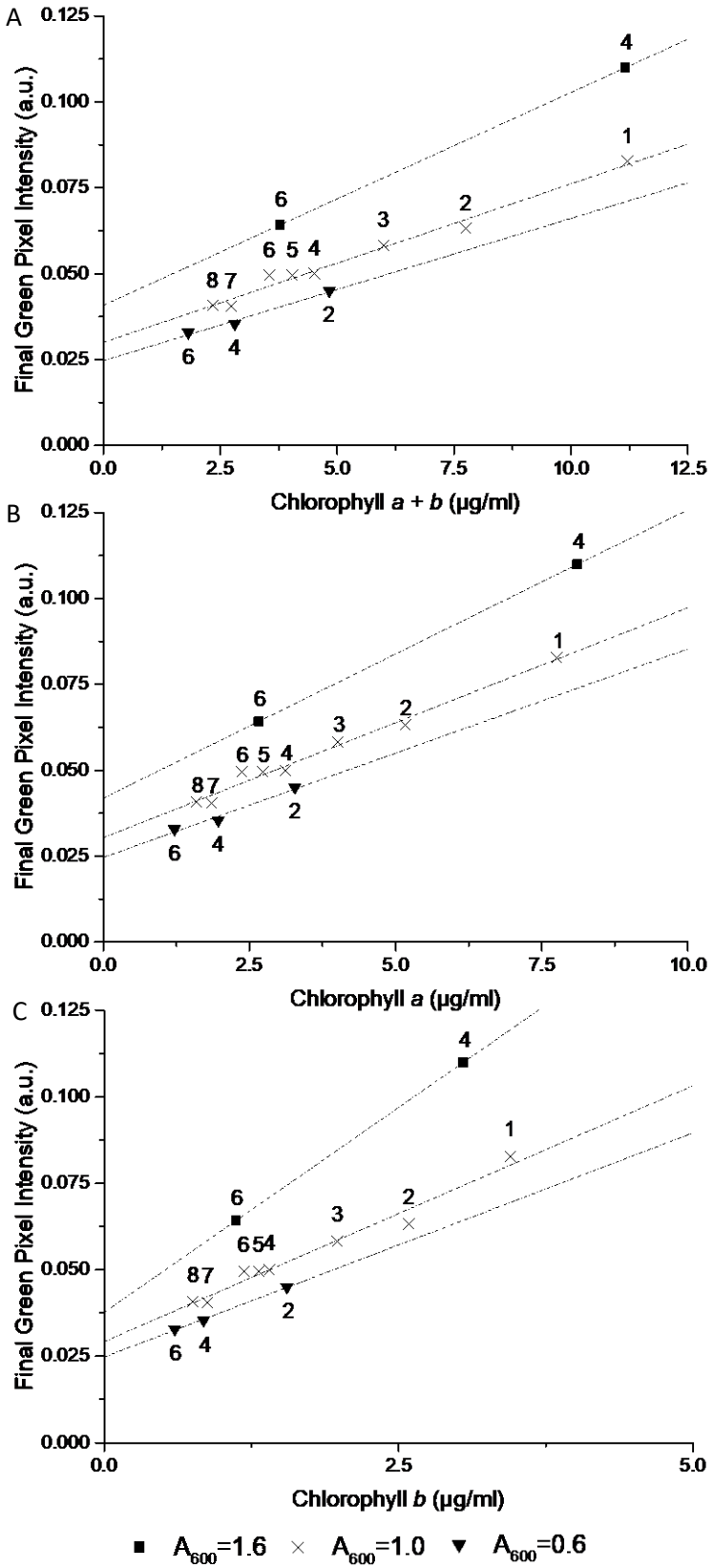

Figure 3.8 Relationship between final GPI, calculated from the RGB colour method, and (A) chlorophyll a + b, (B) chlorophyll a and (C) chlorophyll b concentrations, measured by standard extraction method in 80 % acetone, for C.reinhardtii in TAP-N media and photographed over eight days with three initial starting biomass concentrations as indicated by the different A_{600} values. Numbers above data points represent the number of days after inoculation that analysis took place. Data points are the mean GPI of three photographs (y) and the mean chlorophyll concentration of three sample aliquots (x) and lines represent linear fits through the points.

Table 3.6 gives the error generated, as a percentage of the actual value, if the standard curve for the control dataset is used to estimate chlorophyll concentration for each environmental variable; TAP-N correlations are not included owing to the poor similarity with the control. In each case, the green pixel intensity corresponding to the maximum and half maximum measurable chlorophyll concentrations for the control dataset are used to calculate the predicted and actual chlorophyll concentrations for each variable in order to calculate the generated errors.

*Table 3.6 Percentage error generated when using control data standard curve to estimate chlorophyll concentration in the presence of environmental interference.**

	Total Chlorophyll		**Chl *a***		**Chl *b***	
	% error at max	**% error at half max**	**% error at max**	**% error at half max**	**% error at max**	**% error at half max**
Low Volume	4.3	4.6	3.9	4.4	5.1	5.2
High pH	8.8	5.2	12.9	10.2	0.1	-4.8
+1.5 ml E.coli	14.9	21.1	17.8	25.3	7.9	11.4
+0.325 ml E.coli	6.4	10.7	8.1	12.4	2.4	6.2

**Percentages are calculated at the maximum measurable and half maximum measurable chlorophyll concentration from the control data standard curve.*

For the low volume, high pH and low *E.coli* concentration the errors are typically ≤ 10 % indicating only a relatively small overall error in the estimate of chlorophyll concentration. The standard curve for the control dataset could be used in each of these cases with relatively small errors. In contrast, there is a large error introduced when there is larger *E.coli* contamination with errors typically between 15-25 %. Use of the standard curve of the control dataset would yield greater errors when high levels of contamination are present. The errors shown also corroborate that *E.coli* contamination induces a zero error in the intercept of the standard curve as can be seen from the increased percentage error at lower chlorophyll concentrations, while high pH results in an increased slope of the fit seen from the reduced error at lower total chlorophyll and chlorophyll *a* concentrations.

3.4 Discussion

This study presents a simple and non-destructive method by which the concentration of chlorophyll *a*, *b* and total chlorophyll of an algal culture can be estimated from the green pixel intensity of digital photographs using a standard calibration curve. Compared with other digital image analysis methods, this method is shown to be applicable over a wide range of biomass

concentrations where the sample can be analysed *in situ* thus removing the risk of sample contamination and the need for sample destruction.

There is an excellent linear relationship (R^2 = 0.988) between green pixel intensity, calculated from the tested method, and total chlorophyll concentration, as measured by a standard spectroscopic method with chlorophyll extraction in 80 % (v/v) acetone/20 % methanol (Porra *et al*., 1989) for a sterile culture of *C.reinhardtii* in TAP media (pH 7.0-8.5), photographed at a sample volume of 5 ml, up to a concentration of 16 µg/ml total chlorophyll (green pixel intensity = 0.125). Above this, the gradient of the slope decreases indicating the curve tends towards a plateau at high chlorophyll concentrations. From this, the limit of sensitivity for the method has been estimated at a green pixel intensity of 0.125 and therefore, samples with higher chlorophyll concentration should be diluted to fall within the linear interval of the RGB method.

A selection of commonly encountered environmental variables were chosen to investigate the sensitivity of the method to environmental interference. For each variable investigated, the excellent linear relationship between green pixel intensity and chlorophyll concentration was maintained.

Statistical analysis revealed no significant difference in the green pixel intensity/chlorophyll correlation when the photographed sample volume was decreased. This indicates that the method is insensitive to this factor and a single standard curve created could be used to estimate chlorophyll concentration despite relatively small changes in culture volume. This is particularly important for time-course studies where the culture volume may be reduced gradually over time as a result of other analyses.

In contrast, we found that there is a statistically significant increase in the slope of the green pixel intensity/chlorophyll correlation for both total chlorophyll and chlorophyll *a* when pH is increased. Figure 3.9 shows the visible range absorbance spectra for a culture of *C.reinhardtii* at pH 7.0 and 9.5. For the sake of comparison, the pH 9.5 spectrum has been adjusted to a total chlorophyll concentration equivalent to that of the pH 7.0 sample assuming a directly proportional relationship between total chlorophyll concentration and biomass optical density. As can be seen from the spectra, the higher pH sample has a lower absorbance in the green region of the spectrum (approximately 520-560 nm) and higher absorbance in both the red (approximately 630-750 nm) and blue (approximately 450-490 nm) regions of the spectrum. These differences will result in the culture presenting with a stronger green colour and are likely responsible for the increased green pixel intensity of the high pH samples at similar chlorophyll concentrations given that green pixel intensity is defined as the ratio of the green pixel

component over the sum of red, green and blue components (Eq. 3.1). This increase in green colour at high pH may be as a result of chlorophyll conversion to chlorophyllin which occurs *via* the removal of a hydrocarbon side chain and replacement of the central magnesium ion with copper; copper chlorophyllin has a much more intense green colour compared with non-copper chlorophyll (Kendrick, 2012).

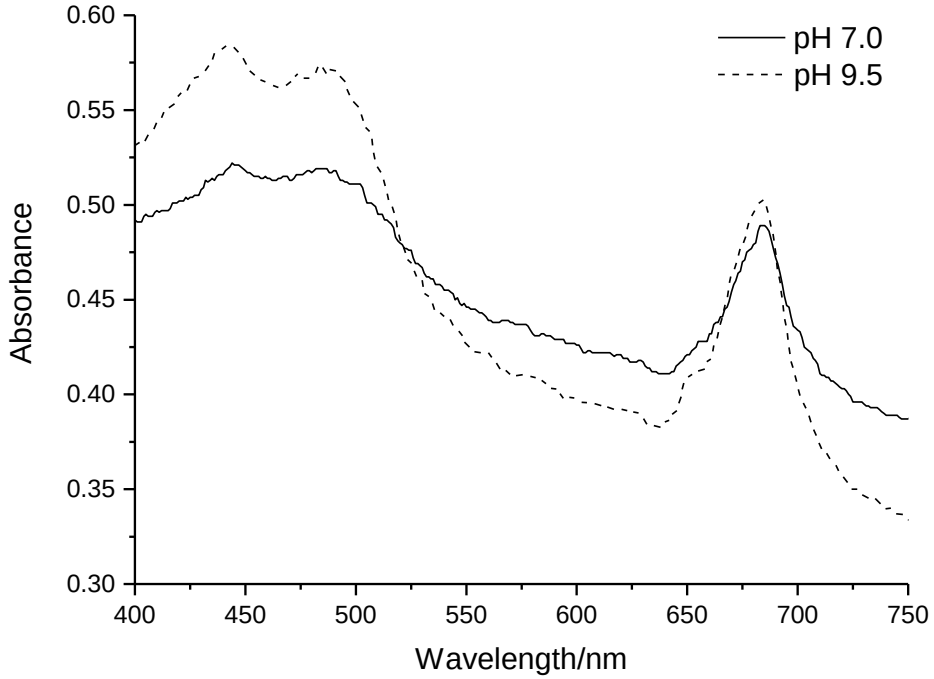

Figure 3.9 Absorption spectra of C.reinhardtii in Tris-Acetate Phosphate (pH 7.0) and CAPS-Acetate Phosphate (pH 9.5) media. In each case spectra have been normalised to a chlorophyll a + b concentration = 7.5 µg/ml.

Addition of *E.coli* (A_{600} = 1.0) revealed a significant increase in the intercept of the green pixel intensity/chlorophyll regression for total chlorophyll and chlorophyll *a* as can be seen from Figure 3.7. It is likely that a zero error in the intercept is being induced by the opacity of *E.coli* even in the absence of algal biomass. The magnitude of this error was, as expected, higher for higher levels of contamination. Given that there is no significant difference in the slope of the line with *E.coli* contamination, the zero error in the intercept could likely be corrected for where the level of contamination is known.

These observed differences in the lines for the *E.coli* and high pH cases were much lower, or absent, for chlorophyll *b* than total chlorophyll and chlorophyll *a*. The reason for this is not understood but indicates chlorophyll *b*, as calculated from the RGB method, is less sensitive to changing environmental conditions. The control correlation could be used as a

standard curve to estimate chlorophyll *b* concentration from green pixel intensity despite the environmental interferences investigated.

In contrast to the other environmental interferences investigated, there is a very clear difference between the correlations for nitrogen starved samples compared with that of the control dataset. For each initial biomass concentration, the slope of the correlation is much shallower than that of the control dataset and there is a clear increase in the intercept of the correlation with increasing initial biomass concentration. Both these factors would result in a significant overestimation of the chlorophyll concentration from the green pixel intensity if the original standard curve is used. We propose that this is most likely due to the yellow colour induced by the lipids as chlorophyll concentration decreases. Given the proximity of yellow and green within the visible spectrum, the residual yellow colour will likely cause significant interference with the green pixel intensity. The green component of the RGB scale has previously been shown to be significant when estimating the lipid content of a microalgal culture using digital image analysis (Su *et al*., 2008). Without a significant correction for lipid accumulation, the developed method is not suitable for estimating chlorophyll concentration when chlorophyll concentration is reduced as a result of nitrogen starvation due to interference from neutral lipid accumulation. Despite this, the method could be applied to qualitatively determine if chlorophyll concentration is increasing/decreasing.

This method extends other digital analysis methods by investigating its applicability over a wide range of commonly encountered environmental variables. The insensitivity of this method to sample volume and low concentrations of bacterial contamination means that the method could be used with a single standard curve in spite of these changes making this method versatile to a range of experimental investigations. The method is also shown to be useful when high levels of bacterial contamination are present or with a variable culture pH however these conditions may lead to higher errors in the estimation of total chlorophyll and chlorophyll *a*. In addition, the method is unique in its minimal use of equipment and data processing all of which can be conducted through a digital camera (e.g. within a smartphone) and widely accessible software packages present as standard on most MS Windows operated PCs.

3.5 Conclusions

Digital image analysis has been used to develop an inexpensive and rapid method to estimate chlorophyll *a*, *b* and total chlorophyll concentration of a microalgal culture without sample destruction. A standard curve between the proposed method and a standard spectroscopic method for chlorophyll quantification of a culture of *C.reinhardtii* CC-1690 revealed an excellent linear correlation up to a green pixel intensity of 0.125, corresponding to

a total chlorophyll concentration of 16 µg/ml in this case. The standard curve created can be used without modification in spite of small changes in volume, culture pH and small quantities of bacterial contamination with only small errors. Large quantities of bacterial contamination however result in an error in the intercept of the standard curve and as such overestimation of the chlorophyll concentration.

This method has the potential to be applied very widely to different algal culture situations or even environmental samples, particularly in situations where sample and equipment availability may be limited (e.g. during fieldwork). It would require following the methodology described to construct a standard curve relating chlorophyll content to GPI for the specific algal species, culture vessel and photographic set up. Although the experiments presented here used an iPhone 5S and Microsoft Paint, in principle any digital camera and software capable of analysing RGB pixel intensity could be used as long as the conditions used for establishing the standard curve (growth, photography set up and software) are subsequently replicated precisely for the experimental samples. To the best of our knowledge, the simplicity and accessibility of this method is unique compared with other non-invasive chlorophyll quantification methods, requiring very little equipment, expertise or specialist software.

Chapter Four – Assessing the Effect of Wastewater Culture Conditions on the Growth, Nutrient Uptake and Lipid Accumulation in *C.reinhardtii*

4.1 Background

Microalgae have gained extensive interest for their ability to accumulate oils, which can be used for the production of biodiesel. However, the production of microalgal biodiesel is expensive owing largely to the cultivation costs (water, nutrients etc.) of microalgae grown in raceway ponds (Campbell *et al*., 2011; Delrue *et al*., 2012; Nagarajan *et al*., 2013; Slade and Bauen, 2013).

The ability of microalgae to accumulate large quantities of nutrients has more recently generated interest for the potential applications in nutrient recycling from wastewater. Current wastewater treatment practice sees a focus on nutrient removal with little attention given to the potential for nutrient recovery. The most common nutrient control methods are through chemical precipitation for phosphorus removal and bacterial nitrification/denitrification for nitrogen removal, both of which are expensive and result in the loss of nutrients. A discussion of these and other technologies for nutrient removal are provided in Chapter 1, Section 1.3.3.

Cultivating microalgae within a wastewater treatment facility provides a free source of water and nutrients whilst also contributing to the wastewater treatment process and enabling recycling of valuable nutrients which may otherwise be lost to the environment. The resultant microalgal biomass can then be processed for extraction of nutrients for fertilisers and/or oils for the production of biodiesel. Residual biomass can additionally be anaerobically digested to produce biogas (Ehimen *et al*., 2011; Sforza *et al*., 2017; González- González *et al*., 2018).

There is a wealth of research reporting the growth and nutrient removal of microalgae cultivated in various real and synthetic wastewaters. Despite this, there is very limited research aimed at understanding the effect of wastewater conditions on the growth of microalgae and accumulation of useful products.

Similarly, there is much research aimed at understanding the triggers of oil and, to a much lesser extent, phosphate accumulation within microalgae. However, the best-known trigger of oil accumulation, nitrogen deprivation, is not practical within a wastewater medium owing to the high ammonium content. Nitrogen deprivation also leads to the rapid cessation of biomass growth (Siaut *et al*., 2011; Park *et al*., 2015) thus limiting the overall yield of useful biomass.

Wastewater treatment works (WWTW) contain a range of culture conditions depending on the composition of the wastewater and the treatment stage. Concentrations of N and P are commonly high in influent wastewater, however microalgae have previously been shown capable of removing almost 100 % of the N and P present within wastewater streams (van Harmelen and Oonk, 2006; Sun *et al*., 2013; Zhang *et al*., 2014a; Caporgno *et al*., 2015) meaning there is the possibility of nutrient starvation towards the end of the wastewater treatment process. Additionally, while nitrogen in wastewater is predominantly present as ammonium (Eckenfelder and Argaman, 1991), current nitrification practice, converting ammonium to nitrate for ammonium removal, means that different nitrogen sources can be utilised depending on the treatment stage.

Similarly, pH varies considerably during the wastewater treatment process as a result of microalgal carbon assimilation and in pond pH can reach values >10 (Mara, 2003; Camargo-Valero and Mara, 2007a). Indeed, the high pH values present are utilised within the treatment system for the removal of pathogens (Curtis *et al*., 1992; Mara, 2003). Microalgal growth is typically optimised by near-neutral pH (Kong *et al*., 2010; Ochoa-Alfaro *et al*., 2019) however, high pH has previously been reported to aid lipid accumulation in some species (see Chapter 1, Section 1.5.2) although no research has been found in *Chlamydomonas* investigating the effect of pH in the absence of either CO_2 or bicarbonate addition. The impact of pH on microalgal growth and nutrient uptake is a vital consideration for the cultivation of microalgae in wastewater.

In order to realise the potential of microalgae for simultaneous wastewater treatment, nutrient recycling and biodiesel production, it is necessary to understand the effect of individual culture conditions present within a WWTW on each of these factors. Only then can an informed decision be made as to the most useful outcomes of microalgal cultivation and a strategic decision be made about the optimum treatment stage from which to harvest microalgae.

The first part of this chapter details an initial study monitoring the growth of three *C.reinhardtii* strains on TAP medium and a synthetic wastewater (SWW) in order to identify potential conditions influencing growth and lipid accumulation. The remainder of the chapter investigates the effect of individual factors in isolation and in greater detail, investigating also the nutrient bioremediation properties and potential biodiesel production from *C.reinhardtii* in each case.

4.2 Comparing the Growth of *C.reinhardtii* on TAP medium and a Synthetic Wastewater

The focus of this initial study was to investigate the effect of wastewater culture conditions, namely pH (and the absence of buffering capacity) and nutrient concentrations in combination, on the growth and carbon storage of *C.reinhardtii*.

To do this, the growth of three strains of *C.reinhardtii* were monitored during cultivation in Tris-Acetate-Phosphate medium (TAP, a commonly used medium for the growth of *Chlamydomonas*) and a synthetic wastewater. The use of synthetic, rather than real, wastewater allows for more control and a comprehensive knowledge of the medium composition. The synthetic wastewater chosen is from the PhD thesis of Dr Anie Yulistyorini (Yulistyorini, 2016) and is based on Bold's Basal Medium (BBM, Culture Collection of Algae and Protozoa). The concentrations of nitrogen, phosphorus and carbon in the media are modified to reflect the concentrations found in raw wastewater obtained from Esholt Wastewater Treatment Works, Bradford, UK (Yulistyorini, 2016). Like wastewater, the medium is unbuffered to allow for natural fluctuations in pH due to biomass growth.

The three strains selected were CC-1690, CC-125 and CC-400. Strain CC-1690 can assimilate both nitrate and ammonium nitrogen sources and is therefore versatile to the nitrogen sources present in wastewater treatment works (WWTW). Strain CC-125 carries mutations at the *nit1* and *nit2* loci and is therefore unable to grow on nitrate as the sole available nitrogen source. Use of these strains allows for potential investigation into the effect of growth under nitrogen replete/deplete conditions by use of mixed nitrogen sources.

The final strain, CC-400 contains the *cw15* mutation and has a greatly reduced cell wall. The *cw15* mutation is present in many *Chlamydomonas* strains, of which CC-400 is the most widely used, owing to the comparative ease with which genetic modifications can be incorporated (Davies and Plaskitt, 1971; The Chlamydomonas Resource Center,d). Cell cracking is typically energy intensive, the reduced cell wall of CC-400 therefore has the potential to reduce the cost and energy requirements of processing biomass for the extraction of useful products.

4.2.1 Growth of C.reinhardtii is significantly reduced on SWW compared to TAP medium

C.reinhardtii cultures were grown each in synthetic wastewater (SWW) and TAP medium until stationary phase was reached. Cultures were monitored daily during lag and stationary phase and twice daily during exponential phase for OD (measured at 750 nm) and chlorophyll concentration. On the final day of cultivation additional samples were taken for observation of

any neutral lipid bodies by Nile-red fluorescence imaging. Full methodology is provided in Chapter 2.

Like all microorganisms, in a batch system under preferential growth conditions microalgal growth kinetics comprise three phases: lag phase where microalgal cells acclimatise to the new culture conditions; exponential (or log) phase where cell doubling occurs at regular intervals known as the doubling time (typically 6-8 hours for *Chlamydomonas* under optimal growth conditions, Harris *et al*., 1988) and stationary phase where the net rate of cell division decreases and cell population reaches a plateau.

Measurement of optical density demonstrated clear lag, exponential and stationary phases of growth for all strains of *C.reinhardtii* grown in TAP medium with cultures reaching a final optical density of 3.2-4.7 (Figure 4.1 A(i)). Total chlorophyll concentration followed a similar trend (Figure 4.1 A(ii)) and a linear relationship between chlorophyll concentration and optical density was maintained during growth (Figure 4.2 A).

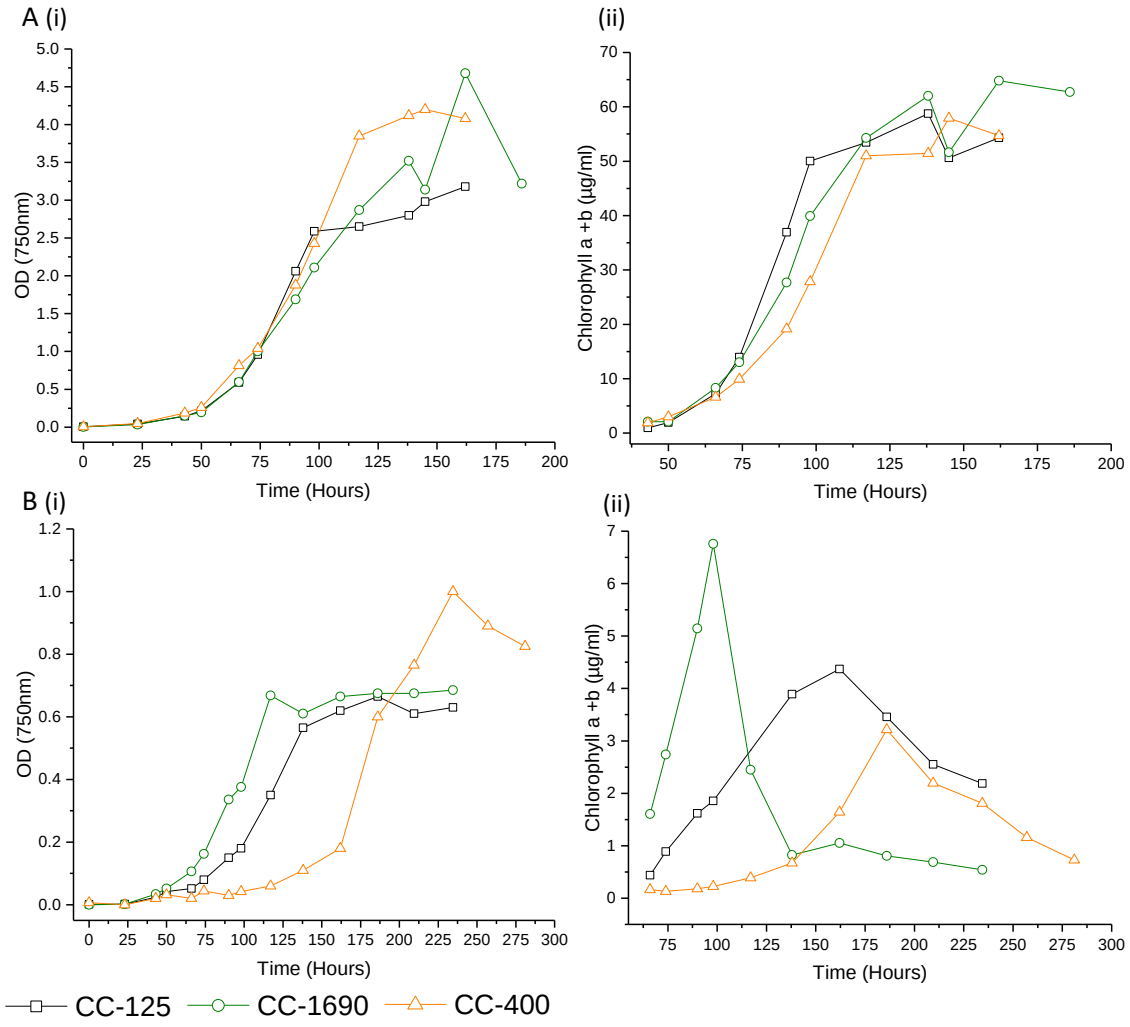

Figure 4.1 Growth of three strains of C.reinhardtii in (A) TAP media and (B) Synthetic Wastewater. (i) Optical density measured at 750 nm, (ii) chlorophyll a + b concentration. Note the different scales on each plot. Data is for single replicates only.

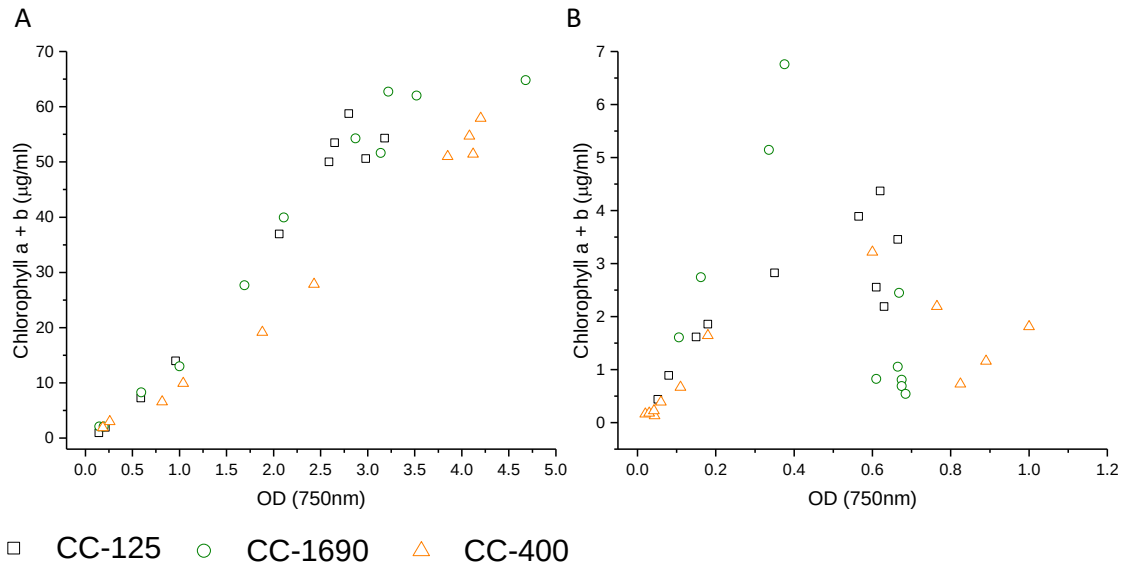

Figure 4.2 Correlation between optical density (measured at 750 nm) and total chlorophyll concentration for three strains of C.reinhardtii cultured in (A) TAP medium and (B) Synthetic wastewater.

Measurement of optical density for cultures grown in SWW was significantly reduced compared to growth on TAP medium. Optical density reached a maximum of 0.67-1.00 depending on culture strain (Figure 4.1 B(i)) indicating that one or more of the culture conditions present in SWW is limiting for growth. Chlorophyll concentration initially increased linearly with optical density (Figures 4.1 B(ii) and 4.2 B) but reached a peak between 98-186 hours, comparable with the time at the onset of stationary phase, after which a sharp drop in chlorophyll concentration was observed.

The significantly longer doubling times at exponential phase for growth on SWW compared to TAP medium confirm that the composition of SWW is significantly inhibiting culture growth. In TAP medium the observed doubling times ranged from 10.5-11.5 hours whereas in SWW the minimum doubling time observed was 18.9 hours for the strain CC-1690 while strain CC-400 has the longest doubling time of 29.1 hours (Table 4.1).

Table 4.1 Doubling times at exponential phase for three strains of C.reinhardtii grown in TAP medium and a synthetic wastewater (SWW).

	Doubling Time (hours)	
Strain	**TAP**	**SWW**
CC-125	11.1	18.9
CC-1690	10.5	15.9
CC-400	11.5	29.1

4.2.2 Cultivation in SWW leads to accumulation of TAGs after a short period of growth

Under stress conditions, the most well studied being nitrogen starvation, microalgae are known to exhibit breakdown of plastidial membranes, including the chloroplast membrane, and subsequent loss of chlorophyll in the process of recycling membrane lipids into triacylglycerols (TAGs) as an energy store (Moellering and Benning, 2010; Siaut *et al*., 2011; Valledor *et al*., 2014; Gonçalves *et al*., 2016). TAGs are stored in the cell as discrete oil bodies and can be observed by staining with the lipophilic stain Nile-red which exhibits a strong fluorescence in the presence of neutral lipids.

To test for the presence of TAG droplets, samples taken on the final day of cultivation were stained with Nile-red and any oil bodies present were observed (see Chapter 2, Section 2.5.4 for full methodology). Observation of microscopy images (Figure 4.3) reveal clear oil bodies in all cultures grown in SWW whereas negligible oil bodies were observed in cells cultivated in TAP medium. The results observed confirm that the sudden reduction in chlorophyll concentration seen for cultures grown in SWW is part of a stress response also responsible for the accumulation of TAG lipid bodies.

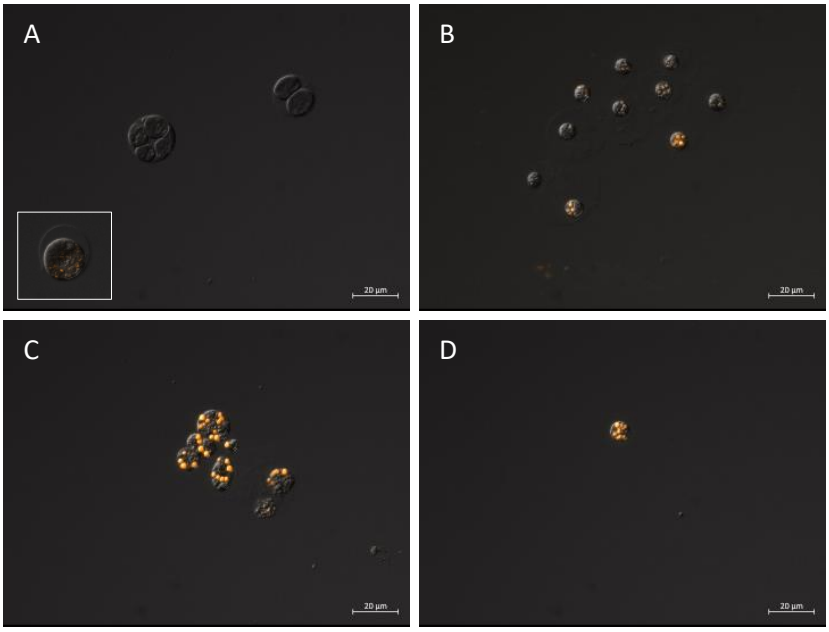

Figure 4.3 Nile-red fluorescent staining of lipid droplets present in C.reinhardtii grown in TAP and synthetic wastewater minus sodium bicarbonate (A) CC-125 in TAP; (B) CC-125 in SWW; (C) CC-1690 in SWW; (D) CC-400 in SWW. Scale bar = 20 µm. White box inset inserted from a separate image of the same culture. Fluorescence intensity not to scale and artificial colour applied.

4.2.3 Comparison of TAP and SWW reveals pH to be a potential trigger of lipid accumulation

Many factors are known to affect the growth rate of microalgae, including nutrient concentrations (Bajhaiya *et al*., 2016; Siaut *et al*., 2011) and pH (Kong *et al*., 2010; Ochoa-Alfaro *et al*., 2019). It is evident that there are one or more factors present in SWW and not in TAP medium that are both restricting the growth rate, and final optical density of the culture, and, either directly or indirectly, resulting in a sudden cessation of biomass growth and simultaneous accumulation of TAGs stored in discrete oil droplets.

By comparison of SWW and TAP medium (Table 4.2), the differences in media composition and external environmental factors that could be contributing to the results seen here are summarised as follows:

- Nutrient (N and/or P) deprivation
- Inorganic carbon availability (Sodium bicarbonate addition)
- pH
- Increased light penetration due to lower biomass density

Table 4.2 Molecular composition and pH properties of Tris-Acetate-Phosphate (TAP) medium and Synthetic Wastewater (SWW). Red, blue and green highlighting represent major differences in the macronutrients, micronutrients and pH properties respectively.

	TAP	SWW	Comments
NH_4	7.48 mM	1.78 mM	SWW has less total nitrogen than TAP
NO_3		1.80 mM	
PO_4	1.03 mM	0.48 mM	SWW< TAP
C (org.)	34.9 mM	8.56 mM	SWW< TAP
C (inorg.)		33.2 mM	SWW> TAP
EDTA	0.13 mM	0.17 mM	SWW>TAP
Mg	0.41 mM	0.30 mM	SWW≈ TAP
Na	0.27 mM	37.9 mM	SWW>> TAP
SO_4	0.51 mM	0.35 mM	SWW≈ TAP
Cl	8.22 mM	0.78 mM	SWW≈ TAP
Fe	0.018 mM	0.018 mM	SWW≈ TAP
Ca	0.34 mM	0.17 mM	SWW< TAP
Zn	76.51 µM	30.67 µM	SWW> TAP
Mn	25.57 µM	7.28 µM	SWW≈ TAP
Cu	6.29 µM	6.29 µM	SWW> TAP
Mo	6.23 µM	4.93 µM	SWW> TAP
Co	6.77 µM	1.68 µM	SWW> TAP
Initial pH	7.0	9.1	SWW>>TAP
Buffering capacity	Tris buffer (range 7.0-9.0)	N/A	

While both bicarbonate addition and increasing light intensity have been shown capable of increasing TAG accumulation, the results seen in this study are unique in that the cultures are first capable of (albeit slow) growth and the cessation of growth, sudden chlorophyll depletion and accumulation of lipids occurs suddenly and without interference – i.e. without addition of chemicals or exchange of the culture medium, approximately 4-8 days after inoculation. The cause of the observed TAG accumulation in SWW cultures is therefore likely to be a factor which allows growth initially, but which reaches a critical point, part way through the experiment, at which growth is no longer supported – i.e. depletion of critical nutrients or increasing pH.

The most well studied trigger of TAG accumulation is nutrient starvation. There is a wealth of research linking nitrogen starvation to lipid accumulation and while there is more controversy regarding the effect of phosphorus starvation on TAG accumulation, several studies report an increase in TAGs during phosphate deprivation (Chapter 1, Section 1.5.2).

In order to test whether the TAG accumulation observed is as a result of nutrient starvation, the proposed algal molecular composition of Stumm and Morgan (1996) (Eq. 4.1) was used to estimate the maximum theoretical biomass concentrations (presented as biomass potential) based on each media composition (Table 4.3). The wt% of nutrients estimated by this equation are in agreement with algal elemental analysis reported later in this report (see Appendix). In each case nitrogen is predicted to be the limiting nutrient based on compositional requirements and media composition.

$$Algal\ molecular\ composition = C_{106}H_{263}O_{110}N_{16}P \quad (4.1)$$

where *C*, *H*, *O*, *N*, *P* represent the proportions of carbon, hydrogen, oxygen, nitrogen and phosphorus respectively.

Table 4.3 Potential biomass concentration based on media nutrient concentrations and the proposed algal molcular composition $C_{106}H_{263}O_{110}N_{16}P$ (Stumm and Morgan, 1996).

		Biomass Potential (g/L)	
		TAP	SWW
Nitrogen	$NH_4^+ + NO_3^-$	-	0.83
	NH_4^+ only[a]	1.66	0.42

[a] *Presented separately for strain CC-125 which is unable to grow on* NO_3^-

Maximum biomass concentration was estimated by use of a correlation between optical density and volatile suspended solids (VSS) (Figure 4.4, Table 4.4) and compared to the theoretical biomass potential (Table 4.3).

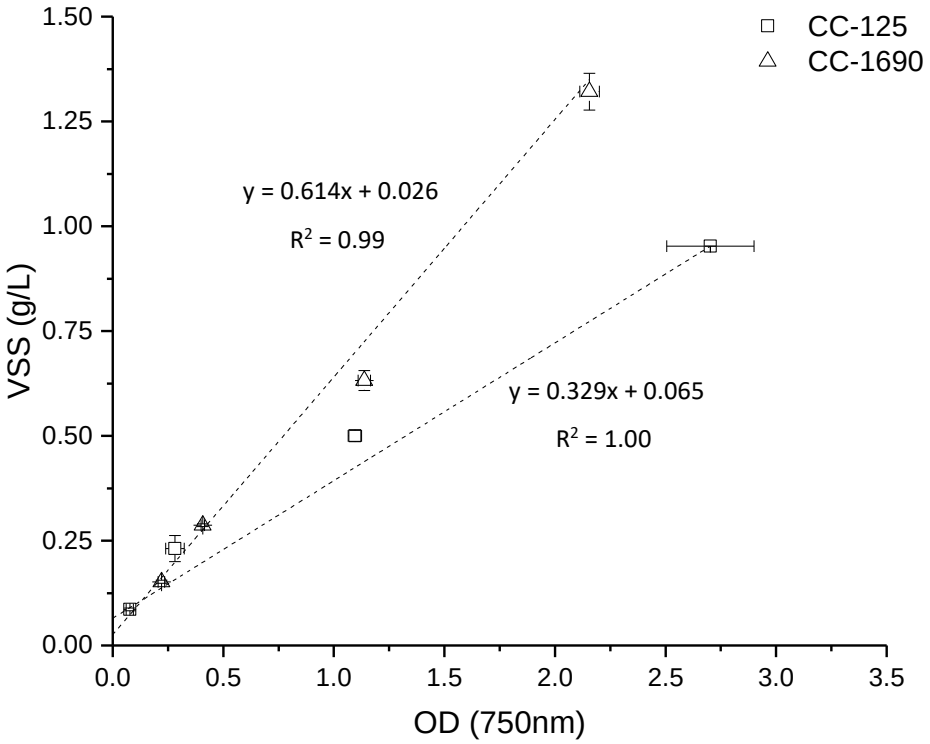

Figure 4.4 Correlation between optical density (measured at 750nm) and volatile suspended solids (VSS) for 'wild-type' C.reinhardtii strains.

Table 4.4 Maximum estimated biomass concentration for each strain of C.reinahrdtii grown in TAP and SWW. Biomass concentration was calculated from the maximum measured OD and the OD/VSS correlation.

	Estimated Maximum Biomass Concentration (g/L)	
Strain	**TAP**	**SWW**
CC-125	1.11	0.28
CC-1690	2.90	0.45
CC-400[a]	2.56	0.57

[a] *Calculated from CC-1690 correlation to estimate max VSS (due to GMO restrictions)*

Comparing Tables 4.3 and 4.4, strains CC-1690 and CC-400 exceeded the predicted biomass potential when grown in TAP medium. Nitrogen deprivation is known to trigger TAG accumulation however cultures grown in TAP medium did not contain oil bodies. It is most likely therefore that either the OD/VSS correlation overestimates VSS (strain CC-1690 showed high levels of flocculation in correlation samples and this a possible cause of VSS overestimation from this correlation) or that nutrient requirements are lower than predicted by the equation of Stumm and Morgan under these conditions.

The maximum estimated biomass concentration for each strain cultivated in SWW is significantly lower than that predicted by nutrient compositional requirements and the medium

composition. We can therefore conclude that the observed stress response is not as a result of nitrogen deprivation. Furthermore, if nitrogen stress were a factor it would be expected that strain CC-125, which is unable to grow on nitrate, would begin chlorophyll degradation at a significantly lower biomass density than strains CC-1690 and CC-400 due to the lower concentration of available nitrogen; this is not the case. Both nitrogen and phosphorus are in significant excess given the resultant biomass density and are therefore unlikely to be responsible for the slower growth rate of cultivation in SWW compared to TAP.

Microalgae are known to cause increases in media pH owing to the assimilation of acidic CO_2 or acetate from the medium (Mara, 2003). In unbuffered cultures such as the synthetic wastewater used here, this pH rise can be more dramatic. pH is known to impact the growth of microalgae, growth of *Chlamydomonas* is most efficient on neutral or marginally acidic pHs (Kong *et al*., 2010; Ochoa-Alfaro *et al*., 2019), it is therefore foreseeable that a rise in pH over time could result in conditions unable to support microalgal growth.

Cultures grown in TAP medium rose from pH 7.00 to approximately 8.30 representing the top of the buffering range for Tris-buffer (Table 4.5). The pH of SWW cultures similarly increased over the cultivation period with the pH of cultures rising from 9.09 to between 9.61 and 10.28 depending on the strain. Most significant is the difference between initial culture pH for TAP and SWW. The increased initial pH of SWW occurred upon autoclaving with the pH rising from near neutral to 9.09 after autoclaving. This is proposed to be a result of the added sodium bicarbonate which exists predominantly as HCO_3^- within the medium at room temperature and neutral pH. Upon heating, the carbonate/bicarbonate/carbonic acid equilibrium is affected and promotes the release of CO_2 as its solubility in water is significantly reduced, driving off CO_2 gas and resulting in an increase in the medium pH (Wiebe and Gaddy, 1940).

Table 4.5 Initial and final pH for each strain of C.reinhardtii grown in TAP and SWW until stationary phase (approx. 7 days in TAP or 9.5-12 days in SWW). Initial pH was measured before addition of biomass. Final pH was measured after centifugation to remove biomass.

	TAP		SWW	
Strain	**pH @ start**	**pH @ end**	**pH @ start**	**pH @ end**
CC-125	7.00	8.36	9.09	10.28
CC-1690	7.00	8.23	9.09	10.07
CC-400	7.00	8.34	9.09	9.61

A plausible explanation for the results presented in this section is that the higher initial pH of SWW severely restricts the growth of *C.reinhardtii* resulting in the much longer doubling times reported. The gradual rise in pH from one capable of supporting growth to one too alkaline

could explain the initial growth of *C.reinhardtii* in SWW followed by the cessation of growth and the observed stress response. pH also represents a major difference between SWW and BBM (known to support efficient growth of *Chlamydomonas,* Yulistyorini, 2016). While the media compositions are largely similar, BBM has a starting pH of approximately 6.7 (Culture Collection of Algae and Protozoa) compared with 9.1 in SWW.

4.3 Investigating the Effect of Initial Culture pH on the Growth of *C.reinhardtii*

Comparing the growth of *C.reinhardtii* on synthetic wastewater (SWW) and TAP medium revealed a much reduced growth rate for each culture grown in synthetic wastewater compared with TAP medium. Based on a comparison of the culture conditions (Table 4.2), pH was identified as the most probable cause of the observed difference in growth rates; SWW has an initial pH of 9.1 compared to 7.0 for TAP. In order to test this hypothesis, 3.5 mL cultures of *C.reinhardtii* were grown in SWW contained within 7 mL Bijou flasks for 12 days at a range of initial media pH values. Bijou flasks were placed upside down on a shaking platform to facilitate light to enter the cultures from the light panel above, and the cultures were cultivated under the conditions previously reported (see Chapter 2, Section 2.4.2). Cultures were opened once daily under sterile conditions to allow for gas exchange and the culture growth was monitored daily by use of the photographic method presented in the previous chapter (see Chapter 3, Section 3.2 for full methodology). Sodium bicarbonate was removed from the medium to allow for control of the initial medium pH.

4.3.1 Increasing initial medium pH results in a significant decrease in the growth rate of C.reinhardtii

Measurement of green pixel intensity (GPI) revealed initially successful growth of all cultures up to a starting medium pH of 8.62 (Figure 4.5). However, similarly to growth on SWW (see Section 4.2), after an initial period of growth, a sudden drop in GPI was observed for all cultures after approximately 3-6 days depending on the strain. In contrast, no growth was observed for cultures cultivated at an initial pH of 9.60 indicating that there is a critical point between pH 8.62-9.60 where the pH of the medium is no longer able to support the growth of *C.reinhardtii*.

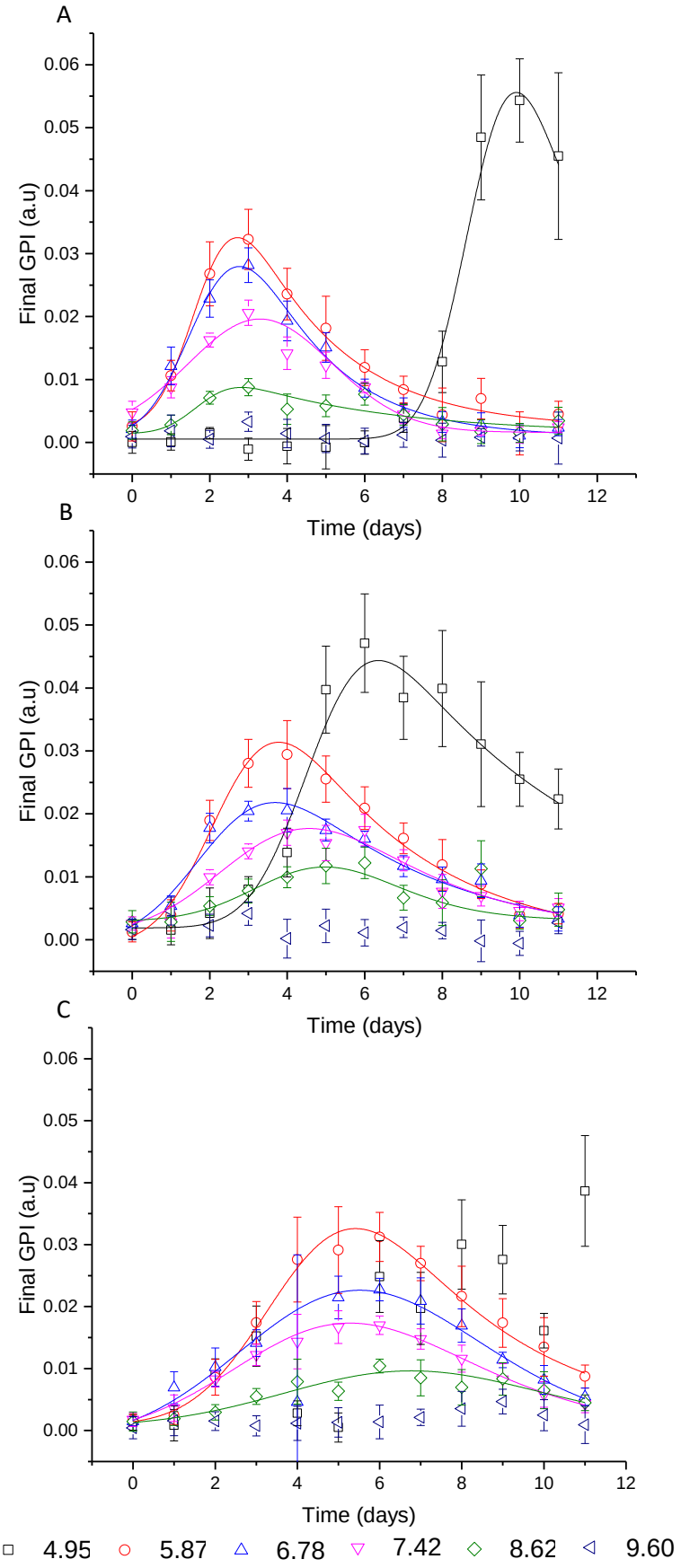

Figure 4.5 Final Green Pixel Intensity obtained from digital photographs of three strains of C.reinhardtii (A) CC-125; (B) CC-1690 and (C) CC-400 grown in SWW in the absence of sodium bicarbonate at six initial culture pH values. Data are the mean and combined standard deviations of two replicates. Data fit by OriginPro9.1 to a GaussMod fit.

Considering the initial growth of cultures, before the observed decrease in GPI, the peak height of each strain is seen to be highly dependent on the initial medium pH. Increasing pH led to a significant decrease in the peak height observed for each strain and this is supported by the decreasing specific growth rate and increasing GPI doubling time with increasing medium pH (Table 4.6). Despite the shorter doubling time and increased peak height, cultures grown at an initial medium pH of 4.95 demonstrated significantly longer lag times than those at higher pH (lag times for pH 5.87-8.62 were comparable within strains). It is proposed that pH 4.95 is unable to support efficient growth of *C.reinhardtii* however small amounts of growth are sufficient to raise the pH to one favourable for growth thus allowing for the delayed exponential phase growth observed.

Table 4.6 Doubling times at exponential phase for three strains of C.reinhardtii grown in SWW at six initial culture pH values. pH 9.60 is not shown due to lack of growth.

Strain	Initial pH	GPI Doubling Time (h)[a]
CC-125	**4.95**	0.61
	5.87	0.79
	6.78	0.82
	7.42	1.73
	8.62	1.10
CC-1690	**4.95**	1.15
	5.87	0.65
	6.78	1.15
	7.42	1.63
	8.62	2.65
CC-400	**4.95**	-[b]
	5.87	1.20
	6.78	1.46
	7.42	1.59
	8.62	2.34

[a] *Time taken for GPI to double. This does not necessarily represent the cell doubling time.*
[b] *Fit did not converge and so a specific growth rate and doubling time could not be calculated*

The results presented show that growth of *C.reinhardtii* is significantly favoured by near-neutral medium pH with increasing alkalinity significantly hindering both the final biomass density and growth rate of cultures. This supports the hypothesis that the initial pH value of

SWW is responsible for the reduced growth rate observed when compared with cultivation in standard TAP medium.

4.3.2 The accumulation of TAGs is independent of initial pH

In order to test for the presence of oil bodies, samples were taken on the final day of cultivation and stained with Nile-red fluorescent stain. Nile-red staining shows clear oil droplets in all cultures regardless of the initial media pH (Figure 4.6) and confirms the occurrence of a similar stress response to that seen for cultures grown in full SWW independent of the initial media pH. Microscopy images are presented for strain CC-125 and are representative of the results observed for all strains. Noticeably different is the size of cells from cultures with initial media pH of 4.95 compared with higher initial pH. Cells have previously been shown to increase in size in response to stressors such as phosphate deprivation (Bajhaiya *et al*., 2016). Assuming that the response to stress begins at the peak pixel intensity, it is likely that the increase in size of higher pH cultures is due to the prolonged period in which they have been under stress conditions compared with the pH 4.95 sample which has a noticeably longer lag-phase.

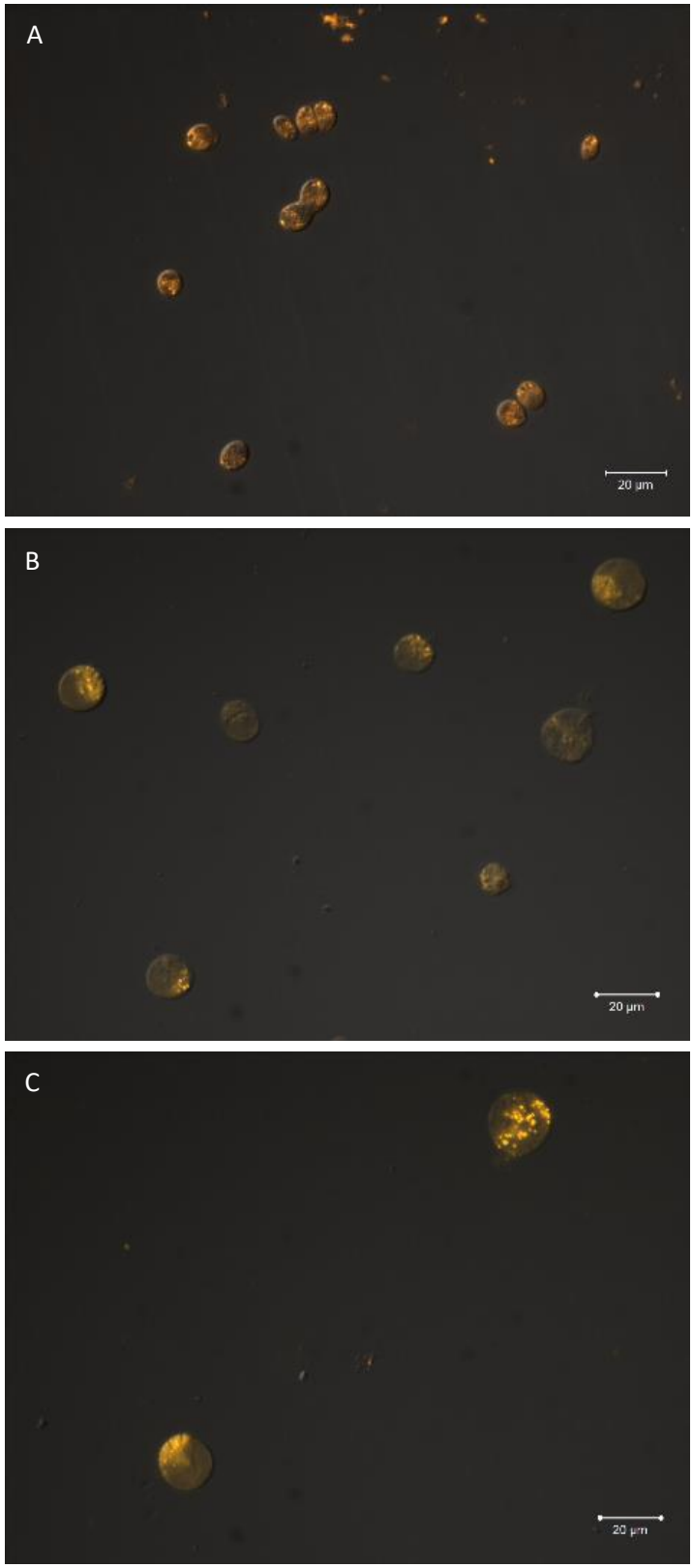

Figure 4.6 Nile-red fluorescent staining of lipid droplets (orange) present in C.reinhardtii strain CC-125 grown in synthetic wastewater minus sodium bicarbonate at initial pH (A) 4.95, (B) 5.87 and (C) 7.42. Scale bar = 20 µm. Fluorescence intensity not to scale and artificial colour applied.

Despite the varying initial medium pH, all cultures (excluding those where no growth was observed) reached a final pH between 9.29 and 9.83; no correlation was observed between the initial and final pH (Table 4.7). This supports the hypothesis that the sudden drop in chlorophyll concentration (proportional to GPI) observed here and when cultures were grown on full SWW (see Section 4.2) is due to a rise in pH from one able to support growth to one which leads (either directly or indirectly) to cessation of growth and subsequent lipid accumulation.

Table 4.7 Initial and final pH of three strains of C.reinhardtii grown for 12 days in SWW at a range of initial media pH values.

Strain	Initial pH	Final pH
CC-125	4.95	9.29
	5.87	9.57
	6.78	9.63
	7.42	9.62
	8.62	9.69
CC-1690	4.95	9.75
	5.87	9.69
	6.78	9.69
	7.42	9.82
	8.62	9.83
CC-400	4.95	9.50
	5.87	9.59
	6.78	9.72
	7.42	9.61
	8.62	9.67

4.4 Investigating the Effect of pH with Varying Nitrogen Source and Availability of Bicarbonate

Growth of *C.reinhardtii* on a synthetic wastewater (SWW) revealed an initial period of slow growth before chlorophyll concentration suddenly dropped and neutral lipids were accumulated in the form of oil droplets within the cells (Section 4.2). In order to understand this effect more fully, eight media preparations were chosen for investigation of individual culture conditions in isolation. For simplicity, all experiments were conducted in TAP medium with modifications made to investigate each condition of interest separately. Furthermore, strain CC-1690 was chosen for ongoing experiments since it is capable of growth on either ammonium

or nitrate as the sole nitrogen source. Its 'wild-type' status also allows for analysis in laboratories with restrictions on the use of GMOs.

To investigate thoroughly the effect of high pH, TAP buffer was replaced with CAPS (buffering range 9.7-11.1) in four media preparations and the media set to an initial pH of 9.5. At high pH, ammonium ions (*pKa* = 9.3) readily dissociate to produce free ammonia (NH_3) which is toxic to microalgae even at low concentrations (Azov and Goldman, 1982; Källqvist and Svenson, 2003; Gutierrez *et al*., 2016). In order to investigate the effect of high pH with and without the possibility of ammonia toxicity, ammonium chloride was replaced with an equal molar concentration of sodium nitrate ('TAP (NO3) High pH') in two of the four 'high pH' media. Cultivation was also performed in TAP (NO3) at an initial pH of 7.00 to individually investigate the effect of a shift in nitrogen source at neutral pH.

The effect of pH on lipid accumulation has previously been reported in some organisms and with varying effect (see Chapter 1, Section 1.5.2), however rarely in the absence of additional carbon, either as bubbled CO_2 or as bicarbonate. It is therefore hard to determine whether reported lipid accumulation as a result of high pH is due to the pH or is in fact due to the additional availability of carbon. In order to test this, sodium bicarbonate was added to two of the high pH media (one each of ammonium and nitrate based) but left absent in the remaining media preparations.

Finally, nutrient starvation (nitrogen starvation 'TAP-N' and phosphorus starvation 'TA-') was included as a positive control for high lipid accumulation (TAP-N) and because, if bioremediation by microalgae is successful, there is likely to be a period of nutrient starvation at the end of the wastewater treatment process. Standard TAP medium was included as a control.

To test the effect of each media preparation, cultures were first grown to mid log phase ($OD_{750} \approx 1.5$) in TAP medium ('TAP Initial') before being exchanged into fresh media of interest to an initial $OD_{750} = 1.0$. A high starting biomass concentration was chosen in order that the light penetration was similar across cultures at the point of exchange and such that both culture growth and death could be observed. All cultures were grown on a shaking platform at constant temperature and 24-hour light for seven days after media exchange. Cultures were monitored daily for OD (measured at 750 nm), chlorophyll concentration and pH and samples were collected for analysis of the media and biomass. On the final day of cultivation, samples were also taken for observation of any neutral lipid droplets by Nile-red fluorescent imaging. Full methodology and media recipes are provided in Chapter 2.

4.4.1 Growth of C.reinhardtii is severely restricted by nitrogen starvation and high pH

Cultures grown in TAP (NO3) and TA- grew very similarly to the control (TAP) to a maximum optical density of approximately 3.0 and demonstrate a typical sigmoidal fit for optical density, chlorophyll concentration and dry weight (Figure 4.7). The similar doubling times (17.88, and 15.06 hours respectively, Table 4.8) and final biomass concentrations of cultures grown in TAP with either ammonium (TAP) or nitrate (TAP (NO3)) as the sole nitrogen source indicate that growth of *C.reinhardtii* is unaffected by the source of nitrogen. The effect of nitrogen source on the growth of *C.reinhardtii* is investigated further in Chapter 5 and is used here predominantly as a control to understand the effect of high pH with either an ammonium or nitrate nitrogen source.

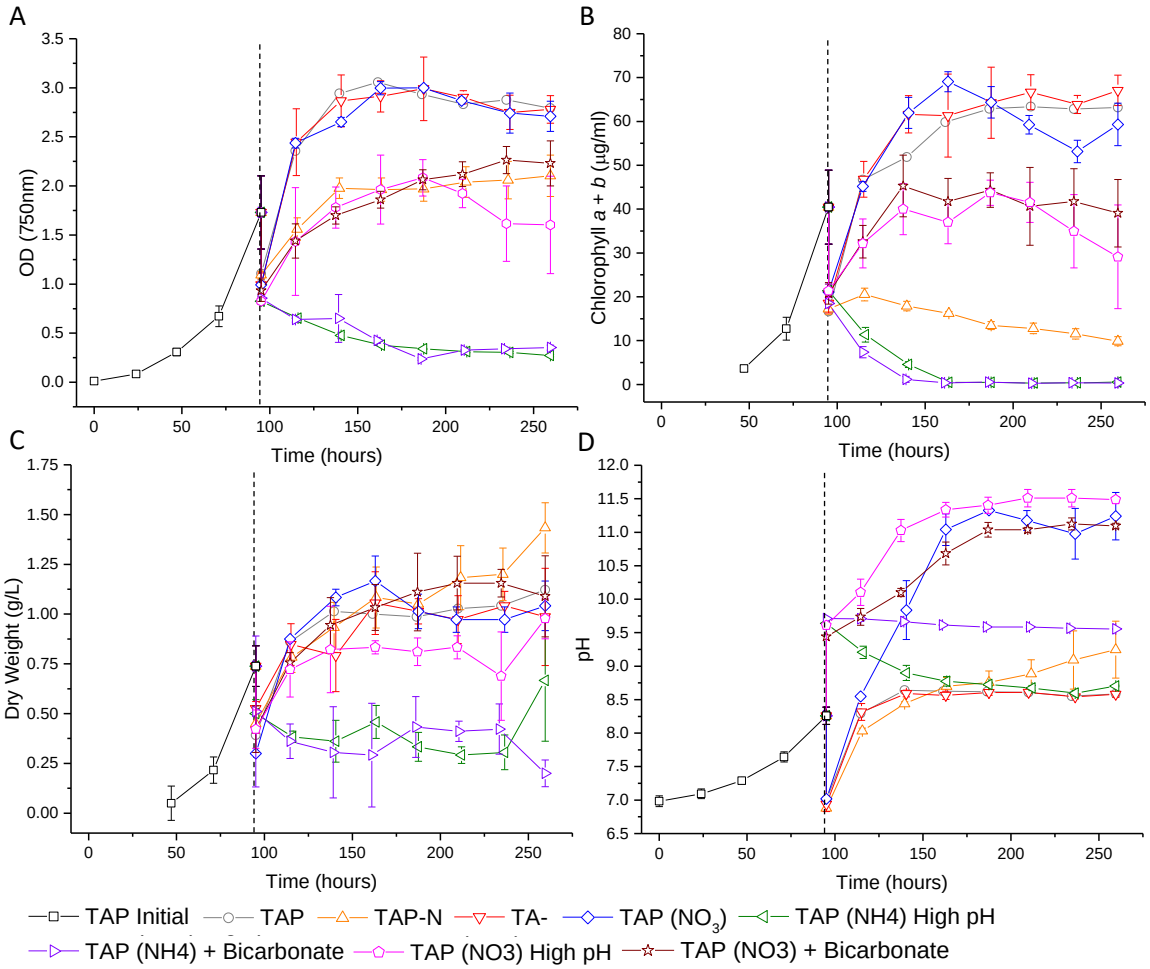

Figure 4.7 (A) Optical density measured at 750 nm, (B) total chlorophyll concentration, (C) dry biomass weight and (D) pH of wild-type C.reinhardtii strain CC-1690 cultured in eight media preparations. All cultures were first grown to mid-log phase in standard TAP media (TAP Initial) before being washed and exchanged into the media of interest. Dashed lines represent the time at media exchange. All points are the mean and standard deviation of nine (TAP Initial) or three (all others) biological replicates.

Table 4.8 Doubling times for C.reinhardtii grown in eight different media preparations based on standard Tris-Acetate-Phosphate (TAP) medium. Data shows the mean of nine (TAP initial) or three (all others) biological replicates. Doubling times were determined from optical density at exponential phase growth (47-95 and 95 to approx. 115 hours for TAP initial and all others respectively.

	Doubling Time (hours)
TAP Initial	19.25
TAP	17.88
TAP-N	39.98
TA-	15.38
TAP (NO3)	15.06
TAP (NH4) High pH	-61.86
TAP (NH4) + Bicarbonate	-46.36
TAP (NO3) High pH	24.56
TAP (NO3) + Bicarbonate	31.17

Phosphorus deprivation has previously been shown to significantly reduce the growth rate of wild-type *C.reinhardtii* (Bajhaiya *et al*., 2016) however, cultures grown in TA- had a similar doubling time to those grown in full TAP medium. Under phosphate replete conditions, microalgae are known to accumulate phosphorus in excess of that required for growth ("luxury phosphorus uptake") and which can subsequently be used to maintain cell division in the absence of phosphate (Powell *et al*., 2009). It is likely that at the point of exchange into phosphate deprived medium, the inoculum biomass had accumulated sufficient stored phosphorus to sustain growth until stationary phase.

It is well reported that, when starved of nitrogen, cellular chlorophyll concentration decreases, proposed as a means to recycle membrane lipids (including the chloroplast membrane) into TAGs as an energy store (Moellering and Benning, 2010; Siaut *et al*., 2011; Valledor *et al*., 2014; Gonçalves *et al*., 2016). Subsequently, biomass productivity is severely restricted with cell division reported to halt within 24 hours of nitrogen removal (Schmollinger *et al*., 2014). On exchange into nitrogen deprived medium (TAP-N), cultures initially grew slowly (doubling time = 39.98 hours) for approximately 48 hours before growth ceased and stationary phase was reached at a maximum optical density of approximately 2.1. Chlorophyll concentration decreased steadily after 24 hours of nitrogen deprivation to approximately one sixth that for cultures grown in full TAP medium. In contrast, biomass dry weight increased steadily, similarly to that seen for the TAP control and likely represents the additional accumulation of carbon into neutral lipids within existing cells.

Of the four 'high pH' cultures (initial pH = 9.5), those grown in nitrate as the sole nitrogen source maintained growth after media exchange with doubling times of 31.17 and 24.56 hours

with and without bicarbonate respectively. Like all organisms, pH has a significant effect on the growth of microalgae with the growth of *Chlamydomonas reinhardtii* optimised by near-neutral pH (Figure 4.5; Kong *et al*., 2010; Ochoa-Alfaro *et al*., 2019). The doubling time for 'high pH (NO3)' cultures is significantly longer than the control TAP cultures (initial pH = 7.0) as is expected given the much higher starting pH.

In contrast, 'high pH' cultures grown in ammonium as the sole nitrogen source saw a significant decrease in the optical density and chlorophyll concentration on media exchange; optical density plateaued at a final optical density of approximately 0.3 both with and without bicarbonate addition. Within 72 hours, chlorophyll concentration had fallen to < 0.9 μg/mL for all cultures and a clear colour change was observed from green to pale yellow/cream. Cultures were also observed to flocculate as has previously been observed in response to unfavourable pH (Vandamme *et al*., 2012; Wu *et al*., 2012; Byrd and Burkholder, 2017). In contrast, biomass dry weight remained largely constant after media exchange suggesting that the changes in chlorophyll concentration and optical density are likely a result of mixed cell necrosis, changing cell morphology and flocculation of the remaining cells; flocculation will result in an underestimation of biomass density from OD measurements. The results presented here are comparable to those seen for other algal species in response to ammonia toxicity afforded by the conversion of ammonium to free ammonia at high pH (Azov and Goldman, 1981; Källqvist and Svenson, 2003).

The addition of bicarbonate to 'high pH' cultures had no observable effect on the optical density, chlorophyll concentration and dry weight profiles.

During photosynthetic growth, microalgae assimilate carbon dioxide from the medium causing the pH to rise (Mara, 2003; Chi *et al*., 2011). With the exception of high pH ammonium cultures, the pH for all cultures rose steadily until a plateau was reached at the emergence of stationary phase. TAP, TAP-N and TA- cultures reached a final pH of approximately 8.5 representing the top of the buffering range for Tris buffer. Both high pH nitrate cultures saw a similar increase in the pH of the medium, rising from 9.5 to approximately 11.1 and 11.5 with and without bicarbonate addition respectively, within the buffering range of CAPS buffer. Cultures grown in nitrate medium (TAP (NO3)) saw a substantial increase in the pH beyond the buffering range of Tris buffer from an initial pH = 7.0 to pH 11.2 by the end of the experiment. This is due to the different equilibrium reactions involved in the uptake and assimilation of NO_3^- compared to NH_4^+ and is explored in more detail in the following chapter (Chapter 5). Unlike other cultures, high pH ammonium cultures saw a reduction in pH from approximately 9.7 to 9.6 and 8.7 with and without bicarbonate addition respectively and is likely due to the reduction in

biomass concentration, as a result of ammonia toxicity, allowing for additional CO_2 absorption into the medium.

4.4.2 The fate of N and P in different culture conditions

One of the main goals of combining microalgal cultivation with wastewater treatment is as a means by which to efficiently remove and potentially recover nutrients, namely nitrogen and phosphorus from wastewater (see Chapter 1, Section 1.3.4). Microalgae are similarly able to accumulate carbon (as biomass or in carbon storage products, lipids and starch), using an organic carbon source from wastewater or as CO_2 from the atmosphere (during photosynthesis), thus contributing to carbon sequestration and providing a carbon source ideal for the production of biodiesel. Indeed, simultaneous wastewater treatment during microalgal cultivation has been suggested as a necessity to make the production of microalgal biodiesel economically feasible (Park *et al*., 2011). An added advantage of bioremediation by microalgae is that nitrogen and phosphorus incorporated into the biomass can be recycled into fertilisers either by extraction (e.g. precipitation as struvite, either from microalgal anaerobic digestate liquor or from microalgal biomass prior to lipid extraction for biodiesel production) or by the direct use of microalgae as a fertiliser (Mulbry *et al*., 2005; Mulbry *et al*., 2007; Barbera *et al*., 2017; Teymouri *et al*., 2016; Wuang *et al*., 2016).

4.4.2.1 Total nutrient removal is optimised by near-neutral pH

In order to test the N and P removal and bioremediation ability of microalgae under the eight different media preparations, the nutrient concentrations in the media were monitored during cultivation. Phosphorus concentration, as soluble orthophosphate, was monitored daily. Nitrogen content (as either ammonium or nitrate) was measured at the start and end of the experiment. All samples were filtered (0.2 µm) immediately after collection to remove precipitants and remove the possibility of precipitant re-solubilisation during analysis. Nutrient removal reported is the total removal from all mechanisms (i.e. precipitation, volatilisation and uptake by algal biomass).

After approximately seven days of cultivation, cultures grown in TAP medium had removed an average of 67.5 mg/L N and 13.3 mg/L P (from starting concentrations of 105 mg/L N and 32 mg/L P respectively based on the media composition) from the medium after exchange at mid-log phase (Figure 4.8). Both N and P removal in each of the remaining seven media preparations are found to be statistically different from the control (TAP) values ($p < 0.05$).

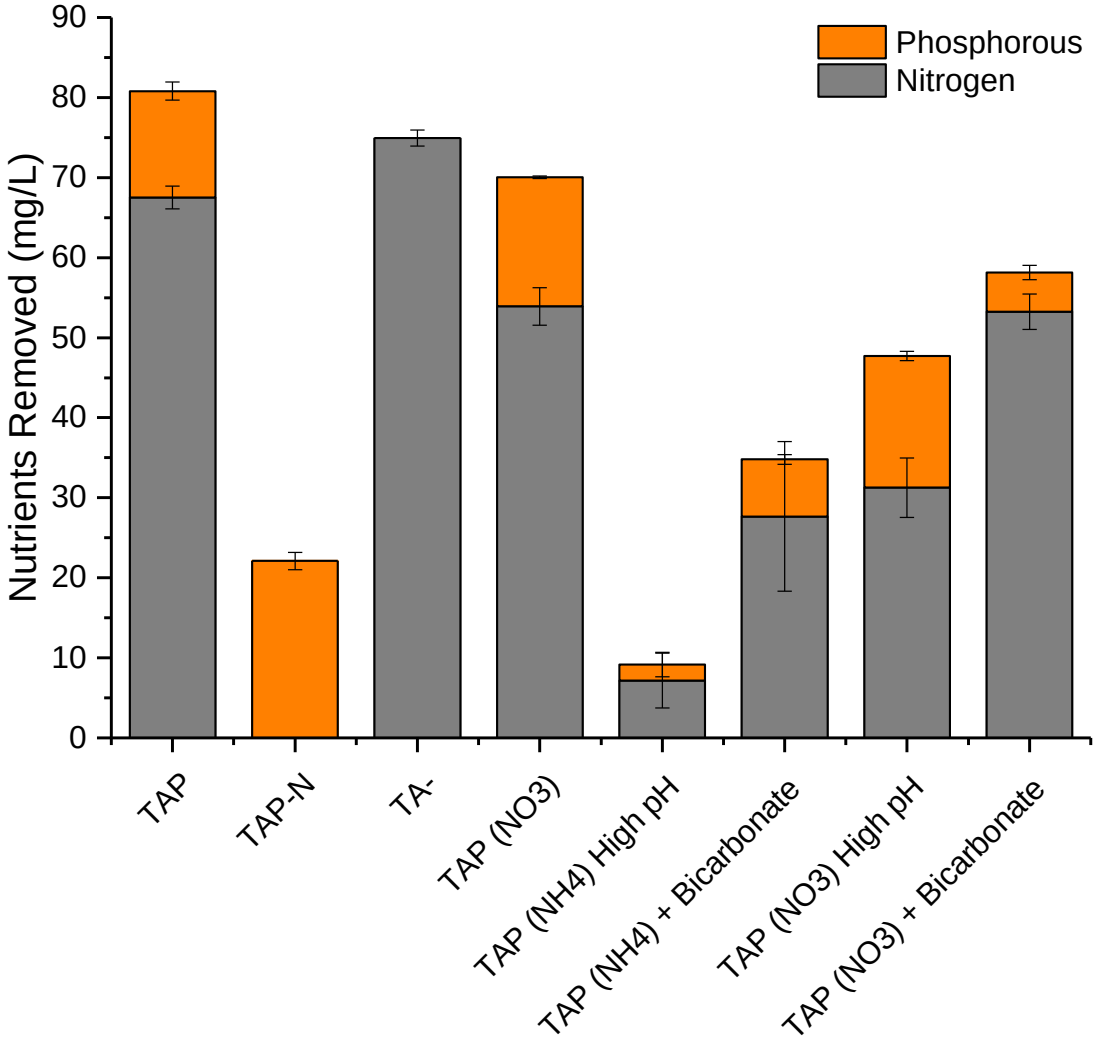

Figure 4.8 Total N and P removed from the medium after exchange from TAP into the medium of interest. Values are the mean and standard deviations of average final nutrient concentration in the medium minus known starting concentration (from media composition, 105 mg/L N, 32 mg/L P) for three biological replicates. All values are statistically different from the control (TAP) ($p < 0.05$).

Comparing nutrient removal with biomass density (measured as dry biomass weight) reveals a loose positive correlation indicating that microalgal uptake is the dominant method of nutrient removal (Figure 4.9). However, the relatively poor correlation is evidence that other factors are affecting either nutrient losses and/or the ability of microalgae to uptake nutrients from the medium.

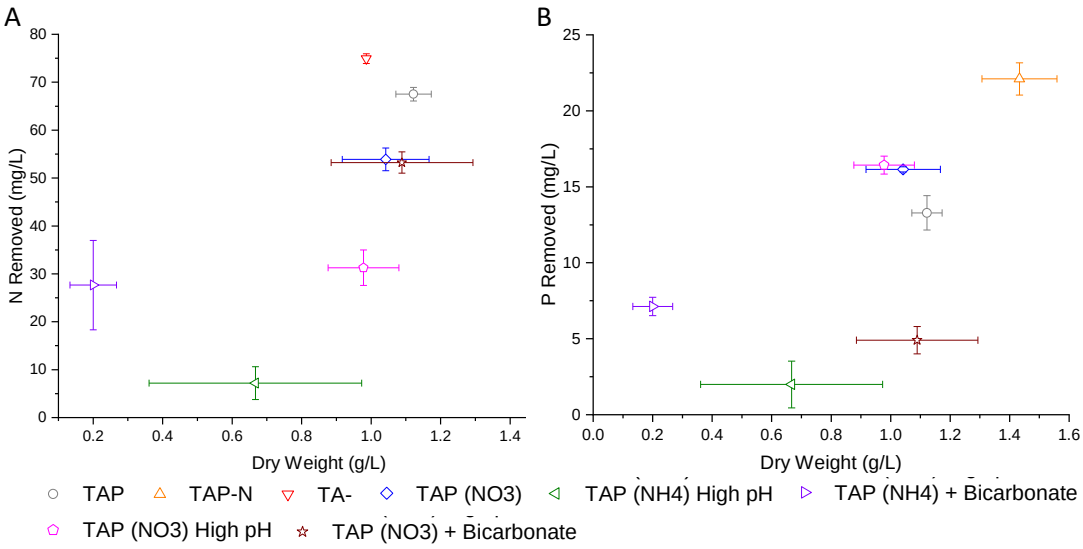

Figure 4.9 Correlation between (A) Nitrogen removal, (B) Phosphorus removal and biomass density, measured as dry biomass weight, after seven days cultivation. Data points represent the mean and standard deviation of biological triplicates.

Total nutrient removal (N + P) was highest in the control cultures (near-neutral pH with ammonium as the sole nitrogen source) with a total nutrient removal of 80.8 mg/L over the seven-day period reflecting the high biomass density of TAP cultures compared to others. The results indicate that ammonium based medium at near-neutral pH is preferable for overall nutrient removal to form a part of the wastewater treatment process.

Changing to nitrate as the sole nitrogen source saw a small drop in total nutrient removal to 70.0 mg/L largely due to the decreased nitrogen removal (53.9 mg/L compared to 67.5 mg/L for TAP ammonium cultures). This agrees with the slight reduction in biomass density observed but both the reduced biomass density and reduced nitrogen removal may also reflect the additional energy needed for nitrate assimilation in contrast to ammonium (Fernandez and Galvan, 2007; Lachmann *et al.*, 2018).

All high pH media preparations resulted in significantly reduced total nutrient removal (< 60 mg/L). This is partly reflected in the significantly reduced biomass densities of most high pH cultures however, at high pH, additional factors such as ammonia volatilisation and phosphate precipitation are known to play a role in nutrient removal, particularly in well mixed cultures with low biomass density (Diamadopoulos and Benedek, 1984; Mara, 2003). These factors likely the explain the breakdown of a correlation between biomass density and nutrient removal for these cultures.

The addition of bicarbonate to both high pH media resulted in an increase in the nitrogen removal from 7.2 mg/L to 27.7 mg/L for ammonium media and from 31.3 to 53.2 mg/L for nitrate-based media. In contrast, addition of bicarbonate had a mixed effect on phosphorus

removal, demonstrating an increase or decrease in phosphorus removal when ammonium or nitrate were present as the sole nitrogen source respectively. This is most likely due to changes in pH close to the *pKas* of phosphoric acid (pKa_2 = 7.2 and pKa_3 = 12.1) resulting in differences in the levels of phosphate precipitation and is discussed further in the following section (see Section 4.4.2.2).

Shifting from ammonium to nitrate as the sole nitrogen source even at near-neutral initial pH resulted in increased phosphate removal despite a decrease in biomass density. As with high pH cultures, this is likely as a result of increased phosphate precipitation due to the elevated pH afforded by nitrate uptake.

Interestingly, the highest nitrogen removal was found in phosphate deplete media and *vice versa* (74.9 mg/L N and 22.1 mg/L P removal respectively). Despite nitrogen starved cultures harbouring the highest biomass density, cell division is known to cease within 24 hours of nitrogen removal (Schmollinger *et al*., 2014) and as such the increase in biomass density is not expected to naturally correlate with an increase in nutrient uptake as with other cultures. The increased biomass density is instead attributed predominantly to an increase in stored neutral lipids, TAGs, within the cell. An increase in polyphosphate accumulation in response to nitrogen starvation has previously been demonstrated in the microalgae *Chlorella* (Zhu *et al*., 2015; Chu *et al*., 2015), the yeast *Saccharomyces cerevisiae* (Breus *et al*., 2012) and in some bacteria. The reason for over-accumulation of phosphate under nitrogen starvation is poorly understood; the different functionalities of N and P within the cell limit the possibility that phosphate is accumulated as a replacement to nitrogen. The similarity between the phosphoanhydride bonds in polyphosphate and those in ATP has led to the suggestion that polyphosphate may have a role as an energy store within the cell (Solovchenko *et al*., 2016). The over-accumulation of phosphate under nitrogen starved conditions may therefore be as part of a stress response, similar to that of neutral lipid accumulation, to produce an energy store which can be rapidly remobilised once favourable growth conditions are restored.

4.4.2.2 Total nutrient removal is a combination of microalgal uptake and environmental losses

During wastewater treatment, the culture conditions affect not only the bioremediation ability of the microalgae present but can also directly affect nutrient removal. Culture conditions, particularly increasing pH, are known to affect the loss of nutrients through mechanisms such as ammonia volatilisation in highly aerated/well mixed systems (e.g. photobioreactors) (Mara, 2003) and phosphate precipitation (Diamadopoulos and Benedek, 1984). While the removal of nutrients through factors other than biological remediation is useful for the treatment of wastewater, nutrients not taken up by biomass are often lost to the environment therefore limiting the potential for nutrient recycling.

In order to understand the fate of N and P and the usefulness of the biomass grown as a source of nutrients for fertiliser, the nutrient concentrations within the biomass were monitored. Nitrogen content was measured by elemental analysis of freeze-dried biomass at the end of the cultivation period. Biomass phosphorus analysis is far more laborious and was therefore calculated as the difference between total removed phosphate from the media and the estimated phosphate precipitation.

To estimate the loss of phosphate from the media due to precipitation, cultures of TAP medium in the absence of biomass were set to six initial pH values (Tris base was excluded to allow for control of the initial pH) and incubated under the same conditions as microalgal cultures. Samples were taken daily and filtered for measurement of pH and soluble orthophosphate. Full methodology is described in Chapter 2, sections 2.7.1 and 2.7.2.

The availability of phosphate within the media remained approximately constant between pH 7.0-8.5 before a sharp drop was observed between pH 8.5-9.5 followed by a second period of constant concentration between pH 9.5-11.5 (Figure 4.10). The *pKas* of phosphoric acid (pKa_1 = 2.3; pKa_2 = 7.2 and pKa_3 = 12.1) are such that at pH 7.0, phosphate is present predominantly as the soluble species $H_2PO_4^-$. Increasing the pH beyond this point decreases the proportion of $H_2PO_4^-$ in favour of HPO_4^{2-} which is able to associate with metal ions producing insoluble precipitates; the presence of high concentrations of calcium in TAP medium likely results in the precipitation of HPO_4^{2-} as calcium phosphates.

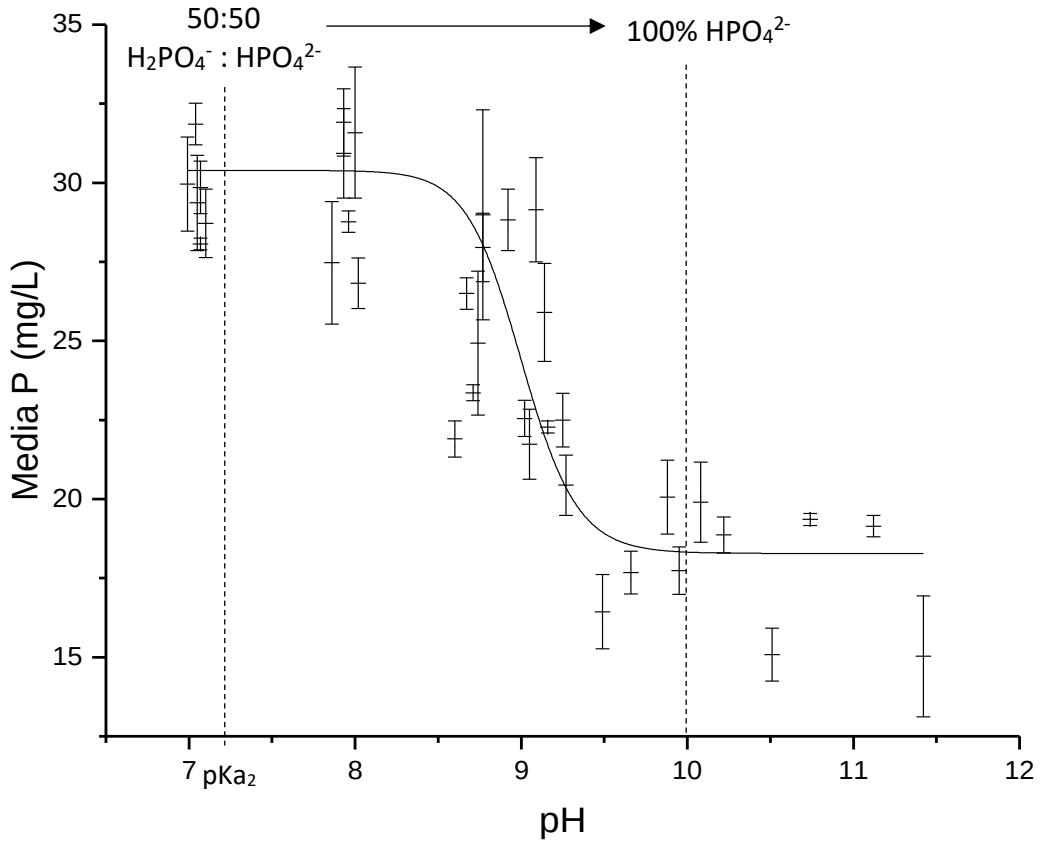

Figure 4.10 Relationship between media phosphate and pH for TAP medium in the absence of biomass growth. Tris base was eliminated and the media set to a range of initial pH values (7-11.5). Cultures were incubated under cultivation conditions and the pH and phosphate concentration measured over 8 days. Data points represent the mean and standard deviation of technical triplicates. Data has been fit using OriginPro9.1. Logistic fitting function of the form y = A2 + (A1-A2)/(1+(x/x0)^p). A1 = 30.3907; A2 = 18.2809; x0 = 9.0031; p = 53.9417.

From the relationship between soluble phosphate and pH (Figure 4.10), the percentage (%) phosphate precipitation was calculated daily for each media preparation based on the measured pH. From this, the predicted phosphate precipitation and subsequent phosphate removal through microalgal remediation were estimated (Figure 4.11).

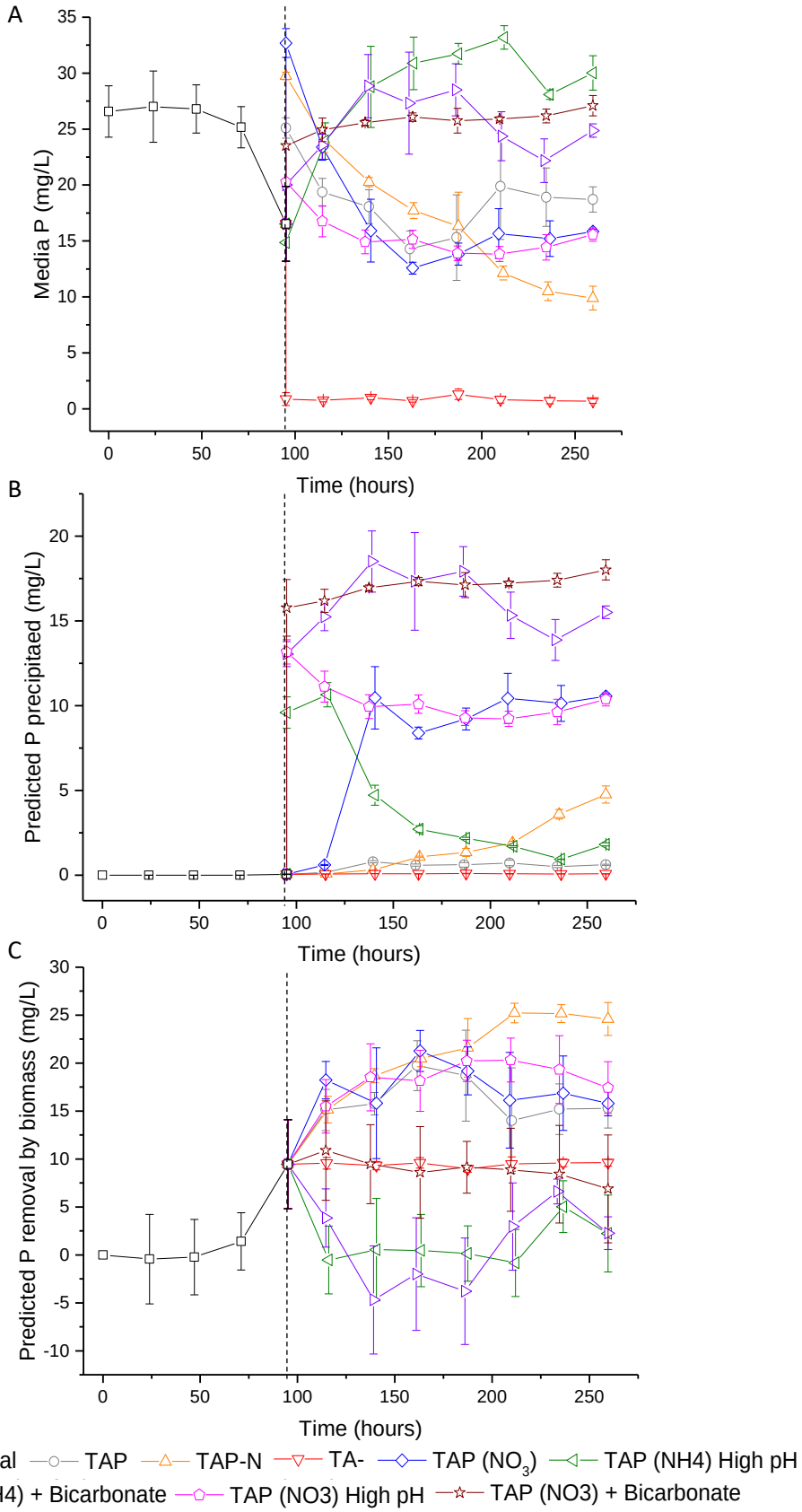

Figure 4.11 (A) Phosphorus concentration (present as PO_4) remaining in the medium after filtration; (B) Predicted phosphorus precipitation and (C) predicted phosphorus removal by biomass during growth of C.reinhardtii in eight different media preparations. All concentrations are mg/L phosphorus present as PO_4^-. Dashed lines represent the time at media exchange. All points are the mean and standard deviation of nine (TAP Initial) or three (all others) biological replicates.

Cultures grown in TAP, TAP(NO3) and TAP(NO3) High pH all resulted in a similar positive removal of phosphate by microalgae (Figure 4.11 C) however the increased pH of both nitrate cultures resulted in an overall increased removal of media phosphate as a result of significant phosphate precipitation; TAP cultures retained a pH < 8.65 throughout, precipitation of phosphates is therefore estimated to be negligible. The addition of bicarbonate to TAP(NO3) high pH cultures resulted in a significantly reduced removal of media phosphate. Given the predicted precipitation afforded by the sustained high pH, it is estimated that negligible quantities of phosphate were removed by the biomass; this may be in part due to the reduced phosphate availability due to precipitation.

Nitrogen starved cultures ('TAP-N') demonstrated the highest overall phosphate removal from the medium (Figure 4.11 A). Despite small quantities of phosphate precipitation predicted (Figure 4.11 B), phosphate removal by microalgal uptake is estimated to be approximately 8 mg/L higher than any other media preparation investigated (Figure 4.11 C). Proposed reasons for this are discussed above (see Section 4.4.2.1).

In contrast, both TAP(NH4) high pH cultures saw a rise in media phosphate concentration in the seven days following inoculation (Figure 4.11 A). Given the reduction in pH and biomass density observed during cultivation (Figure 4.7), it is proposed that the increase in media phosphate is a combination of phosphate released back into the media during cell necrosis and the re-solubilisation of precipitated phosphates as the pH decreased.

Based on the estimated microalgal uptake of nutrients (Figure 4.11) and the measured dry weight of cultures (Figure 4.7), the phosphate content within the biomass was estimated as a percentage of dry biomass weight (Table 4.9). Nitrogen content within the biomass was measured by elemental (CHNS-O) analysis. Dry microalgal biomass typically contains approximately 10 % N and 1 % P by weight (Stumm and Morgan, 1996, van Harmelen and Oonk, 2006) when grown under favourable conditions. This is similarly demonstrated here in TAP cultures which are shown to contain approximately 10 % N and 1 % P. Microalgae grown under phosphate deplete conditions demonstrated similar nitrogen content within the biomass despite a slight increase in total N removal from the medium (Figure 4.8); this discrepancy is likely the result of small errors in measurement of nitrogen or biomass dry weight. As expected, the estimated phosphorus concentration is much lower for microalgae grown under phosphate starvation compared to full medium and confirms the consumption of phosphate reserves within the cell in order to sustain cell growth.

Table 4.9 Nitrogen content and predicted P content of C.reinhardtii after 7 days growth in eight different media preparations. Nitrogen is reported as weight % of dry biomass measured through CHNS elemental analysis. Phosphorus is reported as weight % of dry biomass estimated from the calculated microalgal P uptake and the measured culture dry biomass weight (g/L).

	N Content (% dry biomass)	Predicted P Content (% dry biomass)
TAP initial		1.3
TAP	9.7 ± 0.28	1.0
TAP-N	2.5 ± 0.18	1.5
TA-	9.6 ± 0.17	0.7
TAP (NO3)	8.8 ± 0.15	1.0
TAP (NH4) High pH	10.6 ± 0.07	≈ 0
TAP (NH4) + Bicarbonate	8.3 ± 0.12	≈ 0
TAP (NO3) High pH	5.7 ± 1.01	1.4
TAP (NO3) + Bicarbonate	5.0 ± 0.51	0.3

Cultures grown under nitrogen starvation ('TAP-N') similarly demonstrated low concentrations of nitrogen present in the biomass, however biomass phosphate is significantly higher than the control or the 1 % reported 'typical' concentration (Stumm and Morgan, 1996, van Harmelen and Oonk, 2006). The additional phosphate indicates the accumulation of polyphosphate storage compounds as has previously been reported under nitrogen deplete conditions (Zhu *et al*., 2015; Chu *et al*., 2015).

On shifting to nitrate based media ('TAP(NO3)'), phosphate concentration within the cell is comparable with that of the control; the increased total phosphate removal is likely the result of additional phosphate precipitation in response to the elevated pH afforded by the nitrate assimilation (Figure 4.7 D). Nitrogen content within the cell is reportedly approximately 1 % lower in cultures grown in nitrate compared to ammonium and this is similarly reflected in the total N removal from the medium (Figure 4.8). The reduction in N content may reflect the additional energy requirement of nitrate assimilation compared to ammonium (Fernandez and Galvan, 2007; Lachmann *et al*., 2018).

Reduced N content in nitrate grown cultures is similarly seen for 'high pH' ammonium and nitrate cultures. High pH ammonium-based media resulted in the highest biomass N concentration however the poor biomass yield limited total nutrient removal under these conditions. The increase in phosphate concentration in the media after media exchange also resulted in estimated negligible quantities of phosphate present in the biomass, significantly limiting the potential for biomass grown under these conditions to be used for the recycling of phosphorus for fertiliser.

Despite the additional nitrogen removal on addition of bicarbonate in 'high pH' cultures, the nitrogen content of the biomass was lower in each case. For nitrate media, the addition of

bicarbonate resulted in a significant increase in biomass dry weight and the additional nitrogen removal is likely simply due to the increased biomass growth. In contrast, the dry weights of both high pH ammonium medium were similar. Ammonia volatilisation is known to occur in wastewaters when the pH is elevated (*pKa* $NH_4^+ \leftrightarrow NH_3$ = 9.26) and photosynthetic activity is low (Mara, 2003); ammonia volatilisation as a result of the increased pH afforded by the addition of bicarbonate (final pH = 9.56 compared to 8.70 for bicarbonate deplete media) is therefore proposed to explain the observed increase in total N removal when *C.reinhardtii* was cultured in high pH ammonium-based medium in the presence of high quantities of sodium bicarbonate.

The results presented here indicate that near-neutral media with ammonium as the sole nitrogen source are the preferable conditions to maximise both the overall nutrient removal from wastewater and the nutrient concentrations in the resultant biomass which can be extracted for use in fertiliser production as a means to recycle nutrients otherwise lost through the wastewater treatment process. Despite these conditions being favourable for overall nutrient removal and recycling potential, depending on the specific goal (i.e. phosphate removal or production of a high phosphate biomass etc.), other culture conditions within a wastewater treatment system may be preferentially utilised to meet specific goals – i.e. high pH nitrate medium and nitrogen deplete medium are shown to be most effective for producing high phosphate biomass and a period of nitrogen starvation is shown to maximise phosphate removal from the medium.

4.4.3 Microalgal biodiesel potential under different culture conditions

In order to evaluate the potential of each culture condition for the production of biodiesel from *C.reinhardtii*, biomass samples were extracted (2:1 $CHCl_3$:MeOH) and lipids esterified (0.6M HCl in MeOH) to produce fatty acid methyl esters (FAMEs). FAMEs were analysed quantitatively by GC-MS using C17:0 as an internal standard (Figure 4.12). Full methodology is provided in Chapter 2, Section 2.6.3.1.

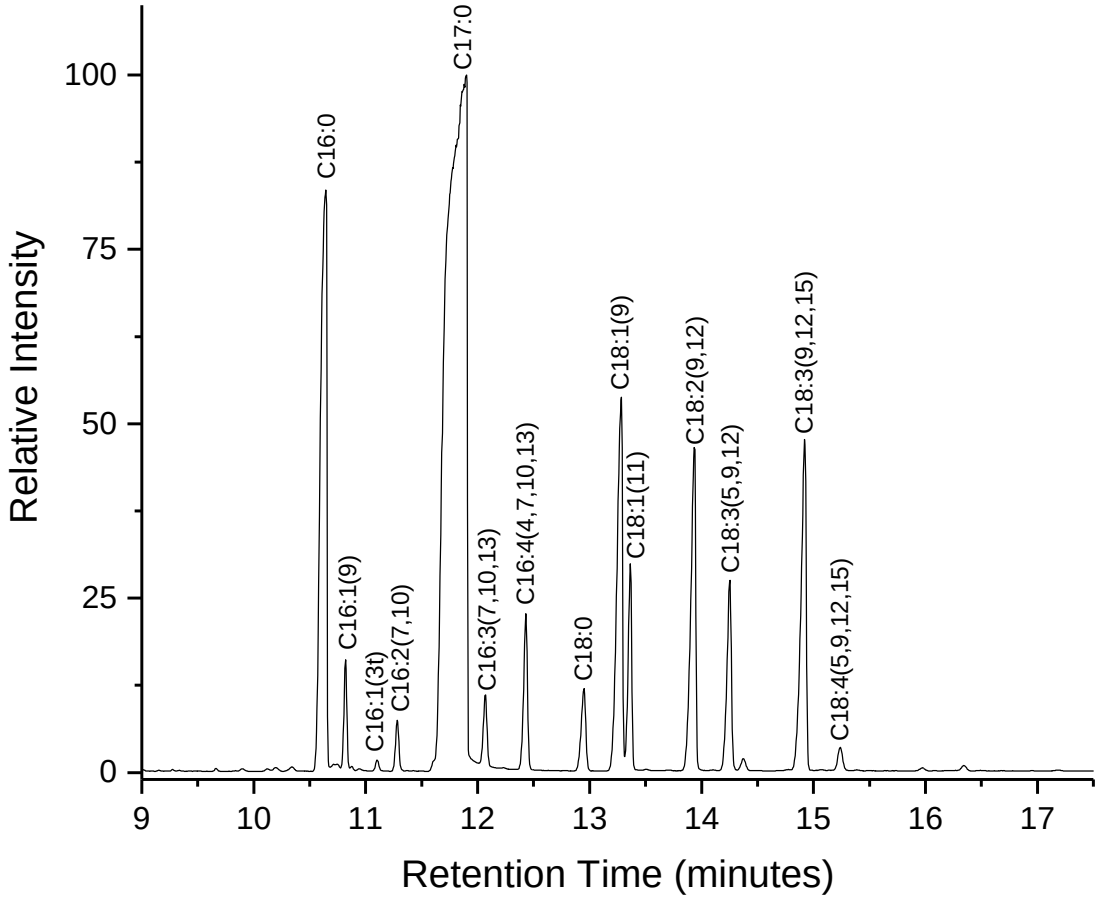

Figure 4.12 GC-MS separation of fatty acid methyl esters prepared from C.reinhardtii total lipids. Peaks were assigned with reference to an external standard and relevant literature (Siaut et al., 2011). Heptadecanoic (C17:0) is present as an internal standard only.

4.4.3.1 FAME content is unaffected by phosphate starvation or choice of nitrogen source but decreased by high pH in the presence of ammonium

Biomass samples were analysed for FAME content immediately before media exchange (Day 0), at the end of exponential phase (Day 4) and at the end of the cultivation period (Day 7, Figure 4.13). Immediately prior to exchange, approximately 13 % FAME content was observed (wt% of biomass dry weight). Cultures grown in standard TAP medium throughout largely retained this FAME content throughout exponential (Day 4) and stationary (Day 7) phase. Similarly, cultures grown in phosphate starved medium and all cultures grown in TAP medium with nitrate as the sole nitrogen source showed no appreciable difference in the FAME content compared to the control ($p > 0.05$).

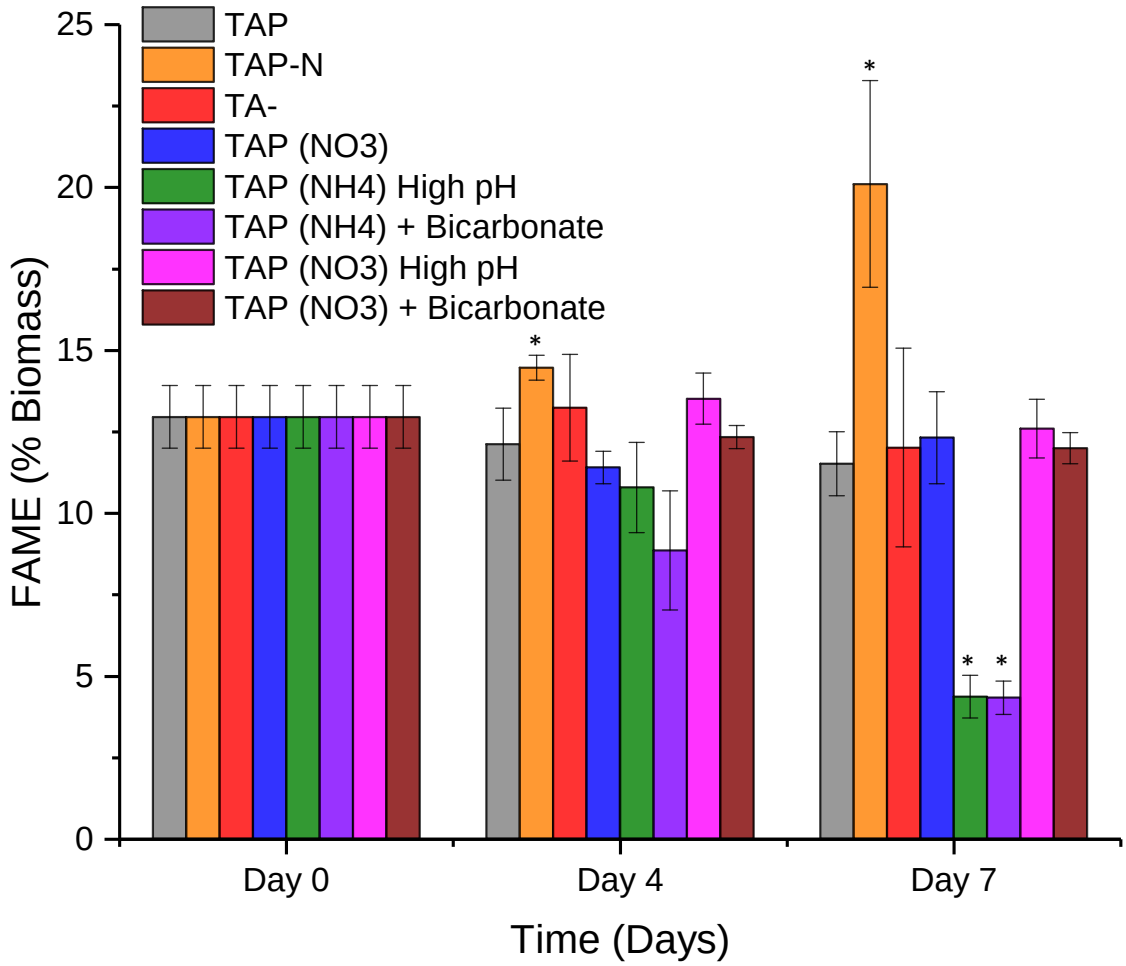

*Figure 4.13 FAME content as % of dry biomass weight for C.reinhardtii cultures grown in eight different media preparations immediately before media exchange (Day 0), at the end of exponential phase (Day 4) and at the end of the cultivation period (Day 7). All points are the mean and standard deviation of biological triplicates. * denotes a statistically significant difference from TAP cultures (two-sided independent t test, $p < 0.05$).*

Cultures exchanged into nitrogen starved medium, showed significantly increased FAME content compared to the control ($p < 0.05$) as has been extensively reported (Siaut *et al* 2011; Schmollinger *et al*., 2014; Valledor *et al*., 2014; Park *et al* 2015) and reached a final FAME content of 20 % biomass dry weight with the majority of lipid accumulation occurring during stationary phase. In contrast, cultures exchanged into TAP medium with elevated pH and ammonium as the sole nitrogen source displayed significantly reduced FAME content compared to the control reaching a final FAME content of 4.3 and 4.4 % with and without the addition of bicarbonate respectively.

Under certain unfavourable growth conditions, most notably nitrogen starvation, microalgal cells are known to accumulate neutral lipids in discrete oil bodies within the cell. Additionally, cells have been shown to break down internal cellular membranes as a means to recycle membrane lipids into additional neutral lipids as part of this stress response (Moellering

and Benning, 2010; Siaut *et al*., 2011; Gonçalves *et al*., 2016). Degradation of the chloroplast membrane has been widely reported under nitrogen starvation and leads to bleaching and cessation of cell division (Valledor *et al*., 2014). Oil bodies within the cell can be readily observed by use of the fluorescent lipophilic stain Nile-red which fluoresces in the presence of neutral lipids but is bleached in polar environments.

Fluorescence microscopy in the presence of Nile-red revealed negligible fluorescence in cultures of *C.reinhardtii* grown in standard TAP and phosphate starved media and in near-neutral pH media with nitrate as the sole nitrogen source (Figure 4.14) indicating no appreciable accumulation of neutral oil bodies. Cultures in nitrogen starved media were observed to have a granular appearance, likely representing the accumulation of storage compounds such as oils, starch and polyphosphate and demonstrated significant fluorescence in the majority of cells indicating significant neutral lipid accumulation. Additionally, nitrogen starved cells were significantly larger than those grown under favourable growth conditions. Increased cell size has previously been shown in response to stressful stimuli proposed as a result of increasing storage products within the cell (Dean *et al*., 2010; Work *et al*., 2010; Bajhaiiya *et al*., 2016).

Despite the similar overall FAME content, high pH nitrate cultures demonstrated fluorescence in a limited proportion of cells however significant debris was also observed. Given necrotic cells are known to fluoresce, it is hard to draw conclusions as to the source of the observed fluorescence. Additionally, the relatively small cell size is comparable with cultures grown without stressful stimuli. In contrast, high pH ammonium cultures demonstrated fluorescence more concentrated even than nitrogen starved cultures. The clearly spherical structure of the cells observed limits the likelihood that this is due to cell necrosis and indicates significant neutral lipid accumulation. Indeed, a significant number of distinct bright spots can be observed similar to previously reported observations of discrete oil bodies (Siaut *et al*., 2011). The sudden bleaching observed on exchange of these cultures supports the hypothesis that high pH ammonium-based media triggers a stress response leading to the accumulation of neutral lipids (see Figure 4.7 B).

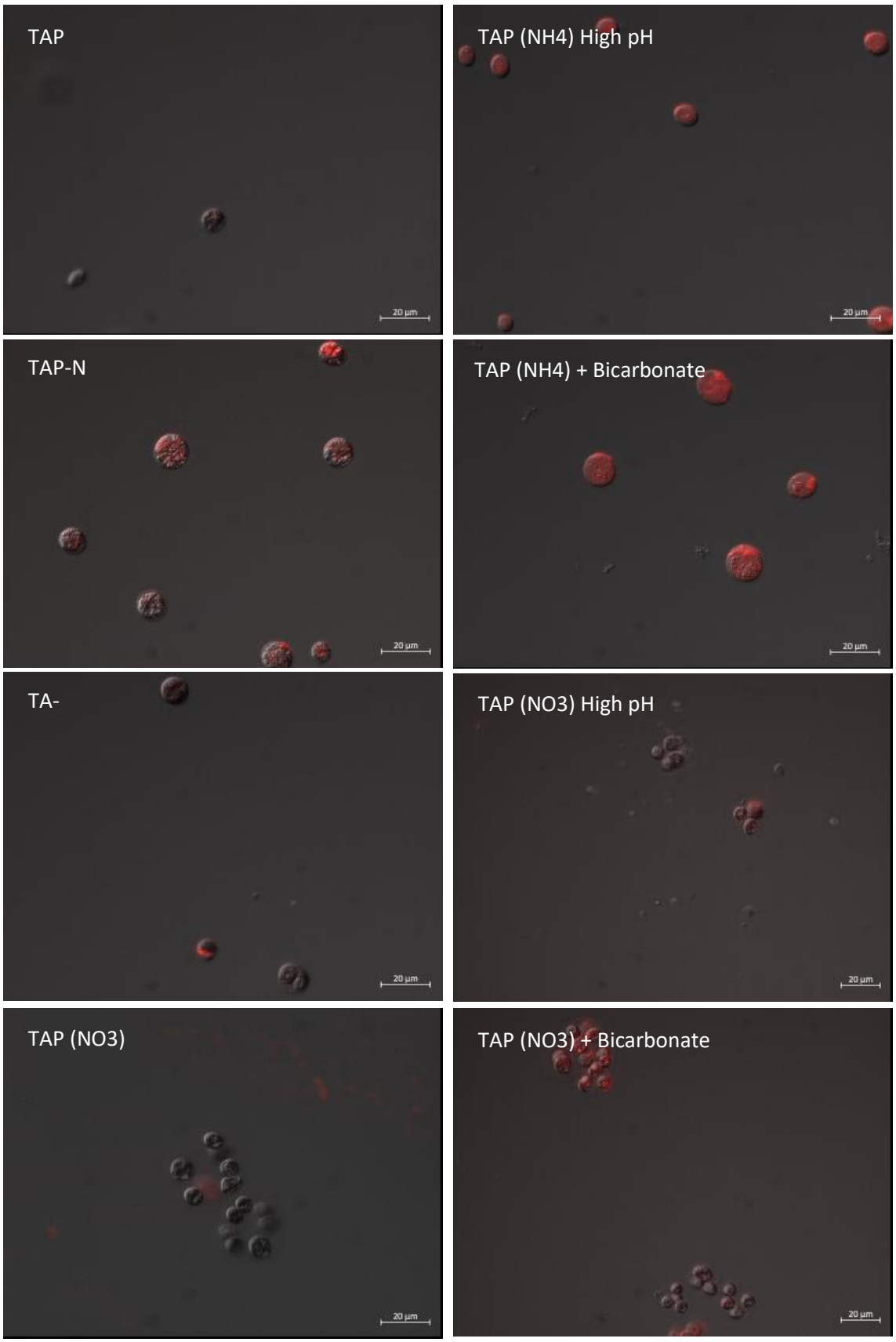

Figure 4.14 Nile-red fluorescent staining of neutral lipid bodies (red) present in C.reinhardtii strain CC-1690 grown in eight media preparations after seven days cultivation. Scale bar = 20 µm. Fluorescence intensity not to scale and artificial colour applied.

4.4.3.2 Lipid quality for biodiesel production is dependent upon FAME composition

In addition to the quantity of useful lipids produced, the quality of lipids for biodiesel is also an important consideration when choosing cultivation conditions. Typically, biodiesels are blended with petrochemical diesel to improve engine performance (Alternative Fuels Data Center) however, biodiesels closer in quality to regulation standards (e.g. EN 14214 European Biodiesel Standard) could be blended at higher proportions with petrochemical diesel.

A number of parameters are commonly used to assess biodiesel quality including the cetane number (CN), iodine value (IV), saponification value (SV), cold filter plugging point (CFPP), kinematic viscosity (υ), density (ρ), oxidative stability index (OSI) and the higher heating value (HHV) (see Chapter 2, Section 2.6.3.3). These factors are determined by the FAME composition, in particular the saturation, chain length and branching of fatty acid methyl esters (Krisnangkura *et al*., 1986; Ramos *et al*., 2009; Islam *et al*., 2013).

FAME compositional analysis revealed that C16:0, C16:4, C18:1(9), C18:2 and C18:3(9,12,15) were the predominant fatty acids present in *C.reinhardtii* (Figure 4.15). Nitrogen deprivation is known to cause accumulation of large quantities of neutral lipids (TAGs), the favoured starting product for biodiesel production from microalgae. The aforementioned fatty acids have previously been reported as key fatty acids in determining TAG abundance with C16:0, C18:1(9) and C18:2 maximised under high TAG accumulation while C16:4 and C18:3 are minimised when the proportion of lipids present as TAGs is increased (Yang *et al*., 2017). Cultures exchanged into nitrogen deprived medium here portray these trends clearly.

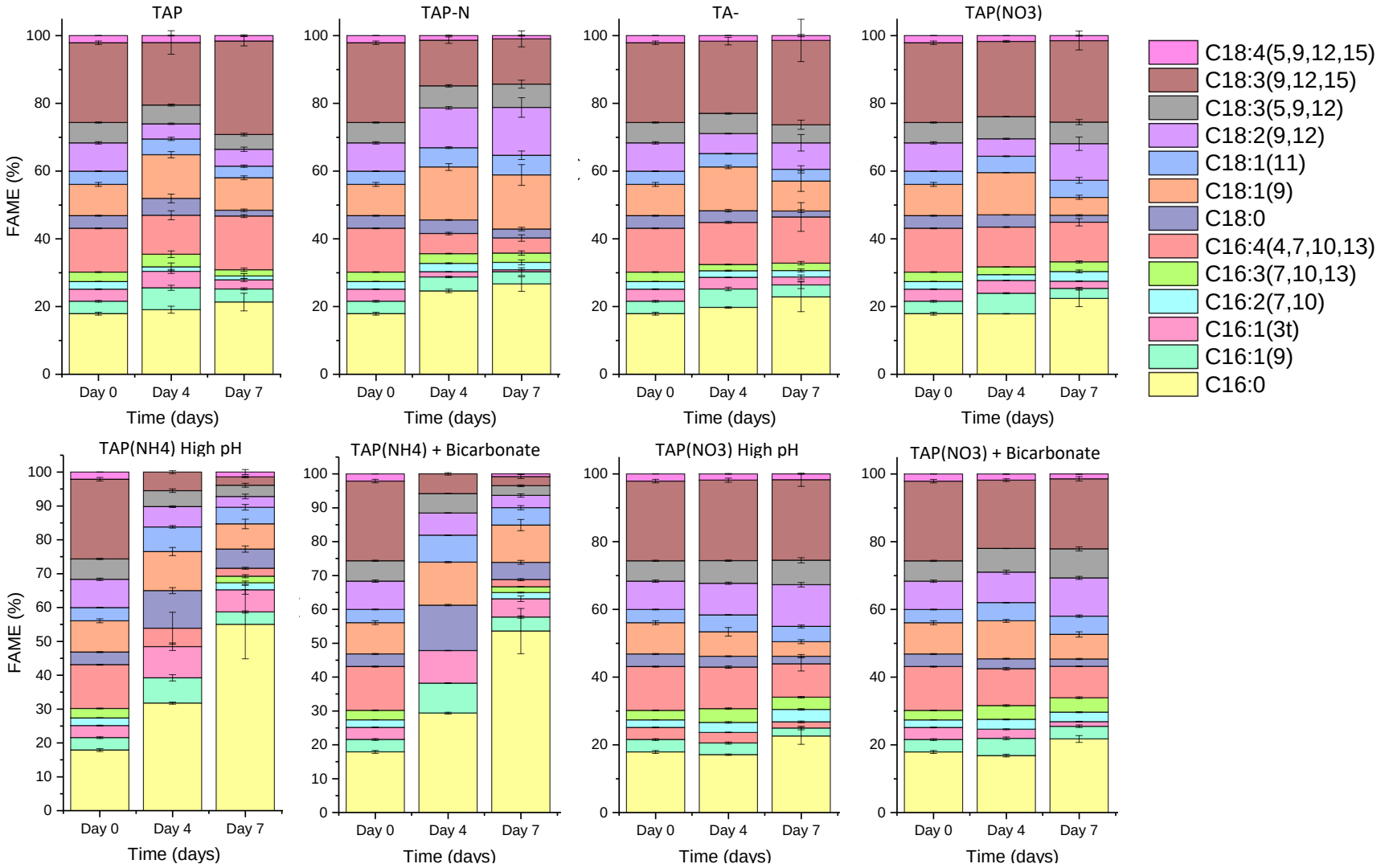

Figure 4.15 FAME composition of C.reinhardtii grown in eight different media preparations. Day 0 represents the point at which cultures were exchanged into the medium of interest after a pre-cultivation period in standard TAP medium. All points are the mean and standard deviation of biological triplicates.

With the exception of high pH cultures with ammonium as the sole nitrogen source, all remaining media preparations resulted in elevated levels of C18:3(9,12,15) at stationary phase (Day 7) compared to exponential phase (Day 4). Similarly, proportions of C18:1(9) are observed to decrease over the cultivation period. While the proportion of C16:0 increases in all cultures, the effect is smaller than that seen for nitrogen deprived cultures. Compositional analysis therefore reveals that these conditions retain a fatty acid composition similar to that of the control (TAP) rather than nitrogen starved cultures (known to be favourable for the production of biodiesel).

In contrast, both high pH ammonium cultures saw significantly increased C16:0 within the FAME profile from approximately 18 to 54 and 55 % with and without bicarbonate respectively. Similarly, cultures retained high abundance of C18:1(9) and C18:2 given the large proportion already comprised of C16:0. Both C16:4 and C18:3 were minimal in each culture by the end of the cultivation period (Day 7). Compositional results support evidence from fluorescent imaging that cultures grown at high pH with high ammonium content accumulate large quantities of TAGs similarly to nitrogen starved cultures.

Based on compositional analysis of FAMEs produced, biodiesel properties were calculated and are compared to the European Biodiesel Standard (EN 14214) (Table 4.10). All cultures met EN 14214 standard for density and kinematic viscosity and the observed HHVs comply with the typical range of regular biodiesel (39.8-40.4 MJ kg^{-1}) (Ramírez-Verduzco *et al.*, 2012).

Table 4.10 Biodiesel properties calculated from the FAME composition of C.reinhardtii grown in eight different media preparations. Day 0 represents the point at which cultures were exchanged from TAP medium into the medium of interest. All points are calculated from the mean FAME composition of biological triplicates.

		DU	*LCSF*	*CN*	*SV* ($mg\ KOHg^{-1}$)	*IV* ($g\ I_2 100g^{-1}$)	*CFPP (°C)*	*OSI (h)*	*Density (ρ)* (gcm^{-3})	*Kinematic Viscosity (υ)* (mm^2s^{-1})	*HHV* ($MJ\ kg^{-1}$)
Biodiesel Standard EN 14214		-	-	≥51	-	≤120	Variable	≥6	0.86-0.90	3.5-5.0	-
TAP Initial	**Day 0**	136.4	3.6	33.6	198.3	178.9	-5.0	5.7	0.89	3.54	39.4
TAP	**Day 4**	123.1	4.4	37.7	198.7	160.4	-2.7	6.7	0.88	3.65	39.4
	Day 7	134.4	3.0	32.4	199.1	183.5	-7.1	5.8	0.89	3.48	39.4
TAP-N	**Day 4**	115.8	4.5	43.1	197.3	137.1	-2.4	6.3	0.88	3.85	39.5
	Day 7	115.5	4.0	44.0	197.0	133.4	-3.9	6.0	0.88	3.88	39.6
TA-	**Day 4**	127.9	3.7	36.3	198.4	166.7	-4.9	6.1	0.89	3.62	39.4
	Day 7	132.7	3.2	34.1	198.9	176.1	-6.6	5.7	0.89	3.53	39.4
TAP (NO3)	**Day 4**	130.0	3.6	35.8	198.2	168.9	-5.2	6.1	0.89	3.61	39.4
	Day 7	135.7	3.3	34.2	198.6	175.9	-6.2	5.4	0.89	3.53	39.4
TAP (NH4)	**Day 4**	78.8	8.7	53.4	199.0	90.2	10.9	9.9	0.88	4.13	39.6
High pH	**Day 7**	56.0	8.3	58.6	202.2	65.3	9.7	15.7	0.87	4.15	39.6
TAP (NH4) +	**Day 4**	75.3	9.7	56.4	197.6	77.9	13.8	9.1	0.87	4.25	39.7
Bicarbonate	**Day 7**	56.9	7.9	59.0	201.6	64.0	8.4	15.4	0.87	4.18	39.6
TAP (NO3)	**Day 4**	140.6	3.3	32.7	198.3	182.9	-6.1	5.6	0.89	3.50	39.4
High pH	**Day 7**	137.3	3.4	34.3	198.4	175.5	-5.8	5.3	0.89	3.54	39.4
TAP (NO3) +	**Day 4**	136.1	3.2	34.9	198.1	173.2	-6.5	5.9	0.89	3.58	39.4
Bicarbonate	**Day 7**	134.4	3.3	35.5	198.2	170.2	-6.2	5.5	0.89	3.58	39.4

Predictive oxidation stability (OSI) is comparable with the European standard for all cultures, with high pH ammonium cultures significantly above the minimum oxidation stability of 6 hours. Nitrate based cultures had the lowest oxidation stability as a result of the increased proportion of C18:2 and C18:3 FAMEs.

Of all the culture conditions investigated, only cultures grown in the high pH ammonium-based medium have FAME composition meeting the European standard for cetane number (CN) and iodine value (IV) due to the low degree of unsaturation (DU). In contrast, the cold filter plugging point, which increases with increasing saturation is significantly higher than other media preparations.

4.4.3.3 Ammonia toxicity causes preferential degradation of PUFAs and FAMEs of better quality for biodiesel production

On exchange into ammonium based media (105 mg/L NH_4Cl) at elevated pH (pH 9.5), *C.reinhardtii* cultures were observed to bleach rapidly and growth ceased, as a result of ammonia toxicity, as can be seen from a sudden drop in the chlorophyll concentration and optical density of the culture (see Figure 4.7). In addition, the quantity of lipids accumulated in the biomass was significantly lower than that observed in standard TAP medium (pH = 7.0), however the degree of unsaturation (DU) and long chain saturation factor (LCSF) were considerably lower and higher than the control respectively (Table 4.10) resulting in lipids of better quality for biodiesel production. The results presented indicate that under these conditions there is a compromise to be had between lipid quality and quantity for the production of biodiesel.

In order to further investigate the effect of ammonia toxicity on *C.reinhardtii* and the balance between lipid quality and quantity under these conditions, the above experiment (Section 4.4) with TAP (NH_4) High pH media was repeated to facilitate daily sampling for GC-MS lipid analysis. On exchange into high pH ammonium medium, the optical density, chlorophyll concentration, dry weight and pH acted similarly to that previously observed (Figure 4.7) and cultures were noticeably yellow in colour within 48 hours with significant biomass flocculation observed within 24 hours.

Biomass samples (ca. 4.5 mL) were taken daily, freeze-dried and analysed for FAME content (see Chapter 2, section 2.6.3.1). Within 4 days of exchange into high pH ammonium based medium, the total FAME content had dropped from approximately 11 % to approximately 4 % of biomass dry weight (Figure 4.16). The PUFA content similarly dropped significantly over the four-day period from approximately 6.7 % to 1.0 % of dry biomass weight while the concentration of MUFA and SFA remained approximately constant throughout indicating that

the loss in total FAME content is as a result of preferential degradation of poly-unsaturated lipids.

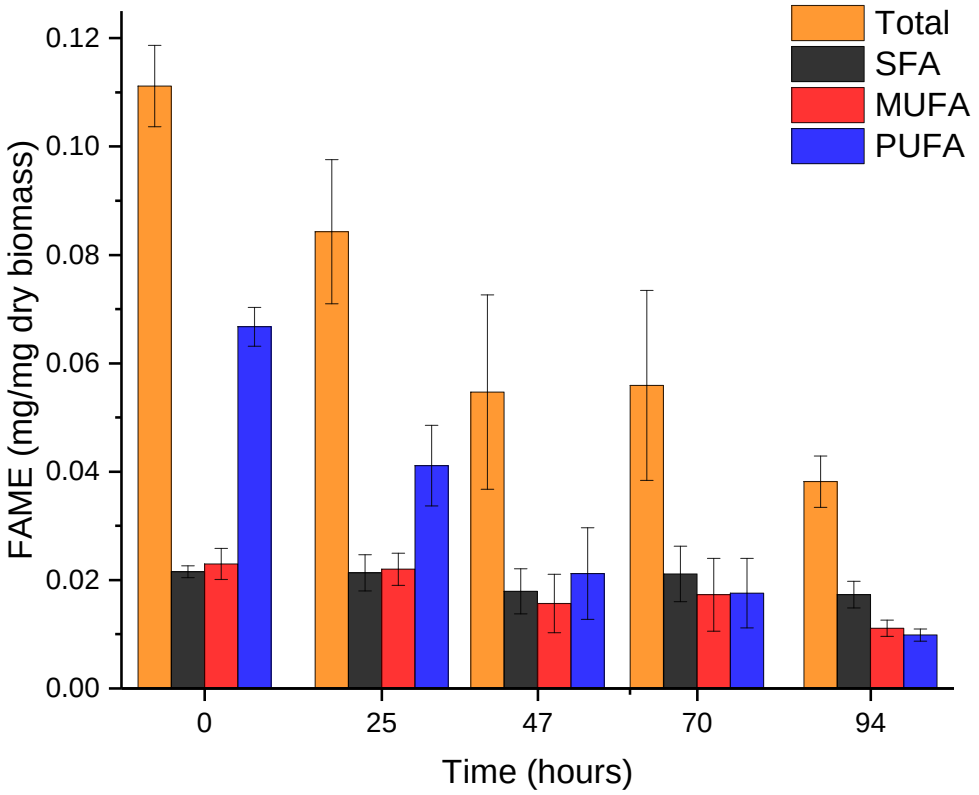

Figure 4.16 Total FAME, SFA, MUFA and PUFA content as % of dry biomass weight for C.reinhardtii cultures grown in ammonium based medium at high initial pH (pH 9.5) for four days after an pre-cultivation period in standard TAP medium. t = 0 hours represents samples taken immediately after exchange from standard TAP medium. All points are the mean and standard deviation of biological triplicates.

Storage lipids (triacylglycerols) are typically rich in saturated and mono-unsaturated fatty acids (Yang *et al*., 2017). The preferential degradation of PUFAs and the observed bleaching, distinctive to chlorophyll degradation, indicates specific depletion of membrane lipids in favour of retention of storage compounds. The presence of storage lipids (TAG droplets) is confirmed by comparison with Nile-red fluorescence imaging (Figure 4.14).

The quality of FAME composition for biodiesel production is largely determined by the relative proportions of saturated, mono-unsaturated and poly-unsaturated fatty acids with the majority of factors optimised by low quantities of poly-unsaturated fatty acids (see Chapter 2, Section 2.6.3.3). Due to the preferential degradation of poly-unsaturated fatty acids, the percentage of poly-unsaturated fatty acids drops rapidly from 60 to 26 % of FAMEs within the four days following exchange into high pH ammonium media (Figure 4.17). Subsequently, both

the percentage of saturated and, to a lesser extent, mono-unsaturated fatty acids increase following exchange to approximately 45 and 29 % of FAMEs respectively.

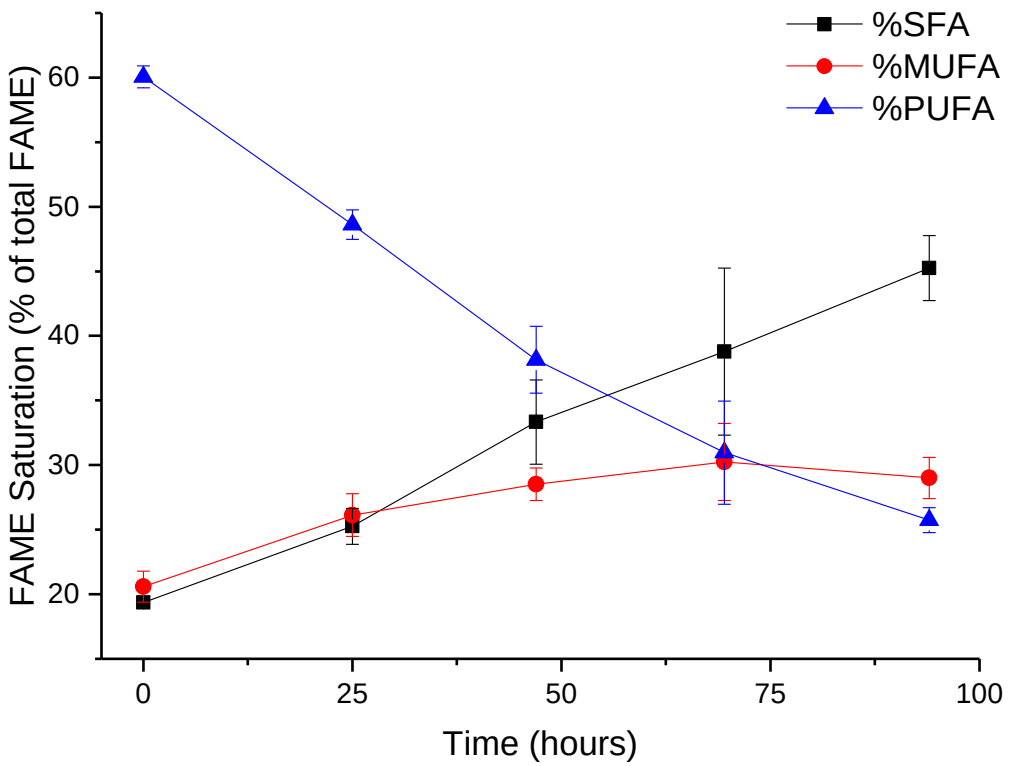

Figure 4.17 Relative quantity (wt%) of saturated (SFA), mono-unsaturated (MUFA) and poly-unsaturated (PUFA) fatty acids present in C.reinhardtii cultures grown in ammonium based medium at high initial pH (pH 9.5) for four days after a pre-cultivation period in standard TAP medium. t = 0 hours represents samples taken immediately after exchange from standard TAP medium. All points are the mean and standard deviation of biological triplicates.

Based on the compositional results, the given biodiesel that would be obtained each day can be analysed for quality according to the parameters explained above. Density, kinematic viscosity and oxidation stability were all within EU limits from the point of exchange. Prior to the effects of ammonia toxicity (Figure 4.18, t = 0 hours), the cetane number and iodine value are well below and above the EU biodiesel standard respectively. However, over the cultivation period, the standard of FAMEs were observed to increase towards the EU limits set. Cetane number and iodine value reached the EU standard after approximately 86 and 60 hours respectively.

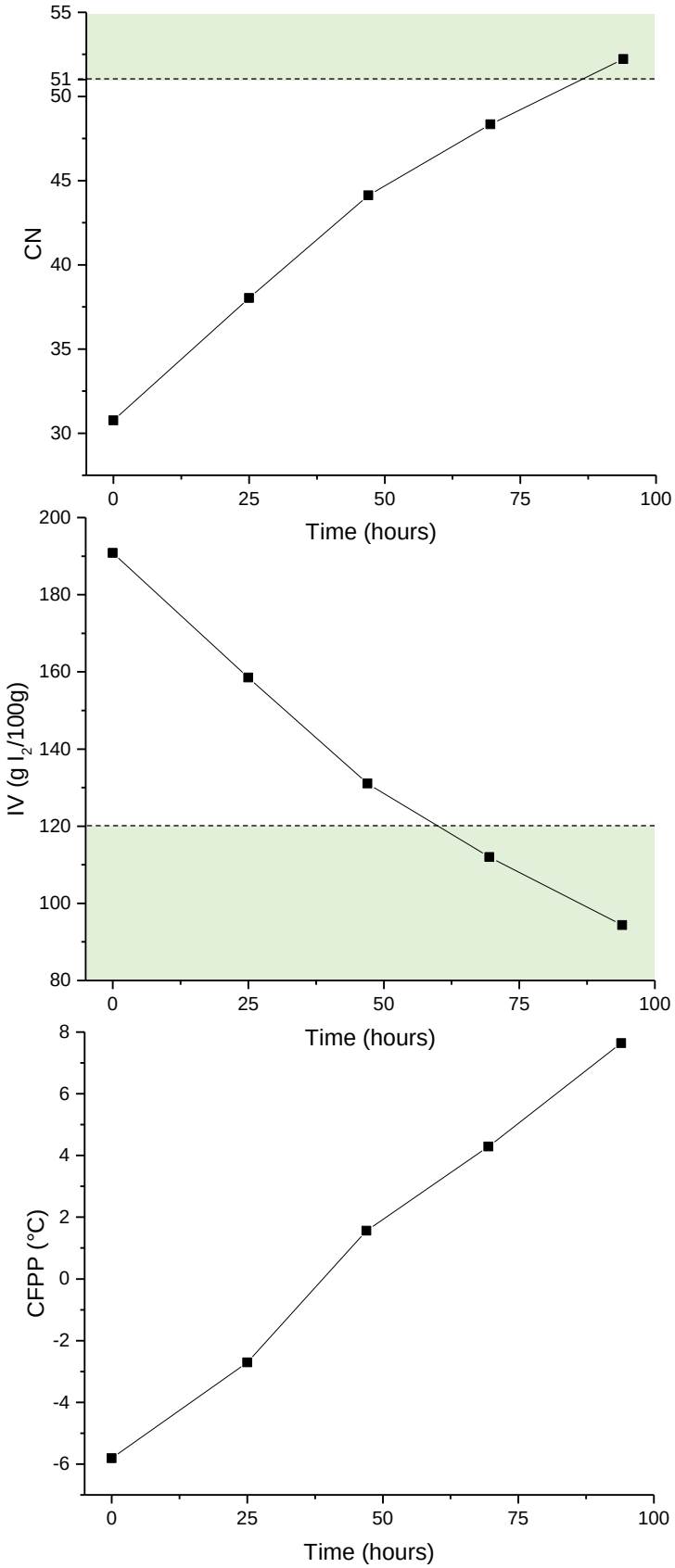

Figure 4.18 Biodiesel Cetane number (CN), Iodine value (IV) and Cold filter plugging point (CFPP) calculated from the mean (n = 3) FAME composition of C.reinhardtii cultures grown in ammonium based medium at high initial pH (pH 9.5) for four days after pre-cultivation in standard TAP medium. t = 0 hours represents samples taken immediately after exchange from standard TAP medium. Green shading represents EU biodiesel standard EN 14214.

There is no definitive standard set for the cold filter plugging point as the necessary range varies from country to country and is season dependent, however in contrast to both the cetane number and iodine value, CFPP becomes decreasingly favourable with the effects of ammonia toxicity given the inverse relationship between FAME saturation and CFPP.

4.5 Conclusions

The culture conditions afforded by wastewater vary considerably depending on the wastewater composition and treatment stage within a wastewater treatment facility. In order to realise the potential of microalgae for combined wastewater treatment and lipid production, the individual effects of these conditions on the growth and nutrient uptake in microalgae need to be understood.

An initial study comparing the growth of *C.reinhardtii* on a synthetic wastewater (SWW) and TAP medium revealed pH to be a possible cause of triacylglycerol (TAG) accumulation within microalgae. From a comparison of SWW and TAP, eight media preparations were chosen to investigate the effect of pH on the growth, nutrient and lipid accumulation in *C.reinhardtii*.

Uptake of total nitrogen and phosphorus was optimised by near-neutral pH media. There is evidence to suggest that ammonium is the preferred nitrogen source for the uptake of nutrients however investigations conducted here were done so only through a sudden change in conditions when cultures reached mid-log phase and therefore some of the response may be due to the shock in growth conditions. The following chapter therefore investigates the effect of nitrogen source on growth and nutrient uptake in further detail.

The effect of high pH is shown to be highly dependent on the nitrogen source available. High pH medium with nitrate as the sole nitrogen source was able to support the growth of *C.reinhardtii* to pH values > 11.0. In contrast, above pH 9.5, ammonium-based medium caused sudden bleaching, cessation of biomass growth and accumulation of TAGs. The results are indicative of a stress response as a result of ammonia toxicity.

Until now, no triggers of TAG accumulation have been demonstrated that would be feasible within a wastewater treatment facility. In contrast, the high ammonium concentrations in wastewater and the high pH resulting from microalgal growth mean that ammonia toxicity is replicable during wastewater treatment and could therefore be harnessed for the production of high quality lipids for biodiesel production. However, while ammonia toxicity results in increased TAG accumulation and subsequently lipid composition of better quality for biodiesel production, the quantity of total lipids is severely reduced. In addition, the poor biomass yield and

bioremediation properties mean that care should be taken to avoid cultivation in conditions able to provoke ammonia toxicity where biomass quantity or nutrient removal is the priority.

Chapter Five – Investigating the Significance of Ammonium and/or Nitrate as the Nitrogen source for *C.reinhardtii* Cultivation

5.1 Background

Current wastewater treatment practice sees nitrogen removed from wastewater through bacterial mediated nitrification/denitrification processes. In untreated municipal wastewater, nitrogen species are present predominantly as ammonium (i.e. from hydrolysed urea present in urine or organic nitrogen compounds appearing in faeces, Eckenfelder and Argaman, 1991). During nitrogen removal, ammonium is first nitrified to nitrate before denitrifying bacteria convert nitrate to N_2 gas which can be released into the environment without harm (Halling-Sørensen and Jørgensen, 1993). However, during nitrification and denitrification, NO and N_2O are produced as intermediates, of which a proportion are similarly released into the atmosphere, contributing to the greenhouse effect; wastewater treatment is estimated to account for 3.2-10 % of all N_2O emissions (Law *et a*l., 2012; Adouani *et al*., 2015). In addition, to facilitate the removal of ammonium *via* nitrification, wastewater tanks are aerated (a costly and highly energy intensive process) to provide oxygen for microbial growth (see Chapter 1, Section 1.3.3); aeration is estimated to account for approximately 45-80 % of electrical energy used in wastewater treatment works (WWTW) (Gandiglio *et al*., 2017 and sources therein). There is, therefore, support for processes that allow for the elimination of nitrification/denitrification processes within WWTW.

Photosynthetic microalgae have been shown capable of removing up to 100 % of the nitrogen from wastewaters (van Harmelen and Oonk, 2006; Sun *et al*., 2013; Zhang *et al*., 2014a; Caporgno *et al*., 2015) and do not require the addition of oxygen for growth. If this can be realised within a WWTW, it could remove the need for nitrification/denitrification processes. However, if this is to be feasible, a thorough understanding of how the nitrogen source affects microalgal growth and nutrient uptake is necessary.

The nitrification process means that depending on the treatment stage, the nitrogen present within a WWTW is present either predominantly as ammonium (influent wastewater), as nitrate (after nitrification) or as a mixture of the two (partial nitrification). With the focus shifting from simply nutrient removal within WWTW to nutrient recovery, existing nitrification technology offers flexibility over the nitrogen source for microalgal cultivation, should a particular form prove preferable for the production of high-value biomass.

Ammonium has long been thought of as the preferred source of inorganic nitrogen for phytoplankton growth (Dortch, 1990). Unlike nitrate, ammonium can be incorporated directly

into the carbon skeleton by the glutamine synthase/glutamate synthase pathway. In contrast, for nitrate assimilation, it is first necessary to reduce nitrate to nitrite and then ammonium for incorporation. A review of ammonium and nitrate assimilation of *Chlamydomonas* can be found in Fernandez and Galvan (2007), nevertheless our understanding of the effect of nitrogen source on algal physiology is lacking, especially given the emergence of microalgae as a useful tool for nutrient bioremediation from wastewater.

The reduced energy requirement of ammonium assimilation compared to nitrate has led to the hypothesis that growth on ammonium will lead to more remaining energy for other cellular processes, thus increasing growth rate (Lachmann *et al*., 2018), however the results of varying nitrogen source on microalgal growth to date have been highly variable, dependent on both the environmental conditions and microalgal species.

Patel and co-workers demonstrated that *Chlamydomonas reinhardtii* (strain CC-2936), when grown under constant light in a mixture of ammonium and nitrate, did not begin nitrate uptake until the concentration of ammonium had fallen to <2.5 mg/L (Patel *et al*., 2015). Despite this, Thacker and Syrett revealed very little difference in the growth of *Chlamydomonas reinhardtii* on a mixed N source with ammonium and nitrate consumed similarly under a range of light regimes (Thacker and Syrett, 1972). They demonstrated that the inhibition of nitrate assimilation by ammonium was limited to approximately 4 hours after which nitrate assimilation resumed normally, however the total N concentration was below the 2.5 mg/L inhibition limit reported by Patel *et al.*, (2015).

In contrast, the growth and lipid production of *Scenedesmus abundans* and *Chlorella ellipsoidea* can be optimised by a mixed nitrogen source proposed to be due to the distinct nitrate and ammonium transporters; nitrogen can therefore be assimilated at a faster rate before transporter saturation (González-Garcinuño *et al*., 2014). Some species including *Tetraselmis* sp. (Kim *et al*., 2016) and *Chlamydomonas acidophila* (Lachmann *et al*., 2018) have additionally been reported to show increased growth on nitrate as the sole nitrogen source.

Previous work has indicated that a shift from ammonium to nitrate leads to increased intracellular phosphate accumulation in *C.reinhardtii* (Yulistyorini, 2016) proposed to be due to an artificial nitrogen stress response induced as a result of the additional energy requirement needed to accumulate nitrate once ammonium resources are depleted. However, the results are inconclusive owing to the use of strain (11/32c) which harbours the *nit1* and *nit2* mutations, but which reportedly grew successfully on nitrate. The work presented in this chapter extends on the work of Yulistyorini by investigating the effect of ammonium/nitrate ratio on the growth, nutrient accumulation and lipid accumulation in *C.reinhardtii*. It is hypothesised that if a natural

shift from ammonium to nitrate assimilation, once ammonium reserves are exhausted, does cause a stress response, that lipid accumulation will be increased by a mixed nitrogen source. The initial total nitrogen content was modelled to reflect that present in real wastewater (after partial primary sedimentation) as measured at Esholt Wastewater Treatment Works, Bradford, UK (Yulistyorini, 2016).

5.2 Results and Discussion

Depending on the treatment stage, nitrogen within a wastewater treatment works is present primarily as ammonium, nitrate or a mixture of the two. As a result, there is flexibility over the choice of nitrogen source for microalgae grown to aid the wastewater treatment process. To test the effect of nitrogen source on the growth, bioremediation properties and lipid accumulation of microalgae, *Chlamydomonas reinhardtii* strain CC-1690 (capable of growth on either nitrate or ammonium) was grown in modified TAP medium with varying proportions of ammonium and nitrate; ammonium chloride was replaced with the same molar concentration of sodium nitrate for nitrate-based media. The total initial nitrogen concentration was kept constant throughout at 50 mg/L N (see Chapter 2, Section 2.2.1.1 for full media recipe). Cultures were monitored daily for optical density (measured at 750nm), chlorophyll concentration and pH and samples were collected daily for analysis of the media and biomass. Full methodology is provided in Chapter 2.

5.2.1 Culture growth was largely unaffected by the ammonium/nitrate ratio

Cultures of *C.reinhardtii* grown in varying proportions of ammonium and nitrate grew similarly with all cultures reaching a final optical density of 2.3-2.4, chlorophyll concentration of 29-33 µg/mL and dry biomass weight of 0.8-1.2 mg/L after seven days cultivation (Figure 5.1). This is corroborated in the similar doubling times for each culture (Table 5.1).

Previous reports have indicated that the presence of ammonium can halt nitrate uptake, indeed the presence of ammonium is shown to inhibit the action of specific nitrate transporters in *Chlamydomonas* (Fernandez and Galvan, 2007). Based on these results, under constant light, there is no apparent difference in the growth of *C.reinhardtii* as a result of differing proportions of ammonium and nitrate present in the media, directly contradicting previous hypotheses proposing that the additional energy required to assimilate nitrate over ammonium may result in a slowing of growth (Lachmann *et al*., 2018).

In contrast to the other tested growth parameters, the culture pH changes dramatically depending on the nitrogen source used (Figure 5.1 (D)). In theory, the presence of Tris buffer in TAP medium should limit the pH to between 7.0 and 9.0 as is observed for growth on ammonium only, however, the presence of nitrate in the medium resulted in an increasing final pH

dependent on the proportion of nitrate; nitrate only medium achieved the highest final pH of 11.0. The assimilation of positively charged ammonium ions causes release of H^+ ions back into the medium in order to maintain a constant intracellular pH. As such, growth on ammonium has previously been shown to cause acidification of culture medium (Scherholz and Curtis, 2013); here under photosynthetic conditions, the uptake of CO_2 and release of oxygen results in a net increase in pH despite ammonium assimilation. In contrast, uptake of negatively charged nitrate ions causes an increase in media pH owing to the uptake of H^+ ions from the medium (Scherholz and Curtis, 2013) and explains the increasing media pH with proportionately increasing nitrate.

While the growth of *C.reinhardtii* appears unaffected by the ammonium/nitrate ratio, the high pH afforded by nitrate assimilation will likely affect nutrient availability and therefore the bioremediation potential for nutrient recycling.

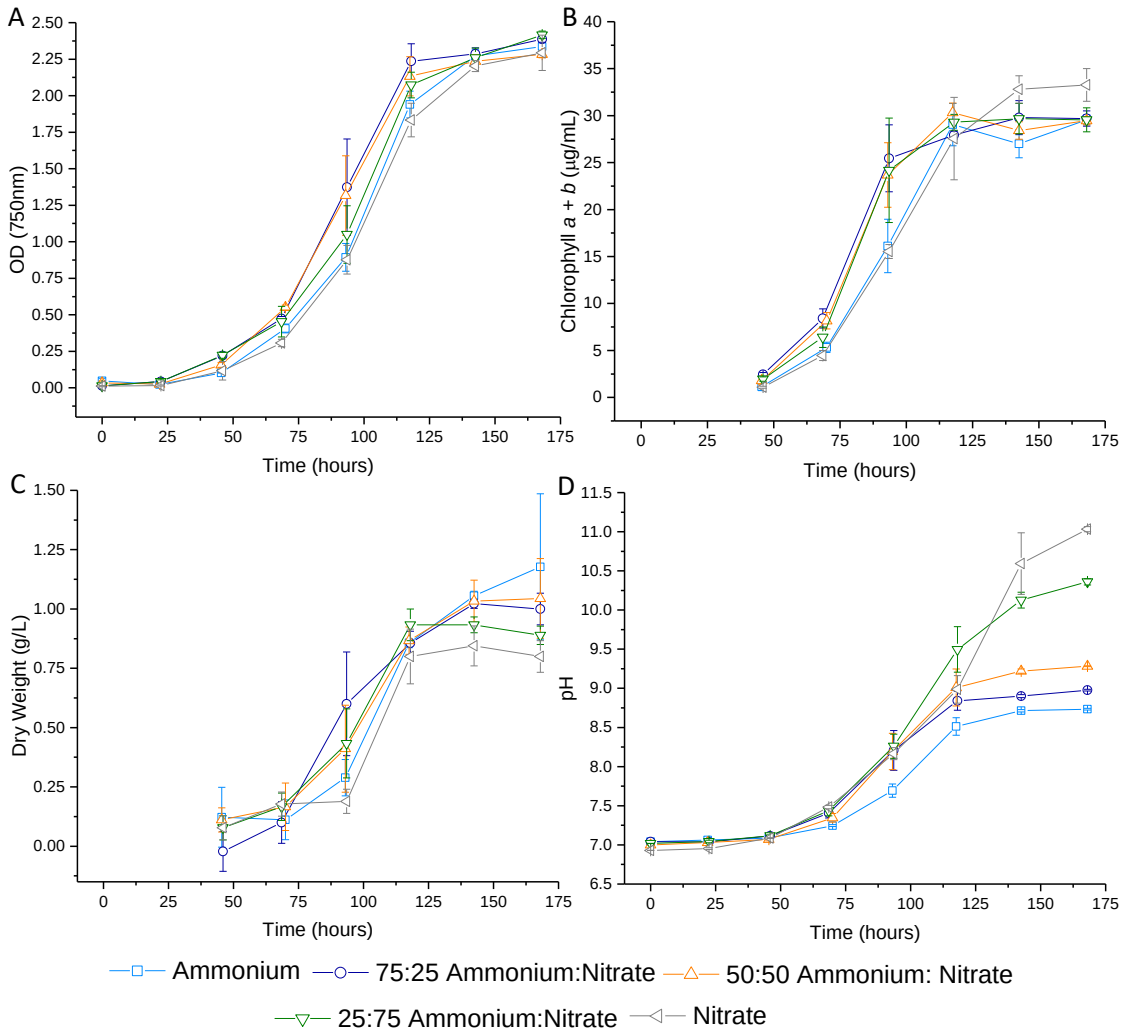

Figure 5.1 Growth of C.reinhardtii in five different ratios of ammonium and nitrate as the only available nitrogen sources for growth (total N concentration = 50 mg/L). (A) Optical density measured at 750 nm, (B) total chlorophyll concentration, (C) dry biomass weight and (D) pH. All points are the mean and standard deviation of biological triplicates.

Table 5.1 Doubling times for C.reinhardtii grown varying ratios of ammonium and nitrate. Doubling times were determined from the optical density at exponential phase growth (between 22 and 93 hours after inoculation). Doubling times shown are calculated from mean optical density of three biological replicates.

	Doubling Time (hours)
Ammonium	13.4
75:25 Ammonium:Nitrate	14.2
50:50 Ammonium:Nitrate	12.5
25:75 Ammonium:Nitrate	15.4
Nitrate	12.3

5.2.2 Bioremediation is optimised by high ammonium content

Some microalgal species show a preference for a specific nitrogen source, indeed the presence of ammonium has been shown to cause an inhibition of nitrate assimilation in some cases (Patel *et al*., 2015; Thacker and Syrett, 1972; Yulistyorini, 2016). In order to test this in *Chlamydomonas reinhardtii* under constant light conditions, the concentrations of ammonium and nitrate in the culture media were measured at the start and end of the cultivation period and daily during exponential phase (Figure 5.2). At high pH, nitrogen may additionally be lost through volatilisation of free ammonia. To be sure that losses observed are due to microalgal uptake, free ammonia concentration was calculated based on the pH and measured ammonium concentration according to the equations of Emerson *et al*., (1975). Estimated concentrations of free ammonia never exceeded 2 mg/L (data not shown) and pH values capable of high NH_3 fractions were only observed once total nitrogen concentrations were low. Losses due to ammonia volatilisation are therefore assumed to be negligible.

Measurement of total inorganic species (NH_4 + NO_3) within the culture media demonstrates that overall nitrogen uptake from the medium was largely unaffected by the differing ammonium/nitrate ratios (Figure 5.2 (C)). Nitrogen removal was initially slow (i.e. lag growth phase) before the majority of nitrogen was removed between approx. 70-120 hours (i.e. exponential phase growth). Within approximately five days, almost all the nitrogen had been removed from the media in all cases. The onset of stationary phase after five days likely reflects the lack of nitrogen availability beyond this point.

In contrast, the uptake of ammonium and nitrate differ from one another and between media preparations (Figure 5.2 (A, B)). The uptake rate of individual nitrogen species is increased with increasing proportional concentration however there is a clear initial preference for ammonium when both ammonium and nitrate are present as can be seen from the near constant nitrate concentration in the first approx. 70 hours of cultivation.

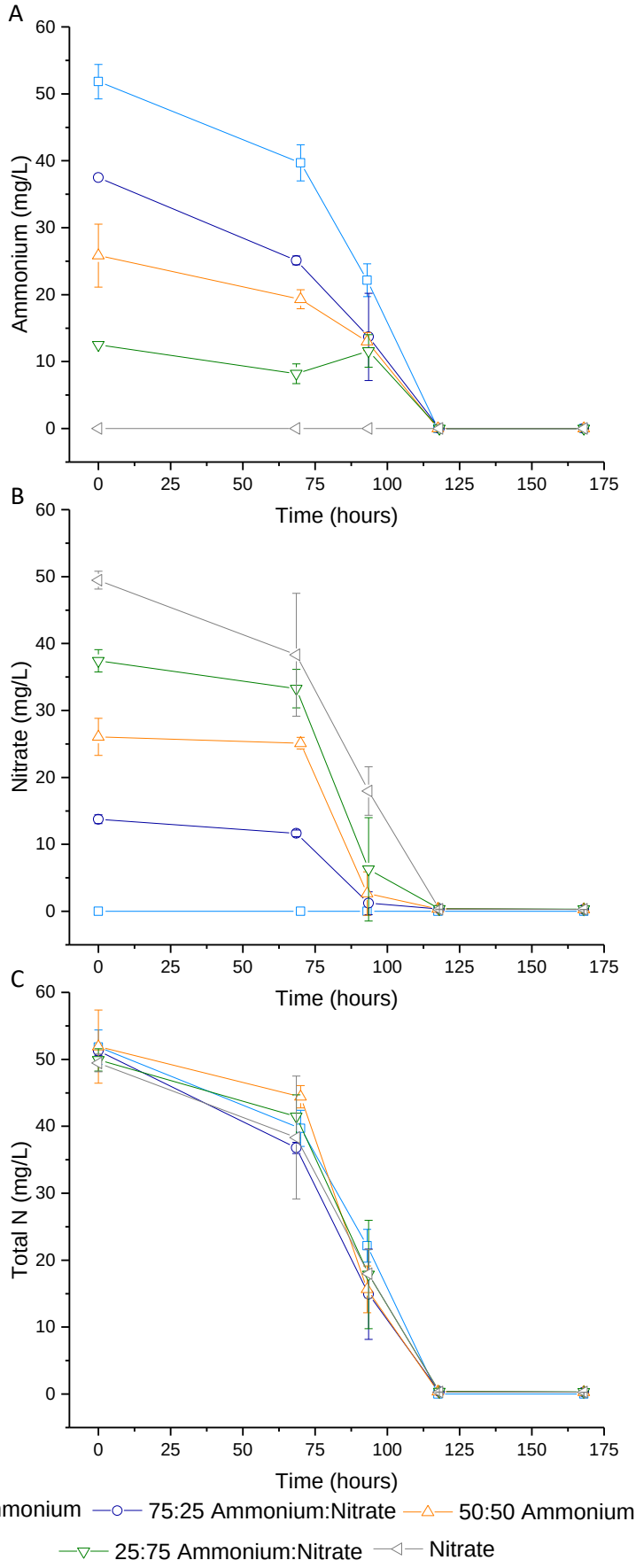

Figure 5.2 (A) Ammonium concentration; (B) Nitrate concentration and (C) total nitrogen concentration in culture medium during growth of C.reinhardtii in five different ratios of ammonium and nitrate as the only available nitrogen sources (total N = 50 mg/L). Points are the mean and standard deviation of biological triplicates.

Comparing the uptake rates of ammonium and nitrate under each media preparation clearly demonstrates that the initial uptake rate of nitrate is lower than that of ammonium with the exception of medium containing a sole nitrogen source (100 % N species) where uptake rates are similar (Figure 5.3 (A)). The presented uptake rates show a clear initial preference for ammonium assimilation over nitrate, as has previously been shown (Patel *et al*., 2015; Yulistyorini, 2016) proposed to be due to the increased energy requirement of nitrate assimilation. In contrast to some reports, the presence of ammonium does not cause complete inhibition of nitrate assimilation, rather a slowing of nitrate uptake in preference for ammonium.

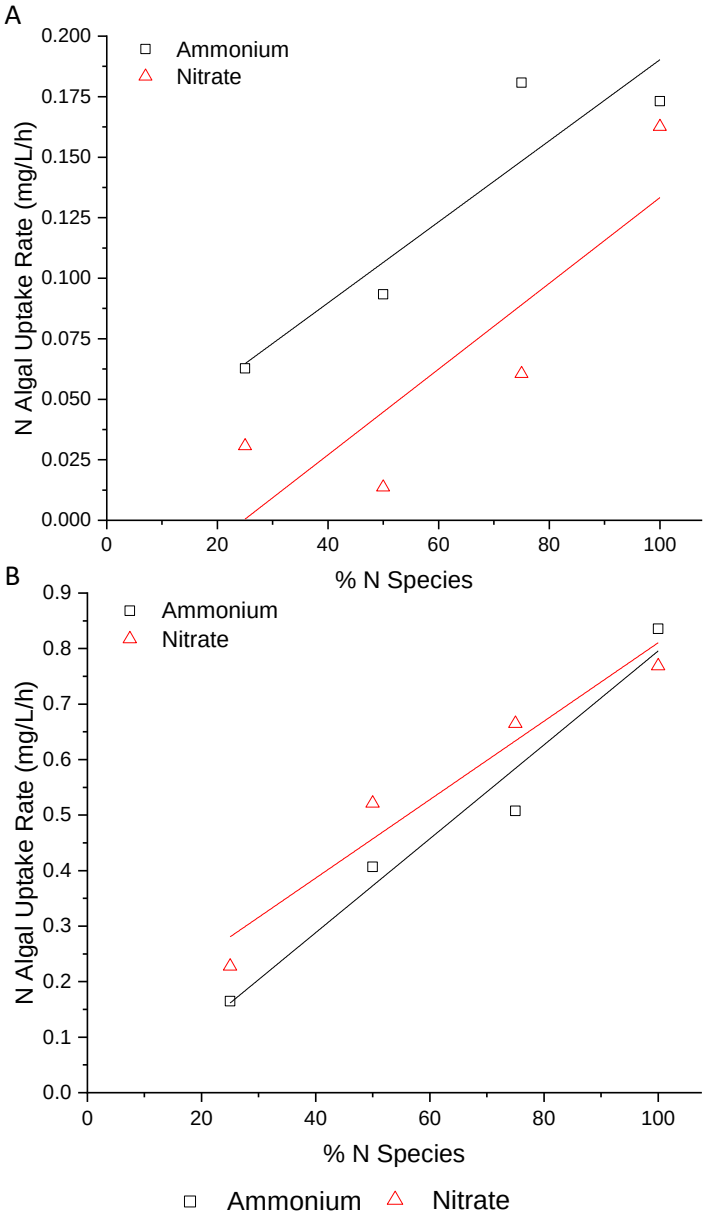

Figure 5.3 Removal rates of ammonium and nitrate between (A) 0-70 hours and (B) 70-118 hours after inoculation. X axis represents the % ammonium for ammonium uptake points and nitrate for nitrate uptake points. Points are calculated as the N removed between the time points indicated/the number of hours. Linear fit of the points shown for comparison purposes only.

In contrast, during exponential phase growth, there appears to be no preference for nitrogen source as can be seen from the similar nitrogen uptake rates for ammonium and nitrate between 70 and 118 hours after inoculation (Figure 5.3 (B)). The loss of preference is possibly as a result of the now much reduced ammonium concentration, however the concentration is still considerably above that previously reported to cause inhibition of nitrate uptake (Patel *et al*., 2015). Alternatively, the lack of preference may be because the rapid uptake of both nitrogen species simultaneously aids rapid growth during exponential phase when nitrogen is limited as is shown due to the total removal of nitrogen within 5 days of inoculation.

Phosphate concentration within the media was measured daily and, by comparison with the relationship between available phosphate and pH demonstrated previously (see Chapter 4, Figure 4.10), the concentration of precipitated phosphate and subsequently the concentration of phosphate removed through microalgal remediation were estimated (Figure 5.4).

The final media phosphate concentration was similar in all cultures ranging from 5.5-8.4 mg/L phosphorus after seven days of *C.reinhardtii* cultivation from an initial media concentration of 32 mg/L. Total P removal therefore appears to be unaffected by the nitrogen source available, however the increased media pH afforded by nitrate assimilation will increase the proportion of phosphate lost through precipitation.

Estimation of phosphate precipitation shows that cultures grown in 100 or 75 % ammonium demonstrate little precipitation of phosphate owing to the near-neutral media pH throughout. In contrast, increasing nitrate to 50 % of the available nitrogen results in a sharp increase in the amount of phosphate precipitated. The final pH for cultures containing ≥ 50 % nitrate ranges from 9.3-11.0 in contrast to ammonium-heavy cultures which reached a final pH of 8.7-9.0 (Figure 5.1). A sharp drop in available media phosphate in response to increasing pH is demonstrated between pH 8.5-9.5 (see Figure 4.10) on either side of which the available phosphate concentration remains approximately constant, thus explaining the similar phosphate precipitation observed between 100 and 75 % ammonium-based cultures and cultures containing 50-100 % nitrate (Figure 5.4 (B)).

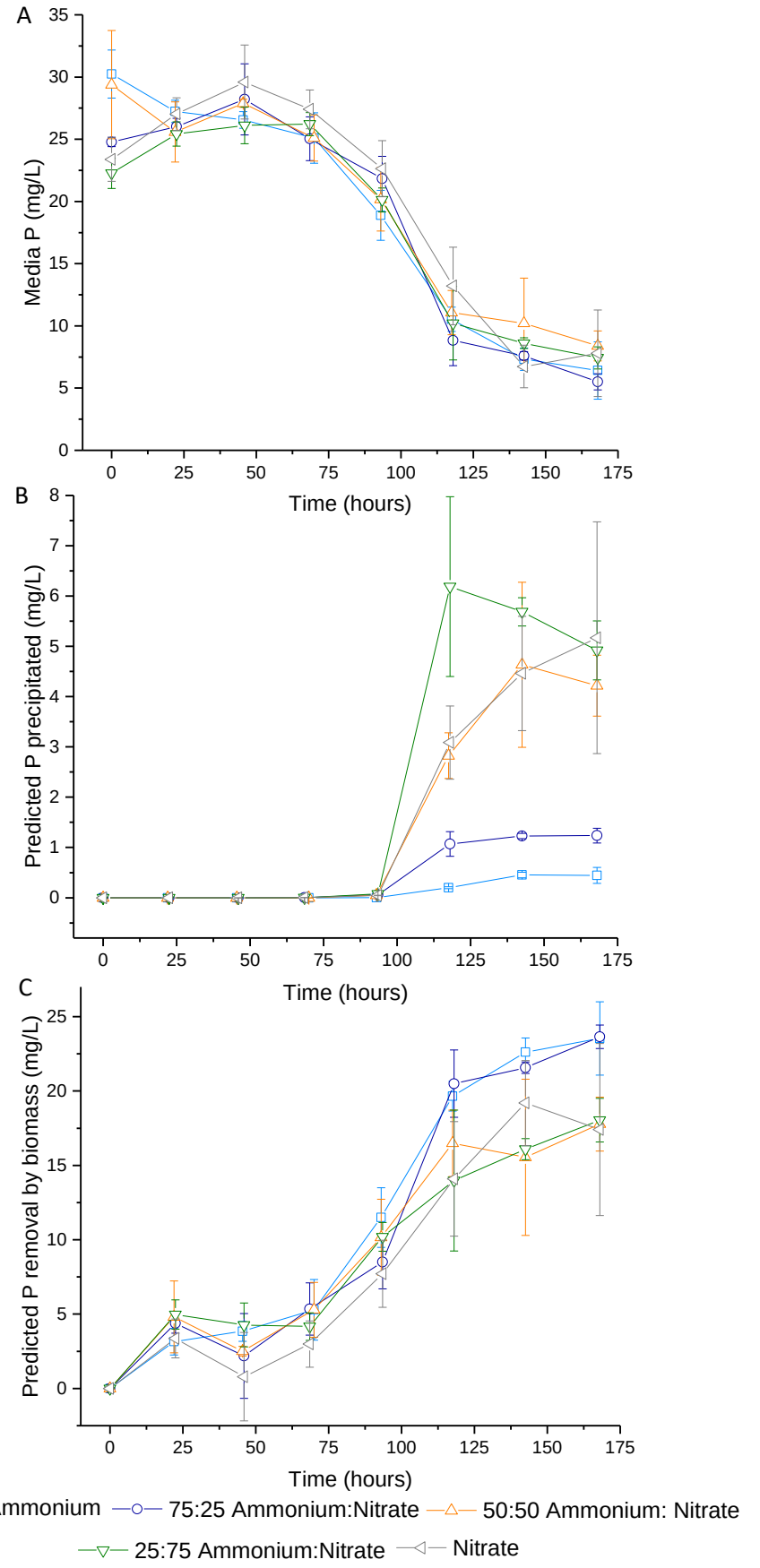

Figure 5.4 (A) Phosphorus concentration (present as PO_4) remaining in the media after filtration; (B) predicted phosphorus precipitation and (C) predicted phosphorus removal by biomass during growth of C.reinhardtii in varying ratios of ammonium and nitrate as the only available nitrogen sources. Points are the mean and standard deviation of biological triplicates.

Subtracting the predicted phosphate precipitation from total phosphate removed gives an estimate of the phosphate assimilated during microalgal growth (Figure 5.4 (C)). There is a clear inverse correlation between the amount of precipitated phosphate and that estimated to be removed by microalgal remediation. Cultures grown in 100 or 75 % ammonium demonstrated approximately 24 mg/L phosphate assimilated in contrast to approximately 18 mg/L by cultures of *C.reinhardtii* grown in ≥50 % nitrate. The almost complete removal of phosphate and inverse correlation between precipitated and bioremediated phosphate indicates that the reduced phosphate assimilation by microalgae in high nitrate-based medium is as a direct result of the reduced availability of phosphate due to precipitation. The significance of this is that nitrate-based culture wastewater will lead to an increase in the amount of phosphate lost (and therefore unavailable for recycling) but affords no advantage to the amount of phosphate remaining in the effluent.

Based on the estimated microalgal uptake of phosphate (Figure 5.4 (C)) and the dry biomass weight of cultures (Figure 5.1 (C)), the phosphate concentration within the biomass was estimated as a weight % of dry biomass (Table 5.2). The data reported are the median and range of [Phosphate (mean – SD)/Dry weight (mean + SD)] and Phosphate (mean + SD)/ Dry weight (mean – SD)] (i.e. the minimum and maximum estimated cellular phosphate concentration) where the phosphate and dry weight means and standard deviations have been calculated from biological triplicates. Nitrogen content within the biomass was measured by elemental (CHNS-O) analysis.

Table 5.2 Nitrogen content and predicted P content of C.reinhardtii after 7 days grown in five different ratios of ammonium and nitrate. Nitrogen is reported as mean and standard deviation weight % of dry biomass measured by CHNS elemental analysis of biological triplicates. Phosphorus is reported as median ± range weight % of dry biomass estimated from the calculated microalgal P uptake and the measured culture dry biomass weight for biological triplicates.

	N Content (% dry biomass)	Predicted P Content (% dry biomass)
Ammonium	5.0 ± 0.18	2.2 ± 0.79
75:25 Ammonium:Nitrate	4.9 ± 0.35	2.4 ± 0.24
50:50 Ammonium:Nitrate	5.0 ± 0.06	1.8 ± 0.46
25:75 Ammonium:Nitrate	5.4 ± 0.20	2.0 ± 0.25
Nitrate	5.9 ± 0.30	2.3 ± 0.91

There is a slight increase in cellular nitrogen concentration with increasing proportion of nitrate in the medium (Table 5.2). This is largely due to a slight reduction in dry weight (Figure 5.1) compared to nitrogen uptake rather than improved nitrogen removal from the medium. Microalgae typically contain approximately 10 % nitrogen by weight (Stumm and Morgan, 1996, van Harmelen and Oonk, 2006); the reduced nitrogen content seen here confirms that cultures

had undergone a period of nitrogen starvation as is inferred from the total removal of nitrogen within five days of cultivation (Figure 5.2).

In contrast, the cellular concentrations of phosphorus are very similar regardless of the nitrogen source, likely because the conditions leading to the highest phosphate uptake (Figure 5.4) also led to the highest biomass dry weight (Figure 5.1). The results contradict those of Yulistyorini (2016) who demonstrated that the natural shift from ammonium to nitrate assimilation once ammonium reserves are depleted resulted in an increase in phosphate accumulation within the cell. If this were the case here, we would expect to see a lower concentration of cellular phosphorus in cultures grown in a single nitrogen source. Microalgae are typically reported to contain approximately 1 % by weight phosphorus (Stumm and Morgan, 1996, van Harmelen and Oonk, 2006). In all media conditions investigated here, the cellular phosphorus concentration is significantly higher than the 'typical' concentration, indicative of significant polyphosphate accumulation. This is most likely as a result of the nitrogen starvation experienced 5-7 days after inoculation; nitrogen deprivation has previously been shown to increase polyphosphate accumulation in microalgae (Zhu *et al*., 2015; Chu *et al*., 2015).

Under the conditions investigated, cultures of *C.reinhardtii* successfully removed 100 % of nitrogen species and approximately 73-83 % of phosphates within seven days, independent of the nitrogen source present. The high proportion of nutrient removal is significant for the prospects of microalgal wastewater treatment. A slight advantage toward phosphorus bioremediation is afforded by a high proportion of ammonium (≥ 75 %) compared to nitrate owing to the comparatively high pH afforded by nitrate assimilation leading to heavy phosphate precipitation. Domestic wastewaters typically contain approximately 6-20 mg/L P (Pescod, 1992), as such, based on these results, microalgal remediation will likely be sufficient for complete removal; microalgal remediation is preferable over precipitation owing to the ability to recycle the assimilated phosphate into agricultural fertilisers. A nitrate-based wastewater may however be utilised for optimising phosphate removal *via* precipitation in extreme phosphate-rich wastewaters where complete nutrient removal may not be possible by microalgal remediation alone.

It is a limitation, however, that this study was performed under conditions of constant light only and that the culture conditions included the presence of a buffer (range 7.0-9.0). The effect of inorganic nitrogen source on the growth and nutrient accumulation in microalgae is a relatively understudied topic especially in the context of wastewater treatment. It stands however that the use of a nitrate-heavy wastewater will lead to an increase in culture pH in comparison with a wastewater containing predominantly ammonium. More research is needed

to fully understand the effect of ammonium/nitrate ratio under 'typical' day/night cycles and in more realistic wastewater conditions.

5.2.3 Biodiesel production favours a nitrate-heavy medium

Oils produced from microalgae grown to aid wastewater treatment can be extracted as a valuable by-product in order to produce biodiesel. In order to test the effect of inorganic nitrogen source on the production of oils and suitability for biodiesel production, *C.reinhardtii* samples were extracted (2:1 $CHCl_3$:MeOH) and lipids esterified (0.6M HCl in MeOH) to produce fatty acid methyl esters (FAMEs). FAMEs were analysed quantitatively by GC-MS using C17:0 as an internal standard (Figure 5.5). Full methodology is provided in Chapter 2, section 2.6.3.1.

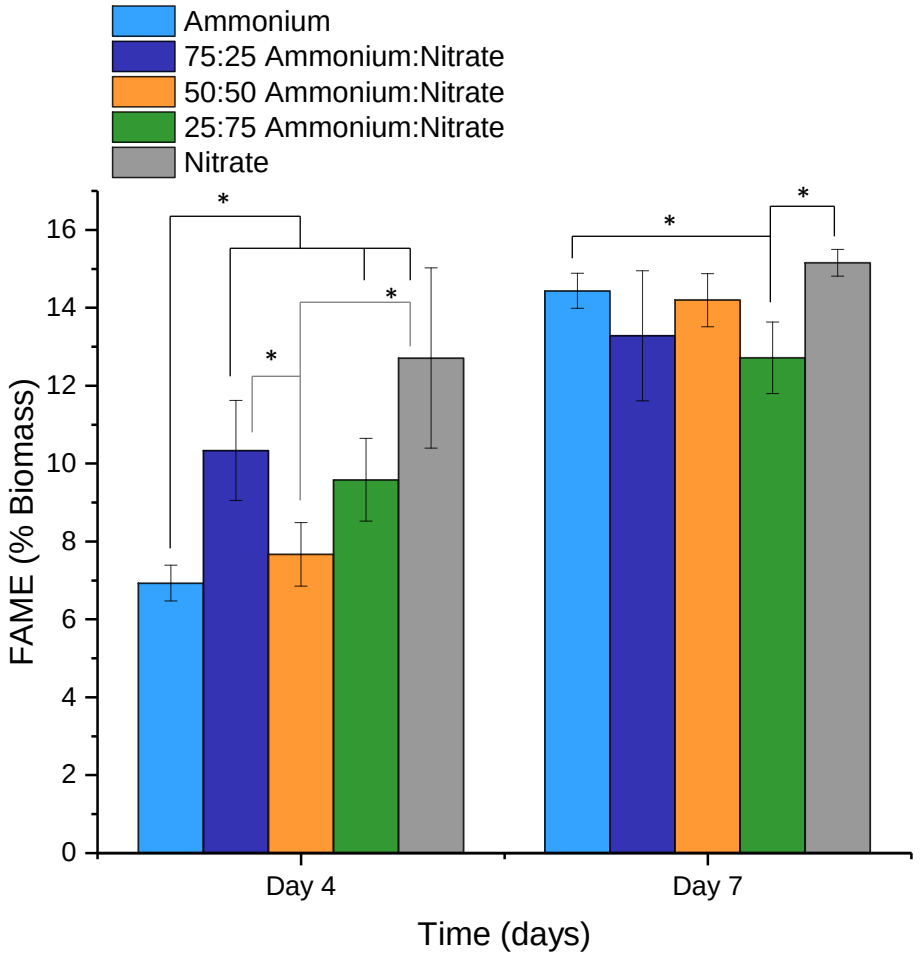

*Figure 5.5 FAME content, measured by GC-MS analysis, as % of dry biomass weight of C.reinhardtii grown in five ratios of ammonium and nitrate as the only available nitrogen sources. Day 4 and 7 represent samples taken four and seven days after inoculation respectively. All points are the mean and standard deviation of biological triplicates. * denotes a statistically significant difference (two-sided independent t test, $p < 0.05$).*

After four days cultivation, there was a large variation in the FAME content observed, dependent on the ratio of ammonium and nitrate. Cultures grown in 100 % ammonium contained the lowest fatty acid concentration (6.9 % of dry biomass weight) in contrast to

cultures grown in 100 % nitrate which contained a significantly higher proportion of fatty acids (12.7 % dry biomass weight, $p < 0.05$). Cultures grown in a mixed nitrogen source were observed to contain approximately 7.5-10.5 % FAME. No correlation was observed between the ammonium/nitrate ratio and FAME content in cultures grown in a mixed nitrogen source.

After a further three days cultivation, the FAME content was increased in all cultures, almost certainly as a result of nitrogen starvation following the depletion of all media nitrogen five days after inoculation (Figure 5.2). Increased lipid content in response to nitrogen starvation has been extensively studied (Moellering and Benning, 2010; Siaut *et al*., 2011; Schmollinger *et al*., 2014; Valledor *et al*., 2014; Gonçalves *et al*., 2016). In contrast to during exponential phase, however, no difference in the FAME content was observed between cultures following the short period of nitrogen starvation with all cultures containing a final FAME concentration of 12.7-15.2 % dry biomass weight.

For biomass harvested during exponential phase, the results presented here demonstrate a significant advantage of a nitrate-based wastewater over one containing ammonium owing to the significant increase in fatty acid accumulation. However, given that the primary goal of using microalgae for wastewater treatment is to aid in the complete removal of nutrients, it would be preferable to harvest biomass once complete removal of nitrogen had been achieved. The significant increase in lipid production once media nitrogen reserves had been depleted is highly promising for the production of biodiesel from wastewater; the quantity of fatty acids could likely be increased by a prolonged period of nitrogen starvation before harvesting. The increase in lipids following a natural depletion of nitrogen (i.e. not by sudden nitrogen removal) has previously been reported in only a limited number of studies (Caporgno *et al*., 2015).

Compositional analysis can be used to estimate the properties of biodiesel from microalgae; biodiesel of better quality can be blended at higher proportions with petrochemical diesel. The composition of FAMEs was similar for all cultures (Figure 5.6) regardless of ammonium/nitrate ratio however significant changes were observed from four to seven days after inoculation; a significant increase in C16:0, C18:2 and C18:3 was observed in all cultures.

Unlike sudden nitrogen starvation, where the degree of unsaturation is generally reduced compared to cultures grown under nitrogen sufficiency, the degree of unsaturation here is seen to increase marginally in all but 75 % nitrate cultures (Table 5.3). This may simply be due to the limited time under which cultures have experienced nitrogen deficiency or may be as a result of the gradual nitrogen decrease opposed to a sudden removal of nitrogen as is more usual in previous studies of nitrogen deprivation and lipid accumulation.

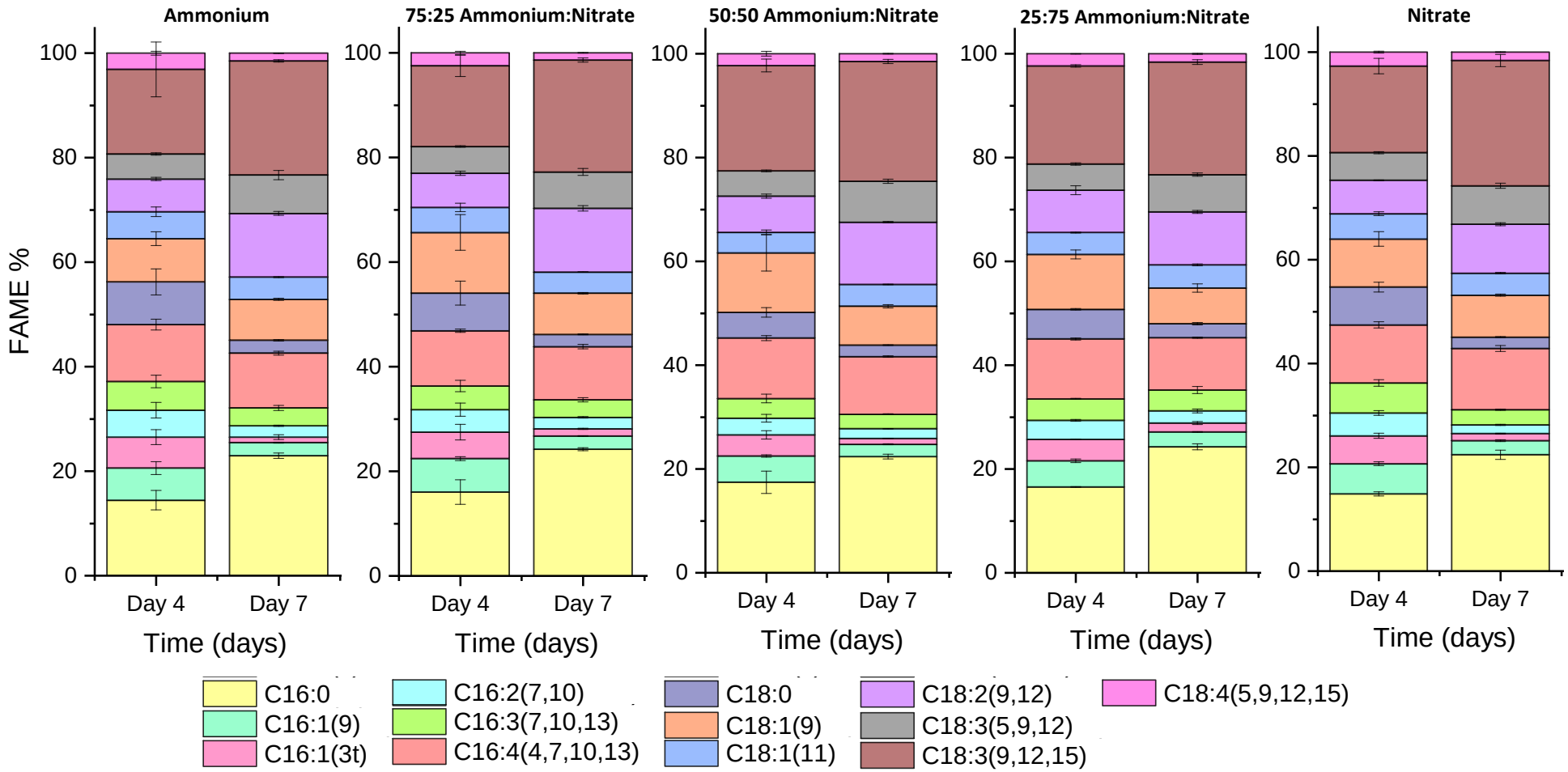

Figure 5.6 FAME composition of C.reinhardtii grown in five ratios of ammonium and nitrate as the only available nitrogen sources. Day 4 and 7 represent samples taken four and seven days after inoculation respectively. All points are the mean and standard deviation of biological triplicates.

Table 5.3 Biodiesel properties calculated from the FAME composition of C.reinhardtii grown in five different ratios of ammonium and nitrate as the only available nitrogen sources. Days represent the time after inoculation to the nearest day. All points are calculated from the mean FAME composition of biological triplicates.

		DU	*LCSF*	*CN*	*SV* ($mg\ KOHg^{-1}$)	*IV* ($g\ I_2 100g^{-1}$)	*CFPP (°C)*	*OSI (h)*	*Density (ρ)* (gcm^{-3})	*Kinematic Viscosity (υ)* (mm^2s^{-1})	*HHV* ($MJ\ kg^{-1}$)
Biodiesel Standard EN 14214		-	-	≥51	-	≤120	Variable	≥6	0.86-0.90	3.5-5.0	-
Ammonium	**Day 4**	129.3	5.5	36.4	199.0	166.0	0.9	6.9	0.89	3.6	39.4
	Day 7	133.6	3.5	35.4	198.1	170.8	-5.4	5.4	0.89	3.6	39.4
75:25	**Day 4**	125.8	5.2	37.9	198.7	159.5	-0.2	6.9	0.88	3.7	39.4
Ammonium:	**Day 7**	131.1	3.6	36.2	198.2	167.2	-5.2	5.5	0.89	3.6	39.4
Nitrate											
50:50	**Day 4**	130.7	4.2	35.8	198.5	168.9	-3.2	6.3	0.89	3.6	39.4
Ammonium:	**Day 7**	135.7	3.3	34.6	197.9	174.8	-6.0	5.3	0.89	3.6	39.4
Nitrate											
25:75	**Day 4**	131.6	4.5	35.8	198.5	168.7	-2.3	6.3	0.89	3.6	39.4
Ammonium:	**Day 7**	130.2	3.8	36.0	198.5	167.9	-4.6	5.6	0.89	3.6	39.4
Nitrate											
Nitrate	**Day 4**	130.4	5.1	36.0	199.0	167.8	-0.3	6.7	0.89	3.6	39.4
	Day 7	134.5	3.3	34.2	198.2	176.0	-6.0	5.5	0.89	3.6	39.4

All cultures possess very similar properties for biodiesel production which get worse with increasing cultivation time from four to seven days, as such there is a trade-off to be had between lipid quality and quantity. The quality of biodiesel produced may however be improved by a prolonged period of nitrogen starvation (i.e. delayed harvesting) once nitrogen reserves have been depleted. The similarity between lipid production and quality regardless of ammonium/nitrate ratio indicates that there is no advantage to be gained from wastewater nitrification prior to microalgal growth.

In addition, the ability of *C.reinhardtii* to remove all of the nitrogen and >70 % of phosphorus from the media, as well as producing high quality biomass for the production of biofuels, regardless of the inorganic nitrogen source present (ammonium or nitrate), confirms that microalgae may offer a suitable alternative to the nitrification/denitrification process and subsequent energy intensive aeration. Furthermore, emerging research has demonstrated that microalgae can reduce nitrate to nitrous oxides, which are released into the atmosphere as harmful greenhouse gases (Plouviez *et al*., 2017), thus further supporting the use of ammonium as the primary nitrogen source.

5.3 Conclusions

Cultivation of *C.reinhardtii* under constant light on a range of ammonium/nitrate ratios as the only available nitrogen sources revealed little difference in microalgal growth or lipid accumulation. In contrast, phosphorus bioremediation was improved when cultivation was performed in a high ammonium-containing (≥75 %) medium owing to the increased pH afforded by nitrate assimilation leading to loss of phosphate through precipitation. The results presented are promising for the use of microalgal bioremediation and biodiesel production as a valuable by-product in place of microbial nitrification/denitrification thus offering the ability for savings in both cost and energy from aeration (required for bacterial growth).

This study provides robust data on the effect of inorganic nitrogen source on microalgal growth, nutrient uptake and lipid accumulation under constant light and with phosphate concentration in excess. Much more research is required into the effect of nitrogen source under realistic day/night cycles, in the absence of buffer, under varying nutrient concentrations and with a wide range of microalgal strains and species in order to fully understand the effect of nitrogen source on microalgal wastewater treatment objectives.

Chapter Six – Investigating the Effect of Diphenyl methylphosphonate on Lipid Catabolism in *C.reinhardtii*

6.1 Background

The majority of research concerned with increasing lipid accumulation in microalgae for the production of biodiesel is concerned with increasing the quantity of neutral lipids (triacylglycerols, TAGs) accumulated, either through manipulation of environmental conditions (the most studied being nitrogen starvation) or through genetic upregulation of the lipid biosynthesis pathway.

Attempts at genetically upregulating the lipid biosynthesis pathway have had limited success in increasing the yield of neutral lipids (Deng *et al*., 2012; Tan and Lee, 2016; Zhu *et al*., 2018; see Chapter 1, section 5.1). This has been proposed to be due to competition for substrates, such as acyl-CoA and other carbon compounds, between the pathways for TAG synthesis and cellular growth (Tan and Lee, 2016). Subsequently, attempts at increasing lipid accumulation have been at the expense of biomass yield (Deng *et al*., 2012; Tsai *et al*., 2014; Tan and Lee, 2016; Zhu *et al*., 2018;).

Emerging research has aimed at increasing lipid yield through downregulation of the lipid catabolism pathway. To date, however, only one TAG lipase (Warakanont *et al*., 2019), one DAG lipase (Li *et al*., 2012) and one acyl-oxidase (responsible for catalysing the first committed step in fatty acid beta-oxidation) (Kong *et al*., 2017) have been identified in *Chlamydomonas* and a much better understanding of the enzymes responsible for lipid catabolism is needed.

The drug Brefeldin A (BFA), known to cause endoplasmic reticulum (ER) stress, has been shown to act as both a trigger for TAG accumulation and a suppressor of TAG mobilisation following nitrogen resupply (Kato *et al*., 2013, Kim *et al*., 2013) but at the expense of cell growth. Cells of *C.reinhardtii* were shown to cease growth immediately after addition of 2.5 µM BFA (Kato *et al*., 2013) and a reduction in optical density has been observed after 15 hours exposure to 75 µg/mL (0.27 mM) BFA (Kim *et al*., 2013). In addition, sonication may be required for BFA induced TAG accumulation in walled microalgal strains (Kim *et al*., 2013).

Brown and co-workers identified that diphenyl methylphosphonate (DMP) acts as a specific chemical inhibitor of TAG mobilisation in seedlings of the terrestrial plant *Arabidopsis thaliana* (Brown *et al*., 2013). Seedlings grown in the presence of 25 µM DMP retained 64 % of TAGs from dry seed compared to 7 % in untreated controls, however growth was significantly hindered in DMP treated seedlings, with seedlings reportedly stunted and pale after four weeks. Although the precise target was not found, comparison of DMP treated seedlings with β-

oxidation and lipase mutants indicates that DMP is responsible for specific inhibition of the β-oxidation pathway, responsible for the degradation of fatty acids into acetyl-CoA, and not inhibition of TAG lipolysis.

Here, the effect of DMP on lipid mobilisation in *Chlamydomonas reinhardtii* is reported. Like in *Arabidopsis thaliana*, DMP inhibits TAG catabolism following nitrogen resupply but much higher concentrations of DMP are required to elicit a response. In contrast to BFA, growth is only marginally affected by high concentrations of DMP and investigation over a wider concentration range will help to identify the best compromise between growth and TAG content.

6.2 Results and Discussion

Diphenyl methylphosphonate (DMP) has previously been shown to inhibit lipid catabolism in seedlings of *Arabidopsis thaliana* (Brown *et al*., 2013). To test whether a similar effect is observed in microalgae, samples of *C.reinhardtii* strain CC-1690 were cultured in TAP medium to mid-log phase (four days) before being exchanged into nitrogen deficient medium (TAP-N) to an initial OD_{750} = 0.8 and allowed to accumulate lipids for 96 hours. Four days of nitrogen starvation has previously been shown to be sufficient to obtain high quantities of neutral lipid accumulation in *C. reinhardtii* (Siaut *et al*., 2011). Finally, cultures were exchanged into fresh TAP medium + 0.1% (v/v) DMSO containing DMP (0 µM – 250 µM, initial OD_{750} = 1.5). Each concentration of DMP was performed in triplicate cultures. Cultures were monitored daily after exchange into DMP containing medium for optical density (measured at 750 nm), chlorophyll concentration and pH. Samples (ca. 3mL) were also taken daily and the biomass harvested by centrifugation for GC-MS lipid analysis. Full methodology is provided in Chapter 2. Initially the experiment was performed with 25 µM DMP (as Brown *et al*., 2013), and following a screening study at small scale over a range of DMP concentrations (50 µM – 250 µM), was repeated at two higher concentrations of DMP. A separate untreated control (0 µM DMP) was run in each case and, as such, different experiments are presented on separate plots throughout.

6.2.3 Diphenyl methylphosphonate inhibits growth on reintroduction of nitrogen

Like most microalgae, *C.reinhardtii* accumulates neutral lipids (stored as oil droplets) under nitrogen starvation (Siaut *et al*., 2011; Schmollinger *et al*., 2014; Valledor *et al*., 2014; Park *et al*., 2015). On reintroduction of nitrogen, cultures resume rapid growth (Siaut *et al*., 2011; Gonçalves *et al*., 2016) and the catabolism of neutral lipids (mobilised as a rapid energy source for the restoration of growth) can be monitored by staining with the lipophilic dye Nile-Red.

Measurement of optical density, chlorophyll concentration, pH and dry biomass weight (Figure 6.1) demonstrated resumed growth on reintroduction of nitrogen but growth rate was significantly reduced in a dose dependent manner under treatment with DMP.

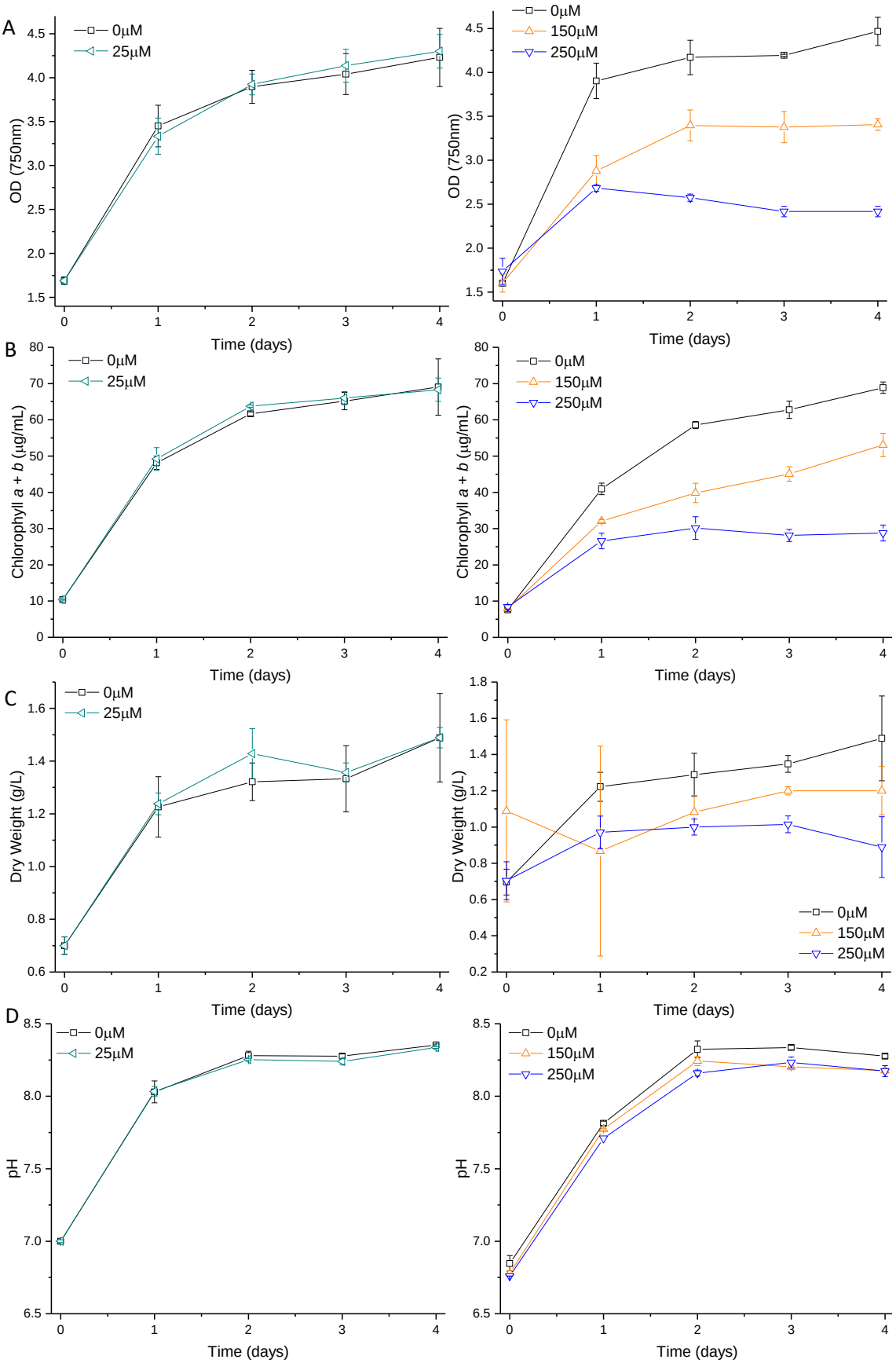

Figure 6.1 Growth of C.reinhardtii on TAP medium + DMP at six concentrations after cultivation in TAP-N medium for four days to accumulate neutral lipids. (A) Optical density; (B) Total chlorophyll concentration; (C) Dry biomass weight (note the difference scales), (D) pH. A control concentration (0 μM DMP) was run for each batch of experiments and batches are therefore presented separately. Points are the mean and standard deviations of three biological replicates.

Measurement of optical density revealed a sharp increase from 1.5 to approximately 3.5-4.0 within 24 hours of exchange into full TAP medium in the absence of DMP (Figure 6.1A). Addition of DMP to TAP medium resulted in a marked decrease in the growth rate, dependent on the concentration of DMP. Cultures treated with the lowest concentration of DMP (25 µM) grew indistinguishably from the control (0 µM) however addition of 150 µM and 250 µM caused increasing levels of growth inhibition. After 24 hours in TAP + 25, 150 and 250 µM DMP, cultures had reached an optical density of 3.3, 2.9 and 2.7 respectively. The chlorophyll concentration and dry weight profiles largely mimic those of the optical density in each case with all cultures reaching stationary phase within 48 hours of exchange into full TAP medium. (Figure 6.1B-D). The pH was similar for all cultures (Figure 6.1D).

While an increase in optical density and dry weight suggest the resumption of growth, variations in cell size, and therefore light scattering behaviour, interfere with the use of optical density and biomass weight to predict cell division and confirm the exit of quiescence. Cell counting is commonly used to determine cell number and hence the rate of cell division, however the reduced chlorophyll concentration severely reduces cell visibility when viewed under an optical microscope, thus limiting the accuracy of this method unless automated cell counters are available. Furthermore, cell counting does not distinguish between dead and living cells and is therefore prone to overestimating the number of viable (divisible) cells. In order to confirm whether the reduced optical density observed for DMP treated cultures is due to inhibition of cell division, the number of viable cells was determined daily by spreading diluted aliquots of culture onto TAP-Agar plates and counting the resulting colonies (colony forming units) after a period of incubation (see Chapter 2, section 2.5.3).

A significant increase in colony forming units (cfu) was observed in all cultures during the first 48 hours after exchange from TAP-N into full TAP medium and confirms that DMP treatment did not result in complete inhibition of cell division (Figure 6.2). Immediately after exchange, all cultures had an initial 2.5-3.8 million colony forming units per mL of culture however, within 24 hours, the measured number of colonies was noticeably fewer for DMP treated cultures (150 µM and 250 µM) compared to the untreated control (0 µM). Over the course of the experiment, the control reached a maximum of 44 million cfu/mL in contrast to 15 million for 150 µM DMP treated and 6 million for 250 µM DMP treated cultures indicating a significant inhibition of cell division which increases with increasing DMP concentration. On the final day of testing, measured cfu for DMP treated cultures was significantly different ($p < 0.05$) from the control. Similarly, 250 µM treated cultures had significantly fewer cfu than 150 µM treated cultures ($p < 0.05$), confirming a dose dependent response of *C.reinhardtii* to DMP. Care

should be taken however due to errors associated with the measure of colony forming units and cell separation.

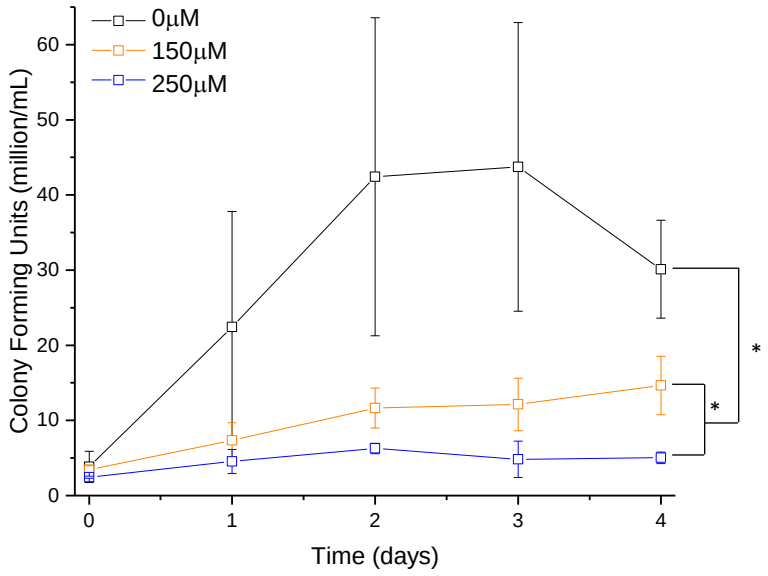

*Figure 6.2 Colony forming units of C.reinhardtii cultures grown in varying concentrations of DMP after four days cultivation in TAP-N medium. Aliquots of culture were spread onto TAP-Agar plates and incubated (20°C, 16-hour photoperiod, ~50 µmol m^{-2} s^{-1}) for 7 days or until visible colonies had appeared. Colonies were counted manually. Values are the mean and standard deviations of three biological replicates. * denotes a statistically significant difference (two-sided independent t test, $p < 0.05$).*

To be accurate, measurements of colony forming units rely on complete separation of cells at the time of plating. Under stress conditions, microalgal cells have been observed to cluster together which will lead to an underestimation of viable cell count from colony forming units. To account for this, average colony area was estimated using Image J software (see Chapter 2, Section 2.5.3) from digital photographs of TAP-agar plates taken seven days after plating. Colonies formed from several initial cells, due to cell clustering at the time of plating, are expected to increase in size at a faster rate than those formed initially from single cells.

Immediately prior to exchange from nitrogen deprived medium, colony size was estimated at an average of 3.6 mm^2 seven days after plating (TAP-N, Figure 6.3). Day 0 samples taken immediately after exchange similarly had an average area of 3.4-4.5 mm^2 independent of the DMP concentration. After four days in full TAP medium, the average colony size of control cultures (0 µM DMP) had reduced to approximately one quarter of that immediately after exchange (0.95 mm^2). In contrast DMP treated cultures retained an average colony area comparable with that of TAP-N and Day 0 cultures with the average colony area for 150 µM DMP treated cultures smaller than that of the 250 µM treated cultures (2.8 and 4.0 mm^2 respectively).

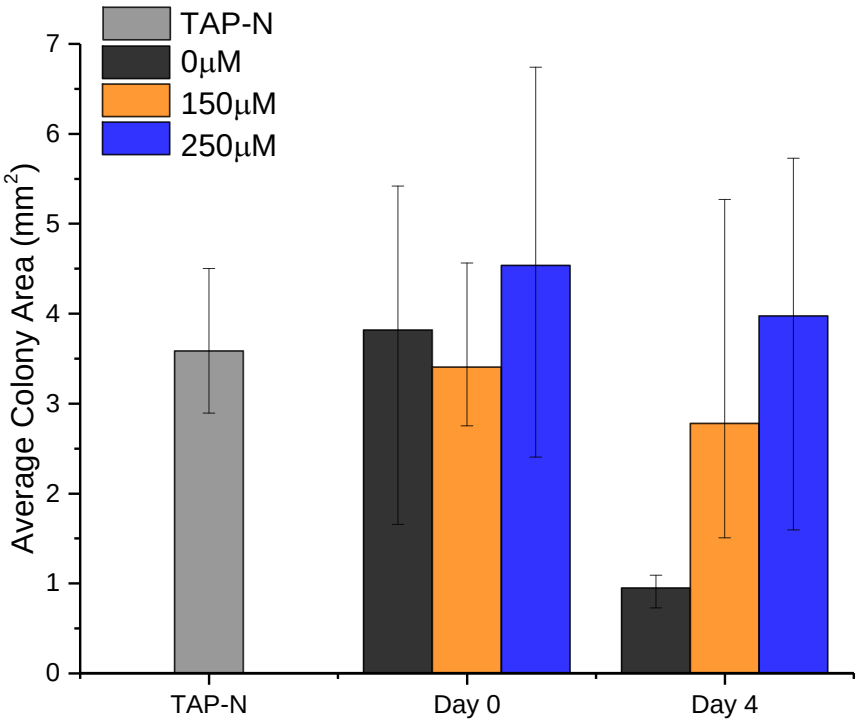

Figure 6.3 Average area of colonies grown in varying concentrations of Diphenyl methylphosphonate (DMP), immediately before media exchange (TAP-N), after 0 (Day 0) and 4 (Day 4) days in DMP. Aliquots of culture were spread onto TAP-Agar plates and allowed to grow under constant conditions (20°C, 16-hour photoperiod, ~50 µmol m^{-2} s^{-1}) for 7 days before photographing. Average colony area was calculated for all colonies using ImageJ software. Data shows the mean and range average colony area for three biological replicates.

The colony area for nitrogen starved (TAP-N) samples is approximately four times that observed after seven days in full TAP medium in the absence of DMP and is indicative of cell clustering at the time of plating. In contrast, the similarity in colony size between nitrogen starved and 250 µM DMP treated cultures hints at the presence of a continued stress stimulus resulting in maintained cell clustering. Colony area of 150 µM treated cultures is between that of 0 and 250 µM treated cultures and corroborates the dose dependent effect of DMP. Considering colony area, and assuming a linear relationship between colony area and colony population, the apparent effect of DMP on the rate of cell division is slight.

Qualitative analysis of TAP-agar plates (Figure 6.4) confirm the results observed by colony area analysis (Figure 6.3). Despite large variation between biological replicates, a clear reduction in colony size is observed when cultures were moved from TAP-N medium into full TAP medium in the absence of DMP. In contrast 250 µM DMP treated cultures have a much larger colony size, comparable with that seen for nitrogen starved cultures.

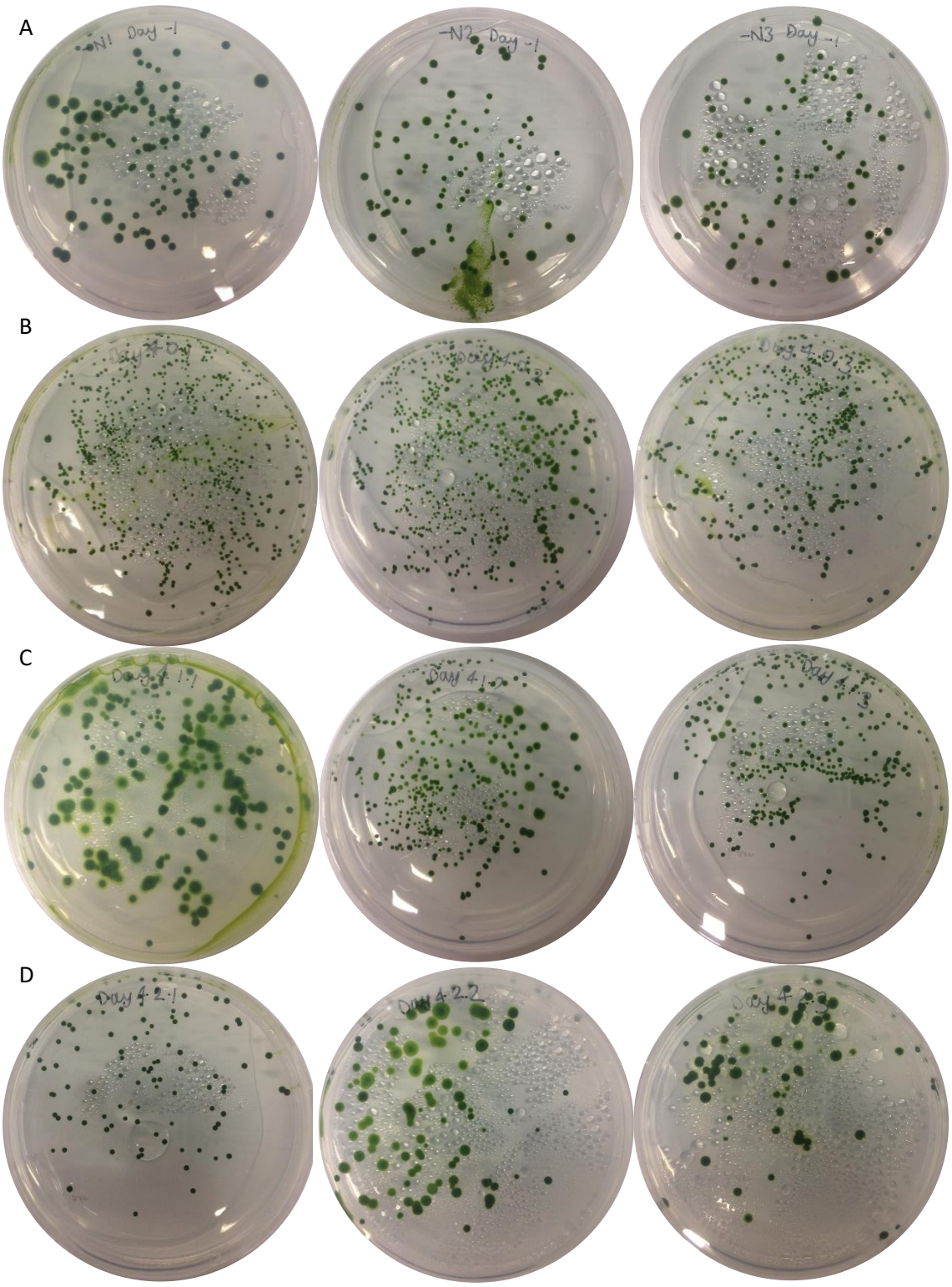

Figure 6.4 C.reinhardtii colonies on TAP-Agar from cultures grown in (A)TAP-N (Day 0); (B) TAP + 0µM DMP; (C) TAP + 150µM DMP; (D) TAP + 250µM DMP. Aliquots of culture were spread onto TAP-Agar plates and incubated (20°C, 16-hour photoperiod, ~50 µmol m^{-2} s^{-1}) for 7 days before photographing. (A) shows aliquots taken from cultures grown for 4 days in TAP-N immediately before exchange into TAP + DMP. (B-D) show aliquots taken from cultures after 4 days growth in TAP + DMP. biological triplicates are shown in each case.

6.2.2 Diphenyl methylphosphonate inhibits TAG catabolism on reintroduction of nitrogen

To test for specific retention of neutral lipid bodies in DMP treated cultures, 4 days after reintroduction of nitrogen samples were stained with Nile-red fluorescent stain for qualitative analysis (see Chapter 2, Section 2.5.4 for full methodology and microscope settings).

Observation of microscopy images (Figure 6.5) confirms the clustering of cells in DMP treated cultures inferred from colony area analysis. Control cultures (0 µM DMP) were present almost exclusively as single cells. In contrast cells imaged from 150 µM and 250 µM DMP treated cultures were commonly observed in small clusters of two or four cells respectively. No difference in cell size was observed for control and DMP treated cultures. The common presence of four-cell clusters in 250 µM DMP treated cultures is in agreement with the reported colony area four times that of untreated cultures. A similar conclusion can be drawn from the presence of two-cell clusters in 150 µM treated cultures. Additionally, the mobility of cells was noticeably reduced with increasing DMP concentration; cells treated with 250 µM DMP were stationary in most cases confirming the continued presence of stressful stimuli in DMP treated cultures but not in the control.

Negligible fluorescence was observed in control cultures indicating a lack of neutral lipid droplets in untreated cells; microalgal cells have previously been reported to degrade all additional accumulated lipids within 48 hours of nitrogen resupply (Siaut *et al*., 2011; Valledor *et al*., 2014). Cells treated with 150 µM DMP demonstrated small amounts of fluorescence in some cells but no fluorescence was observed in the majority of cells. In contrast, approximately half of the observed cells from 250 µM DMP treated cultures demonstrated significant Nile-red fluorescence. Observation of 40x images reveals fluorescence is present as distinct spherical droplets within cells indicative of neutral lipid bodies (Figure 6.5 (ii)). The increased fluorescence and cell clustering in 250 µM treated cultures supports the hypothesis that DMP causes dose dependent TAG retention.

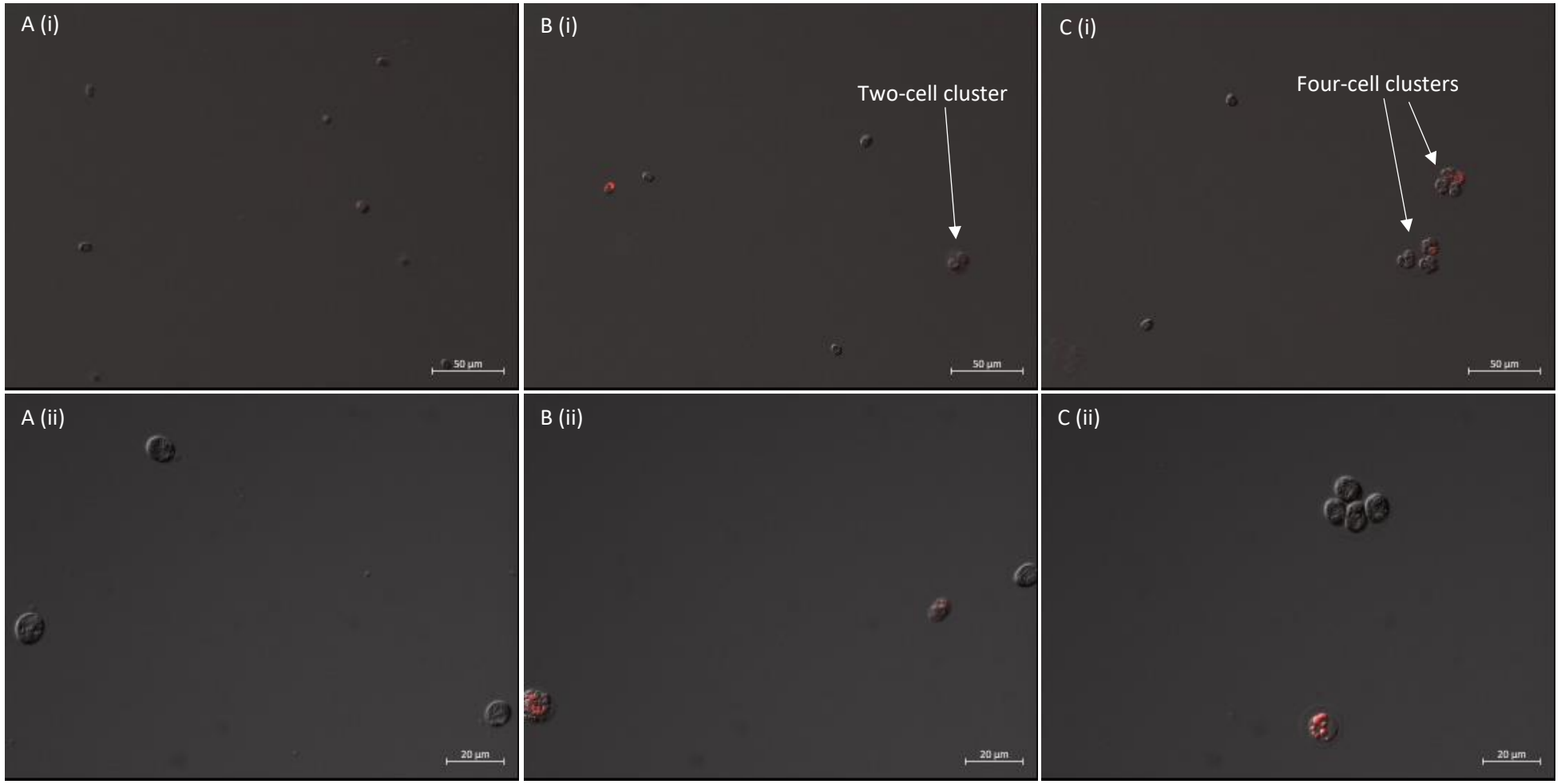

Figure 6.5 Nile-red images taken from samples of culture grown in (A) TAP; (B) TAP + 150µM DMP and (C) TAP + 250µM DMP at two magnifications (i) 20x, scale bar = 50µm; (ii) 40x, scale bar = 20µm. Fluorescence intensity not to scale and artificial colour applied.

Previous results demonstrate that DMP inhibits TAG catabolism but does not increase TAG accumulation (Brown *et al*., 2013). The presence of neutral lipid bodies is therefore assumed to be as a result of retained TAGs from nitrogen starved cultures and not due to additional TAG accumulation.

For quantitative analysis of neutral lipids, lipids were extracted from freeze-dried biomass using the non-polar solvent hexane and measured gravimetrically to 0.01 mg (see Chapter 2, Section 2.6.3.2). Quantitative analysis of neutral lipids confirms the observations of neutral lipid bodies using Nile-red fluorescence staining. Cultures treated with high concentrations of DMP revealed significantly higher neutral lipid concentration compared to untreated cultures ($p < 0.05$) with cultures containing approximately 3.3, 5.9 and 5.3 % neutral lipid by dry biomass weight for 0, 150 and 250 µM DMP treated cultures respectively (Figure 6.6). No statistically significant difference was observed between 25 µM treated and untreated cultures nor between 150 and 250 µM treated cultures. The trend observed here was confirmed by quantitative GC-MS analysis of FAMEs after transesterification however the additional processing resulted in larger errors.

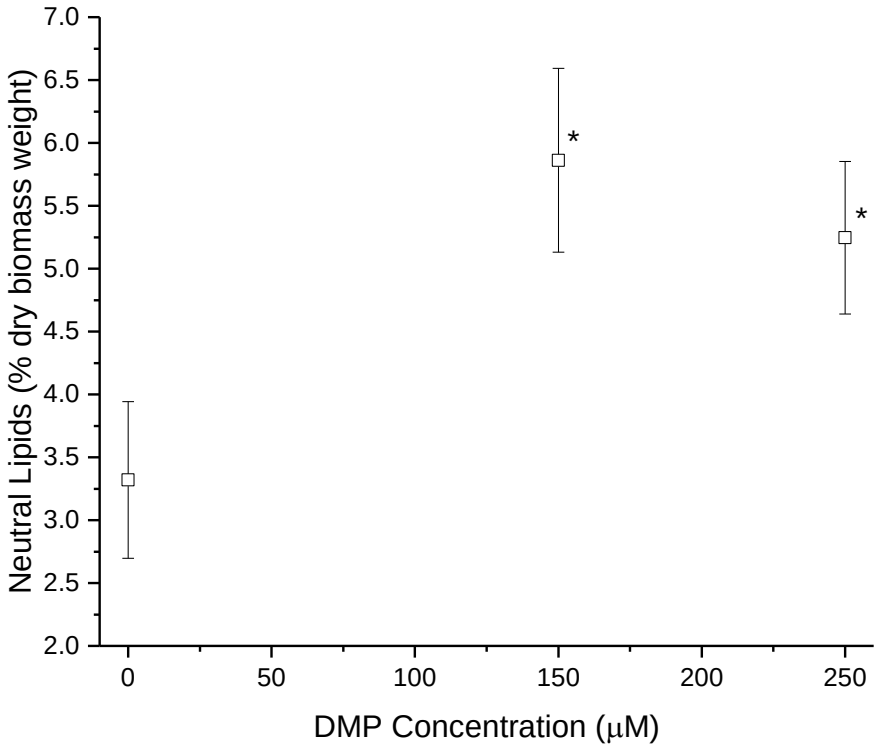

*Figure 6.6 Neutral lipid content as weight % of dry biomass for cultures of C.reinhardtii grown in varying concentrations of DMP following four days cultivation in TAP-N medium to accumulate neutral lipids. Values are the mean and standard deviations of three biological replicates. * denotes a statistically significant difference from the control (0 µM DMP) (two-sided independent t test, p < 0.05).*

The increased TAG retention on nitrogen resupply in DMP treated cultures is consistent with a block in the TAG degradation pathway. Little is currently understood about the catalysis of lipid catabolism in microalgae. However, the major pathways of galactolipid, sulfolipid and phosphatidyglycerol (PtdGro) synthesis are predicted to be conserved between *Chlamydomonas* and *Arabidopsis* (Li-Beisson *et al*., 2015). Similarly, the chloroplast localised synthesis of C16 and C18 fatty acids and the TAG biosynthesis pathway in microalgae are presumed to contain the same enzymatic steps as in higher plants (Li-Biesson *et al*., 2015). Together, these indicate that the main lipid pathways have been evolutionarily conserved between algae and higher plants.

So far only one TAG lipase (catalysing the hydrolysis of TAGs to glycerol and fatty acids), LIP4, which demonstrates 44 % identity with the major *Arabidopsis* lipase, SDP1 (Warakanont *et al*., 2019) and one acyl-CoA oxidase (responsible for the first step of fatty acid β-oxidation), CrACX2, demonstrating 54 % identity with the *Arabidopsis* acyl-CoA oxidase, AtACX2 (Kong *et al*., 2017) have been characterised in microalgae, in the model species *Chlamydomonas reinhardtii*.

Brown and co-workers demonstrated that DMP inhibits an early step in the fatty acid β-oxidation spiral in *Arabidopsis thaliana* (Brown *et al*., 2013). Recently the first algal acyl-CoA oxidase, CrACX2, catalysing the first committed step in the fatty acid β-oxidation spiral, was characterised in the alga *Chlamydomonas reinhardtii*. BlastP analysis revealed 68 % similarity (54 % identity) with the *Arabidopsis* acyl-CoA oxidase, AtACX2 (Kong *et al*., 2017). Defective mutants demonstrate compromised oil degradation on resupply of nitrogen and elevated acyl-CoA levels, similar to that observed in DMP treated *Arabidopsis* (Brown *et al*., 2013). Similarly, CrACX2 has been localised to microalgal peroxisomes ('microbodies') conclusively demonstrating a peroxisomal β-oxidation pathway in the chlorophyte *Chlamydomonas* (Kong *et al*., 2017).

The similarity between *Chlamydomonas* and *Arabidopsis* TAG degradation pathways complements the hypothesis that DMP plays a similar role in *Chlamydomonas* to that previously reported in *Arabidopsis*. Analysis of acyl-CoAs and the effect of DMP on TAG content during nitrogen deficiency would be useful to further corroborate this hypothesis.

Furthermore, *Chlamydomonas lip4* mutants, deficient in the lipase LIP4, demonstrate both increased TAG retention on resupply of N and an increase in TAG accumulation under normal growth conditions (Warakanont *et al*., 2019), in contrast to the *cracx2-1* mutant which shows no increase in TAG accumulation during nitrogen sufficiency (Kong *et al*., 2017). An increase in TAG content has similarly been reported during nitrogen sufficiency on addition of Brefeldin A, proposed to induce endoplasmic reticulum stress (Kato *et al*., 2013; Kim *et al*.,

2013). Analysis of TAG content under nitrogen sufficiency in the presence of DMP will aid in narrowing down the action of DMP on individual steps in the lipid catabolism pathway.

6.2.3 Total lipid content is largely unaffected by DMP treatment

To monitor total lipid catabolism over time, total lipid was extracted from biomass (2:1 $CHCl_3$:MeOH) with simultaneous transesterification (0.6M HCl in MeOH) and FAMEs were analysed quantitatively by GC-MS analysis using C17:0 as an internal standard (Chapter 2, Section 2.6.3.1).

Exchange into full TAP medium led to rapid degradation of lipids with the majority of lipid catabolism observed within the first 48 hours after nitrogen resupply (Figure 6.7), in agreement with previous reports (Siaut *et al*., 2011; Valledor *et al*., 2014). In general, the addition of DMP had little effect on the total lipid content observed, with only the 48-hour time point revealing any significant difference between control and treated cultures (Figure 6.7 (B)). After 48 hours, the continued reduction in lipid content of DMP treated cultures resulted in no significant difference in lipid content between treated and untreated cultures beyond this point. No significant difference in lipid content was observed between untreated and 25 µM treated cultures throughout indicating that 25 µM DMP is insufficient to elicit a response (Figure 6.7 (A)). DMP therefore appears to result in a slowing of the lipid catabolism process rather than complete inhibition.

The similar total lipid content despite elevated neutral lipid content in cultures treated with high concentrations of DMP compared to the control indicates a reduction in membrane lipid concentration as a result of DMP treatment. In *Arabidopsis*, the major lipids of the chloroplast membrane, galactolipids, are shown to be conserved in control and DMP treated cultures (Brown *et al*., 2013) however, the reduced chlorophyll concentration observed here in DMP treated *Chlamydomonas* indicates a significant reduction in the chloroplast membrane (Figure 6.8). It appears as if the retention of TAGs causes a deficiency in available fatty acids for restoration of plastidial membranes since some preference must be given to the loss of fatty acids through β-oxidation to produce sucrose (essential for carbon transport and energy production within the cell, Kong *et al*., 2018). The slow growth observed in both *Arabidopsis* and *Chlamydomonas* as a result of DMP treatment is therefore likely a direct result of the reduced oil mobilisation restricting reconstruction of plastidial membranes essential for growth.

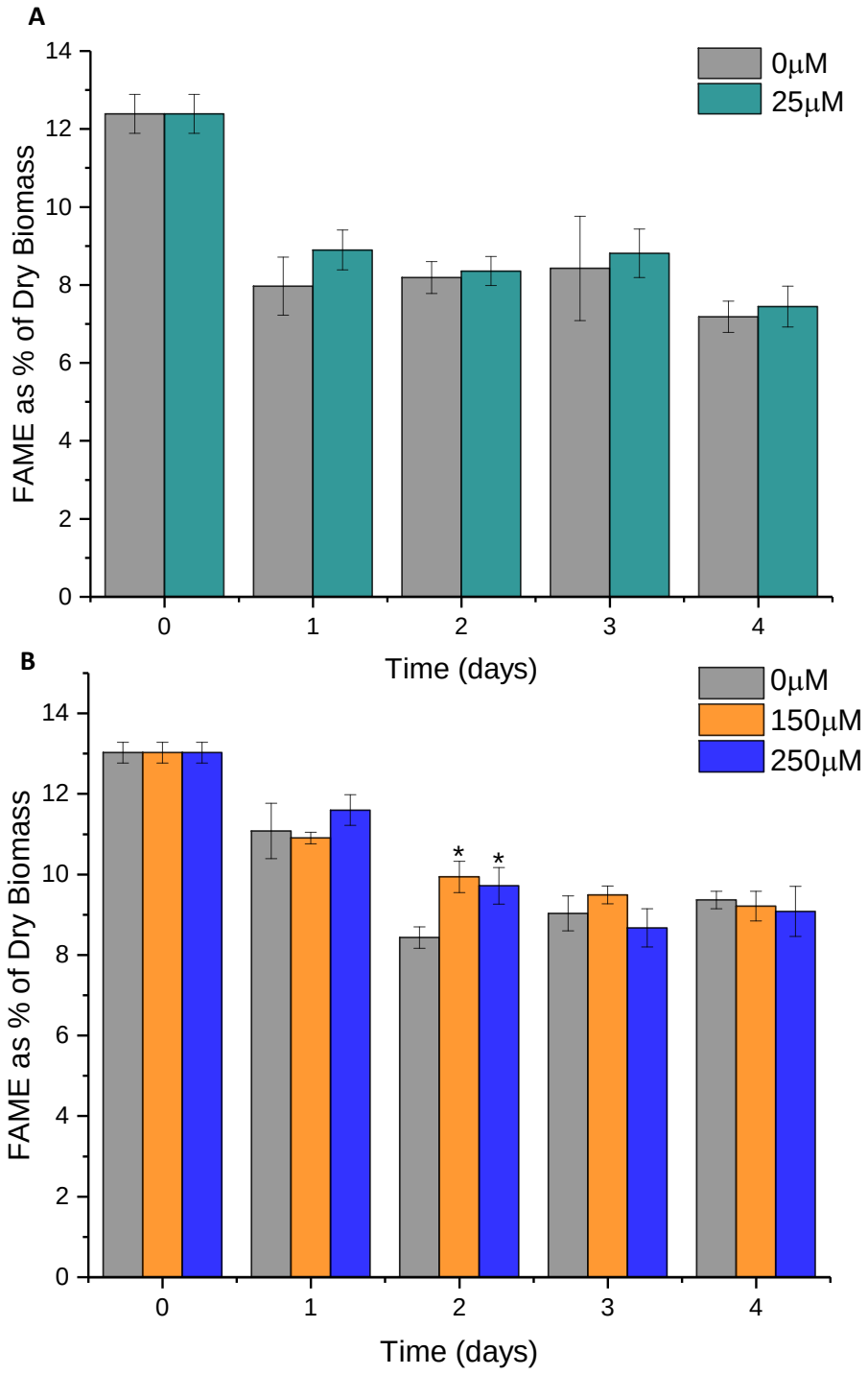

*Figure 6.7 FAME content as a % of dry biomass weight for C.reinhardtii cultures grown in varying concentrations of DMP following four days cultivation in TAP-N medium to accumulate neutral lipids. Values are the mean and standard deviations of three biological replicates. * denotes a statistically significant difference from the control (0uM DMP) (two sided independent t test, $p < 0.05$).*

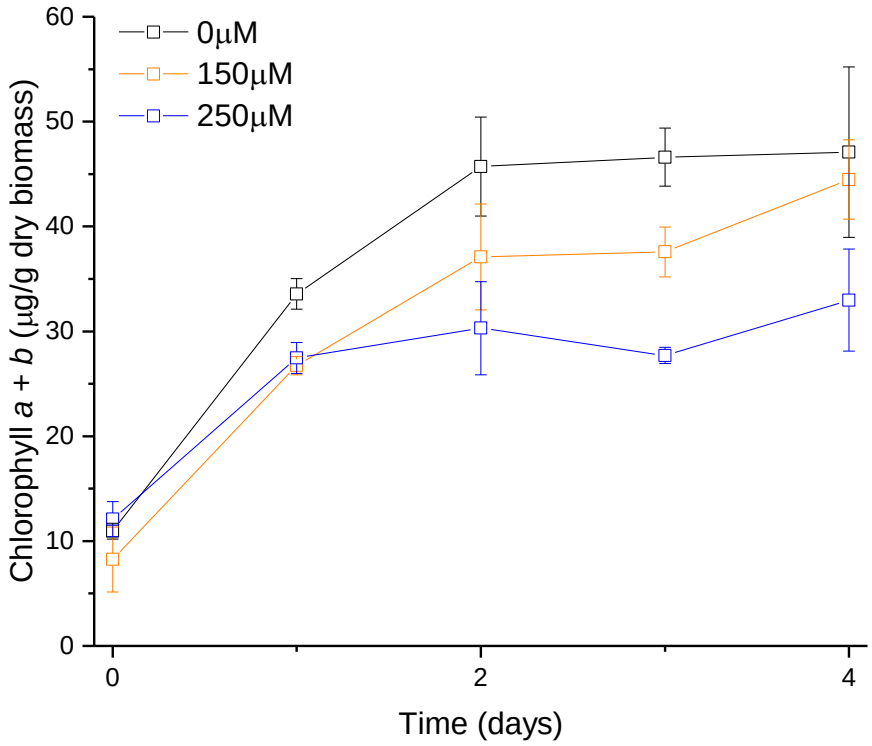

Figure 6.8 Chlorophyll concentration per gram of dry biomass in C.reinhardtii cultures grown in varying concentrations of DMP following four days cultivation in TAP-N medium to accumulate neutral lipids. Values are the mean and standard deviations of chlorophyll concentration/dry weight for three biological replicates.

Compositional analysis of FAMEs reveals that the majority of changes in lipid composition occur within the first 24-48 hours after reintroduction of nitrogen (Figure 6.9). In particular, fatty acids reported to demonstrate significant changes in abundance during TAG accumulation (C16:0, C16:4, C18:1(9) and both C18:3) (Yang *et al.*, 2017) show the largest changes in composition of all fatty acids observed with changes in abundance similarly occurring predominantly within 48 hours after nitrogen resupply. Given additional lipids accumulated as a result of nitrogen starvation are reported to be degraded within 24-48 hours of nitrogen resupply, the changing composition most likely reflects a direct result of TAG catabolism and the restoration of plastidial membranes. In general, the relative abundance of different fatty acids in 250 μM DMP treated cultures demonstrates much greater similarity with nitrogen starved cultures (i.e. before exchange into full TAP medium) than either 150 μM DMP treated or untreated cultures (Figure 6.10) as a result of the greater retained TAG content. Indeed, compositional analysis, similarly to Nile-red fluorescence, indicated significantly higher TAG content in 250 μM treated cultures compared to 150 μM in contrast to quantitative analysis (Figure 6.6) and suggests a continued improvement in TAG retention with rising DMP concentration. The contradiction is most likely as a result of the relatively large errors in quantitative neutral lipid accumulation.

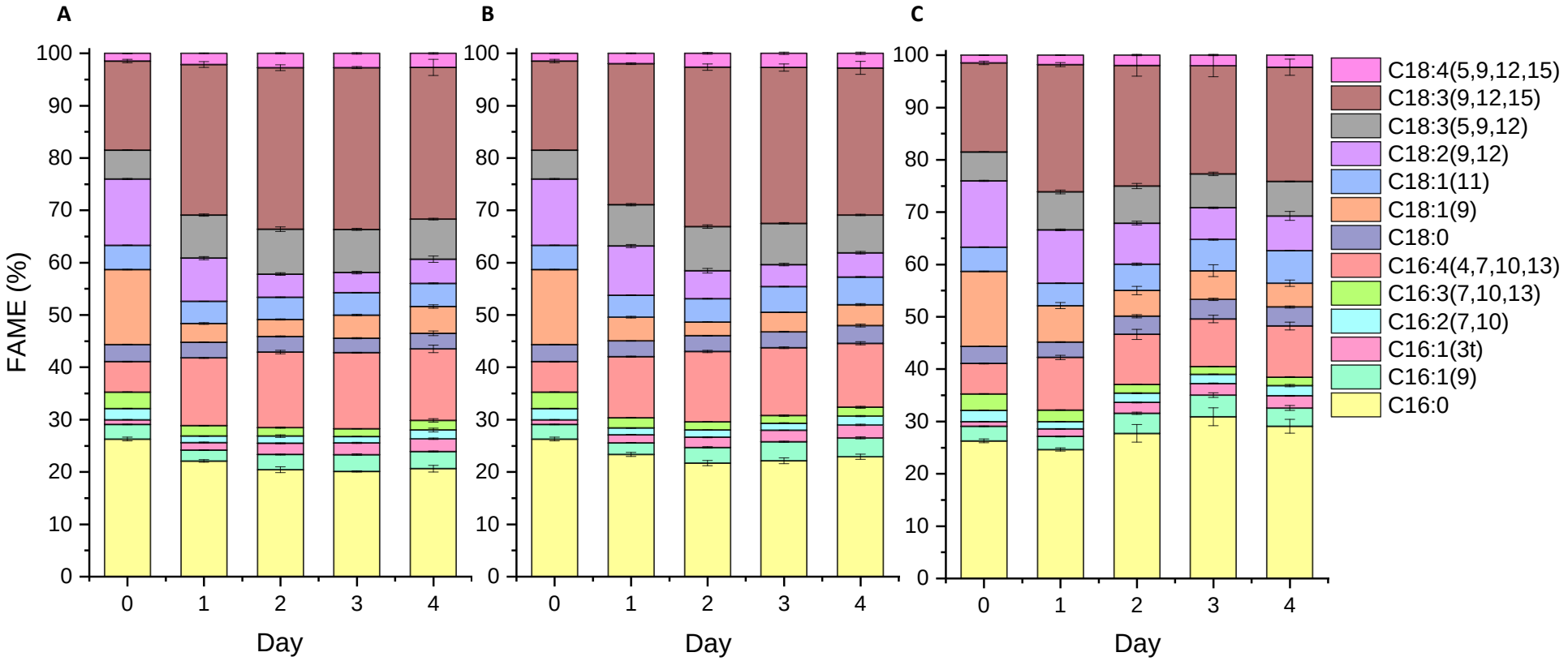

Figure 6.9 Daily FAME profiles for C.reinhardtii grown in TAP medium treated with (A) 0 µM, (B) 150 µM or (C) 250 µM Diphenyl methylphosphonate following 96 hours cultivated in TAP-N medium. Day 0 represents TAP-N samples immediately before exchange into full TAP medium.

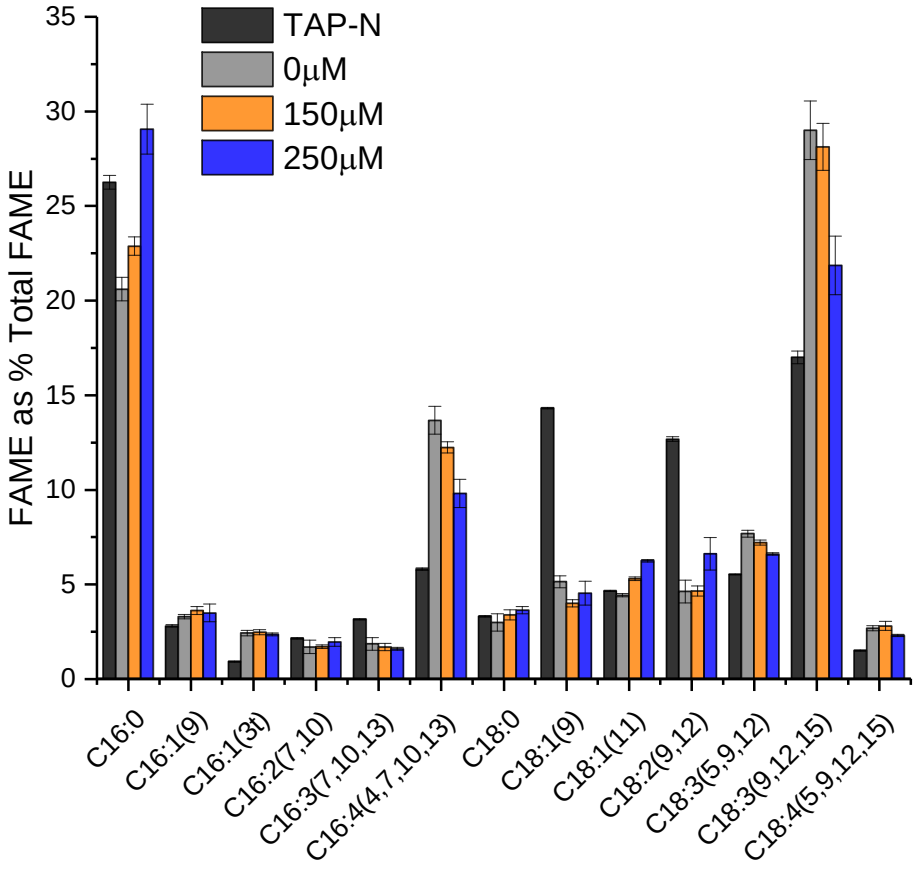

Figure 6.10 Relative abundance of FAMEs observed immediately prior to N-resupply (TAP-N) and 96 hours after N-resupply to C.reinhardtii cultures cultured in TAP medium with 0, 150 or 250 μM *DMP after a period of nitrogen starvation.*

6.3 Significance for Wastewater Treatment and Biodiesel Production

Addition of DMP to *C.reinhardtii* cultures on nitrogen resupply following four days of nitrogen starvation is shown to partially inhibit TAG catabolism with a dose dependent response. Cultures grown in high concentrations of DMP (150, 250 μM) demonstrate increased TAG content four days after nitrogen resupply compared to an untreated control (0 μM DMP). In contrast to *Arabidopsis*, 25 μM DMP elicited no response. The higher concentration required may be as a result of the increased biomass density/uptake area of microalgae compared to plants, a reduced sensitivity of the target to DMP, or the increased rate of algal metabolism compared to *Arabidopsis*; indeed, microalgae have gained attention in part due to their exceptionally fast growth rate compared to conventional biomass sources.

Despite the retention of neutral lipids as a result of DMP treatment, total fatty acid yield is largely unaffected due to the growth reduction caused by DMP treatment, indicating that DMP can be used to elicit changes in lipid quality but not quantity (Table 6.1).

Table 6.1 Total lipid yield for cultures of C.reinhardtii treated with DMP on nitrogen resupply following a four-day nitrogen starvation period. Biomass and lipid yield calculated from the average biomass dry weight and lipid yield (% dry biomass) from Days 2-4 (stationary phase). Total lipid yield calculated from biomass yield and lipid yield (% dry biomass).

	Biomass Yield (g/L)	Lipid Yield (% biomass)	Total Lipid Yield (g/L)
TAP-N (Day 0)	0.70	13.0	0.09
0 µM	1.38	8.94	0.12
150 µM	1.16	9.55	0.11
250 µM	0.97	9.16	0.09

Studies aimed at improving oil yield through upregulation of the TAG biosynthesis pathway have done so with limited success. A recent review by Tan and Lee (2016) proposed that the competition between carbon and substrates (particularly acyl-CoA) fundamentally limits the ability of cells to both accumulate large quantities of TAGs and continue efficient growth (Tan and Lee, 2016). Furthermore, the widespread belief that TAGs are preferentially accumulated during stress conditions, as an energy store available for rapid mobilisation when favourable conditions are restored, suggests an essential role of TAGs in the restoration of growth; no known study has yet successfully repressed TAG mobilisation without compromising growth (Li *et al*., 2012; Brown *et al*., 2013; Kato *et al*., 2013; Kim *et al*., 2013; Kong *et al*., 2017; Warakanont *et al*., 2019).

It may therefore be unrealistic to expect that downregulation of the lipid catabolism pathway can be achieved without significantly limiting biomass yield and therefore overall lipid yield. This study does, however, demonstrate that inhibition of TAG degradation may offer a means of improving biodiesel quality without significantly limiting yield.

In order to assess the quality of microalgal fatty acids for biodiesel production, a series of parameters can be estimated. Parameters affecting biodiesel quality such as cetane number (CN), iodine value (IV), saponification value (SV), cold filter plugging point (CFPP), kinematic viscosity (υ), density (ρ), oxidative stability index (OSI) and the higher heating value (HHV) can be estimated based on biomass FAME composition and are determined chiefly by the saturation, chain length and branching of fatty acid methyl esters (Krisnangkura *et al*., 1986; Ramos *et al*., 2009; Islam *et al*., 2013, see Chapter 2, Section 2.6.3.3). In general, most properties are optimised by a low proportion of polyunsaturated fatty acids (PUFA) in contrast to CFPP which is optimised by a lower proportion of saturated fatty acids (SFA). Nitrogen starvation has become the favoured cultivation condition to produce microalgal biodiesel due to the high proportion of TAGs, rich in saturated and mono-unsaturated (MUFA) fatty acids (Yang *et al*., 2017).

Prior to nitrogen resupply, cultures were observed to contain approximately 30, 23 and 48 % SFA, MUFA and PUFA respectively (Day 0, Figure 6.11). On resupply of nitrogen, the proportions of SFA and MUFA are observed to fall while the proportion of PUFA increases; nitrogen resupply has been shown to cause upregulation of lipid desaturases (Zienkiewicz *et al*., 2020). The observed changes in saturation are less significant in DMP treated cultures as a result of significant TAG retention. The similarity in saturation between control (0 μM) and 25 μM treated cultures confirms the lack of TAG retention at low DMP concentrations.

After 24 hours, the proportion of PUFA in DMP treated cultures (150 and 250 μM) begins to fall tending back towards the proportion seen for nitrogen starved cultures (Day 0). A similar effect is observed for the proportions of SFA and MUFA. Comparison with raw FAME content (Figure 6.12) reveals that the apparent increase in PUFA followed by a reduction after 24 hours is as a result of a delayed onset of PUFA degradation in comparison with SFA and MUFA. The results indicate that, despite the presence of nitrogen, DMP treated cultures have the potential to produce biodiesel with similar properties to that of nitrogen starved cultures from 24 hours after nitrogen resupply.

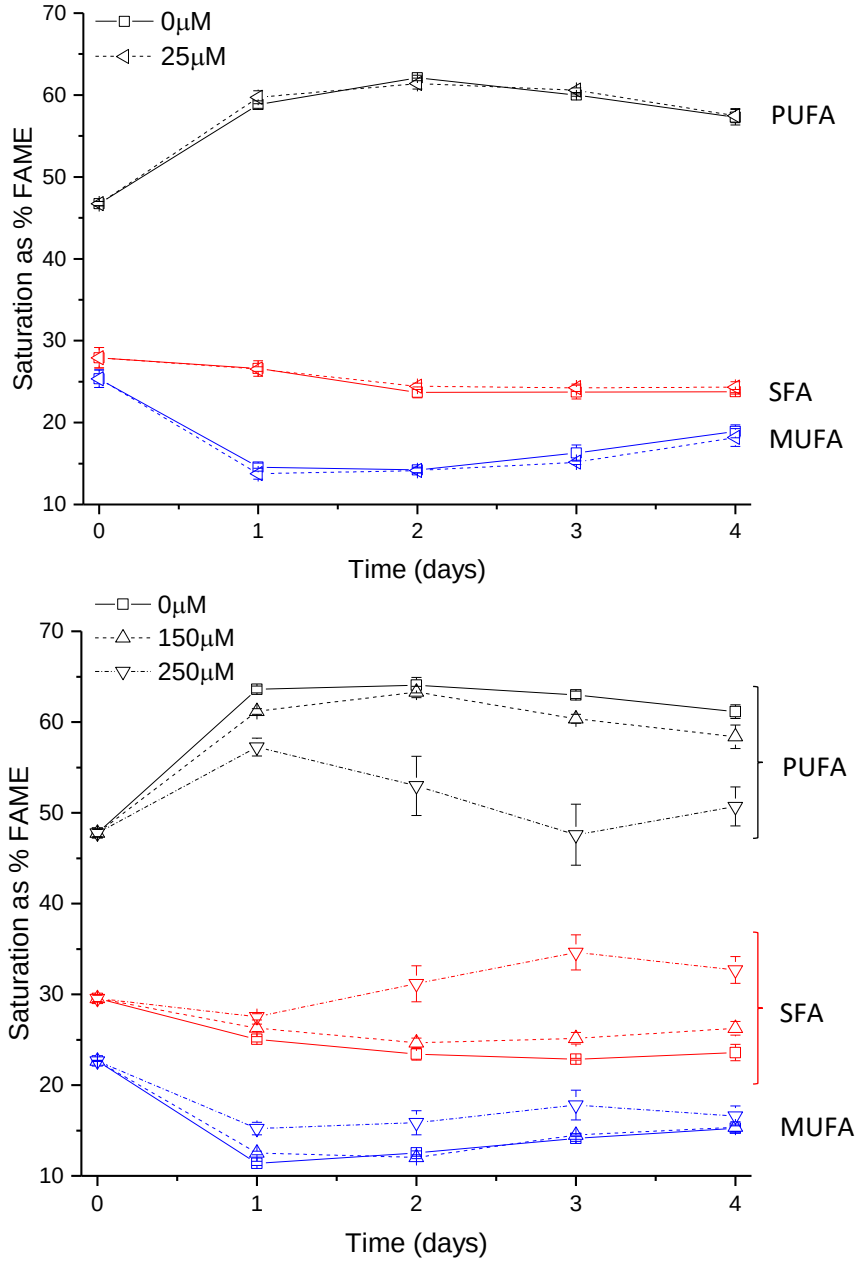

Figure 6.11 % content of saturated (SFA), mono-unsaturated (MUFA) and poly-unsaturated (PUFA) fatty acids in C.reinhardtii grown in varying concentrations of DMP following four days cultivation in TAP-N medium. Time in days after exchange into TAP + DMP. Day 0 represents samples taken immediately before exchange into full TAP medium. Values are the mean and standard deviations of three biological replicates.

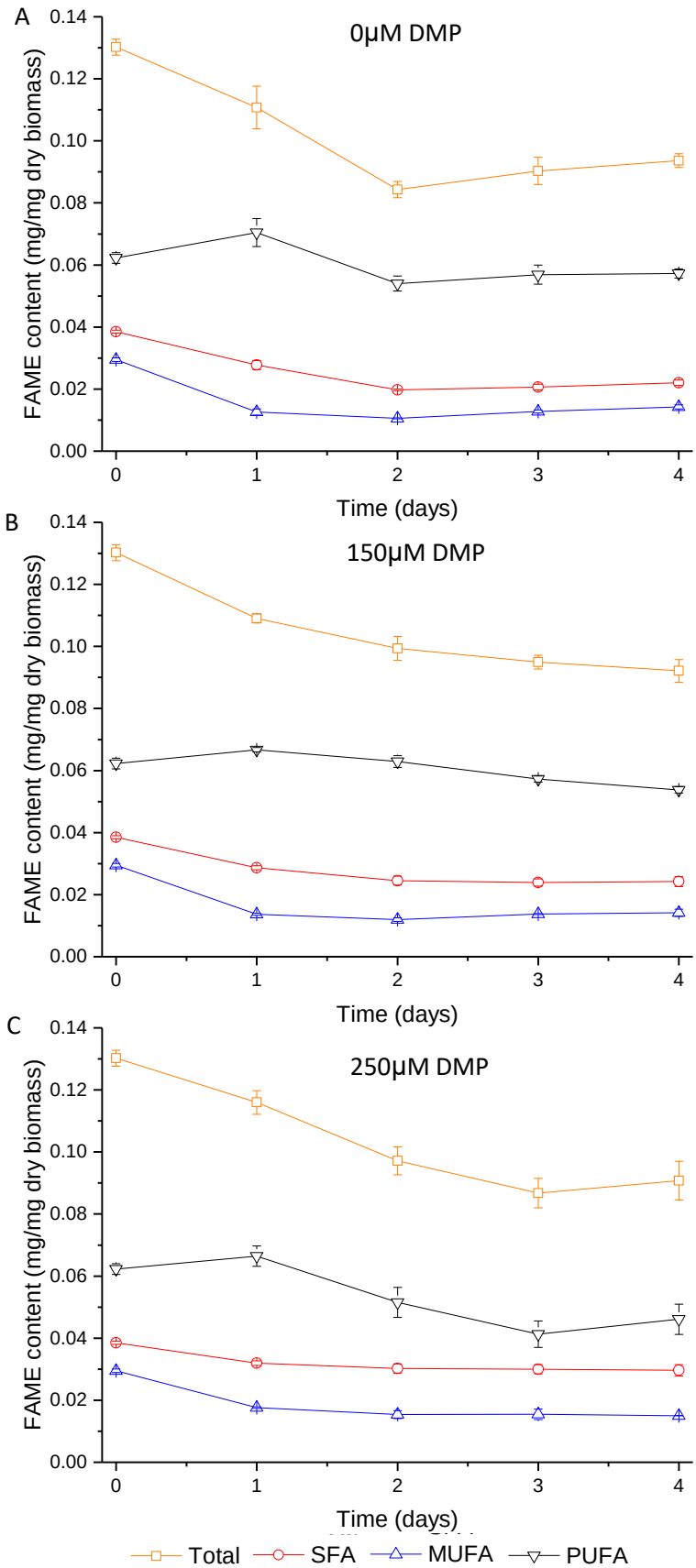

Figure 6.12 Fatty Acid content of C.reinahrdtii grown in TAP + DMP following four days cultivation in TAP-N.(A) 0µM DMP, (B) 150µM DMP, (C) 250µM DMP. Time in days after excahnge into TAP + DMP. Day 0 represents samples taken immediately before exchange into full TAP medium. Values are the mean and standard deviation of three biological replicates.

Based on the compositional analysis of FAMEs in treated and untreated *C.reinhardtii* cultures, biodiesel properties were calculated and are compared to the European Biodiesel Standard (EN 14214) for 100 % biodiesel fuel (B100) (Table 6.2). All cultures met the EN 14214 standard for density and the observed higher heating values (HHVs) comply with the typical range of regular biodiesel (39.8-40.4 MJ kg^{-1}) (Ramírez-Verduzco *et al*., 2012). The saponification value is not controlled by the European Biodiesel Standard but is largely similar for all cultures (197.3 – 199.1) and is comparable with currently used oil feedstocks such as Soybean, Jatropha and Rapeseed (Martínez *et al*., 2014).

In general, TAP-N cultures were closest to meeting the limits for European Biodiesel however the similarity in calculated values between nitrogen starved and 250 µM DMP treated cultures demonstrates that inhibition of TAG catabolism offers a means to maintain good biodiesel quality under nitrogen sufficiency. Indeed, the predictive oxidation stability (OSI) is improved in 250 µM treated cultures compared to those nitrogen starved. In contrast, the biodiesel quality of untreated cultures rapidly deteriorated on nitrogen resupply as a result of depleting TAG reserves.

It is a frustration that nitrogen depletion, while promising for TAG accumulation, results in the cessation of biomass growth. Furthermore, nitrogen resupply, to restart biomass growth, is useful for increasing overall lipid yield but does so at the expense of biodiesel quality due to rapid TAG degradation. It is recommended that future work assess if cycling between nitrogen starvation and DMP treatment under nitrogen sufficiency may offer a way to further improve both lipid yield and quality.

Table 6.2 Biodiesel properties calculated from the FAME composition of C.reinhardtii cultured in TAP + varying concentrations of DMP following four days cultivation in TAP-N medium. TAP-N represents samples measured immediately prior to exchange into full TAP medium (Days 1-4). Data calculated from the mean FAME composition of biological triplicates.

		DU	*LCSF*	*CN*	*SV* (*mg KOHg^{-1}*)	*IV* (*g $I_2$100g^{-1}*)	*CFPP (°C)*	*OSI (h)*	*Density (ρ)* (*gcm^{-3}*)	*Kinematic Viscosity* (*υ*) (*mm^{2}s^{-1}*)	*HHV (MJ kg^{-1})*
Biodiesel Standard EN 14214 (B100)		-	-	≥51	-	≤120	Variable	≥6	0.86-0.90	3.5-5.0	-
TAP -N	**Day 0**	118.2	4.3	42.0	197.3	141.8	-3.0	5.9	0.88	3.81	39.5
0 µM	**Day 1**	138.5	3.7	31.8	198.1	186.7	-4.9	5.2	0.89	3.48	39.4
	Day2	140.7	3.5	30.0	198.5	194.6	-5.4	5.3	0.89	3.42	39.4
	Day 3	140.1	3.4	30.2	198.4	193.8	-5.8	5.3	0.89	3.43	39.4
	Day 4	137.6	3.6	31.5	198.5	188.0	-5.3	5.4	0.89	3.46	39.4
150 **µM**	**Day 1**	134.9	3.8	33.6	198.1	178.8	-4.4	5.3	0.89	3.53	39.4
	Day 2	138.6	3.7	31.0	198.4	190.2	-5.0	5.3	0.89	3.45	39.4
	Day 3	135.2	3.7	32.1	198.5	185.2	-4.7	5.4	0.89	3.48	39.4
	Day 4	132.1	4.0	33.4	198.6	179.4	-4.0	5.5	0.89	3.52	39.4
250 **µM**	**Day 1**	129.7	3.9	36.1	197.9	168.1	-4.1	5.4	0.89	3.61	39.4
	Day 2	121.8	4.5	38.0	198.7	159.2	-2.3	5.7	0.88	3.64	39.4
	Day 3	113.0	5.0	40.4	199.1	147.9	-0.9	6.1	0.88	3.71	39.5
	Day 4	118.0	4.7	38.8	198.9	155.4	-1.6	6.0	0.88	3.66	39.4

To conclude, the use of chemical inhibitors of TAG catabolism are shown here to have potential for aiding the production of high quality microalgal biodiesel feedstocks without the need for genetic modification. Furthermore, the similar lipid yield and quality achieved with DMP treatment compared to that of nitrogen starved biomass but with a greater overall biomass yield could be used to aid in achieving primary wastewater treatment targets, namely nutrient bioremediation, without limiting biodiesel potential.

This study also continues research on the effect of phosphonates on algal growth. Phosphonates are present in abundance in wastewaters owing to their use in detergents (Jaworska *et al*., 2002); the phosphonate DMP exhibits a clear reduction in algal growth from 150 µM (37.2 mg/L) in line with the published 'no observed effect concentration' (NOEC) of the most common detergent phosphonates = 0.1 mg/L (Steber, 2007).

Further research is needed to fully characterise the effect of DMP on TAG catabolism in microalgae. Furthermore, additional research would be useful to investigate whether DMP can elicit an improvement in biodiesel quality without the need for a nitrogen starvation step. Additionally, if the specific target of DMP can be found, genetic manipulation may be able to create a mutant with improved lipid quality. Lipid accumulation has been shown to depend on diurnal variations with lipids accumulated during the day and catabolised during the hours of darkness as a source of carbon in the absence of photosynthesis (Kong *et al*., 2017); research under 'traditional' day night cycles is needed to fully understand the potential advantages of lipid catabolism inhibition in a wastewater treatment scenario.

Chapter Seven – General Discussion, Conclusions and Recommendations for Further Work

This thesis addresses the hypothesis that microalgae may be cultivated, within a wastewater treatment works (WWTW), to simultaneously recover essential nutrients and produce a biomass suitable for biodiesel production whilst contributing to the wastewater treatment process through nutrient removal.

Individually, these goals have been researched extensively. The use of high rate algal ponds (HRAPs) for nutrient removal in WWTW, which were first developed in California in the middle of the twentieth century, are now well established in both warm and more temperate climates such as France, New Zealand and the United Kingdom (Park *et al*., 2011; Craggs *et al*., 2014; Young *et al*., 2017). There is also a wealth of research investigating the growth and nutrient removal ability of various microalgal strains in various wastewaters (Asmare *et al*., 2014; Zhang *et al*., 2014a; Karemore *et al*., 2015; Lu *et al*., 2015; Morales-Amaral *et al*., 2015; Tsolcha *et al*., 2015; Xu *et al*., 2015; Yu *et al*., 2015; Lutzu *et al*., 2016).

Additionally, research into the use of microalgae either as a bio-fertiliser or as a source of biofuels is advanced. Microalgae can be applied directly to crops as a slow-release fertiliser with great success (Coppens *et al*., 2016; Dineshkumar *et al*., 2018) and research includes the use of microalgae grown in various wastewaters (Mulbry *et al*., 2005; Mulbry *et al*., 2007; Wuang *et al*., 2016). The gradual release of nutrients from organic fertilisers additionally helps to minimise nutrient losses (Mulbry *et al*., 2007) which will in turn reduce nutrient loads to surface waters from agricultural run-off. In practice however, the focus of nutrient control in WWTW is on removal with little attention given to the potential for nutrient recovery and reuse.

Similarly, triggers for producing high quantities of oil in microalgae are well understood, with nitrogen starvation being by far the most successful known lipid trigger (Siaut *et al*., 2011; Valledor *et al*., 2014; Schmollinger *et al*., 2014). Other triggers of lipid accumulation such as phosphorus or iron deficiency, as well as several physicochemical factors including light intensity and temperature, have also been studied (Liu *et al*., 2008; Rodolfi *et al*., 2009; Feng *et al*., 2012; Boyle *et al*., 2012; Paveenkumar *et al*., 2012; Urzika *et al*., 2013; Fan *et al*., 2014; Ferreira *et al*., 2017; Morales *et al*., 2018). The overarching problem, however, is that microalgal biodiesel is unlikely to become economically feasible without interaction from WWTW (Park *et al*., 2011). Current costs for microalgal biodiesel range from US $1.40-3.53/L (Chisti, 2007; Campbell *et al*., 2011; Delrue *et al*., 2012; Slade and Bauen, 2013) compared with the average price of petrochemical diesel which as of 2019 stands at US $1.02/L (Global Petrol Prices, 2019a).

While microalgal cultivation in WWTW has been proposed as an effective means of reducing costs through the provision of free water and nutrients, current known triggers for oil accumulation are largely unfeasible within a WWTW and have instead been developed for use in heavily controlled environments such as photobioreactors, which will likely never be economically feasible due to high capital and operational costs (Delrue *et al*., 2012; Slade and Bauen, 2013). Limitations therefore centre on the fact that it is very difficult to engineer the conditions within a WWTW to meet those we know to trigger high oil accumulation. Triggers such as temperature and light intensity require control over external conditions while achieving nutrient starvation is unlikely to be reliable given varying nutrient loading to WWTW. The most successful trigger of oil accumulation, nitrogen starvation, as with many other known triggers, simultaneously results in the cessation of growth (Siaut *et al*., 2011; Park *et al*., 2015) thus limiting overall lipid yield and nutrient recovery. With biomass density and nutrient bioremediation optimised by high nutrient availability and lipid accumulation favoured by stress conditions such as nutrient starvation there will inevitably need to be a compromise between nutrient removal from WWTW, nutrient uptake into microalgal biomass and microalgal lipid accumulation.

In order to understand this compromise, and therefore understand how, and indeed whether, combined wastewater treatment, nutrient recovery and biodiesel production from microalgae is feasible, an interconnected approach towards realising these goals is required

Choosing to take a different approach therefore, the overall aim of this project was to understand how the conditions already present within a WWTW affect the growth, nutrient uptake and lipid accumulation in microalgae, using *C.reinhardtii* as a model species. To do this, conditions present within a WWTW that could influence microalgal growth, nutrient uptake and lipid accumulation were first identified and then the effect of these conditions were individually investigated in order to understand their effects. The rationale behind this approach centres on the fact that the primary goal of wastewater treatment must be the treatment of wastewater; engineering the conditions within a WWTW with the primary objective of increasing oil accumulation will most likely hinder the ability of the WWTW to achieve their primary goal (e.g. removing nitrogen for the sake of increased lipid accumulation would limit overall biomass density and therefore the removal rate of other nutrients). By understanding the effect of individual conditions, such as pH and nitrogen source, informed decisions can be made regarding both the feasibility of combined wastewater treatment, nutrient recovery and biodiesel production, and the most strategic stage of wastewater treatment to utilise for microalgal cultivation.

7.1 A New Method to Measure Biomass Concentration

Growing interest in microalgae to support a green, circular, bioeconomy has led to extensive research aimed at increasing biomass density. At the centre of this is a need for rapid and accurate methods to measure algal biomass concentrations. In particular, there is a need for methods that work for very small cultures, such as in screening studies, where destructive methods are not appropriate.

As a surrogate parameter for biomass density, chlorophyll concentration can achieve a measure of culture density without interference from non-photosynthetic organisms such as bacteria, present in abundance in WWTW. A decrease in chlorophyll concentration can also be used as an early indicator of TAG accumulation due to the breakdown and recycling of the chloroplast membrane (Moellering and Benning, 2010; Siaut et al., 2011). Current methods for chlorophyll quantification involve destructive solvent extraction or, more recently, non-destructive fluorescence methods have emerged, with commercial products available, but both are unsuited to repeated sampling of small volume cultures which need to remain axenic (Vincent, 1983; Wang *et al*., 2018).

This project began with a new method to measure the chlorophyll concentration of algal cultures non-destructively and *in-situ* (Chapter 3). The method was developed from the need to test a range of culture conditions for their effect on the growth of *C.reinhardtii* however, due to space limitation, culture volume was compromised for the sake of time and as such traditional destructive methods were not appropriate. A handful of methods using similar principles of digital image analysis have been developed, predominantly for the measurement of chlorophyll in plant leaves (Gupta *et al*., 2013; Dey *et al*., 2016; Friedman *et al*., 2016) and one using a marine alga (Su *et al*., 2008) but, while effective, complex mathematical processing and a need for advanced modelling software make these methods difficult to replicate. In addition to being much simplified compared with other similar methods, the method developed here can be used over a range of biomass densities. Furthermore, the work reported here is the first to our knowledge to test such a method under changing environmental conditions.

In summary, the developed method is robust to a final green pixel intensity (GPI) of 0.125 corresponding to a total chlorophyll concentration of 16 µg/ml. A single standard curve created for the specific species, culture vessel and photographic set-up can be used despite changes in sample volume with negligible errors. In contrast, an elevated pH or high levels of bacterial contamination lead to increased errors (ca. 5-25 %) but the method can be used effectively for qualitative analyses nonetheless. In contrast, the correlation between GPI and chlorophyll concentration for nitrogen starved cultures varied significantly from that of the

control and as such, the method as it stands is not appropriate for use on cultures with depleted chlorophyll as a result of TAG accumulation.

The method has provided a useful tool facilitating rapid investigations throughout this project including to measure the effect of initial culture pH on the growth of *C.reinhardtii* (see Chapter 4, Section 4.3) and for initial screening studies of environmental conditions and the effect of varying DMP concentrations on *C.reinhardtii* growth and lipid accumulation (Chapter 6). And, while developed initially to support the further work of this project, the method has much wider applications and I can envision it being a useful tool both for small volume screening studies as well as outside of a specialist laboratory setting – e.g. during fieldwork, or in laboratories where access to specialist equipment may be limited. One obvious use, in relation to the aim of this project, is within a WWTW itself as a simple and rapid way of monitoring algal growth on-site.

Further work investigating additional environmental variables as well as a wider range of species and samples, including algal consortia found in WWTW, would help to demonstrate the wider applicability of this method. Additionally, it is plausible that correction factors could be found and applied to reduce errors associated with changing pH and chlorophyll depletion in response to lipid accumulating triggers. Finding correction factors for these conditions would require substantial investigation both mathematically with existing data and then in the laboratory to confirm the result with an expanded range of each variable. It would be prudent to confirm any correction factor for our nitrogen starved samples with other known lipid triggers, such as iron starvation, to further increase the applicability of the method.

7.2 Understanding N, P and C Uptake in Response to Environmental Variation

In order to fully realise the potential of WWTW to support nutrient recovery and biofuel production alongside wastewater treatment, there is a need for a much more critical understanding of the effect of wastewater culture conditions on nutrient uptake and lipid accumulation in microalgae. WWTW contain a range of culture conditions depending on the composition of the wastewater and the stage of treatment. Factors such as nutrient excess or deprivation (i.e. after complete nutrient removal), extreme (>10) or neutral pH and varying nitrogen source could therefore be exploited if they are able to achieve the desired outcomes. This section reviews knowledge gained from this project regarding the effect of these conditions on combined nutrient recovery and lipid accumulation in *C.reinhardtii* to support wastewater treatment.

7.2.1 Combined wastewater treatment, nutrient recovery and biodiesel production is favoured by microalgal cultivation at near-neutral pH

The growth of freshwater algae such as *Chlamydomonas* and other species commonly found in WWTW are typically optimised by neutral or marginally acidic pH (Kong *et al*., 2010; Ochoa-Alfaro *et al*., 2019). However, during growth within WWTW, microalgae impose diurnal variations on pH due to the uptake and release of CO_2 and in-pond pH can reach values >10 (Mara, 2003; Camargo-Valero and Mara, 2007a). The increased pH afforded by microalgal growth can aid nutrient removal through phosphate precipitation (Diamadopoulos and Benedek, 1984) and ammonia volatilisation (Mara, 2003) and is used for considerable pathogen removal in waste stabilisation ponds (Curtis *et al*., 1992; Mara, 2003). With attention turning to nutrient recovery rather than simply removal, neutral pH may be preferential. Use of bubbled CO_2 (e.g. from flue gases) can provide pH control to aid microalgal growth and boost carbon sequestration (Acién *et al*., 2016) and as such both neutral and highly alkaline pH are available to be exploited within WWTW. It is therefore important to understand the effect of pH on nutrient removal, nutrient recovery and the potential for the resultant biomass to be used as a biofuel feedstock.

Microalgae typically contain approximately 10 % N and 1 % P by weight (Stumm and Morgan, 1996, van Harmelen and Oonk, 2006), however under some conditions, microalgae have been reported to accumulate more phosphorus than required for growth (up to 3 %). To the best of our knowledge, before now, only one study has attempted to monitor the specific effect of pH on phosphate concentration within microalgae. Sells and co-workers reported that allowing the pH of a culture to rise naturally (pH>10) increased the concentration of intracellular phosphate compared to CO_2 mediated pH control (pH 7-8 and pH 8-9) (Sells *et al*., 2018). However, the conclusions are somewhat misleading. Initial phosphate concentration within the medium was low (<4 mg/L) with the result that all phosphate had been removed from the medium by the microalgae within 48 hours regardless of culture pH. The uncontrolled pH therefore serves to decrease biomass yield rather than increase phosphate uptake with the result that uncontrolled pH cultures merely have less biomass across which to distribute phosphate, resulting in increased intracellular concentrations. There is no evidence to suggest a similar result would be observed if phosphate was in excess. Indeed, an earlier study in *Chlorella pyrenoidosa* revealed that total phosphate removal is highest at near-neutral pH owing to the increase in biomass density (Huang and Wang, 2003). We therefore question the authors recommendation that pH within waste stabilisation ponds should be uncontrolled for the sake of phosphate bioremediation (Sells *et al*., 2018).

As with other reports, the results presented in this study demonstrate that the growth of *C.reinhardtii* is significantly favoured by near-neutral pH medium, with increasing alkalinity significantly hindering both the final biomass density and the growth rate (Figures 4.5 and 4.7). Total nutrient removal was optimised by maximising biomass density with near neutral pH medium resulting in the highest total nutrient removal from the medium (Figure 4.8).

Owing to difficulties in measuring intracellular phosphate directly, it is commonplace to measure intracellular phosphate using a mass balance approach from the medium, however this approach means that phosphate precipitation is often neglected, which at high pH can lead to overestimations in biomass P. To account for phosphate precipitation in this study, we calculated phosphate availability with increasing pH in a series of cultures containing no biomass (Figure 4.10). The results demonstrated that nearly 50 % of all phosphate may be lost to precipitation when raising the pH from pH 8-10 and this may increase with increasing cation concentration. After factoring in the phosphate lost to precipitation, there is some evidence that increasing pH with nitrate as the sole nitrogen source can increase biomass phosphate (Table 4.9) however the growth rate is reduced such that total nutrient recovery is significantly lower than at near-neutral pH. In the following chapter, pH was increased in some cultures due to nitrate assimilation, while biomass density remained largely similar (Chapter 5) and very similar intracellular P concentrations were observed across all cultures (Table 5.2). It is a limitation however, that in-cell phosphate was estimated rather than directly measured and while accounting for phosphate precipitation arguably makes this study more accurate than others, the methods are still heavily reliant on assumptions regarding phosphate precipitation and availability. Further work should attempt to measure in-cell P directly to ensure these results are reliable.

More importantly, this study demonstrated that overall nutrient removal from the medium is optimised by the conditions which optimise biomass density. Previous work has demonstrated that microalgal uptake is the dominant mechanism of nitrogen removal in WSP maturation ponds (Camargo-Valero and Mara, 2007b) and this work provides evidence of the same for phosphorus removal. As such, maintaining a near-neutral pH through pH control would be preferable for total nutrient removal in WWTW. While high pH is shown to increase phosphate removal from the medium through precipitation, this phosphate is lost to the environment and as such reduces the availability of phosphate for recycling *via* microalgae. High pH as a result of nitrate assimilation (in contrast to ammonium assimilation) was shown to afford no benefit to phosphate removal from the medium owing to the reduction in microalgal uptake proposed to be due to the reduced availability (see Chapter 5, Section 5.2.2).

A crucial problem identified here at high pH is the potential for ammonia toxicity and its effect on algal biomass growth and nutrient uptake. Cultures at high pH grown in ammonium as the sole nitrogen source, had the lowest total nutrient removal of all the conditions tested, likely as a result of cell death and the subsequent reduced biomass density. The effects and significance of ammonia toxicity are discussed in the following section, but they provide additional support for the need for pH control in WWTW reliant on microalgal nutrient removal, especially given ammonium is typically the dominant nitrogen species in influent wastewater (Eckenfelder and Argaman, 1991).

However, alkaline pH has been identified by some studies as a potential TAG accumulating stressor. When subjected to high pH (pH 10) and low salinity, the microalga *Dunaliella viridis* achieved a fatty acid content of 56 % dry biomass weight (Byrd and Burkholder, 2017). Similarly, *Chlorella* has been shown to achieve lipid contents of up to ca. 40 % dry weight when pH stressed compared to approximately 15 % under non-stress conditions (Skrupski et al., 2013). However, these reports are not consistent, with several studies reporting no change in lipid accumulation in response to pH stress (Gardner *et al*., 2013; Zhang *et al*., 2014b). In addition, studies investigating the effect of pH on lipid accumulation often struggle to limit the number of additional variables, with the addition of bicarbonate being a particularly common means by which to raise culture pH. This has led to the hypothesis that additional lipid accumulation is as a result of additional carbon supplied in the form of bicarbonate (or bubbled CO_2 in the case of reports stating that acidic pH causes increased lipid accumulation) rather than as a direct result of the pH. Indeed, the addition of sodium bicarbonate has been linked directly to an increase in lipid accumulation using sodium carbonate as a control (Gardner *et al*., 2013). One question this project aimed to address was whether observed increases in lipid accumulation were indeed due to an increase in culture pH or due to additional carbon sources.

In this study we attempted to eliminate additional variables by using buffers to regulate pH. Nitrate was used as the sole nitrogen source to remove the possibility of ammonia toxicity and bicarbonate was used in separate cultures to independently assess the effect of bicarbonate. Cultures exchanged into high pH medium with nitrate as the sole nitrogen source revealed no increase in the lipid concentration within cells (Figure 4.13) and suggest therefore that pH has no effect on lipid accumulation in *Chlamydomonas reinhardtii*. Interestingly, addition of bicarbonate to high pH cultures resulted in a slightly reduced lipid content than high pH cultures in the absence of bicarbonate, similarly suggesting that under the conditions tested the additional available carbon afforded no advantage to carbon accumulation. Given that cultures were grown in 24-hour light however, it may be that atmospheric CO_2 dissolved in the

media was sufficient for phototrophic growth. Further work should consider repeating the experiments here under heterotrophic or mixotrophic conditions.

In contrast, cultures exchanged into high pH medium with ammonium as the sole nitrogen source rapidly depleted lipid content but preferentially retained saturated and mono-unsaturated fatty acids. Nile-red fluorescent staining revealed the presence of distinct oil bodies indicative of significant TAG accumulation and the rapid chlorophyll depletion supports the recycling of membrane lipids into TAGs. This result suggests that ammonia toxicity, rather than high pH, may be a cause of increased lipid accumulation. The reduction in growth rate and increase in lipid content has previously been suspected in response to ammonia toxicity in the alga *Chlorella pyrenoidosa* (Tan *et al*., 2016). As with high pH nitrate medium, bicarbonate had no significant effect on lipid accumulation. The significance of ammonia toxicity is discussed in more detail in the following section (Section 7.2.2).

With the evidence that nutrient removal, microalgal bioremediation and lipid accumulation is optimised by near-neutral pH, further work should now investigate whether pH could be feasibly controlled within a WWTW without significantly increasing costs or reducing the success of pathogen removal mechanisms.

7.2.2 Ammonia toxicity: a new trigger of TAG accumulation

At the start of this project, a short experiment was conducted to investigate the effect of a synthetic wastewater (SWW) on the growth of *C.reinhardtii* (see Chapter 4, Section 4.2). The synthetic wastewater was modified from Bold's Basal Medium (BBM) to contain nutrient concentrations comparable with that observed at Esholt Wastewater Treatment Works, Bradford, UK (Yulistyorini, 2016). Growth of *C.reinhardtii* on SWW revealed a period of slow growth before chlorophyll concentration suddenly dropped and neutral lipids were accumulated in oil droplets within the cells (Figures 4.1 and 4.3).

Comparison of SWW with standard TAP medium revealed that increasing pH from one first able to support (albeit slow) growth to one which can no longer support algal growth is the most likely cause of the response observed (see Chapter 4, Section 4.2.3); SWW is unbuffered with a starting pH of 9.1 compared to buffered TAP which has a starting pH of 7.0. Alkaline pH has previously been shown to limit the growth of microalgae; *Chlamydomonas reinhardtii* is optimised by growth on neutral or marginally acidic pHs (Kong *et al*., 2010; Ochoa-Alfaro *et al*., 2019, see also Figure 4.5). However, pH is not known to trigger such sudden lipid accumulation; despite some reports that high pH can act as a stressor, inducing TAG accumulation, reports are controversial and there are no known publications reporting lipid accumulation in *Chlamydomonas* as a direct effect of pH (see Chapter 1, Section 1.5.2).

Further investigation (see Chapter 4, Section 4.4) revealed that at high pH, while ammonium as the sole nitrogen source led to a drop in chlorophyll accumulation and accumulation of oil bodies (observed by Nile-red fluorescent staining), growth on nitrate led only to a decrease in the growth rate and no observable TAG accumulation (Figures 4.7 and 4.14). At high pH, ammonium ions (NH_4^+, *pKa* = 9.3) readily dissociate to produce free ammonia (NH_3) which is toxic to microalgae even at low concentrations (Azov and Goldman, 1981; Källqvist and Svenson, 2003; Gutierrez *et al*., 2016). We hypothesise therefore that the sudden cessation of growth and accumulation of TAGs is as a result of stress induced by ammonia toxicity. Indeed, the ability of cultures to grow slowly at pH 9.1 before growth declined with cultures reaching a final pH of 9.6-10.3 (Table 4.5) fits well with the *pKa* of ammonium.

While previously reported to affect microalgal growth and indeed cause cell death, this report is the first to our knowledge that reports ammonia toxicity as an accumulator of TAGs. More importantly, assessment of lipid composition over time (Chapter 4, Section 4.4.3.3) demonstrated that ammonia toxicity causes preferential depletion of poly-unsaturated fatty acids (PUFAs) while the concentration of mono-unsaturated and saturated fatty acids (MUFAs and SFAs) remained largely constant (Figure 4.16). The result of this is that ammonia toxicity has the potential to produce a biomass with lipids of much greater quality for biodiesel production. Of all the cultivation conditions tested in this project, cultures subjected to ammonia toxicity were the only cultures to harbour a lipid composition meeting the EU standard for biodiesel (Table 4.10 and Figure 4.18). One previous study identified a link between lipid accumulation and pH when ammonium was present as the dominant nitrogen source, revealing an increase from 18 to 30 % lipid content in algal blooms harvested from a WWTW during Spring when pH was increased from 5.7-6.5 to 8.3-8.8 as a result of ammonia toxicity (Tan *et al*., 2016). This study however reported a significant increase in PUFA concentration. Nonetheless, their work supports a link between ammonia toxicity and lipid accumulation in microalgae.

Further work should confirm that the results are indeed caused by ammonia toxicity and work should be done to understand the necessary concentration to induce the reported observations. It may be that a reduced concentration of ammonia can give similar results in terms of lipid quality whilst reducing the undesirable effects such as reduced growth, or that the effects of ammonia toxicity can be triggered once high biomass density has been achieved.

Despite the promising result that ammonia toxicity can drastically improve lipid quality for biodiesel production, *Chlamydomonas* did not resist the cell death associated with ammonia toxicity. After media exchange into high pH (pH 9.5) ammonium containing medium, dry biomass weight ceased increasing and optical density was observed to fall to approximately 50 % of the inoculation OD within four days (Figure 4.7). Similarly, total lipid content fell to approximately

one third that at inoculation (Figure 4.13) and phosphate concentration in the medium increased, at least in part due to release from dying microalgal biomass (Figure 4.11). Reduced intracellular phosphate and lipid quantity is therefore compounded by the low biomass yield resulting in significantly reduced total phosphorus and carbon recovery.

The limited biomass growth and crucially the release of phosphate back into the medium, means that ammonia toxicity is a potentially severe problem within WWTW. Given that pH, if uncontrolled, can reach values >10 (Mara, 2003) due to microalgal consumption of CO_2, and ammonium concentrations are often high within influent wastewater (Eckenfelder and Argaman, 1991; Yulistyorini, 2016) and in digestate following the anaerobic digestion of sludge (Morales-Amaral *et al*., 2015b; Stiles *et al*., 2018), ammonia toxicity is highly probable. Therefore, if microalgae are to be grown prior to nitrification of ammonium (see Section 7.2.3 for discussion on why this is favourable), pH control measures such as CO_2 addition may be required in order to keep the pH well below the *pKa* of ammonium. Further work is required to determine the concentration of ammonia required to elicit such a response and the nature of the response to ammonia toxicity during diurnal pH variations as are commonplace within WWTW.

7.2.3 Microalgae can remove the need for nitrification in WWTW

In untreated municipal wastewaters, nitrogen species are present predominantly as ammonium (Eckenfelder and Argaman, 1991) which is typically removed through conversion to nitrate followed by N_2 gas by nitrifying/denitrifying bacteria (Jeyanayagam, 2005; McCarty, 2018; Halling-Sorensen and Jorgensen, 1993). However, nitrifying and denitrifying bacteria release NO and N_2O into the atmosphere as intermediates (Law *et a*l., 2012; Adouani *et al*., 2015) and the process requires extensive aeration to provide aerobic conditions for nitrifiers (Gandiglio *et al*., 2017). As microalgae can remove up to 100 % of nitrogen from wastewaters (van Harmelen and Oonk, 2006; Sun *et al*., 2013; Zhang *et al*., 2014a; Caporgno *et al*., 2015), they may offer an opportunity to replace nitrification/denitrification processes through direct uptake of ammonium, thereby reducing NO/N_2O emissions and offering energy and cost savings through a reduced need for aeration processes.

Ammonium has long been thought to be the preferred source of inorganic nitrogen for phytoplankton growth (Dortch, 1990), likely because of the reduced energy requirement for ammonium assimilation over nitrate (Fernandez and Galvan, 2007). This project revealed a similar result in the species *Chlamydomonas reinhardtii* where uptake rates of ammonium were significantly higher than that of nitrate in the first three days of cultivation (Figure 5.3 (A)). Despite reports that the presence of ammonium inhibits nitrate uptake through inhibition of

specific nitrate transporters in *Chlamydomonas* (Fernandez and Galvan, 2007; Patel *et al*., 2015), the uptake rate of nitrate after the first three days of cultivation (i.e. during exponential-phase growth) exceeded that of ammonium, despite ammonium concentrations of up to 25 mg/L (Figure 5.3 (B)). It may be that under nitrogen limited conditions or during rapid algal growth, the distinct ammonium and nitrate transporters allow for increased nitrogen assimilation before transporter saturation, as has previously been suggested (Gonzales *et al*., 2014). Indeed, similar uptake rates of ammonium and nitrate in *Chlamydomonas reinhardtii* have previously been reported when total nitrogen availability was low (<2.5 mg/L, Thacker and Syrett, 1972). Growth rate and final biomass density were not affected by varying the nitrogen source between ammonium and nitrate (Figure 5.1, Table 5.1).

The preference of microalgae to assimilate ammonium over nitrate has advantages for wastewater treatment both because ammonium is typically the dominant nitrogen species in influent wastewater and, as the more toxic of the two inorganic nitrogen species (i.e. due to ammonia toxicity at high pH, Abdel Raouf *et al.,* 2012), the removal of ammonium is arguably more critical than nitrate removal. Furthermore, there is emerging evidence that microalgae can produce environmentally harmful nitrous oxides during growth in nitrate medium (Plouviez *et al*., 2017). Due to the threats to aquatic life associated with ammonia toxicity, if controlled nitrification processes are to be removed, microalgae must be proven to achieve almost complete removal of ammonium. As with other studies, here we reported that cultures of *C.reinhardtii* were able to remove 100 % of the nitrogen species (50mg/L) present in the medium within 5 days of cultivation. Similarly, high nitrate uptake rates despite the presence of ammonium are advantageous since nitrification processes are still present naturally in alga dominated wastewater treatment processes such as waste stabilisation ponds (Camargo Valero and Mara, 2010b).

With interest in microalgae for wastewater treatment now extending to the search for useful by-products, there is an interest not just in nutrient removal but nutrient uptake, including carbon for processing into biofuels. As such, it is prudent to investigate which the nitrogen source of choice may be to optimise nutrient recovery and lipid accumulation in microalgae.

One recent hypothesis has emerged that a shift from ammonium assimilation to more energy intensive nitrate assimilation might prompt a stress response triggering the accumulation of polyphosphates as is seen during nitrogen deprivation (Yulistyorini, 2016); if this is the case, one might expect a similar accumulation of TAGs. The study in question demonstrated increased polyphosphate accumulation in *Chlamydomonas reinhardtii* as

ammonium availability dropped, forcing growth to continue on nitrate (Yulistyorini, 2016); to date no published studies have tested this hypothesis on TAG accumulation.

Nutrient availability is highly dependent on culture pH which is in turn dependent on the nitrogen source present; up to 50 % of available phosphate may be lost to precipitation due to increasing culture pH from pH 8-10 (Figure 4.10). Due to uptake of H^+ ions from the medium to balance the assimilation of negatively charged nitrate ions, pH during growth on nitrate rises considerably higher than that observed for growth on ammonium (Scherholz and Curtis, 2013). Here the pH is demonstrated to increase proportionately with increasing nitrate concentration in the original medium (Figure 5.1 (D)).

Despite an increase in phosphate precipitation during growth on ≥50 % nitrate (Figure 5.4 (B)), the increase in phosphate lost through precipitation was balanced by a decrease in microalgal phosphate uptake (Figure 5.4 (C)) and no increase in the total phosphate removed from the medium was observed (Figure 5.4 (A)). Phosphate uptake in response to differing availability in the culture medium has previously been shown (Powell *et al*., 2009) and the reduced microalgal uptake demonstrated here as phosphate precipitation is increased likely reflects the reduced phosphate availability. The work here contradicts the hypothesis that a shift from ammonium to nitrate increases microalgal phosphate accumulation however further work on this hypothesis whilst maintaining constant pH (i.e. through CO_2 addition) or with increased nutrient concentrations to remove availability constraints may yield different results.

A critical result of this work is that while microalgal growth in nitrate-based wastewater will lead to an increase in phosphate removal through precipitation, it affords no advantage to the amount of phosphate remaining in the effluent nor the amount available for recycling through algal uptake.

Similarly, a shift from ammonium to nitrate assimilation afforded no additional lipid accumulation. At very short hydraulic retention times (HRT), a slight increase in lipid accumulation may be afforded by growth on nitrate, or a mixed N source, over ammonium only, however after one week cultivation there was no observable difference in the lipid quantity between nitrogen sources (Figure 5.5). No difference in the quality of lipids produced for biodiesel was observed between N sources (Table 5.3). The study here does, however, support the results of the small handful of other studies that show a natural removal of nitrogen (i.e. through microalgal uptake) can lead to a nitrogen starvation response with similar consequences for lipid production as a sudden removal of nitrogen (Caporgno *et al*., 2015; Tsolcha *et al*., 2015; Lutzu *et al*., 2016). However, no significant improvement in lipid quality was observed following the complete exhaustion of nitrogen.

Based on current research, including that provided in this study, during phototropic growth, the microalga *Chlamydomonas reinhardtii* is largely unaffected by a shift in nitrogen source and demonstrates efficient growth on ammonium as well as in a mixed ammonium/nitrate medium. The ability of microalgae to easily assimilate 50 mg/L total N (typical value for influent municipal wastewater) as ammonium, supports the removal of nitrification process in WWTW in place of microalgal uptake. With the interest in microalgae cultivated in WWTW to produce high-value products (i.e. fertilisers and/or biodiesel), there may be rationale for keeping nitrification processes prior to microalgal growth if growth on nitrate can increase the production of useful products. This study contributes to the case for removal of nitrification processes by demonstrating that growth on nitrate affords no advantage in the hunt for valuable by-products. Indeed, nutrient recovery is optimised by a lower culture pH, which is aided by ammonium assimilation over nitrate.

As has previously been stated however (see Sections 7.2.1 and 7.2.2), pH control is recommended to maintain a near-neutral pH in order to avoid the effects of ammonia toxicity where high concentrations of ammonium are present. Since uptake of ammonium helps to maintain a low pH through release of H^+ ions (to maintain intracellular pH), in contrast to nitrate uptake which requires the uptake of H^+ ions, pH control will likely be a smaller challenge in ammonium dominant wastewaters (Scherholz and Curtis, 2013).

As a small-scale laboratory study, the results presented here are promising and help to shed light on the mechanisms of nitrogen uptake during phototrophic growth. Further work should now investigate the effect of nitrogen source during heterotrophic growth as well as during traditional day/night cycles. As with most microalgal research, continued research is needed to scale up testing, particularly in continuous culture where results can be significantly different.

7.3 Chemical Triggers Can Offer Improvements in Lipid Quality but Not Quantity

Until recently, most research concerned with increasing lipid accumulation in microalgae was centred on increasing the quantity of neutral lipids accumulated through the lipid biosynthesis pathway. However, attempts at genetically upregulating the lipid biosynthesis pathway have had limited success at increasing the accumulation of neutral lipids.

Overexpression of DGAT enzymes in *Chlamydomonas reinhardtii*, responsible for the final acylation of a free fatty acid to the glycerol headgroup to form TAGs, resulted in only a ≤50 % increase in lipid content (Deng *et al*., 2012). Similarly, overexpression of the PDAT enzyme resulted in a 22 % increase in total fatty acids and a 32 % increase in TAGs but with a concomitant slowing of growth (Zhu *et al*., 2018). Efforts to increase lipid accumulation through genetic

upregulation, are far from the results achieved by environmental triggers such as nitrogen deprivation.

As such, there is increasing interest in downregulation of the lipid catabolism pathway. To date, only three enzymes responsible for TAG catabolism have been identified in microalgae, all of which demonstrate temporarily reduced TAG remobilisation when downregulated and often at the expense of growth (Li *et al*., 2012; Kong *et al*., 2017; Warakanont *et al*., 2019).

Until we have more knowledge regarding the enzymes involved in TAG catabolism, chemical triggers offer a means to simulate the action of potential mutants as well as enabling the identification of further targets for increasing oil accumulation. The use of chemical triggers may also serve useful in outdoor cultivation systems, such as WWTW, where there are strict controls on the release of genetically modified organisms (GMOs) and, while chemical triggers often impose a growth penalty similar to genetic mutants, in contrast to mutations, chemical triggers can be applied in a controlled manner at strategic points. Indeed, the drug, Brefeldin A (BFA), has had more success at increasing TAG accumulation than alternative genetic approaches (Kato *et al*., 2013; Kim *et al*., 2013).

Use of the drug BFA has similarly been shown to act as a chemical trigger repressing TAG mobilisation; addition of 2.5 µM BFA on nitrogen resupply to cells cultured in TAP-N for 24 hours led to 76 % Nile-red fluorescence retention after 16 hours compared to only 10 % retention in the control (Kato *et al*., 2013). In chapter 6 of this thesis, the small molecule diphenyl methylphosphonate, previously shown to inhibit TAG remobilisation in *Arabidopsis thaliana* (Brown *et al*., 2013), is shown to effect similar results in the microalga *C. reinhardtii* (see Chapter 6). Four days after nitrogen resupply, cultures treated with 150 and 250 µM DMP retained a neutral lipid concentration of 5.9 and 5.3 % of dry biomass weight respectively compared to 3.8 % in the untreated control (Figure 6.6).

However, as with efforts to upregulate the lipid biosynthesis pathway, either by chemical or genetic means, TAG remobilisation has only been repressed at the expense of a full exit from quiescence (the vegetative state cells enter during nitrogen starvation and other TAG accumulating stressors) (Li *et al*., 2012; Kato *et al*., 2013; Kim *et al*., 2013; Kong *et al*., 2017; Warakanont *et al*., 2019). The use of DMP to supress TAG remobilisation here demonstrated a similar result, with DMP treated cultures reaching a dry biomass weight up to half that of untreated cultures after four days (Figure 6.1 (C)) and total lipid yields were similar regardless of DMP treatment (Table 6.1).

We therefore hypothesise that the efficient remobilisation of TAGs following a stress response (e.g. nitrogen starvation) is a necessity for growth to resume in full and that

downregulation of the lipid catabolism pathway cannot be achieved without significantly limiting biomass yield and therefore net lipid yield. The very similar total lipid yields regardless of DMP treatment suggest a direct correlation between lipid concentration within the biomass and biomass yield following N resupply (Table 6.1).

This follows on from the hypothesis that upregulation of the lipid biosynthesis pathway has had limited success due to the competition for substrates (e.g. acyl-CoA) and carbon between pathways for TAG synthesis, cellular growth and other carbon-rich storage products (Tan and Lee, 2016). Indeed, the most successful attempts to increase oil yields through genetic modification have been through downregulation of the starch pathway which competes with TAGs for carbon. Silencing of the STA6 gene, encoding AGPase which catalyses the first committed step in starch synthesis, leads to 2-10 times the TAG accumulation compared with the wild-type when subjected to nitrogen deprivation (Li *et al*., 2010a; Li *et al*., 2010b). Similarly, downregulation of the citrate synthase gene (*CrCIS*) resulted in a 169.5 % increase in TAG content after six days cultivation, compared to the control (Deng *et al*., 2013); both the tricarboxylic acid cycle, of which CIS is the rate-limiting enzyme, and the fatty acid synthesis pathway are thought to compete for pyruvate.

However, chemical triggers have been successful at improving lipid quality for biodiesel production. An exciting study revealed that the fungicide fenpropimorph, leads to rapid mobilisation of membrane lipids, mainly from the chloroplast membrane, to form TAGs, resulting in a four-fold increase in TAG content within one hour (Kim *et al*., 2015). Despite the concomitant cell death, the speed at which polar membrane lipids were converted to TAGs suggests a real opportunity for the late upgrading of microalgal lipids for biodiesel production. Nitrogen starvation has become the favoured cultivation condition to produce microalgal biodiesel due to the high proportion of TAGs, rich in saturated and mono-unsaturated (MUFA) fatty acids (Yang *et al*., 2017). Research in this project shows that DMP treatment on nitrogen resupply can yield lipids of similar quality to those produced under nitrogen starvation but with a much less significant reduction in biomass density (Tables 6.1 and 6.2).

The ability to produce high quality lipids without compromising biomass density is particularly useful if we are to realise the goals of producing biodiesel from wastewater grown microalgae without limiting nutrient removal. In order to confirm this, further research is needed to measure the bioremediation potential of microalgae when subjected to promising chemical triggers. Furthermore, it would be useful to report the effect of DMP during 'traditional' day/night cycles (lipid catabolism is known to occur more quickly in the dark as a carbon source in the absence of photosynthesis, Kong *et al*., 2017). Cycling between nitrogen

starvation and DMP treatment under nitrogen replete conditions may also facilitate increased lipid quantity.

Nevertheless, this study provides further evidence that attempts to increase TAG content through direct manipulation of the TAG biosynthesis or catabolism pathways are likely to be unfruitful due to competition for carbon. These methods instead serve as a fortuitous mechanism to improve lipid quality without compromising nutrient recovery. The similarity between the response of *Chlamydomonas* and *Arabidopsis* to DMP adds further support to the assumptions that the mechanisms of lipid catabolism are likely conserved between microalgae and higher plants.

7.4 Conclusions and Recommendations for Applicability

Based on the work presented in this project as well as previous literature we can summarise our findings into the following recommendations:

Firstly, in order to maximise nutrient removal and nutrient recovery, pH control should be employed to maintain near-neutral pH. Freshwater algae are known to grow best at near-neutral pH and pH control through the addition of bubbled CO_2 or flue gases to algal ponds has been previously identified as a means to reduce carbon limitation and increase carbon sequestration. However, traditional methods for nutrient removal can be improved by increasing water pH (i.e. increasing ammonia volatilisation and phosphate precipitation). While pH has previously been suggested as a possible trigger for TAG and polyphosphate accumulation, we have shown here that increasing pH does not work to increase overall yields of either in *Chlamydomonas reinhardtii*. The main contribution of increasing pH is to significantly reduce both the growth rate and final biomass density of algal cultures.

Furthermore, we have demonstrated here that the increased microalgal biomass density and subsequent increase in nutrient bioremediation outweighs additional nutrient losses through alternative mechanisms. Indeed, the elevated pH caused by nitrate over ammonium assimilation only served to reduce phosphate availability through increased precipitation but afforded no improvement in the final media phosphate concentration (Section 7.2.3). These results are in agreement with previous work demonstrating that microalgal uptake is the dominant nitrogen removal mechanism in waste stabilisation ponds (Camargo-Valero and Mara, 2007b) and provide evidence of the same for phosphorus removal.

With ammonium as the dominant nitrogen source in influent wastewaters, allowing pH to rise uncontrolled increases the chances of cell death due to toxicity from free ammonia (pKa = 9.3). Ammonia toxicity is known to cause algal death, however studies on its possible

effects on microalgae within WWTW are limited. Here we have shown that increasing pH to >9.5 (as is regularly reported within WWTW) leads to cell death, reduced net lipid yield and crucially a release of stored phosphates back into the medium. It is therefore crucial that significant levels of free ammonia be avoided within WWTW; the easiest, and otherwise advantageous, way to achieve this is through pH control.

Secondly, microalgae allow for removal of energy intensive aeration processes to facilitate nitrification. The majority of WWTW employ nitrification/denitrification processes for nitrogen removal, converting ammonium to nitrate and eventually removing nitrogen as N_2 gas to the atmosphere. However, the necessary bacteria require oxygen supplementation through energy intensive and costly aeration, estimated to account for up to 45-80 % of all electricity use within WWTW (Gandiglio *et al*., 2017 and sources therein).

Historically, ammonium has been thought to be the preferred nitrogen source for phytoplankton growth and *Chlamydomonas* conforms to this assumption (Dortch, 1990; Patel *et al*., 2015; and see Figure 5.3(A)), however here we have demonstrated that during exponential phase growth under nitrogen limitation, *Chlamydomonas* can uptake both N species at similar rates (Figure 5.3(B)), contrary to previous reports that ammonium inhibits nitrate assimilation. This is proposed to be because the distinct ammonium and nitrate transporters allow for more rapid nitrogen assimilation if used simultaneously. Despite this, the growth rate, final biomass density, nutrient remediation and lipid production was similar across a range of ammonium/nitrate ratios within the media with growth on nitrate or a mixed N source offering no significant advantage. As such, there is no rationale for nitrification prior to microalgal growth where microalgae serve as the dominant nutrient removal mechanism.

Finally, and most importantly, the production of lipids must become a by-product of nutrient removal goals rather than the focus of efforts within WWTW. Throughout testing varying environmental variables which can be relatively easily replicated within WWTW, the production of high lipid quantities was always at the expense of nutrient removal ability. As with countless other accounts, the removal of nitrogen led to significant increases in lipid quantity, however, as has been argued throughout this project, controlled removal of nitrogen is unfeasible within a WWTW owing to additional costs and time required. Nitrogen deprivation may serve to increase lipid quantity only once nitrogen supplies have been exhausted through microalgal uptake and work here (Figure 5.5) and in previous literature (Caporgno *et al*., 2015; Tsolcha *et al*., 2015; Lutzu *et al*., 2016) has shown this to be similarly effective to manual nitrogen removal, but significant work upscaling research, particularly within continuous culture is required to test if this will work beyond laboratory scale.

Ammonia toxicity was additionally identified as a novel trigger of TAG accumulation in microalgae (see Section 7.2.2), however the effect on biomass density is worse than that reported by most TAG accumulating stressors. Biomass density was found to drop significantly with the result that phosphates previously stored in the cells were released back into the medium and total lipid yield was drastically reduced.

Lipid accumulation in microalgae as a result of stress conditions to create a rapidly mobilisable energy store is now a widely accepted hypothesis. As such, it is almost inevitable that dedicated attempts to significantly increase lipid accumulation will be at the expense of biomass density and therefore nutrient recovery. Research into the use of chemical triggers to inhibit lipid catabolism (see Section 7.3) further supports the hypothesis that high quantities of lipid accumulation cannot be achieved without compromising growth and therefore the nutrient removal ability of microalgae. Fundamentally, the combination of microalgal production within WWTW to reduce costs of microalgal biodiesel rely on some contribution of microalgae to the wastewater treatment process and as such any efforts to improve biodiesel production at the expense of wastewater treatment must be avoided, leaving biodiesel to become a valuable by-product, rather than the focus, of such endeavours. Despite this, promising results regarding the nutrient bioremediation potential of microalgae coupled with small biodiesel yields offer great opportunities for improving the sustainability of wastewater treatment practices.

Bibliography

Abdel-Raouf, N., Al-Homaidan, A. A., & Ibraheem, I. B. M. 2012. Microalgae and wastewater treatment. *Saudi Journal of Biological Sciences*. **19**(3), pp. 257–75.

Abou-Shanab, R. A. I., Ji, M.-K., Kim, H.-C., Paeng, K.-J. & Jeon, B.-H. 2013. Microalgal species growing on piggery wastewater as a valuable candidate for nutrient removal and biodiesel production. *Journal of Environmental Management*. **115**, pp. 257–264.

Abelson, P.H. 1999. A potential phosphate crisis. *Science.* **283**(5410), p. 2015.

Acién, F., Fernández-Sevilla, J., & Grima, E. 2016. Supply of CO2 to Closed and Open Photobioreactors. In: Slocombe, S. P. & Benemann, J. R. eds. *Microalgal Production for Biomass and High-Value Products*. Boca Raton, Florida: Taylor & Francis Group, pp. 225–252.

Adouani, N., Limousy, L., Lendormi, T. & Sire, O. 2015. N_2O and NO emissions during wastewater denitrification step: Influence of temperature on the biological process. *Comptes Rendus Chimie*. **18**, pp. 15–22.

Aksoy, M., Pootakham, W., & Grossman, A. R. 2014. Critical function of a Chlamydomonas reinhardtii putative polyphosphate polymerase subunit during nutrient deprivation. *The Plant Cell*. **26**(10), pp. 4214–29.

AlMomani, F. A. & Örmeci, B. 2016. Performance of *Chlorella Vulgaris*, *Neochloris Oleoabundans* and mixed indigenous microalgae for treatment of primary effluent, secondary effluent and centrate. *Ecological Engineering*. **95**, pp. 280–289.

Alternative Fuels Data Center. *Biodiesel Blends.* [Online]. [Accessed 27th September 2019], Available at: https://afdc.energy.gov/fuels/biodiesel_blends.html

Alvarez, S. & Jerez, C. A. 2004. Copper Ions Stimulate Polyphosphate Degradation and Phosphate Efflux in *Acidithiobacillus ferrooxidans*. *Applied and Environmental Microbiology.* **70**(9), pp. 5177–5182.

Amaro, H. M., Guedes, A. C., & Malcata, F. X., 2011. Advances and perspectives in using microalgae to produce biodiesel. *Applied Energy*. **88**(10), pp. 3402–3410.

Ambulkar, A. & Nathanson, J. A. 2010. Wastewater treatment. *Encyclopaedia Britannica.* [Online]. [Accessed 23rd Jan 2020], Available at: https://www.britannica.com/technology/wastewater-treatment

Andersson, A. J., & Gledhill, D. 2013. Ocean Acidification and Coral Reefs: Effects on Breakdown, Dissolution, and Net Ecosystem Calcification. *Annual Review of Marine Science*. **5**, pp.321-348.

APHA. 2012. *Standard methods for the examination of water and wastewater*. 22nd ed. Washington, DC: American Public Health Association.

Arias, D. M., Solé-Bundó, M., Garfí, M., Ferrer, I., García, J. & Uggetti, E. 2018. Integrating microalgae tertiary treatment into activated sludge systems for energy and nutrients recovery from wastewater. *Bioresource Technology*. **247**, pp. 513–519.

Asmare, A. M., Demessie, B. A., & Murthy, G. S. 2014. Investigation of microalgae co-cultures for nutrient recovery and algal biomass production from dairy manure. *Applied Engineering in Agriculture*. **30**(2), pp. 335–342.

Aitchinson, P. A., & Butt, V. S., 1973. The Relation between the Synthesis of Inorganic Polyphosphate and Phosphate Uptake by Chlorella vulgaris. *Journal of Experimental Botany.* **24**(80), pp. 497-510.

Azov, Y. & Goldman, J. C. 1982. Free Ammonia Inhibition of Algal Photosynthesis in Intensive Cultures. *Applied and Environmental Microbiology.* **43**(4), pp. 735–739.

Bajhaiiya, A. K., Dean, A. P., Zeef, L. A. H., Webster, R. E. & Pittman, J. K. 2016. PSR1 Is a Global Transcription Regulator of Phosphorus Deficiency Responses and Carbon Storage Metabolism in *Chlamydomonas reinhardtii*. *Plant Physiology.* **170**, pp. 1216–1234.

Barbera, E., Teymouri, A. Bertucco, A., Stuart, B. J. & Kumar, S. 2017. Recycling Minerals in MicroalgaeCultivation through a Combined Flash Hydrolysis-Precipitation Process. *ACS Sustainable Chemistry and Engineering*. **5**, pp. 929–935.

Battisti, D. S. & Naylor, R. L. 2009. Historical warnings of future food insecurity with unprecedented seasonal heat. *Science*. **323**, pp. 240–244.

Beddington, J. 2009. Food, Energy, Water and the Climate: A Perfect Storm of Global Events? Available at: https://webarchive.nationalarchives.gov.uk/20121206120858/http://www.bis.gov.uk/assets/goscience/docs/p/perfect-storm-paper.pdf

Beer, L. L., Boyd, E. S., Peters, J. W., & Posewitz, M. C. 2009. Engineering algae for biohydrogen and biofuel production. *Current Opinion in Biotechnology*. **20**(3), pp. 264–271.

Bhatt, N. C., Panwar, A., Bisht, T. S. & Tamta, S. 2014. Coupling of Algal Biofuel Production with Wastewater. *The Scientific World Journal*. **2014**, article no: 210504, [no pagination].

Bhuiyan, M. I. H., Mavinic, D. S. & Koch, F. A. 2008. Phosphorus recovery from wastewater through struvite formation in fluidized bed reactors: a sustainable approach. *Water Science and Technology.* **57**(2), pp. 175–181.

Blackall, L. L., Crocetti, G. R., Saunders, A. M. & Bond, P. L. 2002. A review and update of the microbiology of enhanced biological phosphorus removal in wastewater treatment plants. *Antonie van Leeuwenhoek.* **81**, pp. 681–691.

Blackburn, S. 2004. Water Pollution and Bioremediation by Microalgae: Eutrophication and Water Poisoning. *In: Handbook of Microalgal Culture. Biotechnology and Applied Phycology*. Oxford: Blackwell Publishing.

Bligh, E. G. & Dyer, W. J. 1959. A rapid method for total lipid extraction and purification. *The Canadian Journal of Biochemistry and Physiology.* **37**, pp. 911–917.

Bohutskyi, P., Kligerman, D. C., Byers, N., Nasr, L. K., Cua, C., Chow, S., *et al*. 2016. Effects of inoculum size, light intensity, and dose of anaerobic digestion centrate on growth and productivity of *Chlorella* and *Scenedesmus* microalgae and their poly-culture in primary and secondary wastewater. *Algal Research*. **19**, pp. 278–290.

Bolesch, D. G. & Keasling, J. D. 2000. Polyphosphate Binding and Chain Length Recognition of *Escherichia coli* Exopolyphosphatase. *The Journal of Biological Chemistry.* **275**(43), pp. 33814–33819.

Boyle, N. R., Page, M. D., Liu, B., Blaby, I. K., Casero, D., Kropat, J., *et al*. 2012. Three acyltransferases and nitrogen-responsive regulator are implicated in nitrogen starvation-induced triacylglycerol accumulation in Chlamydomonas. *The Journal of Biological Chemistry*. **287**(19), pp. 15811–15825.

Brauman, K.A., Richter, B. D., Postel, S., Malsy, M. & Flörke, M. 2016. Water depletion: An improved metric for incorporating seasonal and dry-year water scarcity into water risk assessments. *Elementa: Science of the Anthropocene.* **4**, p. 000083.

Breus, N. A., Ryazanova, L. P., Dmitriev, V. V. & Kulakovskaya, T. V. 2012. Accumulation of phosphate and polyphosphate by *Cryptococcus humicola* and *Saccharomyces cerevisiae* in the absence of nitrogen. *FEMS Yeast Research*. **12**, pp. 617–624.

Brown, L., Larson, T. R., Graham, I. A., Hawes, C., Paudyal, R., Warriner, S. L., & Baker, A. 2013. An inhibitor of oil body mobilization in Arabidopsis. *New Phytologist*. **1**, pp. 1–9.

Buchanan, B. B., Gruissem, W. and Jones, R. L. eds. 2006. *Biochemistry and Molecular Biology of Plants*. Maryland, USA: American Society of Plant Physiology.

Bunce, J. T., Ndam, E., Ofiteru, I. D., Moore, A. & Graham, D. W. 2018. A Review of Phosphorus Removal Technologies and Their Applicability to Small-Scale Domestic Wastewater Treatment Systems. *Frontiers in Environmental Science Wastewater Management.* **6**, article no: 8 [no pagination].

Buschmann, C., Langsdorf, G. & Lichtenthaler, H. 2000. Imaging of the Blue, Green, and Red Fluorescence Emission of Plants: An Overview. *Photosynthetica*. **38**, pp. 483–491.

Byrd, S. M., & Burkholder, J. M. 2017. Journal of Experimental Marine Biology and Ecology Environmental stressors and lipid production in Dunaliella spp. II. Nutrients, pH, and light under optimal or low salinity. *Journal of Experimental Marine Biology and Ecology*. **487**, pp. 33–44.

Cai, T., Park, S. Y., & Li, Y. 2013. Nutrient recovery from wastewater streams by microalgae: Status and prospects. *Renewable and Sustainable Energy Reviews*. **19**, pp. 360–369.

Campbell, M. K. & Farrell, S. O. 2008. *Biochemistry*. California, USA: Brooks/Cole CENAGE Learning.

Camargo Valero, M. A. & Mara, D. D. 2007a. Nitrogen removal via ammonia volatilization in maturation ponds. *Water Science and Technology.* **55**(11), pp. 87-92.

Camargo Valero, M. A. & Mara, D. D. 2007b. Nitrogen removal in maturation ponds: tracer experiments with ^{15}N-labelled ammonia. *Water Science and Technology*. **55**(11), pp. 81–85.

Camargo Valero, M. A., Read, L. F., Mara, D. D., Newton, R. J., Curtis, T. P. & Davenport, R. J. 2010a. Nitrification-denitrification in waste stabilisation ponds: a mechanism for permanent nitrogen removal in maturation ponds. *Water Science and Technology.* **61**(5), pp. 1137–1146.

Camargo Valero, M. A., Mara, D. D. & Newton, R. J. 2010b. Nitrogen removal in maturation waste stabilisation ponds via biological uptake and sedimentation of dead biomass. *Water Science and Technology.* **61**(4), pp. 1027–1034.

Campbell, P. K., Beer, T., & Batten, D. 2011. Life cycle assessment of biodiesel production from microalgae in ponds. *Bioresource Technology*. **102**(1), pp. 50–56.

Caporgno, M. P., Taleb, A., Olkiewicz, M., Font, J., Pruvost, J., Legrand, J., & Bengoa, C. 2015. Microalgae cultivation in urban wastewater: Nutrient removal and biomass production for biodiesel and methane. *Algal Research*. **10**, pp. 232–239.

Castro, C. D., Meehan, A. J., Koretsky, A. P. & Domach, M. M. 1995. In Situ ^{31}P Nuclear Magnetic Resonance for Observation of Polyphosphate and Catabolite Responses of Chemostat Cultivated Saccharomyces cerevisiae after Alkalinization. *Applied and Environmental Microbiology.* **61**, pp. 4448–4453.

Castrol, C. D., Koretsky, A. P. & Domach, M. M. 1999. NMR-Observed Phosphate Trafficking and Polyphosphate Dynamics in Wild-Type and *vph1-1* Mutant *Saccharomyces cerevisae* in Response to Stresses. *Biotechnology Progress.* **15**(1), pp. 65-73.

Chen, C.-Y., Kuo, E.-W., Nagarajan, D., Ho, S.-H., Dong, C.-D., Lee, D.-J. & Chang, J.-S. 2020. Cultivating *Chlorella sorokiniana* AK-1 with swine wastewater for simultaneous wastewater treatment and algal biomass production. *Bioresource Technology*. **302**, article no: 122814, [no pagination].

Chi, Z., O'Fallon, J. V., Chen, S. 2011. Bicarbonate produced from carbon capture for algae culture. *Trends in Biotechnology*. **29**(11), pp. 537–541.

Chinnasamy, S., Bhatnagar, A., Hunt, R. W. & Das, K. C. 2010. Microalgae cultivation in a wastewater dominated by carpet mill effluents for biofuel applications. *Bioresource Technology.* **101**(9), pp. 3097–3105.

Chiranjeevi, P., & Mohan, S. V. 2016. Optimizing the critical Factors for lipid Productivity during stress Phased heterotrophic Microalgae cultivation. *Frontiers in Energy Research*. **4**, pp. 1–10.

Chisti, Y. 2007. Biodiesel from microalgae. *Biotechnology Advances*. **25**(3), pp. 294–306.

Cho, D. H., Ramanan, R., Heo, J., Shin, D. S., Oh, H. M., & Kim, H. S. 2016. Influence of limiting factors on biomass and lipid productivities of axenic Chlorella vulgaris in photobioreactor under chemostat cultivation. *Bioresource Technology*. **211**, pp. 367–373.

Chu, F.-F. Shen, X.-F., Lam, P. K. S. & Zeng, R. J. 2015. Polyphosphate during the Regreening of *Chlorella vulgaris* under Nitrogen Deficiency. *International Journal of Molecular Sciences.* **16**, pp. 23355–23368.

Climate Change Act 2008. (c.27). [Online]. London: The Stationary Office. [Accessed 21 April 2020]. Available at: http://www.legislation.gov.uk/ukpga/2008/27/pdfs/ukpga_20080027_en.pdf

CO2 Earth, 2020. CO2 Acceleration [Online]. [Accessed 21 April 2020] Available at: https://www.co2.earth/co2-acceleration

Committee on Climate Change (CCC). 2016. UK Climate action following the Paris Agreement. Available at: https://www.theccc.org.uk/wp-content/uploads/2016/10/UK-climateaction-following-the-Paris-Agreement-Committee-on-Climate-Change-October-2016.pdf

Coppens, J., Grunert, O., Van Den Hende, S., Vanhoutte, I., Boon, N., Haesaert, G. & De Gelder, L. 2016. The use of microalgae as a high-value organic slow-release fertilizer results in tomatoes with increased carotenoid and sugar levels. *Journal of Applied Phycology*. **28**, pp. 2367–2377.

Cordell, D., Drangert, J. O., & White, S. 2009. The story of phosphorus: Global food security and food for thought. *Global Environmental Change*. **19**(2), pp. 292–305.

Craggs, R., Park, J., Heubeck, S. & Sutherland, D. 2014. High rate algal pond systems for low-energy wastewater treatment, nutrient recovery and energy production. *New Zealand Journal of Botany.* **52**(1), pp. 60–73.

Crimp, A., Brown, N. & Shilton, A. 2018. Microalgal luxury uptake of phosphorus in waste stabilization ponds – frequency of occurrence and high performing genera. *Water Science and Technology*. **78**(1), pp. 165–173.

Culture Collection of Algae and Protozoa. BB (Bold's Basal Medium). [Online]. [Accessed 10th November 2016]. Available at: https://www.ccap.ac.uk/pdfrecipes.htm

Curtis, T., Mara, D. D & Silva, S. A. 1992. The Effect of Sunlight on Faecal Coliforms in Ponds: Implications for Research and Design. *Water Science and Technology.* **26**(7-8) pp. 1729–1738.

Curtis, T. 2003. Bacterial pathogen removal in wastewater treatment plants. In: Mara, D. & Horan, N. eds. *Handbook of Water and Wastewater Microbiology*. Academic Press, pp. 477–490.

Davies, D. R. & Plaskitt, A. 1971. Genetical and structural analyses of cell-wall formation in Chlamydomonas reinhardi. *Genetics Research.* **17**, pp. 33–43.

Dean, A. P., Sigee, D. C., Estrada, B. & Pittman, J. K. 2010. Using FTIR spectroscopy for rapid determination of lipid accumulation in response to nitrogen limitation in freshwater microalgae. *Bioresource Technology*. **101**, pp. 4499–4507.

Delrue, F., Setier, P., Sahut, C., Cournac, L., Roubaud, A., Peltier, G., & Froment, A. 2012. Bioresource Technology An economic, sustainability, and energetic model of biodiesel production from microalgae. *Bioresource Technology*. **111**, pp. 191–200.

Demirbas, A., & Demirbas, M. F. 2011. Importance of algae oil as a source of biodiesel. *Energy Conversion and Management*. **52**(1), pp. 163–170.

Deng, X. D., Gu, B., Li, Y. J., Hu, X. W., Guo, J. C., & Fei, X. W. 2012. The roles of acyl-CoA: Diacylglycerol acyltransferase 2 genes in the biosynthesis of triacylglycerols by the green algae Chlamydomonas reinhardtii. *Molecular Plant*, **5**(4), pp. 945–947.

Deng, X., Cai, J. & Fei, X. 2013. Effect of the expression and knockdown of citrate synthase gene on carbon flux during triacylglycerol biosynthesis by green algae *Chlamydomonas reinhardtii*. *BMC Biochemistry.* **14**, article no: 38, [no pagination].

Dey, A. K., Sharma, M., & Meshram, M. R., 2016. An Analysis of Leaf Chlorophyll Measurement Method using Chlorophyll Meter and Image Processing Technique. *Procedia Computer Science*. **85**, pp. 286–292.

Diamadoupoulos, E. & Benedek, A. 1984. The Precipitation of Phosphorus from Wastewater Through pH Variation in the Presence and Absence of Coagulants. *Water Research.* **18**(9), pp. 1175–1179.

Dineshkumar, R., Kumaravel, R., Gopalsamy, J., Sikder, M. N. A. & Sampathkumar, P. 2018. Microalgae as Bio-fertilizers for Rice Growth and Seed Yield Productivity. *Waste Biomass and Valorization*. **9**, 793–800.

Docampo, R. & Moreno, S. N. J. 2001. The acidocalcisome. *Molecular and Biochemical Parasitology.* **33**, pp. 151–159.

Docampo, R., de Souza, W., Miranda, K., Rohloff, P. & Moreno, S. N. J. 2005. Acidocalcisomes – Conserved from Bacteria to Man. *Nature Reviews.* **3**, pp. 251–261.

Dortch, Q. 1990. The interaction between ammonium and nitrate uptake in phytoplankton. *Marine Ecology Progress Series*. **61**, pp. 183–201.

Eckenfelder, W. W. & Argaman, Y. 1991. Principles of Biological and Physical/Chemical Nitrogen Removal. In: Sedlak, R. I. ed. *Phosphorus and Nitrogen Removal from Municipal Wastewater.* 2nd ed. New York: The Soap and Detergent Association, pp. 3–42.

Ehimen, E. A., Sun, A F., Carrington, C. G., Birch, E. J. & Eaton-Rye, J. J. 2011. Anaerobic digestion of microalgae residues resulting from the biodiesel production process. *Applied Energy*. **88**(10), pp. 3454–3463.

Elser, J., & Bennett, E. 2011. A broken biogeochemical cycle. *Nature*. **478**(7367), pp. 29–31.

Emerson, K., Russo, R. C., Lund, R. E. & Thurston, R. V. 1975. Aqueous Ammonia Equilibrium Calculations: Effect of pH and Temperature. *Journal of the Fisheries Research Board of Canada*. **32**(12), pp. 2379–2383.

Etheridge, D.M., Steele, L.P., Langenfelds, R.L., Francey, R.J., Barnola, J.-M. & Morgan, V.I. 1998. Historical CO_2 records from the Law Dome DE08, DE08-2, and DSS ice cores. In Trends: A Compendium of Data on Global Change. Carbon Dioxide Information Analysis Center, Oak Ridge National Laboratory, U.S. Department of Energy, Oak Ridge, Tenn., U.S.A.

Environment Agency. 2019. *Waste water treatment works: treatment monitoring and compliance limits.* [Online]. [Accessed 18th Jan 2020]. Available at: https://www.gov.uk/government/publications/waste-water-treatment-works-treatment-monitoring-and-compliance-limits/waste-water-treatment-works-treatment-monitoring-and-compliance-limits

Fan, J., Andre, C., & Xu, C. 2011. A chloroplast pathway for the de novo biosynthesis of triacylglycerol in Chlamydomonas reinhardtii. *FEBS Letters*, **585**(12), pp. 1985–1991.

Fan, J., Yan, C., Andre, C., Shanklin, J., Schwender, J., & Xu, C. 2012. Oil accumulation is controlled by carbon precursor supply for fatty acid synthesis in Chlamydomonas reinhardtii. *Plant and Cell Physiology*. **53**(8), pp. 1380–1390.

Fan, J., Cui, Y., Wan, M., Wang, W., & Li, Y. 2014. Lipid accumulation and biosynthesis genes response of the oleaginous Chlorella pyrenoidosa under three nutrition stressors. *Biotechnology for Biofuels.* **7**(17), pp. 1–14.

Faul, F., Erdfelder, E., Buchner, A., & Lang, A.-G. 2009. Statistical Power Analyses using G*Power 3.1: Tests for Correlation and Regression Analyses. *Behaviour Research Methods*. **41**(4), pp. 1149–1160.

Feng, P., Deng, Z., Fan, L., & Hu, Z. 2012. Lipid accumulation and growth characteristics of Chlorella zofingiensis under different nitrate and phosphate concentrations. *Journal of Bioscience and Bioengineering*. **114**(4), pp. 405–410.

Fernandez, E. & Galvan, A. 2007, Inorganic nitrogen assimilation in Chlamydomonas. *Journal of Experimental Botany*. **58**(9), pp. 2279–2287.

Ferreira, V. dS. & Sant'Anna, C. 2017. The effect of physicochemical conditions and nutrient sources on maximizing the growth and lipid productivity of green microalgae. *Phycological Research.* **65**, pp. 3–13.

Food and Agriculture Organisation of the United Nations (FAO). 2011a. The state of the World's land and water resources for food and agriculture: Managing systems at risk. Available at: http://www.zaragoza.es/contenidos/medioambiente/onu/869-eng-sum.pdf

Food and Agriculture Organisation of the United Nations (FAO). 2011b. Energy-Smart Food for People and Climate, Issue Paper. Available at: http://www.fao.org/3/a-i2454e.pdf

Food and Agriculture Organisation of the United Nations (FAO). 2014. The Water-Energy-Food Nexus. A new approach in support of food security and sustainable agriculture. Available at: http://www.fao.org/3/a-bl496e.pdf

Francisco, É. C., Neves, D. B., Jacob-Lopes, E. & Franco, T. T. 2009. Microalgae as a feedstock for biodiesel production: Carbon dioxide sequestration, lipid production and biofuel quality. *Journal of Chemical Technology and Biotechnology.* **85**, pp. 395–403.

Friedman, J. M., Hunt Jr, E. R., & Mutters, R. G. 2016. Assessment of Leaf Color Chart Observations for Estimating Maize Chlorophyll Content by Analysis of Digital Photographs. *Agronomy Journal*. **108**(2), pp. 822–829.

Freimoser, F. M., Hürlimann, H. C., Jakob, C. A., Werner, T. P., & Amrhein, N. 2006. Systematic screening of polyphosphate (poly P) levels in yeast mutant cells reveals strong interdependence with primary metabolism. *Genome Biology*. **7**(11), article no: R109 [no pagination].

Gandiglio, M., Lanzini, A., Soto, A., Leone, P. & Santarelli, M. 2017. Enhancing the Energy Efficiency of Wastewater Treatment Plants through Co-digestion and Fuel Cell Systems. *Frontiers in Environmental Science*. **5**, article no: 70, [no pagination].

Gardner, R. D., Lohman, E., Gerlach, R., Cooksey, K. E. & Peyton, B. M. 2012. Comparison of CO_2 and Bicarbonate as Inorganic Carbon Sources for Triacylglycerol and Starch Accumulation in *Chlamydomonas reinhardtii*. *Biotechnology and Bioengineering.* **110**(1), pp. 87–96.

Gardner, R. D., Lohman, E. J., Cooksey, K. E., Gerlach, R., & Peyton, B. M. 2013. Cellular Cycling, Carbon Utilization, and Photosynthetic Oxygen Production during Bicarbonate-Induced Triacylglycerol Accumulation in a Scenedesmus sp. *Energies*. **6**, pp. 6060–6076.

Gargouri, M., Park, J. J., Holguin, F. O., Kim, M. J., Wang, H., Deshpande, R. R., *et al*. 2015. Identification of regulatory network hubs that control lipid metabolism in Chlamydomonas reinhardtii. *Journal of Experimental Botany*. **66**(15), pp. 4551–4566.

Gerber, C. P. & Pepper, I. L. 2019. Municipal Wastewater Treatment. In: Brusseau, M. L., Pepper, I. L. & Gerba, C. P. eds. *Environmental and Pollution Science.* 3rd ed. Academic Press.

Gerasimaitė, R., Sharma, S., Desfougères, Y., Schmidt, A., & Mayer, A. 2014. Coupled synthesis and translocation restrains polyphosphate to acidocalcisome-like vacuoles and prevents its toxicity. *Journal of Cell Science*. **127**(23), pp. 5093–104.

Global Petrol Prices.com. 2019a. *Diesel prices, liter, 18-Dec-2019*. [Online]. [Accessed 18th December 2019]. Available at: https://www.globalpetrolprices.com/diesel_prices/

Global Petrol Prices.com. 2019b. *Gasoline prices, liter, 18-Dec-2019*. [Online] [Accessed 18th December 2019]. Available at: https://www.globalpetrolprices.com/gasoline_prices/

Gómez-García, M. R., & Kornberg, A. 2004. Formation of an actin-like filament concurrent with the enzymatic synthesis of inorganic polyphosphate. *Proceedings of the National Academy of Sciences of the United States of America*. **101**(45), pp. 15876–80.

Gonçalves, A. L., Simões, M., & Pires, J. C. M. 2014. The effect of light supply on microalgal growth, CO2 uptake and nutrient removal from wastewater. *Energy Conversion and Management*. **85**, pp. 530–536.

Gonçalves, E. C., Wilkie, A. C., Kirst, M., & Rathinasabapathi, B. 2016. Metabolic regulation of triacylglycerol accumulation in the green algae: Identification of potential targets for engineering to improve oil yield. *Plant Biotechnology Journal*. **14**(8), pp. 1649–1660.

González-Garcinuño, A., Taberno, A., Sánchez-Álvarez, J. M., del Valle, E. M. M. & Galán, M. A. 2014. Effect of nitrogen source on growth and lipid accumulation in *Scenedesmus abundans* and *Chlorella ellipsoidae*. *Bioresrouce Technology*. **173**, 334–341.

González-González, L. M., Correa, D. F., Ryan, S., Jensen, P. D., Pratt, S. & Schenk, P. M. 2018. Integrated biodiesel and biogas production from microalgae: Towards a sustainable closed loop through nutrient recycling. *Renewable and Sustainable Energy Reviews.* **82**(1), pp. 1137–1148.

Grady, C. P. L., Daigger, G. T., Love, N. G. & Filipe, C. D. M. 2011. *Biological Wastewater Treatment.* 3rd ed. USA: CRC Press and London: IWA Publishing.

Greenfield, N. J., Hussain, M. & Lenard, J. 1987. Effects of growth state and amines on cytoplasmic and vacuolar pH, phosphate and polyphosphate levels in Saccharomyces cerevisiae: a ^{31}P-nuclear magnetic resonance study. *Biochimica et Biophysica Acta.* **926**, pp. 205–214.

Greenwell, H. C., Laurens, L. M. L., Shields, R. J., Lovitt, R. W., & Flynn, K. J. 2010. Placing microalgae on the biofuels priority list: a review of the technological challenges. *Journal of the Royal Society, Interface / the Royal Society*. **7**(46), pp. 703–726.

Guihéneuf, F., & Stengel, D. B. 2013. Carbon Availability in the Marine Haptophyte Pavlova lutheri. *Marine Drugs*. **11**, pp. 4246–4266.

Gupta, S. D., Ibaraki, Y., & Pattanayak, A. K. 2013. Development of a Digital Image Analysis Methods for Real-Time Estimation of Chlorophyll Content in Micropropagated Potato Plants. *Plant Biotechnology Reports.* **7**, pp. 91–97.

Gupta, S. K. & Bux, F. eds. 2019. *Biorefinery Approaches of Wastewater Treatment. Application of Microalgae in Wastewater Treatment,* Vol 2. Springer.

Gutierrez, J., Kwan, T. A., Zimmerman, J. B. & Peccia, J. 2016. Ammonia inhibition in oleaginous microalgae. *Algal Research.* **19**, pp. 123–127.

Haberl, H., Erb, Karl-Heinz., Krausmann, F., Running, S., Searchinger, T. S., & Smith, W. K. 2013. Bioenergy: how much can we expect for 2050? *Environmental Research Letters*. **8**(3), pp. 1-5.

Halfhide, T., Dalrymple, O. K., Wilkie, A. C., Trimmer, J., Gillie, B., Udom, I., *et al*. 2015. Growth of an Indigenous Algal Consortium on Anaerobically Digested Municipal Sludge Centrate: Photobioreactor Performance and Modelling. *Bioenergy Research*. **8**, pp. 249–258.

Halling-Sørensen, B. & Jørgensen, S. E. 1993. *The Removal of Nitrogen Compounds from Wastewater*. Amsterdam, London, New York, Tokyo: Elsevier.

Harris, E., Stern, D. & Witman, G. eds. 1988. *Introduction to Chlamydomonas and Its Laboratory Use. The Chlamydomonas Sourcebook,* Vol 1. Academic Press.

Harold, F. M. 1962. Depletion and Replenishment of the Inorganic Polyphosphate Pool in *Neurospora Crassa*. *Journal of Bacteriology.* **83**, pp. 1047–1057.

Harold, F. M. 1966. Inorganic polyphosphates in biology: structure, metabolism, and function. *Bacteriological Reviews*. **30**(4), pp. 772–794.

Hernández, D., Riaño, B., Coca, M., Solana, M., Bertucco, A., & García-González, M. C. 2016. Microalgae cultivation in high rate algal ponds using slaughterhouse wastewater for biofuel applications. *Chemical Engineering Journal*. **285**, pp. 449–458.

Hoegh-Guldberg, O., Mumby, P. J., Hooten, A., Steneck, R. S., Greenfield, P., Gomez, E., *et al.* 2007. Coral reefs under rapid climate change and ocean acidification. *Science*. **318**(5857), pp.1737–1742.

Hothorn, M., Neumann, H., Lenherr, E. D., Wehner, M., Rybin, V., Hassa, P. O., *et al*. 2009. Catalytic Core of a Membrane-Associated Eukaryotic Polyphosphate Polymerase. *Science*. **324**(5926), pp. 513–516.

Huang, G. & Wang, Y. 2003. Nitrate and Phosphate Removal by Co-immobilized *Chlorella pyrenoidosa* and Activated Sludge at Different pH Values. *Water Quality Research Journal of Canada*. **38**(3), pp. 541–551.

Hurlimann, H. C. 2007. Pho91 Is a Vacuolar Phosphate Transporter That Regulates Phosphate and Polyphosphate Metabolism in Saccharomyces cerevisiae. *Molecular Biology of the Cell*. **19**(1), pp. 308–317.

IEO, 2016. U.S. Energy Information Administration. International Energy Outlook (IEO) 2016. Available at: https://www.eia.gov/outlooks/ieo/pdf/0484(2016).pdf

IRENA, 2014: Nakada, S., Saygin, D. & Gielen, D. 2014. Global Bioenergy Supply and Demand Projections: A working paper for REmap 2030. *International Renewable Energy Agency.* **September 2014**.

IPCC, 2007a: Summary for policymakers. In: Solomon, S., Qin, D., Manning, M., Chen, Z., Marquis, M., Averyt. K. B., Tignor, M. & Miller, H. L. eds. *Climate Change 2007: The Physical Science Basis. Contribution of Working Group I to the Fourth Assessment Report of the Intergovernmental Panel on Climate Change*. Cambridge, United Kingdom and New York, NY, USA: Cambridge University Press.

IPCC, 2007b: *Climate Change 2007: Impacts, Adaptation and Vulnerability. Contribution of Working Group II to the Fourth Assessment Report of the Intergovernmental Panel on Climate Change*. Parry, M.L., Canziani, O.F., Palutikof, J.P., van der Linden, P.J. & Hanson, C.E. eds. Cambridge, UK: Cambridge University Press.

IPCC, 2013: Summary for Policymakers. In: Stocker, T. F., Quin, D., Plattner, G.-K., Tignor, M., Allen, S. K., Boshung, J., *et al*. eds. *Climate Change 2013: The Physical Science Basis. Contribution of Working Group I to the Fifth Assessment Report of the Intergovernmental Panel on Climate Change*. Cambridge, United Kingdom and New York, NY, USA: Cambridge University Press.

IPCC, 2014: Blanco G., R. Gerlagh, S. Suh, J. Barrett, H.C. de Coninck, C.F. Diaz Morejon, R. *et al*. 2014. Drivers, Trends and Mitigation. In: Edenhofer, O., R. Pichs-Madruga, Y. Sokona, E. Farahani, S. Kadner, K. Seyboth, A. *et al*. eds. *Climate Change 2014: Mitigation of Climate Change. Contribution of Working Group III to the Fifth Assessment Report of the Intergovernmental Panel on Climate Change.* Cambridge, United Kingdom and New York, NY, USA: Cambridge University Press.

Islam, M. A., Magnusson, M., Brown, R. J., Ayoko, G. A., Nabi, M. N. & Heimann, K. 2013. Microalgal Species Selection for Biodiesel Production Based on Fuel Properties Derived from Fatty Acid Profiles. *Energies.* **6**, pp. 5676–5702.

Jaworska, J., Genderen-Takken, H. V., Hanstveit, A., van de Plassche, E. & Feijtel, T. 2002. Environmental risk assessment of phosphonates used in domestic laundry and cleaning agents in the Netherlands. *Chemosphere*. **47**, pp. 655–665.

Jeyanayagam, S. 2005. True Confessions of the Biological Nutrient Removal Process. *Florida Water Resources Journal.* **January 2005**. pp. 37–46.

Joyce, S. 2000. The Dead Zones: Oxygen-Starved Coastal Waters. *Environmental Health Perspectives.* **108**(3), pp. 120–125.

Johnson, X., & Alric, J. 2013. Central carbon metabolism and electron transport in Chlamydomonas reinhardtii: Metabolic constraints for carbon partitioning between oil and starch. *Eukaryotic Cell*. **12**(6), pp. 776–793.

Källqvist, T. & Svenson, A. 2003. Assessment of ammonia toxicity in tests with the microalga, *Nephroselmis pyriformis*, Chlorophyta. *Water Research.* **37**, pp. 477–484.

Karemore, A., & Sen, R. 2015. Green integrated process for mitigation of municipal and industrial liquid and solid waste mixes for enhanced microalgal biomass and lipid synthesis for biodiesel. *RSC Advances.* **5**(87), pp. 70929–70938.

Kato, N., Dong, T., Bailey, M., Lum, T., & Ingram, D. 2013. Triacylglycerol mobilization is suppressed by brefeldin A in Chlamydomonas reinhardtii. *Plant and Cell Physiology*. **54**, pp. 1585–1599.

Kendrick, A. 2012. Natural Food and Beverage Colourings. In: Baines, D. & Seal, R. eds. *Natural Food Additives, Ingredients and Flavourings.* Woodhead Publishing, pp. 24–40.

Kim, S., Kim, H., Ko, D., Yamaoka, Y., Otsuru, M., Kawai-, M., *et al*. 2013. Rapid Induction of Lipid Droplets in Chlamydomonas reinhardtii and Chlorella vulgaris by Brefeldin A. *PloS One*. **8**(12), pp. 1–12.

Kim, H., Jang, S., Kim, S., Yamaoka, Y., Hong, D., Song, W.-Y., *et al*. 2015. The small molecule fenpropimorph rapidly converts chloroplast membrane lipids to triacylglycerols in *Chlamydomonas reinhardtii*. *Frontiers in Microbiology.* **6**, article no: 54, [no pagination].

Kim, G., Mujtaba, G. & Lee, K. 2016. Effects of nitrogen sources on cell growth and biochemical composition of marine chlorophyte *Tetraselmis* sp. for lipid production. *Algae*. **31**(3), pp. 257–266.

Klok, A. J., Lamers, P. P., Martens, D. E., Draaisma, R. B., & Wijffels, R. H. 2014. Edible oils from microalgae: Insights in TAG accumulation. *Trends in Biotechnology*. **32**(10), pp. 521–528.

Kochian, L. V. 2012. Rooting for more phosphorus. *Nature.* **488**(7412), pp. 466–467

Komine, Y., Eggink, L. L., Park, H., & Hoober, J. K. 2000. Vacuolar granules in Chlamydomonas reinhardtii: polyphosphate and a 70-kDa polypeptide as major components. *Planta*, **210**(6), pp. 897–905.

Kong, Q., Li, L., Martinez, B., Chen, P. & Ruan, R. 2010. Culture of Microalgae *Chlamydomonas reinhardtii* in Wastewater for Biomass Feedstock Production. *Applied Biochemistry and Biotechnology.* **160**, pp. 9–18.

Kong, F., Liang, Y., Légeret, B., Beyly-Adriano, A., Blangy, S., Haslam, R. P., *et al*. 2017. *Chlamydomonas* carries out fatty acid *β*-oxidation in ancestral peroxisomes using a bona fide acyl-CoA oxidase. *The Plant Journal.* **90**, pp. 358–371.

Kong, F., Romero, I. T., Warakanont, J. & Li-Beisson, Y. 2018. Lipid catabolism in microalgae. *New Phytologist.* **218**, pp. 1340–1348.

Kong, F., Yamaoka, Y., Ohama, T., Lee, Y. & Li-Beisson, Y. 2019. Molecular Genetic Tools and Emerging Synthetic Biology Strategies to Increase Cellular Oil Content in *Chlamydomonas reinhardtii*. *Plant and Cell Physiology.* **60**(6), pp. 1184–1196.

Krisnangkura, K. 1986. A Simple Method for Estimation of Cetane Index of Vegetable Oil Methyl Esters. *Journal of the American Oil Chemists' Society.* **63**(4), pp. 552–553.

Kuenen, J. G. 2008. Anammox bacteria: from discovery to application. *Nature Reviews Microbiology*. **6**, pp. 320–326.

Kulakovskaya, T. V., Andreeva, N. A., Trilisenko, L. V., Suetin, S. V., Vagabov, V. M. & Kulaev, I. S. 2005. Accumulation of polyphosphates and expression of high molecular weight exopolyphosphatase in the yeast *Saccharomyces cerevisiae*. *Biochemistry (Moscow).* **70**, pp. 980–985.

Kumble, K. D., & Kornberg, A. 1996. Endopolyphosphatases for Long Chain Inorganic Polyphosphate in Yeast and Mammals. *The Journal of Biological Chemistry*. **271**(43), pp. 27146–27151.

Kummu, M., Guillaume, J. H. A., de Moel, H., Eisner, S., Flörke, M., Porkka, M., *et al*. 2016. The world's road to water scarcity: shortage and stress in the 20th century and pathways towards sustainability. *Nature*. **6**, article no: 38495 [no pagination].

Lachmann, S. C., Mettler-Altmann, T., Wacker, A. & Spijkerman, E. 2018. Nitrate or ammonium: Influences of nitrogen source of the physiology of a green alga. *Ecology and Evolution*. **9**, pp. 1070–1082.

Lancet and University College London Institute for Global Health Commission. 2009. Managing the health effects of climate change. *Lancet*. **373**, pp. 1693-1733.

Larkum, A. W. D. 2010. Limitations and prospects of natural photosynthesis for bioenergy production. *Current Opinion in Biotechnology*. **21**(3), pp. 271–276.

Law, Y., Ye, L., Pan, Y. & Yuan, Z. 2012. Nitrous oxide emissions from wastewater treatment processes. *Philosophical Transactions of The Royal Society*. **367**, pp. 1265–1277.

Li, Y., Han, D., Hu, G., Dauvillee, D., Sommerfeld, M., Ball, S., & Hu, Q. 2010a. Chlamydomonas starchless mutant defective in ADP-glucose pyrophosphorylase hyper-accumulates triacylglycerol. *Metabolic Engineering*. **12**(4), pp. 387–391.

Li, Y., Han, D., Hu, G., Sommerfeld, M., & Hu, Q. 2010b. Inhibition of starch synthesis results in overproduction of lipids in Chlamydomonas reinhardtii. *Biotechnology and Bioengineering*. **107**(2), pp. 258–268.

Li, X., Benning, C., & Kuo, M. H. 2012. Rapid triacylglycerol turnover in Chlamydomonas reinhardtii requires a lipase with broad substrate specificity. *Eukaryotic Cell*. **11**(12), pp. 1451–1462.

Li-Beisson, Y., Beisson, F., & Riekhof, W. 2015. Metabolism of acyl-lipids in Chlamydomonas reinhardtii. *Plant Journal*, **82**(3), pp. 504–522.

Likosova, E. M., Keller, J., Rozendal, R. A., Poussade, Y. & Freguia, S. 2013. Understanding colloidal FeSx formation from iron phosphate precipitation sludge for optimal phosphorus recovery. *Journal of Colloid and Interface Science.* **403**, pp. 16–21.

Liu, Z., & Wang, G. 2008. Effect of iron on growth and lipid accumulation in Chlorella *vulgaris. Bioresource Technology. 99, pp. 4717–4722.*

Liu, B., & Benning, C. 2013. Lipid Metabolism in Microalgae Distinguishes Itself. *Current Opinion in Biotechnology*. **24**, pp. 300–309.

Liu, J., Yang, H., Gosling, S. N., Kummu, M., Flörke, M., Pfinster, S., *et al*. 2017. Water scarcity assessments in the past, present, and future. *Earth's Future.* **5**, pp. 545–559.

Lobell, D.B. & Asner, G. P. 2003. Climate and management contributions to recent trends in US agricultural yields. *Science*. **299**, p. 1032.

Lonetti, A., Szijgyarto, Z., Bosch, D., Loss, O., Azevedo, C., & Saiardi, A. 2011. Identification of an Evolutionarily Conserved Family of Inorganic Polyphosphate Endopolyphosphatases. *The Journal of Biological Chemistry*. **286**(37), pp. 31966–31974.

Lu, W., Wang, Z., Wang, X., & Yuan, Z. 2015. Cultivation of Chlorella sp. using raw diary wastewater for nutrient removal and biodiesel production: Characteristics comparison of indoor bench-scale and outdoor pilot-scale cultures. *Bioresource Technology*. **192**, pp. 382–388.

Lutzu, G. A., Zhang, W., & Liu, T. 2016. Feasibility of using brewery wastewater for biodiesel production and nutrient removal by Scenedesmus dimorphus, *Environmental Technology.* **37**(12), pp. 1568-1581.

Lynch, J. P. 2011. Root Phenes for Enhanced Soil Exploration and Phosphorus Acquisition: Tools for Future Crops. *Plant Physiology.* **156**, pp. 1041–1049.

Mara, D. 2003. *Domestic Wastewater Treatment In Developing Countries*. London: Earthscan.

Martínez, G., Sánchez, N., Encinar, J. M. & González, J. F. 2014. Fuel properties of biodiesel from vegetable oils and oil mixtures. Influence of methyl esters distribution. *Biomass and Bioenergy*. **63**, pp. 22–32.

McCarty, P. L. 2018. What is the Best Biological Process for Nitrogen Removal: When and Why? *Environmental Science and Technology.* **52**, pp. 3835–3841.

Merchant, S. S., Prochnik, S. E., Vallon, O., Harris, E. H., Karpowicz, S. J., Witman, G. B., *et al*. 2007. The *Chlamydomonas* Genome Reveals the Evolution of Key Animal and Plant Functions. *Science*. **318**(5848), pp. 245–250.

Minnesota Pollution Control Agency (MPCA). 2006. *Phosphorus Treatment and Removal Technologies*. Minnesota: Minnesota Pollution Control Agency.

Miyachi, S., Kanai, R., Mihara, S., Miyachi, S. & Aoki, S. 1964. Metabolic Roles of Inorganic Polyphosphates in *Chlorella* Cells. *Biochimica et Biophysica Acta.* **93**, pp. 625–634.

Moellering, E. R., & Benning, C. 2010. RNA interference silencing of a major lipid droplet protein affects lipid droplet size in Chlamydomonas reinhardtii. *Eukaryotic Cell*. **9**(1), pp. 97–106.

Morales, M., Sánchez, L. & Revah, S. 2018. The impact of environmental factors on carbon dioxide fixation by microalgae. *FEMS Microbiology Letters.* **365**(3), February 2018, fnx262.

Morales-Amaral, M. del M., Gómez-Serrano, C., Acién, F. G., Fernández-Sevilla, J. M., & Molina-Grima, E. 2015. Production of microalgae using centrate from anaerobic digestion as the nutrient source. *Algal Research*, **9**, pp. 297–305.

Morales-Amaral, M. del M., Gómez-Serrano, C., Acién, F. G., Fernández-Sevilla, J. M., & Molina-Grima, E. 2015b. Outdoor production of *Scenedesmus* sp. in thin-layer and raceway reactors using centrate from anaerobic digestion as the sole nutrient source. *Algal Research*. **12**, pp. 99–108.

Moseley, J. L., Chang, C. W., & Grossman, A. R. 2006. Genome-based approaches to understanding phosphorus deprivation responses and PSR1 control in Chlamydomonas reinhardtii. *Eukaryotic Cell*. **5**(1), pp. 26–44.

Mouratiadou, I., Biewald, A., Pehl, M., Bonsch, M., Baumstark, L., Klein, D., *et al*. 2016. The impact of climate change mitigation on water demand for energy and food: An integrated analysis based on the Shared Socioeconomic Pathways, *Environmental Science & Policy*. **64**, pp. 48–58.

Mujtaba, G., Rizwan, M., & Lee, K. 2015. Simultaneous removal of inorganic nutrients and organic carbon by symbiotic co-culture of Chlorella vulgaris and Pseudomonas putida. *Biotechnology and Bioprocess Engineering*. **20**(6), pp. 1114–1122.

Mulbry, W., Westhead, E. K., Pizarro, C. & Sikora, L. 2005. Recycling of manure nutrients: use of algal biomass from dairy manure treatment as a slow release fertilizer. *Bioresource Technology*. **96**, pp. 451–458.

Mulbry, W., Kondrad, S. & Pizarro, C. 2007. Biofertilizers from Algal Treatment of Dairy and Swine Manure Effluents. *Journal of Vegetable Science*. **12**(4), pp. 107–125.

Mulder, A. 1989. *Anoxic ammonia oxidation*. EP 0327184 A1.

Muralikrishna, I. V. & Manickam, V. 2017. Chapter Twelve – Wastewater Treatment Technologies. In: *Environmental Management. Science and Engineering for Industry.* Butterworth Heinemann.

Mus, F., Toussaint, J., Cooksey, K. E., Fields, M. W., Gerlach, R., Peyton, B. M., & Carlson, R. P. 2013. Physiological and molecular analysis of carbon source supplementation and pH stress-induced lipid accumulation in the marine diatom Phaeodactylum tricornutum. *Applied Microbioogy and Biotechnology.* **97***,* pp. 3625–3642.

Nagarajan, S., Kiang, S., Cao, S., Wu, C., & Zhou, Z. 2013. An updated comprehensive techno-economic analysis of algae biodiesel. *Bioresource Technology*. **145**, pp. 150–156.

Nishikawa, K., Yamakoshi, Y., Uemura, I. & Tominaga, N. 2003. Ultrastructural changes in *Chlamydomonas acidophila* (Chlorophyte) induced by heavy metals and polyphosphate metabolism. *FEMS Microbiology Ecology.* **44**, pp. 253–259.

Ochoa-Alfaro, A. E., Gaytán-Luna, D. E., González-Ortega, O., Zavala-Arias, K. G., Paz-Maldonado, L. M. T., Rocha-Uribe, A. & Soria-Guerra, R. E. 2019. pH effects on the lipid and fatty acids accumulation in *Chlamydomonas reinhardtii*. *Biotechnology Progress.* **35**(6), pp. 1–8.

Oehmen, A., Lemos, P. C., Carvalho, G., Yuan, Z., Keller, J., Blackall, L. L & Reis, M. A. M. 2007. Advances in enhanced biological phosphorus removal: From micro to macro scale. *Water Research.* **41**, pp. 2271–2300.

Ogawa, N., DeRisi, J., & Brown, P. O. 2000. New components of a system for phosphate accumulation and polyphosphate metabolism in Saccharomyces cerevisiae revealed by genomic expression analysis. *Molecular Biology of the Cell*. **11**(12), pp. 4309–4321.

Oleszkiewicz, J., Kruk, D. J., Devlin, T., Lashkarizadeh, M., & Yuan, Q. 2015. *Options for Improved Nutrient Removal and Recovery from Municipal Wastewater in the Canadian Context*. Winnipeg: Canadian Water Network.

Oswald, W. J., & Golueke, C. G. 1966. Eutrophication Trends in the USA - A problem? *Journal of the Water Pollution Control Federation*, **38**(6), pp. 964–975.

Pachés, M. Martínez-Guijarro, R., González-Camejo, J., Seco, A. & Barat, R. 2020. Selecting the most suitable microalgae species to treat the effluent from an anaerobic membrane bioreactor. *Environmental Technology.* **41**(3), pp. 267–276.

Paris Agreement 2015. United Nations Framework Convention on Climate Change. [Online]. Available at: https://unfccc.int/sites/default/files/english_paris_agreement.pdf

Park, J. B. K., Craggs, R. J., & Shilton, A. N. 2011. Wastewater treatment high rate algal ponds for biofuel production. *Bioresource Technology*, **102**(1), pp. 35–42.

Park, J. J., Wang, H., Gargouri, M., Deshpande, R. R., Skepper, J. N., Holguin, F. O., *et al*. 2015. The response of Chlamydomonas reinhardtii to nitrogen deprivation: A systems biology analysis. *Plant Journal*. **81**(4), pp. 611–624.

Pascual, M., Ahumada, J. A., Chaves, L. F., Rodó, X., & Bouma, M. 2006. Malaria resurgence in the East African highlands: temperature trends revisited. *Proceedings of the National Academy of Sciences of the United States of America*. **103**(15), pp. 5829–5834.

Pastor, L., Marti, N., Bouzas, A. & Seco, A. 2008. Sewage sludge management for phosphorus recovery as struvite in EBPR wastewater treatment plants. *Bioresource Technology.* **99**, pp. 4817–4824.

Patel, A. K., Huang, E. L., Low-Décarie, E., Lefsrud, M. G. 2015. Comparative Shotgun Proteomic Analysis of Wastewater-Cultured Microalgae: Nitrogen Sensing and Carbon Fixation for Growth and Nutrient Removal in *Chlamydomonas reinhardtii*. *Journal of Proteome Research*. **14**, pp. 3051–3067.

Pescod, M. B. 1992. Wastewater treatment and use in agriculture. Food and Agriculture Organization of the United Nations. [Online]. [Accessed 23rd April 2020]. Available at: http://www.fao.org/3/t0551e/t0551e00.htm#Contents

Pierzynski, G. M. ed. 2000. Methods of Phosphorus Analysis for Soils, Sediments, Residuals, and Waters. North Carolina State University.

Pittman, J. K., Dean, A. P., & Osundeko, O. 2011. The potential of sustainable algal biofuel production using wastewater resources. *Bioresource Technology*. **102**(1), pp. 17–25.

Plouviez, M., Wheeler, D., Shilton, A., Packer, M. A., McLenachan, P. A., Sanz-Luque, E. *et al*. 2017. The biosynthesis of nitrous oxide in the green alga *Chlamydomonas reinhardtii*. *The Plant Journal*. **91**, 45–56.

Poirier, Y., Antonenkov, V. D., Glumoff, T., & Hiltunen, J. K. 2006. Peroxisomal β -oxidation – A metabolic pathway with multiple functions. *Biophysica et Biochemica Acta*. **1763**, pp. 1413–1426.

Porra, R. J., Thompson, W. A., & Kriedemann, P. E. 1989. Determination of accurate extinction coefficients and simultaneous equations for assaying chlorophylls a and extracted with four different solvents: verification of the concentration of chlorophyll standards by atomic absorption spectroscopy. *Biochemica et Biophysica Acta.* **975**, pp. 384–394.

Posadas, E., Morales, M, dM., Gomez, C., Acién, F. G. & Muñoz. 2015. Influence of pH and CO_2 source on the performance of microalgae-based secondary domestic wastewater treatment in outdoors pilot raceways. *Chemical Engineering Journal.* **265**, pp. 239–248.

Powell, N., Shilton, A. N., Pratt, S., & Chisti, Y. 2008. Factors Influencing Luxury Uptake of Phosphorus by Microalgae in Waste Stabilization Ponds. *Environmental Science & Technology*. **42**(16), pp. 5958–5962.

Powell, N., Shilton, A., Chisti, Y., & Pratt, S. 2009. Towards a luxury uptake process via microalgae – defining the polyphosphate dynamics. *Water Research*. **43**(17), pp. 4207–4213.

Praveenkumar, R., Shameera, K., & Mahalakshmi, G. 2012. Influence of nutrient deprivations on lipid accumulation in a dominant indigenous microalga Chlorella sp., BUM11008: Evaluation for biodiesel production. *Biomass and Bioenergy*. **37**, pp. 60-66.

Pröschold, T., Harris, E. H. & Coleman, A. W. 2005. Portrait of a Species: Chlamydomonas reinhardtii. *Genetics*. **170**, pp. 1601–1610.

Prud'homme, M., 2010. World Phosphate Rock Flows, Losses and Uses. In *Proceedings of Phosphates 2010 International Conference, 22-24 March 2010, Brussels*. Brussels: International Fertiliser Industry Association.

Qiu, R., Gao, S., Lopez, P. A. & Ogden, K. L. 2017. Effects of pH on cell growth, lipid production and CO_2 addition of microalgae *Chlorella sorokiniana*. *Algal Research.* **28**, pp. 192–199.

Rachlin, J. W., Jensen, T. E. & Warkentine, B. 1984. The Toxicological Response of the Alga *Anabaena flos-aquae* (Cyanophyceae) to Cadmium. *Archives of Environmental Contamination and Toxicology.* **13**, pp. 143–151.

Rai, M. P. & Gupta, S. 2017. Effect of media composition and light supply on biomass, lipid content and FAME profile for quality biofuel production from *Scenedesmus abundans*. *Energy Conversion and Management.* **141**, pp. 85–92.

Ramírez-Verduzco, L. F., Rodríguez-Rodríguez, J. E., Jaramillo-Jacob, A. R. 2012. Predicting cetane number, kinematic viscosity, density and higher heating value of biodiesel from its fatty acid methyl ester composition. *Fuel*. **91**, pp. 102–111.

Ramos, M. J., Fernández, C. M., Casas, A., Rodríguez, L. & Pérez, A. 2009. Influence of fatty acid composition of raw materials on biodiesel properties. *Bioresource Technology.* **100**, pp. 261–268.

Ramsundar, P., Guldhe, A., Singh, P. & Bux, F. 2017. Assessment of municipal wastewaters at various stages of treatment process as potential growth media for *Chlorella sorokiniana* under different modes of cultivation. *Bioresource Technology*. **227**, pp. 82–92.

Rao, N. N., Gómez-García, M. R., & Kornberg, A. 2009. Inorganic polyphosphate: essential for growth and survival. *Annual Review of Biochemistry*. **78**, pp. 605–647.

Rignon, J. P. G., Capuani, S., Fernandes, D. M., & Guimarães, T. M. 2016. A Novel Method for the Estimation of Soybean Chlorophyll Content using a Smartphone and Image Analysis. *Photosynthetica*. **54**(4), pp. 559–566.

Rodolfi, L., Zittelli, G. C., Bassi, N., Padovani, G., Biondi, N., Bonini, G., & Tredici, M. R. 2009. Microalgae for oil: Strain selection, induction of lipid synthesis and outdoor mass cultivation in a lowcost photobioreactor. *Biotechnology and Bioengineering*. **102**(1), pp. 100–112.

Renman, A. & Renman, G. 2010. Long-term phosphate removal by the calcium-silicate material Polonite in wastewater filtration systems. *Chemosphere*. **79**, pp. 659–664.

Reverdatto, S., Beilinson, V. & Nielsen, N.C. 1999. A multisubunit acetyl coenzyme A carboxylase from soybean. *Plant Physiology*. **119**, pp. 961–978.

Ruiz, F. A., Marchesini, N., Seufferheld, M., Govindjee, & Docampo, R. 2001a. The Polyphosphate Bodies of Chlamydomonas reinhardtii Possess a Proton-pumping Pyrophosphatase and Are Similar to Acidocalcisomes. *Journal of Biological Chemistry*. **26**(49), pp. 46196–46203.

Ruiz, F. A., Rodrigues, C. O. & Docampo, R. 2001b. Rapid Changes in Polyphosphate Content within Acidocalcisomes in Response to Cell Growth, Differentiation and Environmental Stress in *Trypanosoma cruzi*. *The Journal of Biological Chemistry.* **276**(28), pp. 26114–26121.

Salomé, P. A. & Merchant, S. S. 2019. A Series of Fortunate Events: Introducing Chlamydomonas as a Reference Organism. *The Plant Cell.* **31**, pp. 1682–1707.

Samorì, G., Samorì, C., Guerrini, F., & Pistocchi, R. 2013. Growth and nitrogen removal capacity of Desmodesmus communis and of a natural microalgae consortium in a batch culture system in view of urban wastewater treatment: part I. *Water Research*. **47**(2), pp. 791–801.

Saxena, R. C., Adhikari, D. K., & Goyal, H. B. 2009. Biomass-based energy fuel through biochemical routes: A review. *Renewable and Sustainable Energy Reviews.* **13**(1), pp. 167–178.

Sells, M. D., Brown, N. & Shilton, A. N. 2018. Determining the variables that influence the phosphorus content of waste stabilization pond algae. *Water Research.* **132**, pp. 301–308.

Sethuraman, A., Rao, N. N., & Kornberg, A. 2001. The endopolyphosphatase gene: Essential in Saccharomyces cerevisiae. *Proceedings of the National Academy of Sciences of the United States of America*. **98**(15), pp. 18–23.

Scherholz, M. L. & Curtis, W. R. 2013. Achieving pH control in microalgal cultures through fed-batch addition of stoichiometrically-balanced growth media. *BMC Biotechnology*. **13**, article no: 39, [no pagination].

Schröder, J. J., Smit, A. L., Cordell, D., and Rosemarin, A. 2011. Improved phosphorus use efficiency in agriculture: A key requirement for its sustainable use. *Chemosphere.* **84**(6), pp. 822–831.

Schmollinger, S., Mühlhaus, T., Boyle, N. R., Blaby, I. K., Casero, D., Mettler, T., *et al*. 2014. Nitrogen-Sparing Mechanisms in *Chlamydomonas* Affect the Transcriptome, the Proteome, and Photosynthetic Metabolism. *The Plant Cell*. **26**(4), pp. 1410–1435.

Scott, S. A., Davey, M. P., Dennis, J. S., Horst, I., Howe, C. J., Lea-smith, D. J., & Smith, A. G. 2010. Biodiesel from algae: challenges and prospects. *Current Opinion in Biotechnology*. **21**(3), pp. 277–286.

Seckler, D., Amarasinghe, U., Molden, D., de Silva, R. & Barker, R. 1998**.** World water demand and supply, 1990 to 2025: Scenarios and issues. *Colombo, Sri Lanka: International Irrigation Management Institute (IIMI);* IWMI. vi, 40p. (IIMI Research Report 19 / IWMI Research Report 19).

Sforza, E., Barbera, E., Girotto, F., Cossu, R. & Bertucco, A. 2017. Anaerobic digestion of lipid-extracted microalgae: Enhancing nutrient recovery towards a closed loop recycling. *Biochemical Engineering Journal.* **121**, pp. 139–146.

Shilton, A. N., Elmetri, I., Drizo, A., Pratt, S., Haverkamp, R. G. & Bilby, S. C. 2006. Phosphorus removal by an “active” slag filter – a decade of full scale experience. *Water Research.* **40**, pp. 113–118.

Siaut, M., Cuiné, S., Cagnon, C., Fessler, B., Nguyen, M., Carrier, P., *et al*. 2011. Oil Accumulation in the Model Green Alga Chlamydomonas reinhardtii: Characterisation, Variability between Common Laboratory Strains and Relationship with Starch Reserves. *BMC Biotechnology,* **11**, article no: 7, [no pagination].

Sivakumar, G., Xu, J., Thompson, R. W., Yang, Y., Randol-Smith, P., & Weathers, P. J. 2012. Integrated green algal technology for bioremediation and biofuel. *Bioresource Technology*. **107**, pp. 1–9.

Skrupski, B., Wilson, K. E., Goff, K. L. & Zou, J. 2013. Effect of pH on neutral lipid and biomass accumulation in microalgal strains native to the Canadian prairies and the Athabasca oil sands. *Journal of Applied Phycology.* **25**, pp. 937–949.

Slade, R., & Bauen, A. 2013. Micro-algae cultivation for biofuels: Cost, energy balance, environmental impacts and future prospects. *Biomass and Bioenergy*. **53**(0), pp. 29–38.

Smith, B. E. 2002. Nitrogenase Reveals Its Inner Secrets. *Science.* **297**(5587), pp. 1654–1655.

Smith, S., Takacs, I., Murthy, S., Daigger, G. T. & Szabo, A. 2008. Phosphate complexation model and its implications for chemical phosphorus removal. *Water Environment Research*. **80**(5), pp. 428–438.

Solovchenko, A., Verschoor, A. M., Jablonowski, N. D. & Nedbal, L. 2016. Phosphorus from wastewater to crops: An alternative path involving microalgae. *Biotechnology Advances.* **34**, pp. 550–564.

Steber, J. 2007. The Ecotoxicity of Cleaning Product Ingredients. In: Johansson, I. & Somnsundaran, P. eds. *Handbook of Cleaning/Decontamination of Surfaces*. Elsevier. Xu

Stiles, W. A. V., Styles, D., Chapman, S. P., Esteves, S., Bywater, A., Melville, L., *et al*. 2018. Using microalgae in the circular economy to valorise anaerobic digestate: challenges and opportunities. *Bioresource Technology*. **267**, pp. 732–742.

Stumm, W. & Morgan, J. J. 1996. *Aquatic Chemistry: Chemical Equilibria and Rates in Natural Waters.* 3rd ed. New York: John Wiley & Sons Inc.

Su, C.-H., Fu, C.-C., Chang, Y.-C., Nair, G. R., Ye, J.-L., Chu, I.-M., & Wu, W.-T. 2008. Simultaneous Estimation of Chlorophyll a and Lipid Contents in Microalgae by Three-Color Analysis. *Biotechnology and Bioengineering*. **99**(4), pp. 1034–1039.

Sun, X., Wang, C., Li, Z., Wang, W., Tong, Y., & Wei, J. 2013. Microalgal cultivation in wastewater from the fermentation effluent in Riboflavin (B2) manufacturing for biodiesel production. *Bioresource Technology*. ***143***, pp. 499–504.

Tan, K. W. M. & Lee, Y. K. 2016. The dilemma for lipid productivity in green microalgae: importance of substrate provision in improving oil yield without sacrificing growth. *Biotechnology for Biofuels.* **9**, article no: 255, [no pagination].

Tan, X.-B., Zhang, Y.-L., Yang, L.-B., Chu, H.-Q. & Guo, J. 2016. Outdoor cultures of *Chlorella pyrenoidosa* in the effluent of anaerobically digested activated sludge: The effects of pH and free ammonia. *Bioresource Technology*. **200**, pp. 606–615.

Teymouri, A., Kumar, S., Barbera, E., Sforza, E., Bertucco, A. & Morosinotto, T. 2016. Integration of Biofuels Intermediates Production and Nutrients Recycling in the Processing of a Marine Algae. *AIChE Journal.* **63**(5), pp. 1494–1502

Thacker, A. & Syrett, P. J. 1972. The Assimilation of Nitrate and Ammonium by *Chlamydomonas reinhardi*. *New Phytologist*. **71**, pp. 423–433.

The Chlamydomonas Resource Center,a. *About Chlamydomonas*. [Online]. [Accessed 23rd April 2020]. Available at: https://www.chlamycollection.org/resources/about-chlamydomonas/

The Chlamydomonas Resource Center,b. *TAP and Tris-minimal*. [Online]. [Accessed 17th November 2017]. Available at: https://www.chlamycollection.org/methods/media-recipes/tap-and-tris-minimal/

The Chlamydomonas Resource Center,c. *Freezing Chlamydomonas Cells*. [Online]. [Accessed 10th January 2020]. Available at: https://www.chlamycollection.org/methods/freezing-chlamydomonas-cells/

The Chlamydomonas Resource Center,d. CC-400 cw15 mt+. [Online]. [Accessed 14th November 2016]. Available at: https://www.chlamycollection.org/product/cc-400-cw15-mt/

The World Bank. 2020. *Pump price for gasoline (US$ per liter)*. [Online] [Accessed 23rd April 2020]. Available at: https://data.worldbank.org/indicator/EP.PMP.SGAS.CD?end=2016&start=1991&view=chart

Tsai, C. H., Warakanont, J., Takeuchi, T., Sears, B. B., Moellering, E. R., & Benning, C. 2014. The protein Compromised Hydrolysis of Triacylglycerols 7 (CHT7) acts as a repressor of cellular quiescence in Chlamydomonas. *Proceedings of the National Academy of Sciences*. **111**(44), pp. 15833–15838.

Tsolcha, O. N., Tekerlekopoulou, A. G., Akratos, C. S., Bellou, S., Aggelis, G., Katsiapi, M., MoustakaGouni, M., & Vayenas, D. V. 2015. Treatment of second cheese whey effluents using a *Choricystis* based system with simultaneous lipid production. *Journal of Chemical Technology & Biotechnology*, **91**, pp. 2349–2359.

United Nations, Department of Economic and Social Affairs, Population Division. 2015. World Population Prospects: The 2015 Revision, Key Findings and Advance Tables. Working Paper No. ESA/P/WP.241.

Urzica, E. I., Vieler, A., Hong-hermesdorf, A., Page, M. D., Casero, D., Gallaher, S. D., *et al*. 2013. Remodelling of Membrane Lipids in Iron-starved. *The Journal of Biological Chemistry*. **288**(42), pp. 30246–30258.

U.S. Geological Survey. 2020. *Mineral commodity summaries 2020*. [online]. U.S. Geological Survey. [Accessed 23 April 2020]. Available at: https://doi.org/10.3133/mcs2020

Usher, P. K. 2014. Integrating heterotrophic microalgae feedstock into the Brazilian biodiesel industry: A whole systems analysis. Ph.D. thesis, University of Leeds.

Vagabov, V. M., Trilisenko, L. V., Kulakovskaya, T. V., & Kulaev, I. S. 2008. Effect of a carbon source on polyphosphate accumulation in Saccharomyces cerevisiae. *FEMS Yeast Research*. **8**(6), pp. 877–882.

Valledor, L., Furuhashi, T., Recuenco-Muñoz, L., Wienkoop, S., & Weckwerth, W. 2014. System-level network analysis of nitrogen starvation and recovery in Chlamydomonas reinhardtii reveals potential new targets for increased lipid accumulation. *Biotechnology for Biofuels*. **7**, article no: 171, [no pagination].

van Beilen, J. B. 2010. Why microalgal biofuels won't save the internal combustion machine. *Biofuels, Bioproducts and Biorefining*. **4**(1), pp. 41–52.

van Harmelen, T., Oonk, H. 2006. Microalgae biofixation processes: Applications and potential contributions to greenhouse gas mitigation options. *TNO Built Environmental and Geosciences. Apeldoorn. Prepared for the International Network on Biofixation of CO2 and greenhouse gas abatement with Microalgae. Operated under the International Energy Agency Greenhouse Gas R&D Programme., The Netherlands (Order no. 36562).*

Van Kauwenberg, S. J. 2010. *World Phosphate Rock Reserves and Resources.* Technical Bulletin IFDCT-75. Muscle Shoals, Alabama, USA.

Vandamme, D., Foubert, I., Fraeye, I., Meesschaert, B. & Muylaert, K. 2012. Flocculation of *Chlorella vulgaris* induced by high pH: Role of magnesium and calcium and practical implications. *Bioresource Technology*. **105**, pp. 114–119.

Vieler, A., Wu, G., Tsai, C. H., Bullard, B., Cornish, A. J., Harvey, C., *et al*. 2012. Genome, Functional Gene Annotation, and Nuclear Transformation of the Heterokont Oleaginous Alga Nannochloropsis oceanica CCMP1779. *PLoS Genetics*. **8**(11), [no pagination].

Vincent, W F. 1983. Fluorescence Properties of the Freshwater Phytoplankton: Three Algal Classes Compared. *British Phycological Journal*. **18**(1), pp. 5–21.

von Sperling, M. 2007. *Wastewater Characteristics, Treatment and Disposal. Biological Wastewater Treatment Series,* Vol 1. London: IWA Publishing.

Wang, X.-X., Wu, Y.-H., Zhang, T.-Y., Xu, X.-Q., Dao, G.-H., & Hu, H.-Y. 2016. Simultaneous nitrogen, phosphorus, and hardness removal from reverse osmosis concentrate by microalgae cultivation. *Water Research*. **94**, pp. 215–24.

Wang, H., Zhu, R., Zhang, J., Ni, L., Shen, H. & Xie, P. 2018. A Novel and Convenient Method for Early Warning of Algal Cell Density by Chlorophyll Fluorescence Parameters and Its Application in a Highland Lake. *Frontiers in Plant Science.* **9**, article no: 869, [no pagination].

Warakanont, J., Li-Beisson, Y. & Benning, C. 2019. LIP4 Is Involved in Triacylglycerol Degradation in *Chlamydomonas reinhardtii*. *Plant and Cell Physiology.* **60**(6), pp. 1250–1259.

Wase, N., Tu, B., Black, P. N. & DiRusso, C. C. 2015. Phenotypic screening identifies Brefeldin A/Ascotoxin as an inducer of lipid storage in the algae *Chlamydomonas reinhardtii*. *Algal Research.* **11**, pp. 74–84.

Werner, T. P., Amrhein, N. & Freimoser, F. M. 2005. Novel method for the quantification of inorganic polyphosphate (iPoP) in *Saccharomyces cerevisiae* shows dependence of iPoP content on the growth phase. Archives of Microbiology. 184, pp. 129–136.

Wiebe, R. & Gaddy, V. L. 1940. The Solubility of Carbon Dioxide in Water at Various Temperatures from 12 to 40° and at Pressures to 500 Atmospheres. Critical Phenomena. *Journal of the American Chemical Society.* **62**(4), pp. 815–817.

Wijffels, R. H., & Barbosa, M. J. 2010. An Outlook on Microalgal Biofuels. *Science*. ***329***, pp. 796–799.

Wood, A. M., Everroad, R. C., & Wingard, L. M. 2005. Measuring growth rates in microalgal cultures. In: Andersen, R. A. ed. *Algal Culturing Techniques, Measuring Growth Rates in Microalgal Cultures*. Amsterdam: Phycological Society of America, Elsevier, pp. 269–286.

Work, V. H., Radakovits, R., Jinkerson, R. E., Meuser, J. E., Elliott, L. G., Vinyard, D. J., *et al*. 2010. Increased Lipid Accumulation in the Chlamydomonas reinhardtii sta7-10 Starchless Isoamylase Mutant and Increased Carbohydrate Synthesis in Complemented Strains. *Eukaryotic Cell*. **9**(8), pp. 1251–1261.

Wu, Z., Zhu, Y., Huang, W., Zhang, C., Li, T., Zhang, Y. & Li, A. 2012. Evaluation of flocculation induced by pH increase for harvesting microalgae and reuse of flocculated medium. *Bioresource Technology*. **110**, pp. 496–502.

Wuang, S. C., Khin, M. C., Chua, P. Q. D. & Luo, Y. D. 2016. Use of Spirulina biomass produced from treatment of aquaculture wastewater as agricultural fertilizers. *Algal Research*. **15**, pp. 59–64.

Wurst, H., & Kornberg, A. 1994. A Soluble Exopolyphosphatase of Saccharomyces cerevisiae. *The Journal of Biological Chemistry*. **269**(15), pp. 10996–11001.

Wykoff, D. D., Grossman, A. R., Weeks, D. P., Usuda, H., & Shimogawara, K. 1999. Psr1, a nuclear localized protein that regulates phosphorus metabolism in Chlamydomonas. *Proceedings of the National Academy of Sciences of the United States of America*. **96**(26), pp. 15336–15341.

Xu, J., Zhao, Y., Zhao, G., & Zhang, H. 2015. Nutrient removal and biogas upgrading by integrating freshwater algae cultivation with piggery anaerobic digestate liquid treatment. *Applied Microbiology and Biotechnology*. **99**(15), pp. 6493–6501.

Yang, M., Fan, Y., Wu, P.-C., Chu, Y.-D., Shen, P.-L., Xue, S. & Chi, Z.-Y. 2017. An Extended Approach to Quantify Triacylglycerol in Microalgae by Characteristic Fatty Acids. *Frontiers in Plant Science*. **8**, article no: 1949, [no pagination].

Young, P., Taylor, M. & Fallowfield, H. J. 2017. Mini-review: high rate algal ponds, flexible systems for sustainable wastewater treatment. *World Journal of Microbiology and Biotechnology.* **33**, article no: 117 [no pagination].

Yu, J., Su, Z., Wang, P., & Zhou, Y. 2015. The growth traits of microalgae for biofuel and its effect on nitrogen and phosphorus removal in waste water. *International Conference on Advances in Energy and Environmental Science (ICAEES), 25-26 July 2015, Zhuhai, China.* Atlantic Press, pp. 495–498.

Yuan, Z., Pratt, S. & Batstone, D. J. 2012. Phosphorus recovery from wastewater through microbial processes. *Current Opinion in Biotechnology.* **23**, pp. 878–883.

Yulistyorini, A. 2016. Phosphorus Recovery from Wastewater through Enhanced Micro-algal Uptake. Ph.D. thesis, University of Leeds.

Zhang, H., Gómez-García, M. R., Brown, M. R. W., & Kornberg, A. 2005. Inorganic polyphosphate in Dictyostelium discoideum: influence on development, sporulation, and predation. *Proceedings of the National Academy of Sciences of the United States of America*. **102**(8), pp. 2731–2735.

Zhang, B., Wang, L., Hasan, R., & Shahbazi, A. 2014a. Characterization of a native algae species Chlamydomonas debaryana: Strain selection, bioremediation ability, and lipid characterization. *BioResources*. **9**(4), pp. 6130–6140.

Zhang, Q., Wang, T. & Hong, Y. 2014b. Investigation of initial pH effects on growth of an oleaginous microalgae *Chlorella* sp. HQ for lipid production and nutrient uptake. *Water Science and Technology.* **70**(4), pp. 712–719.

Zhang, S., Kim, T.-H., Han, T. H., & Hwang, S.-J. 2015. Influence of light conditions of a mixture of red and blue light sources on nitrogen and phosphorus removal in advanced wastewater treatment using Scenedesmus dimorphus. *Biotechnology and Bioprocess Engineering*. **20**(4), pp. 760–765.

Zheng, J., Hao, J. M., Wang, B. & Shui, C., 2011. Bioremediation of Aquiculture Wastewater by Microalgae Isochrysis zhanjiangensis and Production of the Biomass Material. In: *International Conference on Components, Packaging and Manufacturing Technology, 9-10 December 2010, Sanya, China.* Pp. 460–461.

Zhou, W., Li, Y., Min, M., Hu, B., Chen, P. & Ruan, R. 2011. Local bioprospecting for high-lipid producing microalgal strains to be grown on concentrated municipal wastewater for biofuel production. *Bioresource Technology.* **102**, pp. 6909–6919.

Zhu, S., Wang, Y., Xu, J., Shang, C., Wang, Z., Xu, J. & Yuan, Z. 2015. Luxury uptake of phosphorus changes the accumulation of starch and lipid in *Chlorella* sp. under nitrogen depletion. *Bioresource Technology.* **198**, pp. 165–171.

Zhu, Z., Yuan, G., Fan, X., Fan, Y., Yang, M., Yin, Y., *et al*. 2018. The synchronous TAG production with the growth by the expression of chloroplast transit peptide-fused ScPDAT in *Chlamydomonas reinhardtii*. *Biotechnology for Biofuels.* **11**, article no: 156, [no pagination].

Zienkiewicz, K., Du, Z. Y., Ma, W., Vollheyde, K., & Benning, C. 2016. Stress-induced neutral lipid biosynthesis in microalgae - Molecular, cellular and physiological insights. *Biochimica et Biophysica Acta.* **1861**(9), pp. 1269–1281.

Zienkiewicz, A., Zienkiewicz, K., Poliner, E., Pulman, J. A., Du, Z.-Y., Stefano, G., *et al*. 2020. The Microalga Nannochloropsis during Transition from Quiescence to Autotrophy in Response to Nitrogen Availability. *Plant Physiology*. **182**, pp. 819–839.

Appendix

Table A1. Biomass composition as weight % moisture, ash, volatile matter and fixed carbon as obtained from thermogravimetric analysis (TGA) after 7 days cultivation.

	Moisture (wt%)	Ash (wt%)	Volatile Matter (wt%)	Fixed Carbon (wt%)
TAP	3.9 ± 0.06	9.4 ± 0.10	71.1 ± 0.14	15.5 ± 0.22
TAP –N	4.9 ± 0.18	10.0 ± 0.57	70.0 ± 2.33	15.0 ± 2.61
TA-	4.1 ± 0.27	4.7 ± 0.50	74.8 ± 0.84	16.4 ± 0.67
TAP (NO_3)	4.2 ± 0.84	7.6 ± 1.47	73.2 ± 0.44	14.9 ± 0.31
CAP (NH_4) High pH	5.5 ± 0.19	9.5 ± 0.57	69.1 ± 0.56	15.9 ± 0.27
CAP (NH_4) High pH + Bicarbonate	5.8 ± 0.17	16.7 ± 2.49	63.1 ± 1.86	14.4 ± 0.70
CAP (NO_3) High pH	5.2 ± 0.25	10.6 ± 1.45	68.2 ± 1.11	15.9 ± 1.62
CAP (NO_3) High pH + Bicarbonate	10.4 ± 6.47	6.6 ± 1.54	67.2 ± 3.72	15.8 ± 1.33
TAP with varying ammonium:nitrate ratio				
100:0	4.1 ± 0.11	10.9 ± 0.17	71.4 ± 0.37	13.6 ± 0.32
75:25	4.4 ± 0.12	10.3 ± 0.24	71.9 ± 0.42	13.4 ± 0.49
50:50	4.2 ± 0.08	10.3 ± 0.25	72.3 ± 0.87	13.2 ± 0.71
25:75	4.3 ± 0.38	9.3 ± 0.26	73.0 ± 0.33	13.4 ± 0.23
0:100	4.1 ± 0.18	10.5 ± 0.30	71.5 ± 0.52	13.9 ± 0.37

Table A2. Biomass composition as weight % carbon, hydrogen, nitrogen, sulphur and oxygen (by difference) of dry biomass as obtained from CHNS elemental analysis after 7 days cultivation. Ash and moisture content, to correct to dry basis, were obtained from thermogravimetric analysis (TGA, see Table A1).

	Carbon (wt%, dry)	Hydrogen (wt%, dry)	Nitrogen (wt%, dry)	Sulphur (wt%, dry)	Oxygen (wt%, dry)	Ash (wt%, dry)
TAP	52.1 ± 0.24	5.2 ± 0.39	9.7 ± 0.28	0.2 ± 0.14	22.9 ± 0.48	9.8 ± 0.10
TAP –N	46.9 ± 0.45	5.2 ± 0.47	2.5 ± 0.18	0.0 ± 0.00	34.8 ± 0.98	10.5 ± 0.60
TA-	53.9 ± 0.64	5.4 ± 0.43	9.6 ± 0.17	0.2 ± 0.13	26.0 ± 0.97	4.9 ± 0.51
TAP (NO_3)	52.5 ± 0.36	5.8 ± 0.94	8.8 ± 0.15	0.1 ± 0.10	24.9 ± 1.70	7.9 ± 1.47
CAP (NH_4) High pH	47.6 ± 0.55	5.0 ± 0.01	10.6 ± 0.07	0.0 ± 0.00	27.2 ± 0.61	10.0 ± 0.60
CAP (NH_4) High pH + Bicarbonate	40.8 ± 0.56	4.6 ± 0.86	8.3 ± 0.12	0.0 ± 0.05	28.5 ± 2.46	17.7 ± 2.65
CAP (NO_3) High pH	38.4 ± 5.89	4.9 ± 0.70	5.7 ± 1.01	0.0 ± 0.00	39.8 ± 7.72	11.2 ± 1.50
CAP (NO_3) High pH + Bicarbonate	46.0 ± 4.79	4.6 ± 0.90	5.0 ± 0.51	0.0 ± 0.00	37.0 ± 5.86	7.3 ± 1.24
TAP with varying ammonium:nitrate ratio						
100:0	47.8 ± 0.22	5.5 ± 1.13	5.0 ± 0.18	0.0 ± 0.00	30.3 ± 1.15	11.3 ± 0.17
75:25	48.0 ± 3.66	5.6 ± 1.48	4.9 ± 0.35	0.0 ± 0.00	30.6 ± 5.26	10.8 ± 0.24
50:50	48.1 ± 0.23	5.7 ± 1.22	5.0 ± 0.06	0.0 ± 0.00	30.4 ± 1.21	10.7 ± 0.26
25:75	48.6 ± 0.32	5.7 ± 1.31	5.4 ± 0.20	0.0 ± 0.00	30.6 ± 1.36	9.7 ± 0.27
0:100	49.3 ± 0.46	5.5 ± 0.35	5.9 ± 0.30	0.0 ± 0.00	28.4 ± 0.81	11.0 ± 0.31